GAHNITE AND ITS FORMATION IN THE CONTEXT OF REGIONAL METAMORPHISM AND MINERALIZATION IN THE NAMAQUALAND METAMORPHIC COMPLEX.

by

JUDITH ANNE HICKS
(formerly Evans)

Thesis submitted in fulfilment of the requirements for the degree of Master of Science in the Faculty of Science, University of Cape Town.

Department of Geology

1988

D88/40.

U.T 550 HICK

88/7952

ABSTRACT

Gahnite ($ZnAl_2O_4$) is commonly associated with sulphide mineralization in metamorphosed massive sulphide deposits, and also occurs in marbles, pegmatites and quartz veins. Its formation has been attributed to the breakdown of Zn-staurolite or desulphidation of sphalerite during metamorphism. The stability of zinc-rich spinels under a wide range of metamorphic conditions in a variety of lithologies results in its persistence in rocks where many other prograde, high temperature minerals and sulphides have been altered. This has resulted in various investigations into its use in exploration and potential for determining metamorphic parameters. With the interest in finding new ore bodies and in determining the metamorphic history and mineralogy in Namaqualand, some gahnite-bearing localities have been investigated in this study.

Gahnite occurs in association with massive sulphide mineralization in the Bushmanland Sequence rocks (Aggeneys Subgroup) of the Namaqualand Metamorphic Complex at Aggeneys and Gamsberg. Gahnite also occurs in quartzites and metapelitic rocks at Achab, 8 km east of Gamsberg and in sillimanite-corundum rocks 35 km north-east of Aggeneys. On Oranjefontein farm, 70 km south-west of Aggeneys, co-existing green and blue gahnite occurs in quartzites and garnet-rich rocks in a similar stratigraphic succession to that which occurs in the Bushmanland rocks in the north.

Gahnite mineral chemistry and textural relations indicates that it formed during diagenesis and subsequent metamorphism of precursor sulphide-bearing, aluminous metasediments at Aggeneys, Achab, Swartkoppies and Oranjefontein in the reaction (Spry and Scott, 1987a);
$Al_2Si_2O_5(OH)_4 + ZnS + 0.5O_2 \rightarrow ZnAl_2O_4 + 2SiO_2 + 2H_2O + 0.5S_2$

Calculated maximum metamorphic conditions are 650 ±50 °C at 4.5 - 5 kbar in northern Namaqualand and 650 - 750 °C at Oranjefontein in central Namaqualand. Conditions of the prevailing metamorphic $f(O)_2$ were calculated in the metapelitic assemblages at Aggeneys (-16.0 ±0.7), Achab (-15.8 ±0.7) and Oranjefontein (-16.5 ±0.7). It is possible that there is some re-equilibration of gahnite composition and new gahnite formation during subsequent low grade metamorphism. In the quartzites at Aggeneys and Achab textural evidence supports the continued formation of gahnite along fractures

by infiltration of oxidising metamorphic fluids. Under these circumstances gahnite forms by reactions such as;
$2H_3AlO_3$ (in H_2O) + (Zn,Fe)S -> $(Zn,Fe)Al_2O_4$ + H_2O + H_2S (Moore and Reid, 1988 in press). At Oranjefontein the formation of almost endmember blue gahnite is attributed to alteration of the high grade assemblage by oxidising metamorphic fluids during retrograde, low temperature metamorphism, i.e. $(Zn,Mg)Al_2O_4$ (green gahnite) + Mg-biotite + garnet + quartz + H_2O -> $ZnAl_2O_4$ (green gahnite) + chlorite + rutile + hematite + sericite

Minor zoning in gahnite in a massive gahnite rock at Swartkoppies is attributed to gahnite growth during decreasing metamorphic temperatures and in a sphalerite-quartz-gahnite assemblage at Aggeneys, to Fe/Zn exchange between gahnite and sphalerite.

It was found that gahnite occurs in a wide variety of assemblages and exhibits a range in composition. This is attributed to the ability of Zn-spinel to incorporate increasing quantities of zinc under decreasing metamorphic temperatures and increasing $f(O)_2$ conditions and the complete solid solution between the endmember components of spinel. Gahnite, associated with sulphide mineralization at Aggeneys has the compositional range $Ghn_{70-82}Hc_{18-30}Sp_{3-6}$. At Achab gahnite occurs in quartzites and metapelitic schists and has the compositional range $Ghn_{54-78}Hc_{7-37}Sp_{3-8}$. In the sillimanite-corundum rocks at Swartkoppies, a wide range of compositions are exhibited by zincian hercynite and gahnite i.e. $Ghn_{18-58}Hc_{35-58}Sp_{8-18}$. Green gahnite associated with the high grade metamorphic facies at Oranjefontein has the compositional range $Ghn_{55-65}Hc_{10-17}Sp_{20-34}$. Retrograde blue gahnite has in excess of 90 mol% gahnite component, less than 10 mol% hercynite and less than 3 mol% spinel.

It is concluded that gahnite compositon is affected by various parameters including bulk chemistry, the composition of co-existing minerals, metamorphic $f(O)_2$ and temperature. It will be important to determine the host rock lithology if gahnite composition is to be used to imply the presence of zinc sulphides.

TABLE OF CONTENTS

ABBREVIATIONS USED IN THE TEXT

Alm	almandine
Amphi	amphibole
BIF	banded iron formation
Biot	biotite
Cp	chalcopyrite
Crd	cordierite
Gal	galaxite
Ghn	gahnite
Gn	galena
Fsp	feldspar
Epi	epidote
Gar	garnet
Hc	hercynite
Hem	hematite
Mt	magnetite
Musc	muscovite
Py	pyrope
Pyr	pyrite
Pyrr	pyrrhotite
Pyxm	pyroxmangite
Qtz	quartz
Sill	sillimanite
Sp	spinel
Spess	spessartine
Sph	sphalerite
ss	solid solution
Tourm	tourmaline
LLD	lower detection limit

Chapter 1. INTRODUCTION

1.1 Geological Setting

Gahnite, a zinc aluminium spinel is commonly found in association with zinc mineralization or is related to the breakdown of zincian staurolite in aluminous metasedimentary environments, eg. Broken Hill, New South Wales and the Appalachian Caledonides. In South Africa gahnite occurs in the ore-bearing Bushmanland Group of the Namaqualand Metamorphic Complex.

Recently gahnite has received much attention, because with ever increasing need to find new ore bodies, gahnite has been used as an indicator mineral for exploration purposes, due to its association with massive sulphide deposits and its resistance to weathering.

Although spinel and quartz are incompatible and hercynite-quartz associations are only compatible at granulite grade metamorphism, several studies indicate that the substitution of zinc into spinel or hercynite stabilises the mineral with quartz to amphibolite or lower grades. Spry (1984) and Wall and England (1979) suggest that gahnite composition may be sensitive to changes in temperature and metamorphic $f(O)_2$ and $f(S)_2$. The presence of gahnite in highly metamorphosed rocks, and commonly in association with quartz in Namaqualand provides an opportunity to confirm these theories.

1.2 Present Investigation

Gahnite occurs in rocks in the ore-bearing horizons of the Gamsberg zinc deposit (Rozendaal, 1978) and Aggeneys massive sulphide deposit (Ryan et al. (1982) in northern Namaqualand. Figure 1 is a locality map of northern and central Namaqualand. Gahnite also occurs associated with schists and quartzites on the farm Achab which borders the Gamsberg zinc deposit. Furthermore, very local massive gahnite and gahnite-sillimanite rocks occur on the Swartkoppies sillimanite deposit on the farm Pella Mission, north of Aggeneys and Gamsberg (Fig.1). Near Springbok, gahnite occurs at Vioolskraalberg on the farm Oranjefontein. At this locality, blue and green varieties of gahnite were found to co-exist in quartzites

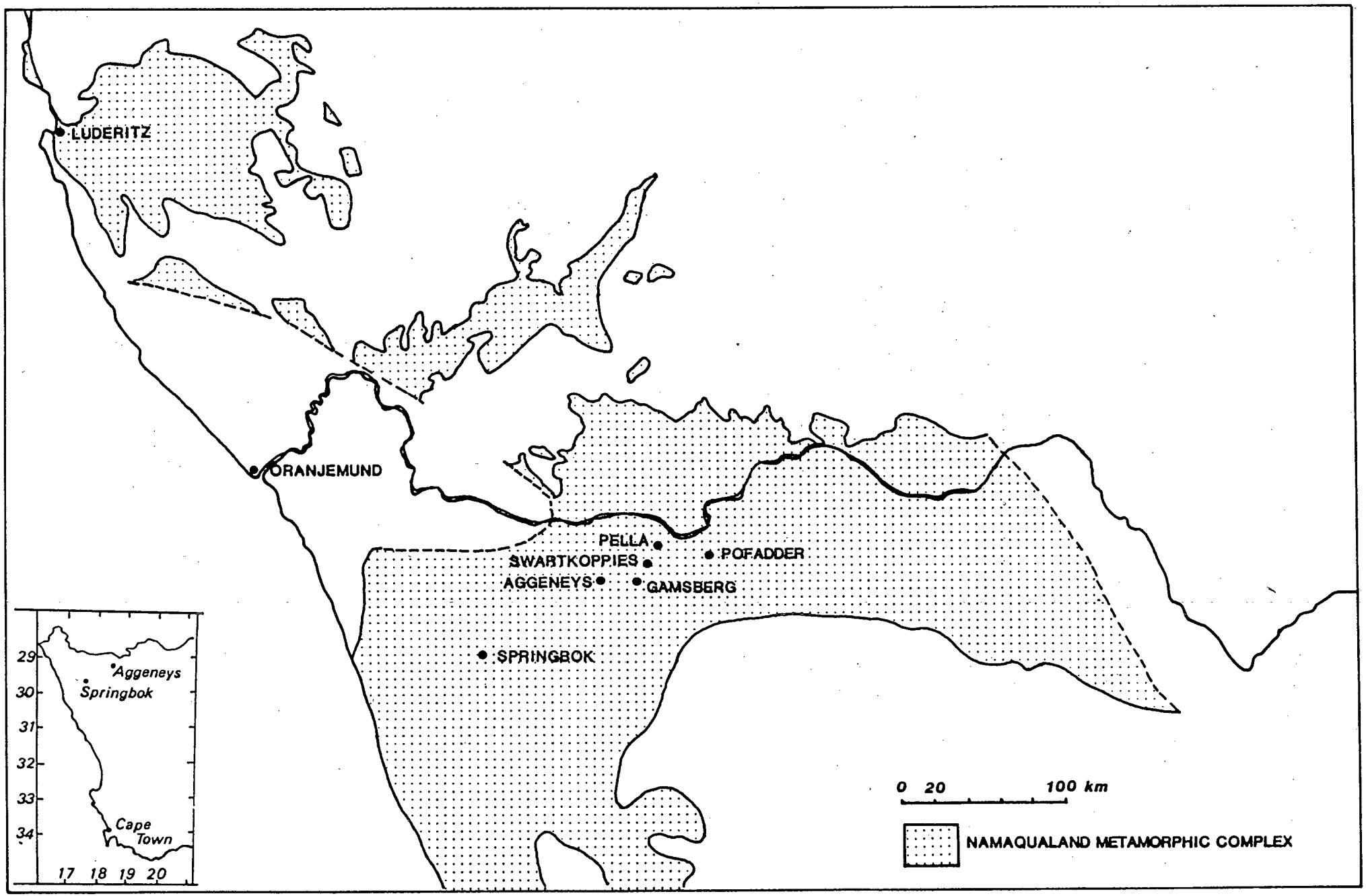

Figure 1: Locality map of northern and central Namaqualand.

and schists in rocks which are believed to be correlatives of the Bushmanland Sequence (Hicks et al., 1985, Strydom 1982).

The work reported on here includes the study of gahnite-bearing lithologies found at Swartkoppies, Achab farm, Broken Hill and Black Mountain at Aggeneys and Oranjefontein farm in Namaqualand (Fig.1). Detailed mapping and sample collection was done at the localities of Achab and Oranjefontein. Samples from Swartkoppies, Broken Hill and Black Mountain were made available to the author by J.Moore. The study includes a mineralogic and petrographic appraisal of gahnite and associated assemblages in order to establish the stability relations of the mineral in the context of regional metamorphism. Microprobe studies of gahnite and associated minerals were done to determine the extent of zinc substitution into mineral phases coexisting with gahnite. Other important aspects of this study include the formation of gahnite in the rocks and a comparison of gahnite composition with those reported in available literature.

According to Spry (1982a, 1984), gahnite associated with massive sulphide mineralization has high zinc and iron contents and low magnesium content. Bernier et al. (1984) found that the ratio of ZnO/ZnO+FeO+MgO in gahnite and staurolite is related to its position relative to mineralized zones and thus an increase in the ratio could indicate the presence of underlying sulphide ores. Ririe and Foster (1984) found gahnite-bearing sillimanite gneiss a potential directional indicator for mineralization. It is one of the aims of this study to elucidate any lithological or compositional characteristic of gahnite which may be associated with its proximity to mineralization.

1.3 Previous Work in Namaqualand

Exsolved zincian spinels from magnetite with up to 14 wt% ZnO are reported from hypersthene-,plagioclase-,phlogopite-,magnetite-,sulphide-bearing noritoids at the O'Okiep mine in Nababeep by Stumpfl et al.(1976). Zincian spinels with 15 wt% ZnO are reported from quartz-,feldspar-,sillimanite-gneiss associated with cupriferous- and magnetite-rich zones from the Kouberg Synform south east of Nababeep (Rozendaal, 1982). Zincian hercynites of similar composition are reported in association with mineralisation in the Kielder District by Gorton (1981).

Lipson (1978) records the presence of trace quantities of gahnite in the aluminous schist and calc silicate rocks from the Big Syncline ore body at Aggeneys . De Waal (1981), Ryan (1982) and Ryan et al. (1982) observed gahnite in association with the ore horizons at Broken Hill. Spry (1986, 1987a) and Spry and Scott (1986a) studied zincian spinel and gahnite in sulphide-rich rocks, garnet quartzites and quartz-magnetite rocks from Black Mountain and Broken Hill ore bodies at Aggeneys. It was found that gahnite associated with massive sulphides is zinc-rich, (65-85 mol% gahnite component), in comparison to gahnite in the garnet quartzites (18-75 mol%) and magnetite quartzite (20-76 mol%).

At Gamsberg Rozendaal (1982) found that gahnite occurs mostly in the C member above the ore horizon where it has a compositional range of $Ghn_{77-78}Hc_{16-18}Sp_{3-6}$. In the B member (ore horizon) gahnite is less common and has the composition $Ghn_{38}Hc_{59}Sp_{3}$.

ACKNOWLEDGEMENT

I am very grateful to Professor A.M. Reid for his encouragement and assistance during this project and to Dr. J.M. Moore who was instrumental in initiating it and who willingly took over supervision when Professor Reid left U.C.T. The C.S.I.R. provided all important funding for a substantial portion of the analytical work and SOEKOR allowed me the use of essential typing, copying and photographic facilities in its compilation. Furthermore I would like to thank the following people whose assistance and expertise in their various fields has been of invaluable help to me ; Dr. D.W. Waters, Dr. P.G. Spry, J.H. Mc Stay, D.S. Rickard. I would also like to acknowledge the support given by the Precambrian Research Unit at U.C.T. in allowing me to make use of their drafting facilities as well as time generously given by Ms R.M. Kovats.
Finally I would like to acknowledge the patience and kindness of the many friends and family both inside U.C.T. and out, whose support was always there when needed.

Chapter 2. GAHNITE MINERAL CHEMISTRY

2.1 Chemistry of gahnite

Gahnite, $ZnAl_2O_4$, is a member of the aluminium Spinel Series of the Spinel Group which also includes a Magnetite Series (Fe^{3+}) and Chromite Series (Cr). The structure of the spinel group has 32 oxygens and 24 cations, of which 8 are in 4-fold coordination (A position) and 16 in 6-fold coordination (B position). Gahnite ($ZnAl_2O_4$) along with spinel ($MgAl_2O_4$), hercynite ($FeAl_2O_4$) and galaxite ($MnAl_2O_4$) are normal spinels with 8 R^{+2} cations in A and 16 R^{+3} in B, as opposed to inverse spinels like magnetite $Fe^{3+}(Fe^{2+}, Fe^{3+})O_4$ or franklinite $Fe^{3+}(Zn^{2+}, Fe^{3+})O_4$ with 8 R^{+2} in A and 8 R^{+2} + 8 R^{+3} cations in B (Deer et al. 1969). $ZnAl_2O_4$, $MgAl_2O_4$ and $FeAl_2O_4$ appear to be miscible in all proportions (Deer et al. 1980, Rumble 1976). The wide variety of compositions exhibited by the Spinel Group minerals enable them to accurately reflect the bulk rock composition of the rocks in which they occur (Rumble, 1976).

2.3 Occurrence of gahnite

Gahnite is named after the Swedish chemist J.G. Gahn and was apparently recorded as early as 1907 (Simpson, 1931). Early references to gahnite include documentation of its occurrence associated with ore-bearing pegmatites (Eskola 1914, Simpson 1930, 1937). Andersen et al. (1937) analysed blue gahnite from the gem gravels of Ceylon and attributed the unusual blue colour to Fe^{2+} in the mineral structure. Generally gahnite is reported as having a blue-green colour (Deer et al., 1980). Pehrman (1948), discussed Zn-Fe exchange in spinel and proposed a hydrothermal origin for spinel in pegmetites. An early reference by Rankin and Merwin (1918), makes note of the incompatibility of spinel ($MgAl_2O_4$) and quartz which react to form sapphirine, garnet and sillimanite, and cordierite with increasing quantities of quartz (Friedman, 1954). Von Knorring and Dearnley (1960), documented the structural characteristics of gahnite. Several early authors record gahnite as a mineral associated with zinc mineralization (Haranczyk and Skiba 1961, Segnit 1961, Vokes 1962, Salotti 1965, Frondel and Klein 1965, Nemec 1972).

Gahnite occurs in a variety of sedimentary, metamorphic and pegmatitic environments. The occurrence of gahnite in sedimentary environments is attributed to its resistance to weathering. Gahnite occurs as an accessory phase in quartz-feldspar pegmatites (Eskola 1914, Simpson 1930, Pehrman 1948, von Knorring and Dearnley 1959, Batchelor and Kinnaird 1984). Weathering of such pegmatites probably produces the detrital gahnite found in sedimentary rocks (Hutton, 1957). Gahnite is infrequently reported from granitic environments (Tulloch, 1981 and Stevenson, 1985). In pegmatites and granites the origin of zinc in gahnite is attributed to closely associated ore lodes. However, Tulloch (1981) proposed that gahnite formed in a highly evolved, garnetiferous-, muscovite-, alkali-feldspar granite by late-stage breakdown of muscovite and concentration of zinc into late-stage aqueous solutions.

In metamorphic rocks gahnite occurs in metapelitic and cordierite-orthoamphibole schists and gneisses. Common assemblages observed are: staurolite + muscovite/biotite + quartz + sillimanite/andalusite + magnetite + gahnite (± K feldspar, plagioclase, garnet, cordierite) and cordierite + orthoamphibole + quartz + gahnite (± staurolite, cummingtonite).
Its presence is most commonly attributed to retrograde breakdown of zinc-rich staurolite, desulphidation of sphalerite under oxidising metamorphic conditions or prograde metamorphism of zinc-bearing sediments. Although staurolite, biotite, muscovite and chlorite may contain significant quantities of zinc in their structures, in aluminous, zinc-rich terranes, gahnite is a common phase.

Gahnite appears to be stable over a range of metamorphic temperatures and is reported from quartz veins, (Gandhi, 1971), low temperature chlorite-sericite schists (Haranczyk and Skiba, 1961), slates (Kramm, 1977) and in a contact metamorphic aureole (Schumacher, 1985). It is stable in the presence of quartz (Kramm 1978, Dietvorst 1980, Schumacher 1985) and also in highly aluminous rocks (Atkin 1978, Spry 1982b, Feenstra 1985). More specifically it is found in cordierite-anthophyllite rocks associated with mineralization (Essene et al. 1982, Wolter and Siefert 1984, Schreurs and Westra 1985, Treloar et al. 1981).

Gahnite is a common accessory phase and may even constitute a major mineral in metamorphosed massive sulphide deposits e.g. the stratiform massive sulphide deposits of Broken Hill, Australia (Segnit 1961, Hobbs 1975, Plimer 1977), the massive sulphide deposits of the Appalachians (Sandhaus 1981, Craig 1983, Field and Haggerty 1984) and Scandinavian Caledonides (Vokes 1962, Sundblad 1982, Spry 1983, Spry and Scott 1986b) and the Colorado Precambrian massive sulphide deposits (Sheridan and Raymond 1977, 1984, Karlsson et al. 1980). Gahnite is reported as an exsolution product of franklinite at the Franklin and Sterling Hill Zn-Fe-Mn deposits, New Jersey (Frondel and Klein 1965, Frondel and Baum 1974). Gahnite is also reported from Cu-Zn Skarns (Salotti, 1965) and an Archean iron formation in association with zinc mineralization (Appel, 1986).

2.4 Gahnite-forming reactions

Various reactions have been put forward to explain the formation of gahnite in metamorphic rocks. These include reactions which occur during prograde metamorphism of zinc-bearing sediments and prograde and retrograde metamorphism of precursor zinc-bearing minerals. Some of the proposed reactions are listed below.

1. from zinc adsorbed onto sediments which are subsequently metamorphosed e.g. Zn (oxide/sulphide/carbonate) + kaolinite = gahnite + quartz + water (Kramm 1978, Karlsson et al. 1980, Appel 1986, Segnit 1981, Field and Haggerty 1984).

2. from breakdown of a zinc-bearing aluminosilicate phase e.g.
   (i) Zn biotite + sillimanite + quartz = cordierite + gahnite + fluid (Dietvorst, 1980) or
   (ii) Zn staurolite + biotite + quartz = sillimanite + K-feldspar + rutile + Zn hercynite + garnet + fluid (Stoddard 1976, 1979).
   Zn staurolite = Zn hercynite + cordierite + sillimanite (Atkin, 1978).
   Zn staurolite + Sn phlogopite = cordierite + corundum + gahnite + nigerite + hogbomite + Sn-poor phlogopite (Spry, 1982b).
   Zn staurolite + muscovite + quartz + O_2 = andalusite + Zn hercynite + magnetite + biotite + H_2O (Schumacher, 1985).

3. by desulphidation of sphalerite during metamorphism e.g.
   Gedrite + sphalerite (+staurolite) + O_2 = gahnite + quartz + S_2 + H_2O (Plimer 1977, Sundblad 1982, Williams 1983, Bernier et al. 1984).
   Sphalerite + pyrite/pyrrhotite + aluminosilicate + O_2 = gahnite + quartz + S_2 or
   Almandine + sphalerite + S_2 = gahnite + pyrite + quartz (Spry and Scott 1986 a,b, Spry 1984).

4. in pegmatites and quartz veins from hydrothermal solutions permeating through sulphide-bearing rocks e.g.
   Zn^{2+} + Al^{3+} + $4H_2O$ = gahnite + $8H^+$ (Hobbs, 1975).
   $2KH_2AlO_3$ (in fluid) + sphalerite = gahnite (+ H_2S + 2KOH in fluid) (Moore and Reid, 1988 in press).

Chapter 3. GEOLOGICAL SETTING OF THE STUDY LOCALITIES

3.1 Regional geology of the Namaqualand Metamorphic Complex

The Namaqualand Metamorphic Complex (NMC) covers a large section of northern and central Namaqualand (Fig.1). It consists of a variety of intrusive, metasedimentary and metavolcanic rock units which have undergone extensive deformation accompanied by regional metamorphism (Table 1). The lithologies encountered at the study localities are correlated with the Bushmanland Sequence which comprises a pretectonic metasedimentary sequence within the NMC (Table 1).

The NMC supracrustal rocks represent a major, east west striking, mobile belt. Deformation varies extensively across the Namaqua province and various interpretations have been applied to the tectonic and stratigraphic units encountered e.g. Joubert (1971) and Blignault et al. (1983). The latter define two main episodes of deformation related to the Namaqua Orogeny. A regional early planar fabric defines the first event. The large-scale intrusion of syntectonic augen gneisses of the Little Namaqua Suite are closely related to an episode of major thrusts and isoclinal folding. To the north of the Aggeneys area, the Groothoek thrust (1000 - 1200 Ma) resulted in the superposition of the calc-alkaline, metavolcanic Orange River Group over the metaquartzite/schist, Aggeneys metasediments. Joubert's (1971) F1 and F2 deformational events are included in this deformational episode.

The second deformational event occurred in the period 1000 to 1100 Ma and is seen as late, macroscopic upright and open to gentle folds on a regional scale (Joubert 1971, Blignault et al. 1983). Late shears impart the last regionally important structural imprint (Joubert 1971, Moore 1977, Blignault et al. 1983) and caused the major deflections in the regional lineation pattern.

In western Namaqualand metamorphic events relate to the two structural episodes described above. Early planar structures and large-scale intrusive augen gneisses are associated with a high temperature, low pressure, prograde event (Moore's, 1977 M1 event in the Namiesberg). Waters (1986) describes the metamorphic regime as largely isobaric and suggests that the high temperatures attained are not related to isostatic uplift in the NMC. Upper amphibolite grades metamorphism are recognised in the north (Ryan et al., 1982) and to the south and in the central area a granulite facies zone is recognised (Albat, 1984). In metapelitic schists the transition is; quartz + K-feldspar + plagioclase + biotite +

Table 1: Lithostratigraphic division of the Namaqualand Metamorphic Complex (after SACS, 1980).

Koperberg Suite	
Spektakel Suite	
Keimoes Suite	Syntectonic intrusive
Hoogoor Suite	rock units
Little Namaqualand Suite	
Gladkop Suite	
Vioolsdrif Suite	
Orange River Group	
Okiep Group	Pretectonic metasedimentary
Bushmanland Group	and metavolcanic rock units
Korannaland Group	
Marydale and Kaaien Groups	

sillimanite ± garnet -> quartz + K-feldspar + plagioclase + cordierite + garnet ± biotite ± sillimanite (Moore 1983, Waters and Whales 1984). Several workers (Clifford et al. 1975 a,b, Zelt 1980, Albat 1984, Waters and Whales 1984, Waters and Moore 1985) describe various aspects of the granulite terrain in Namaqualand.

Various retrograde metamorphic signatures relate to the second deformational event of open folding and shearing. The early folds are associated with a lower amphibolite to amphibolite facies metamorphic event (Moore's, 1977 M2 event). Later structures are associated with lower grade, greenschist facies metamorphism (Moore's, 1977 M3 event).

3.2 General geology of the Bushmanland Sequence

The Bushmanland Group comprises a metasedimentary sequence and overlies a basement gneiss complex. SACS (1980) recognises several lithostratigraphic units within the Bushmanland Group including the Pella and Aggeneys Subgroups which were originally described by Joubert (1974) and later in the Namiesberg area by Moore (1977) (Table 2). A more complex stratigraphic succession is recognised by Praekeldt et al. (1983), however their stratigraphic terminology remains informal and is therefore not being used in this thesis.

A generalised succession of the Bushmanland Group in the Pofadder - Aggeneys area is given by SACS (1980). This consists of a basement porphyroblastic- and pink gneiss and an overlying metasedimentary sequence which comprises metapelitic schists, metaquartzites, iron formation and an overlying quartz - muscovite schist and conglomerate unit. At Aggeneys and Gamsberg, economic barite and massive sulphide mineralization occur within the iron formation. The iron, manganese and barite mineralization is described by Mathias (1941) and Coetzee (1958). Sulphide mineralization at Aggeneys is described by Moore (1974, 1983), Ryan (1982) and Ryan et al. (1982) and at Gamsberg by Rozendaal (1978, 1980, 1982).

At Swartkoppies, on the farm Pella Mission, sillimanite-corundum rocks constituting an aluminium ore deposit, occur within the metapelitic schist unit. Several workers have described various aspects of the aluminous rocks (Coetzee 1941, De Jager and von Backstrom 1961, De Jager 1963, Frick and Coetzee 1974, Joubert 1974 and Moore 1980).

According to Tankard et al. (1982) the Bushmanland Sequence above the pink gneiss represents an accumulation of sediments in a shallow basin or

Table 2: Lithostratigraphy of the Bushmanland Group (after SACS, 1980).

Quartz - muscovite schist and conglomerate unit	Pella
Iron Formation Unit	
Metaquartzite Unit	
Schist Unit	
Mafic gneisses with intercalated metasediments	Guadom
Leucocratic gneisses with intercalated metasediments	Hom
Quartz - muscovite schist and conglomerate unit	Aggeneys
Gams Formation (iron formation)	
Metaquartzite	
Namies Schist Formation	

basins. The association of concentrations of Al, Ca, Na and B suggest that the parent rocks consisted of clays and evaporites formed in a sabkha or playa-like environment (Moore, 1977). Although there is some dispute as to the origin of the sediments evidence indicates a sedimentary basin (basins) initially filled under terrestrial or marginal marine conditions (Tankard et al., 1982).

3.3 General geology of the study areas

Four gahnite-bearing localities hosted in the Bushmanland Sequence were chosen for the basis of this study. The lithostratigraphy of the Bushmanland Sequence is described by SACS (1980). Table 2 shows the subgroup breakdown. Swartkoppies occurs in Bushmanland rocks which are correlated with the Pella Subgroup. Achab locality is part of the Namiesberg area which is correlated with the Aggeneys Subgroup (Moore, 1977). The fourth study locality, Oranjefontein, occurs in central Namaqualand, somewhat distant from the three geographically close areas in northern Namaqualand (Fig.1). Lithological and stratigraphic similarities with the Bushmanland Sequence at Aggeneys have resulted in this locality being correlated with the Bushmanland Sequence (Hicks et al., 1985). Table 3 compares the generalised stratigraphic succession at the 4 localities. Figure 2 is a comparison of the supracrustal rocks at the study localities and shows the similarities in lithology and to correlate the gahnite-bearing horizons in the context of the generalised succession. There is some controversy concerning the stratigraphic succession of the iron formation in the Broken Hill ore body compared to that at the Aggeneysberge and Gamsberg. At the Aggeneysberge and Gamsberg the sulphide-bearing iron formation rocks overly the metaquartzite unit whereas at Broken Hill the iron formation occurs below this unit (Ryan et al. 1982, Rozendaal 1982, Moore 1986).

The Aggeneys ore bodies, Swartkoppies and Achab are believed to be part of the amphibolite facies zone of the NMC. At Oranjefontein, the presence of biotite-cordierite-garnet rocks associated with quartz-feldspar-cordierite-biotite schist indicates a transitional facies which achieved close to granulite grade metamorphism (Hicks 1983, Hicks et al. 1985). Ryan et al. (1982), Moore (1977) and Rozendaal (1978) recognise three metamorphic events in the Aggeneys area for which Tankard et al. (1982) quotes maximum estimated metamorphic conditions of 690 °C at 3 - 5 kbar.

basins. The association of concentrations of Al, Ca, Na and B suggest that the parent rocks consisted of clays and evaporites formed in a sabkha or playa-like environment (Moore, 1977). Although there is some dispute as to the origin of the sediments evidence indicates a sedimentary basin (basins) initially filled under terrestrial or marginal marine conditions (Tankard et al., 1982).

3.3 General geology of the study areas

Four gahnite-bearing localities hosted in the Bushmanland Sequence were chosen for the basis of this study. The lithostratigraphy of the Bushmanland Sequence is described by SACS (1980). Table 2 shows the subgroup breakdown. Swartkoppies occurs in Bushmanland rocks which are correlated with the Pella Subgroup. Achab locality is part of the Namiesberg area which is correlated with the Aggeneys Subgroup (Moore, 1977). The fourth study locality, Oranjefontein, occurs in central Namaqualand, somewhat distant from the three geographically close areas in northern Namaqualand (Fig.1). Lithological and stratigraphic similarities with the Bushmanland Sequence at Aggeneys have resulted in this locality being correlated with the Bushmanland Sequence (Hicks et al., 1985). Table 3 compares the generalised stratigraphic succession at the 4 localities. Figure 2 is a comparison of the supracrustal rocks at the study localities and shows the similarities in lithology and to correlate the gahnite-bearing horizons in the context of the generalised succession. There is some controversy concerning the stratigraphic succession of the iron formation in the Broken Hill ore body compared to that at the Aggeneysberge and Gamsberg. At the Aggeneysberge and Gamsberg the sulphide-bearing iron formation rocks overly the metaquartzite unit whereas at Broken Hill the iron formation occurs below this unit (Ryan et al. 1982, Rozendaal 1982, Moore 1986).

The Aggeneys ore bodies, Swartkoppies and Achab are believed to be part of the amphibolite facies zone of the NMC. At Oranjefontein, the presence of biotite-cordierite-garnet rocks associated with quartz-feldspar-cordierite-biotite schist indicates a transitional facies which achieved close to granulite grade metamorphism (Hicks 1983, Hicks et al. 1985). Ryan et al. (1982), Moore (1977) and Rozendaal (1978) recognise three metamorphic events in the Aggeneys area for which Tankard et al. (1982) quotes maximum estimated metamorphic conditions of 690 °C at 3 - 5 kbar.

Table 3: Comparison of the stratigraphy in the study areas.

PELLA (SACS 1980)	NAMIESBERG (Moore 1977)	AGGENEYS (Ryan et al.1982)	ORANJEFONTEIN (Hicks et al.1985)
		Grey Gneiss with schists and minor amphibolites	
		Quartz muscovite schist and nodular gneiss with amphibolite	
		Magnetite quartzite (Aggeneys Iron Formation)	
Metaquartzite	Metaquartzite	Metaquartzite	Metaquartzite
qtz-biot-sill-musc schist, sill-cor bodies	qtz-biot-sill-musc schist, sill-rich rocks, amphibolite, calc silicate	qtz-biot-sill-musc schist, dark quartzites, amphibolite, sill-rich rocks	qtz-K feld-cord-biot-sill-gar schist
Porphyroblastic gneiss	Quartzo-feldspathic gneiss	Quartzo-feldspathic gneiss	Quartzo-feldspathic gneiss
	Achab gneiss	Porphyroblastic granite gneiss	Biotite gneiss

Swartkoppies	Namiesberg (Achab)	Aggeneys	Oranjefontein
(SACS 1980; de Jager & von Backstrom 1961: Frick & Coetzee 1974)	(Moore, 1977)	(Moore 1983; Ryan et al., 1982)	(Hicks et al., 1985)

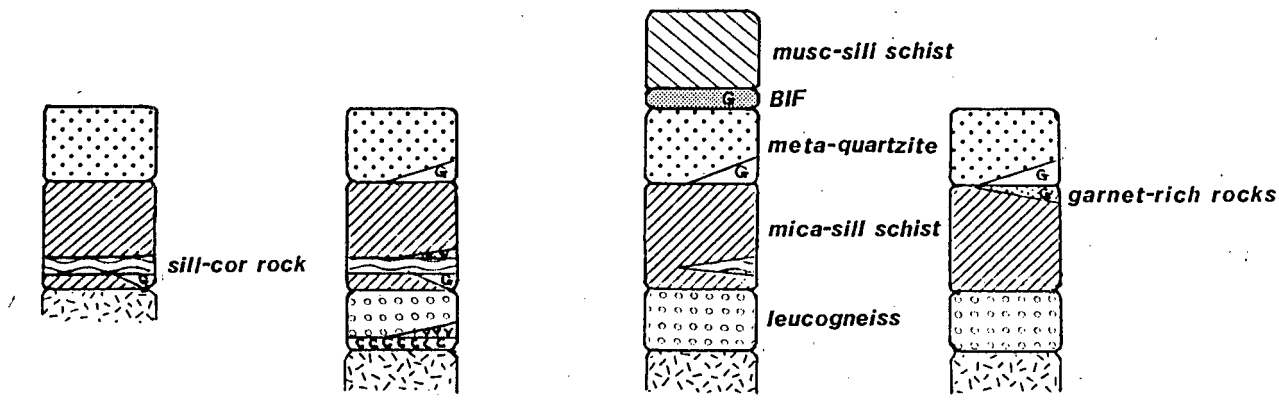

Figure 2: Comparison of the stratigraphic succession of the supracrustal rocks in the study areas.

3.3.1 Aggeneys - Broken Hill ore body

The Aggeneys base metal deposits are situated in northern Namaqualand approximately 80 km west of Pofadder and 110 km north east of Springbok (Fig.1). Three separate ore bodies; Black Mountain, Broken Hill and Big Syncline comprise the Aggeneys deposit (Fig.3). Gamsberg zinc deposit is situated approximately 12 km east of Aggeneys and is similar to Aggeneys deposit with respect to stratigraphic position and ore genesis (Rozendaal, 1982). Samples used in this study were obtained from Broken Hill (Fig.4) and Black Mountain.

Four phases of deformation are recognised in Bushmanland rocks at Aggeneys and Gamsberg. The rocks were subjected to metamorphism with an upper limit bordering on granulite grade, which is correlated with the F2 deformation (Joubert, 1971). Retrograde metamorphism followed and largely overprints evidence of the early metamorphic history. Rozendaal (1978) estimated temperatures of 630 - 670 °C and pressures of 2.8 - 4.5 kbar for the high grade event in the Gamsberg, whereas Ryan et al. (1982) obtained temperatures of 670 - 695 °C at 3.4 - 6 kbar at Aggeneys.

The stratigraphic succession of the Namaqualand Metamorphic Complex at Aggeneys consists of a basal augen gneiss and the overlying Bushmanland Sequence (SACS, 1980). At the Aggeneys deposits, the Bushmanland Sequence comprises a basal pink gneiss overlaid by quartz-biotite-muscovite-sillimanite schists, quartzite and then quartz-feldspar-muscovite-biotite-sillimanite schists. A generalised stratigraphic column according to Ryan et al. (1982) is given in Table 4. The ore bodies associated with banded iron formations (BIF) have a sulphide mineralogy consisting of pyrite, pyrrhotite, sphalerite, galena and chalcopyrite (Ryan et al., 1982).

Various metapelitic rocks and some gahnite-bearing quartzites were obtained from Black Mountain and Dabiepoort, but most of the gahnite-bearing rocks were obtained from Broken Hill (Fig.4).

The ore bodies at Broken Hill consist of a lower sulphide-bearing quartzite, followed by a succession of banded and massive sulphide and baritic rocks which grade into magnetite amphibolite, BIF and garnet quartzites.

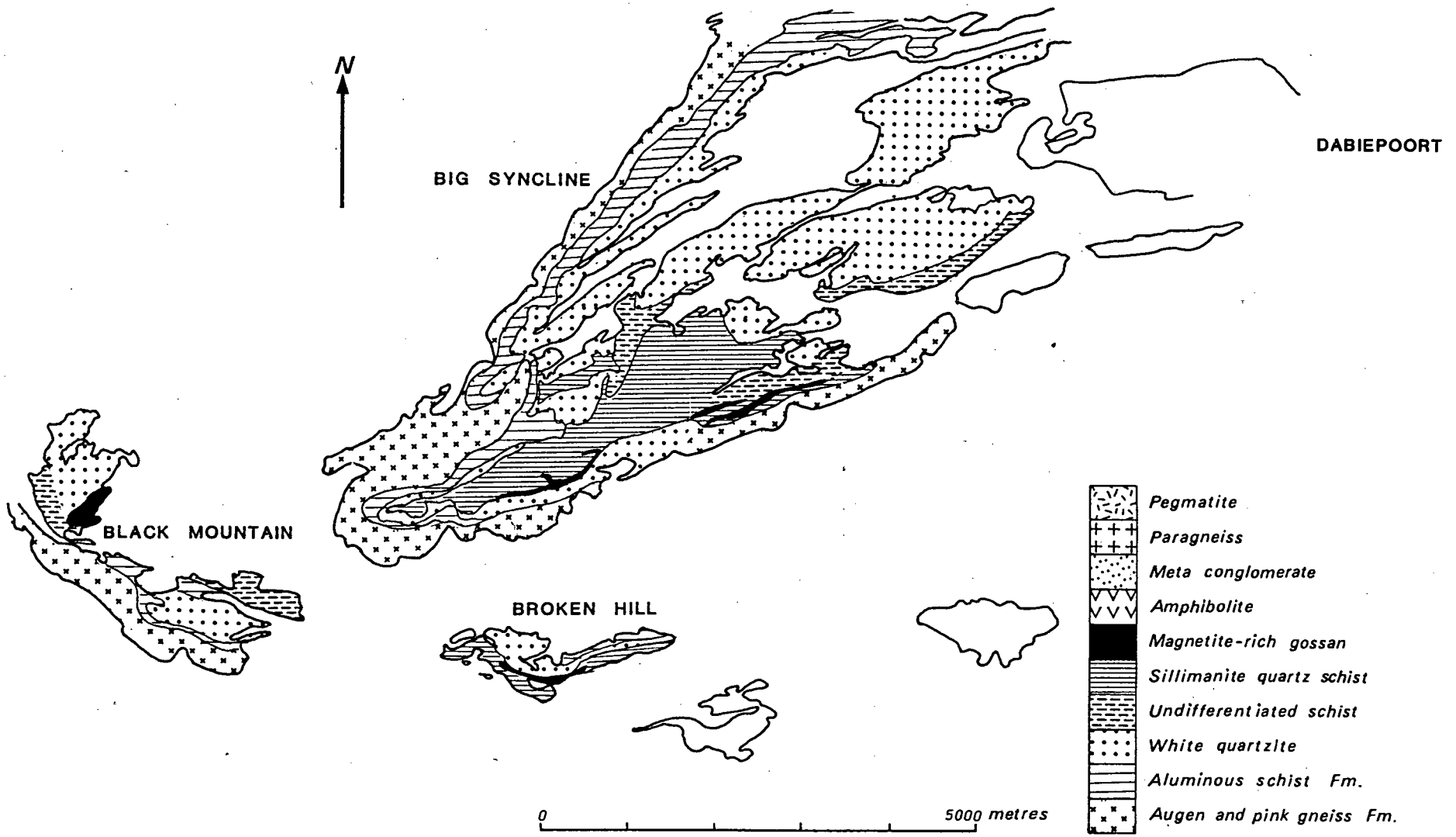

Figure 3: Geological map of Aggeneys massive sulphide deposit, (modified from Ryan et al., 1982).

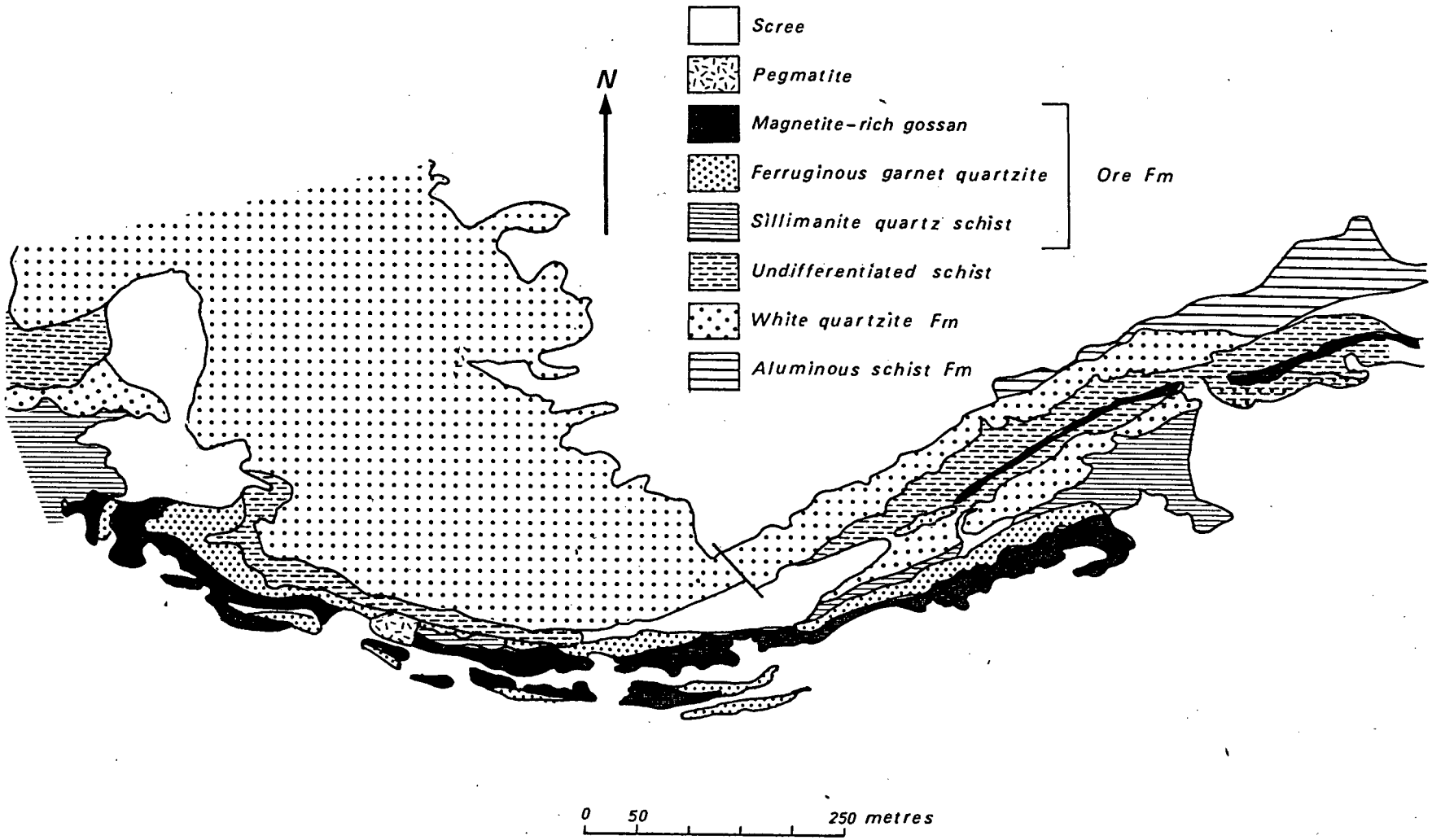

Figure 4: Geological map of Broken Hill ore deposit, Aggeneys, (modified from Ryan et al., 1982).

Table 4: Stratigraphy of the NMC in western Namaqualand (after Ryan et al., 1980).

Amphibolite / Leucocratic Grey Gneiss Formation		
Aggeneys Iron Formation	Bushmanland	
White Quartzite Formation	Sequence	NMC
Aluminous Schist Formation		
Pink Gneiss Formation		
Augen Gneiss Formation		

Ryan et al. (1982) have divided the rock types into sulphide, oxide and silicate facies (Table 5). From Black Mountain in the west to Gamsberg in the east, the mineralization shows a progressive decrease in Cu and Pb and increase in Zn (Ryan et al. 1982, Rozendaal 1982)(Table 6). Metal concentrations in the ores are further divided into a Fe-Pb-Cu dominated succession at Black Mountain and Broken Hill in the south-west and a Mn-Zn dominated succession in the Aggeneysberge and at Gamsberg in the north-east (Moore, 1983). Genetic model interpretation, based on these and other characteristics of the deposits, emphasise a sedimentary basin environment of deposition with an exhalative source, with Gamsberg representing a deeper, more distal environment (Ryan et al. 1982, Moore 1977).

Gahnite has been observed throughout the mineralized zones (Joubert 1971, Moore 1974, 1980, 1986) and also occurs at the contact of crosscutting pegmatites (Ryan et al., 1982). The formation of gahnite has been attributed to desulphidation of sphalerite (Ryan et al. 1982, Spry 1987a).

3.3.2 Achab

Achab farm is situated approximtely 8 km east of Gamsberg. The areas studied occur along the northern flank bordering Gams Noord farm. The position of the gahnite-rich rocks in relation to the surrounding lithologies is shown in Figure 5.

The lithologies which crop out at this locality comprise a basal leucogneiss (correlated with the pink gneiss at Broken Hill), with local bands of calc-silicate rocks and amphibolites towards the base of the unit (Fig.5). This is succeeded by the Namies schist and metaquartzite (Moore, 1977). Impersistent bands of gahnite-quartz rock, cordierite-anthophyllite rock, sillimanite-rich rock, tourmalinite and amphibolite occur towards the base of the aluminous schist. The gahnite-quartzites and gahnite-bearing schists occur at the contact between the leucogneiss and the aluminous schist and locally in the upper horizons of the aluminous schist near the contact with the overlying metaquartzite unit.

Table 5: Distribution of mineralization with respect to rock type at Aggeneys massive sulphide deposit (after Ryan et al., 1982).

FACIES	ROCK TYPE	MINERALS	MINERALIZATION
Silicate	Magnetite Amphibolite	quartz, magnetite, grunerite, cummingtonite, spessartine fayalite	moderate galena (gn)> sphalerite (sp)> chalcopyrite (cp
Oxide	Magnetite quartzite	magnetite, quartz, garnet, biotite	moderate gn >sp >cp
	Ferruginous garnet quartzite	quartz, magnetite garnet, biotite	very weak sp >cp >gn
Sulphide	Massive sulphide	pyrrhotite, pyrite quartz	high gn > pyrite >cp
	Sulphide quartzite	quartz, pyrrhotite pyrite	moderate-high gn >sp >cp

Table 6: Zoning of mineralization between Aggeneys and Gamsberg ore deposits (Ryan et al., 1982).

	OREBODY	BASE METAL CONTENT		
WEST	Black Mountain	0.75 %Cu	2.67 %Pb	0.59 %Zn
	Broken Hill	0.34	3.57	1.77
	Big Syncline	0.04	1.01	2.45
EAST	Gamsberg	0.00	0.50	7.00

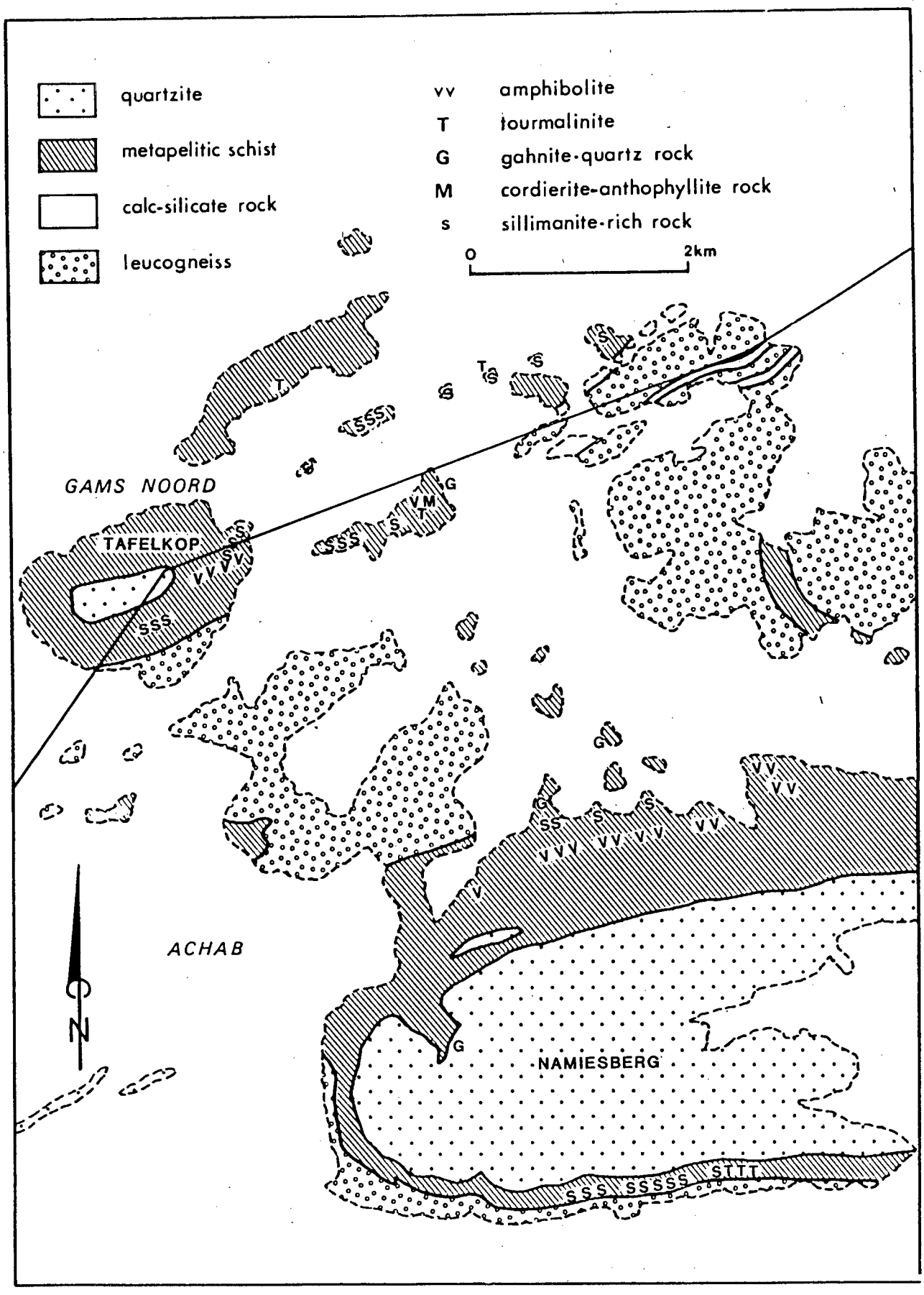

Figure 5: Geological map of Achab study locality, (adapted from Moore, 1977).

The Namiesberg at Achab (Fig.5) has undergone similar polyphase deformational events to the rocks at Aggeneys (Moore, 1977). Three metamorphic episodes were interpreted to have affected rocks in the Namiesberg (Moore, 1977). These are; M1, for which temperature estimates of 650 and 750 °C at
5 - 7 kbar are given, M2 at 600 - 500 °C and 3 - 5 kbar and M3 at less than 500 °C and below 3 kbar pressure (Moore, 1977).

3.3.3 Swartkoppies

Swartkoppies sillimanite-corundum deposit is situated on Pella Mission farm approximately 30 km north-west of Pofadder and 35 km north-east of Aggeneys in northern Namaqualand (Fig.1). It was first described by Coetzee (1941) and the discovery of further sillimanite deposits in northern Namaqualand led to follow up investigations by de Jager and von Backstrom (1961), Frick and Coetzee (1974) and Moore (1977). SACS (1980) correlates the rocks at this locality with the Pella Subgroup of the Bushmanland Sequence (Table 2). Table 3 lists the stratigraphic succession in the area.

The sillimanite-corundum rocks occur as massive bodies in a basal biotite-sillimanite schist. The schist has been correlated with the Aluminous Schist of the Bushmanland Sequence at Aggeneys (Praekelt et al., 1983). The sillimanite-corundum rock consists of radiating fibrolite masses which merge into colourless sillimanite prisms containing corundum cores and ilmenite inclusions (Coetzee, 1941). Biotite-sillimanite schist overlies the sillimanite-corundum rock. Massive quartzite forms the uppermost unit in the Pella area. Limonite specks in the basal schist horizon infer the former presence of sulphides (SACS, 1980). Massive gahnite and gahnite-fibrolite rocks crop out locally in the sillimanite-corundum rock. Secondary copper staining was observed at the sampling locality (Moore, pers. comm.). Similar sillimanite-corundum rocks occur in Achab Pan and are interpreted to result from progressive metamorphism of high aluminium clays (Moore, 1977,1980)

3.3.4 Oranjefontein

Oranjefontein farm is situated in western, central Namaqualand approximately 50 km east of Springbok and 70 km south-west of Aggeneys (Fig.1). Gahnite-bearing lithologies occur on a prominent hill, Vioolskraalberg, in the northwest section of Oranjefontein farm. A geological map of the area is shown in Figure 6.

Vioolskraalberg forms part of a narrow belt of paragneisses enclosed within pretectonic and syntectonic gneisses which form a basal intrusive suite of porphyroblastic grey gneisses in the Little Namaqualand Suite (SACS, 1980). Vioolskraalberg is a flat lying, synformal structure which is correlated with the F3 deformational episode of the Namaqualand Metamorphic Complex (Joubert, 1971). The stratigraphic succession at Vioolskraalberg bears strong resemblance to the lower portions of the Bushmanland Group, as described by SACS (1980), which host the base metal sulphide deposits of Aggeneys and Gamsberg (Table 3).

The basal unit in the vicinity of Vioolskraalberg is a coarse-grained, biotite gneiss, which is locally overlain by lenses of pink weathering, leucocratic, quartzo-feldspathic gneiss. This is succeeded by weathered, brown, aluminous schist. A thick succession of massive, coarsely crystalline, white quartzite forms the uppermost unit at this locality.

Dark green, crystalline spinel coexists with bright blue spinel in a variety of rock types at the interface between the aluminous schist and overlying quartzites (Fig.6). The gahnite-bearing rocks were first described by Joubert (1971) who linked the presence of blue spinel to late stage quartz pegmatites associated with retrograde shearing at the locality.

Within the aluminous schist are narrow, lense-shaped bodies, not longer than 5 m and approximately 0.5 m thick, consisting of garnet-bearing metapelitic rocks. In the uppermost portions of the aluminous schist, massive garnet and garnet-biotite schists locally contain gahnite. At the same stratigraphic level are gahnite-quartz rocks containing green and blue gahnite and locally, galena. The gahnite quartzites show greater

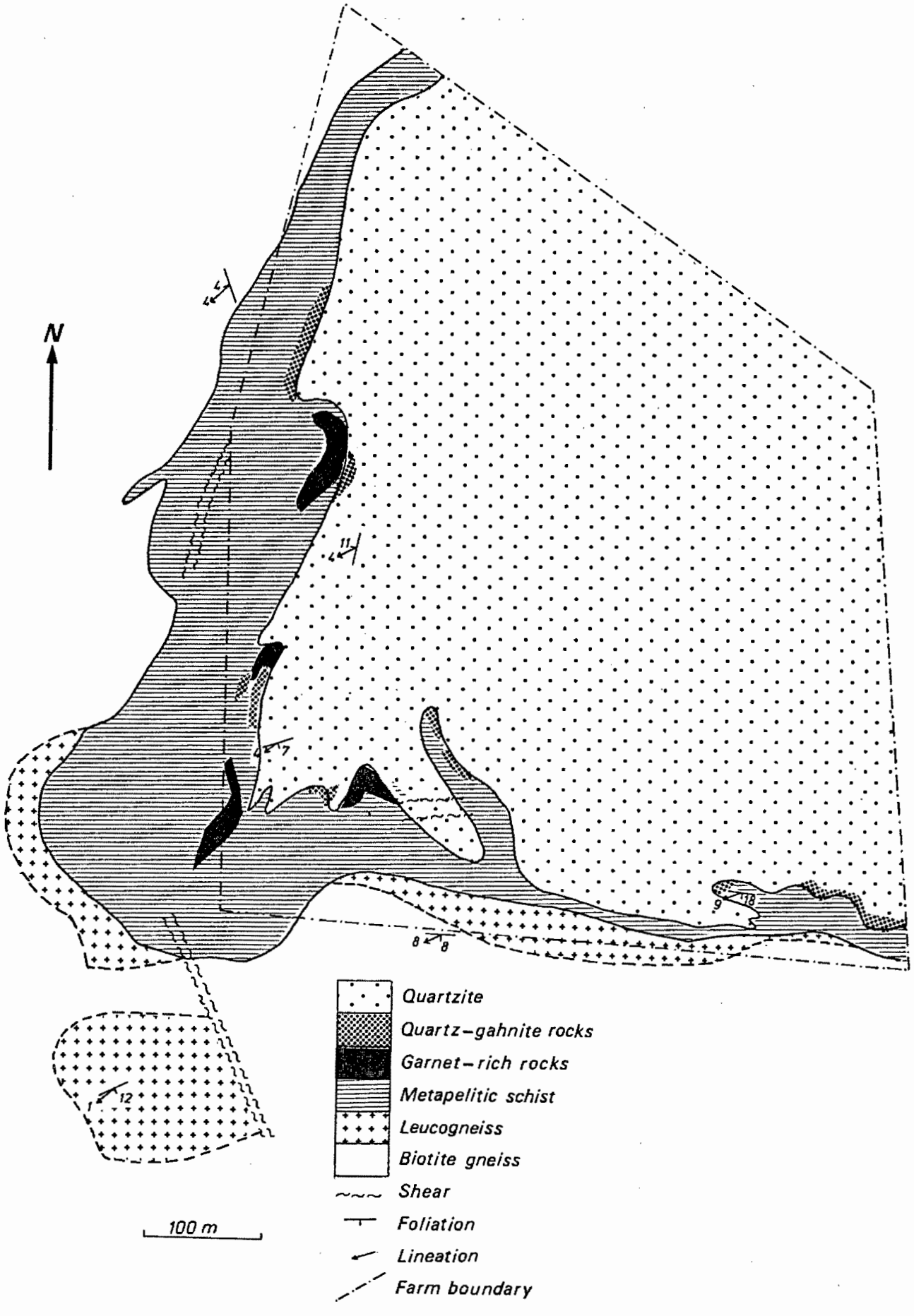

Figure 6: Geological map of Oranjefontein, (adapted from Hicks et al., 1985).

lateral persistence than the massive garnet and garnet-biotite rocks which are restricted to lenses preserved within a major synformal fold closure (Fig.5). In the lower horizons of the massive quartzite, fine-grained blue gahnite fills cracks and fissures and appears to radiate outward from green gahnite cores. Locally, galena and specks of chalcopyrite occur in the lower horizons of the massive quartzite unit. On the southern flanks of Vioolskraalberg at the contact between the schist and quartzite, a green epidote-chlorite contains up to five percent galena.

To the south of Oranjefontein, metapelitic rocks are dominated by granulite facies quartz-K feldspar-garnet-cordierite gneisses (Joubert 1971, Moore 1983,1986, Albat 1984, Waters and Whales 1984, Waters and Moore 1985) and to the north in the Aggeneys/Gamsberg area by quartz-biotite- muscovite-sillimanite schists of upper amphibolite grade (Moore 1977, Rozendaal 1978,1982). Pressure-temperature conditions of 700 - 900 °C and 5 - 6 kbar have been estimated for the granulite terrain (Albat 1984) and 650 - 700 °C and 4 - 5 kbar for the amphibolite grade rocks at Aggeneys/Gamsberg (Moore 1983). The garnet-bearing metapelitic rocks contain biotite, cordierite and rarely sillimanite and K feldspar at Oranjefontein, and appear to represent a transitional zone between the granulite and amphibolite facies. Temperatures of 600 - 750 °C at 4.5 - 5 kbar were calculated by Hicks et al. (1985).

Chapter 4. GAHNITE IN THE CONTEXT OF MINERALIZATION AND METAMORPHISM AT THE STUDY LOCALITIES

4.1 Introduction

The following sections describe gahnite-bearing lithologies at Aggeneys, Achab, Swartkoppies and Oranjefontein. Using petrographic data and mineral analyses an attempt is made to tie the formation of gahnite in to the regional metamorphic history of the Bushmanland rocks in Namaqualand. Geothermometric and oxygen fugacity calculations are applied to metapelitic assemblages. An explanation of the methods employed is given in Appendix 2. Gahnite compositions are compared to similar gahnite occurrences in the literature.

Mineral analyses were made on the Cameca microprobe in the Geochemistry Department at the University of Cape Town and are listed in Appendix 4. Tables of average analyses of minerals are given in the text. Stoichiometric recalculation of Fe^{3+} content of gahnite was necessary for the calculation of endmember compositions. The method used for recalculation is outlined in Appendix 1 and a list of endmember compositions of analysed spinel is given in Appendix 3.

4.2 Aggeneys

4.2.1 Petrography

Samples obtained from the Aggeneys locality include gahnite-bearing quartzite from the Black Mountain ore body and Dabiepoort (east of Aggeneys) and samples of the magnetite quartzite, magnetite amphibolite and massive sulphide horizons at Broken Hill. Estimated modal proportions of most of the samples studied are given in Table 7.

Gahnite-bearing quartzites

Amphibole-,garnet-bearing quartzite from Aggeneys contains pale, pleochroic blue-brown blade-like anthophyllite and gedrite, and small, euhedral garnet grains as major minerals other than quartz. Magnetite, chalcopyrite and green gahnite occur in minor to accessory amounts. The bright green spinel occurs as tiny, rounded grains in the matrix or in association with magnetite.

Quartzites obtained from Dabiepoort contain pale-brown biotite, pale green gahnite and accessory quantities of iron oxides, goethite, galena and pyrite.

Various gahnite-bearing samples associated with sulphide-bearing ores were obtained from the Broken Hill ore body. These are described below.

Magnetite quartzite

(1) Banded Magnetite Quartzite. (Figure 7a)
Compositionally this rock is almost bimineralic consisting of quartz (> 70%) and magnetite (~ 20%). Quartz grains are large (up to 6 mm), strained and tend to be elongate with sutured grain boundaries. Magnetite occurs as elongate grains with ragged outlines; occasionally euhedral forms are present. Magnetite contains 0.2 - 0.4 mm quartz and green hercynite inclusions (Fig.7a). Exsolved hercynite grains most commonly occur along

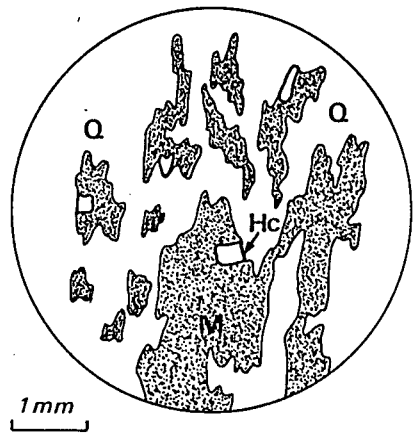

a. Exsolved hercynite in the magnetite-quartzite.

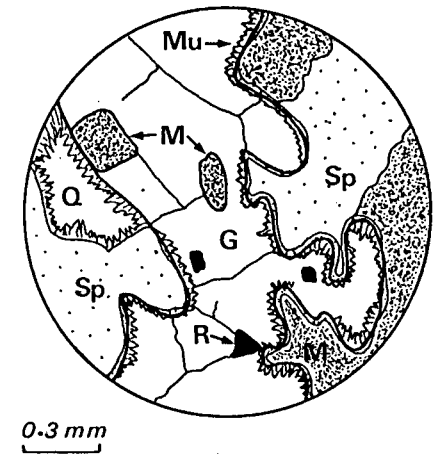

b. Porphyroblastic gahnite with rims of muscovite in the massive sulphide rocks. Alteration to sphalerite occurs along cleavage traces.

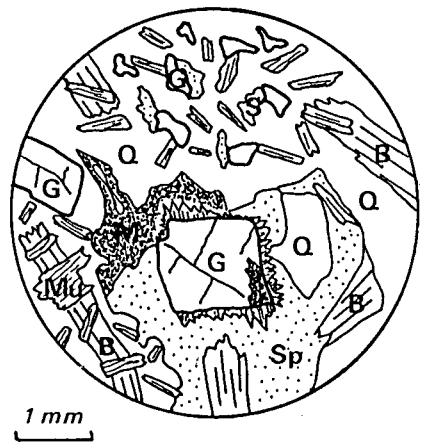

c. Euhedral gahnite associated with sphalerite, muscovite and quartz in the massive sulphide rocks.

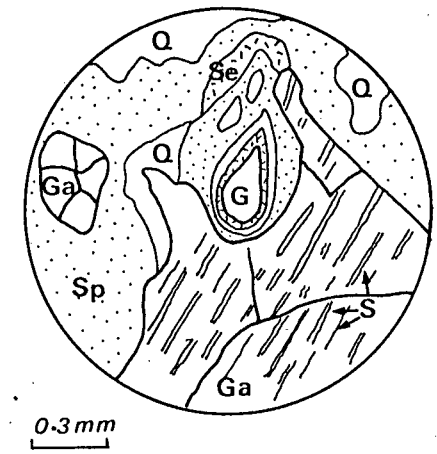

d. Gahnite rimmed by a stacked corona of sericite, quartz and sphalerite in an embayed garnet grain in the brecciated massive sulphide rock.

Abbreviations:
G - gahnite, Ga - garnet, M - magnetite, Mu - muscovite,
Q - quartz, S - sillimanite, Sp - sphalerite, R - rutile.

Figure 7: Textural relations of minerals in rocks from Broken Hill.

Table 7. Estimated modal proportions of minerals present in samples studied from Aggeneys

SAMPLE:	BH-1	BH-3	BH-2	BHLO-1	BHWE-1	BHWE-2	BHG-302	240AG56	DPB
Magnetite	30	15			40	60	20	m	
Hematite	tr								
Chalcopyrite	5	35			m	10	5	tr	
Pyrite			15	tr					tr
Pyrrhotite	25	25	10	10	5	m			
Sphalerite	m	m	10	5	m	m			
Galena	tr	5	40	10				tr	tr
Quartz	25	5	10	55	45	20	75	75	95
Feldspar		5	m						
Pyroxmangite	5	5							
Garnet				5	m			10	
Chlorite	m	tr			tr	m	tr		
Biotite			5		tr	tr			m
Muscovite			5	10				tr	
Gahnite/hercynite			m	tr	tr	tr	tr	m	m
Tourmaline				m					
Amphibole	tr	tr						10	
Sillimanite				tr					

'm' indicates minerals present in minor proportions (5% or less)
'tr' indicates minerals present in trace quantities (1% or less)

Rock Types:

BH-1, BH-3 : sulphide-, amphibole-bearing BIF
BH-2 : massive sulphide rock
BHLO-1 : brecciated massive sulphide
BHWE-1, BHWE-2: sulphide-bearing magnetite quartzite (BIF)
BHG302 : banded magnetite quartzite (BIF)
240AG56 : amphibole-garnet quartzite
DPB-1 : metaquartzite

the edge of magnetite grains, bordering on matrix quartz. The exsolved hercynite contains tiny magnetite and quartz inclusions. Spinel also occurs as tiny grains in quartz inclusions in magnetite. Accessory mineral phases in this rock include muscovite and chlorite (Table 7).

(2) Sulphide-rich Magnetite Quartzite.
Sulphide minerals include chalcopyrite, pyrrhotite and sphalerite (Table 7). The ore minerals form coarse interlocking grains. Minor phases include garnet, phlogopite, chlorite, muscovite and gahnite. Quartz and magnetite are the major phases with quartz occuring as coarse grains, (0.6 - 4 mm), with undulose extinction and sutured grain boundaries. Euhedral magnetite grains occur throughout the rock. Chalcopyrite and pyrrhotite appear to be associated. Sphalerite, like magnetite occurs throughout the matrix.
Pale-green gahnite grains up to 0.35 mm are associated with sulphide minerals and magnetite. Green gahnite is commonly anhedral or occurs as ribbon-like inclusions in chalcopyrite, pyrrhotite or sphalerite. Sphalerite is commonly spatially associated with gahnite and occasionally surrounds it and infills fractures in gahnite. The association of sphalerite with fractures in gahnite suggests that gahnite is replaced by retrograde sphalerite. Gahnite commonly contains quartz inclusions and shows no disequilibrium features towards quartz.
Garnet occurs locally as aggregates interspersed with magnetite and quartz. Garnet and gahnite were not observed in contact.

Sulphide-rich amphibole-bearing BIF.

The samples studied include a quartz-, magnetite-dominated assemblage and a sulphide-dominated assemblage, however both rocks contain the mineral suite; quartz + magnetite + chalcopyrite + pyrrhotite + sphalerite + galena + pyroxmangite + amphibole (Table 7). Quartz is invariably surrounded by a thin rim consisting of small radiating pyroxmangite grains. Pyroxmangite also occurs as pale, (0.4 - 0.8 mm), subhedral grains in the ore assemblage. Amphibole occurs in a blade-like habit, displays excellent twinning, typical amphibole cleavage and has a 2V of 80-90°. Grain size is similar to that of pyroxene. The amphibole contains significant quantities of manganese and appears to fit the description of tirodite described by Ryan et al. (1982). Although sphalerite occurs throughout, no gahnite was observed in the samples studied.

Massive Sulphide. (Figures 7b,c)

This rock contains a sulphide-dominated assemblage. The gangue minerals include quartz as a major phase along with brown phlogopite, colourless muscovite, minor feldspar and pale green gahnite. Sulphides include galena, pyrite, pyrrhotite and sphalerite (Table 7).
Quartz occurs as large poikiloblastic grains (up to 1.7 mm). Large phlogopite and muscovite laths coexist with quartz. Most of the orange-brown phlogopite is corroded and altered. In contrast to this, muscovite is unaltered and exhibits euhedral grain shapes.
Pale green gahnite occurs throughout the assemblage as inclusions in the ore minerals or along with quartz and muscovite as part of the gangue mineral assemblage (Fig.7c). Where it occurs as inclusions in ore, gahnite forms large anhedral grains commonly bordered by sphalerite and magnetite (Fig.7b). Inclusions of magnetite, sphalerite and rutile occur in gahnite. A feature of gahnite in this assemblage is the narrow rim of muscovite which surrounds the grains and forms a boundary between it and the surrounding sulphides. Small grains of quartz are commonly associated with gahnite in the ore and these too are surrounded by muscovite (Fig.7c). Occasional grains of gahnite are surrounded partially by a narrow rim of quartz.
Gahnite surrounded by quartz is generally associated with sphalerite. Large complex gahnite-muscovite-quartz intergrowths on closer inspection comprise inclusions of gahnite and quartz hosted in large, optically continuous muscovite poikiloblasts. Scattered, euhedral grains of gahnite also occur as inclusions in quartz grains in the matrix.

A coarse, brecciated form of the massive sulphide rock consists dominantly of quartz cemented by pyrrhotite, galena and pyrite. Minor sphalerite is present as well as garnet, tourmaline and muscovite (Table 7). The dominant quartz fraction is recrystallised and exhibits a fine mortar texture. Muscovite occurs in elongate, curved laths with stumpy grain terminations and is generally surrounded by sulphides. Tourmaline occurs as 0.06 - 0.4 mm, rounded grains displaying a yellow-orange/orange pleochroic scheme. Garnet tends to be concentrated locally as subhedral, fractured grains of up to 1.7 mm in diameter. Larger grains contain inclusions of quartz, magnetite and fine sillimanite needles. Garnet is

commonly fractured and infilled with sulphides. Pale green gahnite is rare, occurring as anhedral grains in muscovite. A single grain of gahnite occurs in an embayment in garnet surrounded by sphalerite. The gahnite grain is surrounded by a stacked corona consisting of an inner sericite layer, quartz and a wider sphalerite rim (Fig.7d). Quartz and sericite grains surround the complex mineral aggregate.

4.2.2 Mineral Chemistry

Mineral analyses were obtained by use of the Cameca Microprobe in the Geochemistry Department at the University of Cape Town. An explanation of the technique employed and method of data reduction is given in Appendix 1. Natural and synthetic standards were employed. Individual mineral analyses are listed in Appendix 4. Table 8 lists average mineral analyses of the rocks studied.

Muscovite.

Muscovite is a major phase in the massive sulphide rocks (Table 8). The simplified general formula for analysed muscovite is:

$K_2Mg_{0.3-0.35}Fe_{0.4-0.47}Ti_{0.13}Al_{3.37}(Si_6Al_2)O_{20}(OH)_4$.

There is some substitution of Ti, Mg and Fe for octahedral Al and this site is slightly overfull according to the structural formula. A stoichiometric recalculation of the analysed composition did not require that any of the Fe be present in the Fe^{3+} state. Individual muscovite grains contained up to 0.23 wt% CaO but most of the analyses contained no calcium. A single analysis of a Na-muscovite was made but the rest have < 0.5 wt% NaO. None of the muscovite analysed contained zinc above the detection limit for this element (0.2 wt% ZnO).

Biotite/Phlogopite

In the massive sulphide rock orange-brown biotite occurs along with muscovite, the latter replacing earlier brown biotite. The simplified structural formula for biotite in this sample is:

$Na_{0.03}K_{1.7}Mn_{0.13}Mg_{3.3}Fe_{1.9}Ti_{0.2}(Al_{2.6}Si_{5.4})O_{20}(OH)_4$.

Biotite contained significant quantities of manganese (up to 1 wt% MnO). Phlogopite occurs as a minor phase in sulphide-bearing BIF (Table 8), and

Table 8. Average (or representative) analyses of minerals present in samples studied at Aggeneys.

	BIOTITE						PHLOGOPITE
n	7		2		2		1
SAMPLE	BHG156-7		BHG156-5		BH-2		BHWE-2
		σ		σ		σ	
SiO2	34.14	0.91	33.89	0.35	36.91	0.14	41.12
TiO2	4.11	0.34	3.41	0.63	1.84	0.10	0.08
Al2O3	19.22	0.53	19.49	0.69	17.48	0.42	12.98
Cr2O3	nd		0.08	0.01	nd		nd
FeO	24.65	2.17	25.89	1.48	14.57	0.02	9.91
MnO	0.23	0.05	0.24	0.01	0.99	0.01	0.51
MgO	5.17	0.55	5.60	0.42	14.26	0.32	21.32
CaO	nd		nd		nd		nd
ZnO					0.16	0.04	nd
Na2O	0.07	0.04	0.11	0.01	0.10	0.03	1.02
K2O	9.08	0.40	7.61	0.08	8.74	0.08	7.33
Total	96.67		96.32		95.05		94.27

	MUSCOVITE				CHLORITE			
n	1	7		3		1	3	
SAMPLE	BHG156-5	BH-2		BHLO-1		BHG156-5	BHWE-2	
			σ		σ			σ
SiO2	45.30	42.76	0.29	43.64	0.63	29.50	30.42	1.25
TiO2	0.59	1.51	0.12	1.35	0.12	2.46	nd	
Al2O3	35.50	32.10	0.32	32.02	0.24	21.40	9.56	1.01
Cr2O3	nd	nd		nd		nd	nd	
FeO	1.83	3.12	0.47	2.55	0.13	28.32	43.80	0.41
MnO	nd	0.07	0.02	0.09	0.05	0.43	2.04	0.03
MgO	0.34	1.63	0.07	1.38	0.06	7.63	2.15	0.32
CaO	nd	nd		nd		nd	nd	
ZnO		0.13	0.12	nd			0.15	0.09
Na2O	0.22	0.21	0.03	0.51	0.14	0.08	0.14	0.07
K2O	7.13	9.25	0.11	9.64		2.72	0.32	0.07
Total	90.91	90.78		91.18		92.54	88.58	

nd: element was not detected or the amount detected is below the detection limit of the analytical method employed.
σ: is a statistical measure of the range of 'n' number of analyses.
All Fe was analysed as FeO.

Table 8. Average (or representative) analyses of minerals present in samples studied at Aggeneys.

	PYROXMANGITE		TIRODITE		ANTHOPHYLLITE	GEDRITE		TOURMALINE	
n	2		5		1	2		5	
SAMPLE	BH-1		BH-3		240AG56	240AG56		BHLO-1	
		σ		σ			σ		σ
SiO2	47.03	0.19	53.14	0.16	50.98	44.55	0.75	35.00	0.66
TiO2	nd		nd		0.04	0.13	0.02	0.69	0.18
Al2O3	nd		0.19	0.06	4.14	13.06	0.04	34.01	0.50
Cr2O3	nd		nd		nd	nd		nd	
FeO	9.30	1.41	13.97	0.40	24.41	25.66	0.32	9.14	1.12
MnO	40.96	2.98	15.71	0.69	0.30	0.27	0.01	0.22	0.04
MgO	2.16	1.37	14.40	0.49	18.03	13.58	0.37	4.87	0.75
CaO	0.22	0.10	0.20	0.06	0.07	0.12	0.00	0.72	0.23
Na2O	nd		0.11	0.03	0.26	1.04	0.07	1.60	0.21
K2O	nd		nd		nd	nd		0.11	0.05
Total	99.67		97.72		98.23	98.41		86.36	

	GARNET									
n	5		5		2		4		3	
SAMPLE	BHWE 1		BHLO 1		240AG56		BHG 156-7		AG80-195	
		σ		σ		σ		σ		σ
SiO2	36.72	0.20	36.31	0.12	37.37	0.11	37.01	0.16	37.19	0.18
TiO2	nd		nd		nd		nd		nd	
Al2O3	20.89	0.18	21.52	0.04	21.81	0.28	21.19	0.09	21.16	0.11
FeO	21.67	0.48	24.79	0.60	35.34	0.86	32.74	0.38	34.86	0.13
MnO	17.82	0.75	16.33	0.73	1.24	0.01	8.71	0.05	5.73	0.07
MgO	1.47	0.09	0.98	0.10	5.30	0.17	1.45	0.06	1.36	0.07
CaO	1.43	0.36	0.53	0.14	0.34	0.01	1.17	0.04	1.93	0.07
Na2O	nd		nd		nd		nd		nd	
K2O	nd		nd		nd		nd		nd	
Total	100.00		100.46		101.40		102.27		102.23	

nd: element was not detected or the amount detected is below the detection limit of the analytical method employed.
σ: is a statistical measure of the range of 'n' number of analyses.
All Fe was analysed as FeO.

Table 8. Average (or representative) analyses of minerals present in samples studied at Aggeneys.

MAGNETITE

n	3		1	4		4		1
SAMPLE	BH-1		BH-3	BHWE-1		BHWE-2		240AG56
		o			o		o	
SiO2	0.02	0.01	nd	0.04	0.02	0.04	0.01	0.08
TiO2	0.04	0.02	0.21	0.10	0.02	0.15	0.02	0.14
Al2O3	0.13	0.05	0.20	0.33	0.04	0.40	0.08	0.23
Cr2O3	nd		nd	nd		nd		0.18
FeO	95.23	0.25	92.08	96.26	0.43	95.82	0.98	95.13
MnO	1.76	0.04	2.26	0.33	0.06	0.35	0.07	nd
MgO	0.03	0.03	nd	0.02	0.01	nd		nd
CaO	nd		nd	nd		nd		nd
ZnO	nd		nd	nd		nd		0.14
Total	97.21		94.75	97.08		96.76		95.90

GAHNITE

n	11		1	9		10		6		3	
SAMPLE	BH-2		BHLO-1	BHWE-1		BHWE-2		240AG56		DPB-1	
		o			o		o		o		o
SiO2	nd		nd	nd		nd		nd		nd	
TiO2	nd		nd	nd		nd		nd		nd	
Al2O3	57.04	0.35	58.03	56.69	0.24	56.97	0.41	55.77	0.62	56.79	0.42
Cr2O3	0.07	0.04	nd	nd		nd		nd		0.07	0.03
FeO	7.12	0.50	10.41	9.22	0.31	9.51	1.08	16.94	1.44	11.43	0.15
MnO	0.51	0.05	0.49	0.38	0.05	0.56	0.14	nd		0.41	0.03
MgO	1.15	0.11	0.79	1.07	0.06	1.05	0.05	2.77	0.16	0.57	0.02
ZnO	33.60	0.57	32.17	32.47	0.44	31.74	1.02	24.10	1.64	30.14	0.40
Total	99.49		101.89	99.83		99.83		99.58		99.41	

nd: element was not detected or the amount detected is below the detection limit of the analytical method employed.
o: is a statistical measure of the range of 'n' number of analyses.
All Fe was analysed as FeO.

SPHALERITE

n	3	
SAMPLE	BH-2	
		o
Zn	58.94	0.08
Fe	8.13	0.07
Mn	0.30	0.06
S	33.80	0.24
Total	101.17	
Zn/Fe	7.2	

has the structural formula:
$Na_{0.3}K_{1.3}Mn_{0.06}Mg_{4.5}Fe_{1.3}Al_{0.3}(Al_2Si_6)O_{20}(OH)_4$. It was found to contain less manganese than biotite (0.5 wt% MnO). Stoichiometric recalculation of biotite and phlogopite did not require that any Fe occurs in the Fe^{3+} state. Analysis for zinc in biotite and phlogopite gave values of less than 0.2 wt% ZnO (0.2 wt% ZnO is the lower detection limit for this element in the analyses).

Chlorite

The only chlorite observed in the rocks studied occurred in the phlogopite-bearing BIF (see above). Chlorite is significantly rich in iron and silica and contains in excess of 2 wt% MnO. A simplified formula is $Na_{0.1}K_{0.1}Mg_{0.7}Mn_{0.4}Fe_{8.5}Al_{1.5}(Al_1Si_7)O_{20}(OH)_4$.

Garnet

In the massive sulphide and sulphide-bearing BIF, garnet has high spessartine contents. Average core compositions of garnet in the samples studied are $Alm_{56.7}Spess_{37.8}Py_4Gross_{1.5}$ and $Alm_{48.5}Spess_{40.9}Py_{5.9}Gross_{4.2}$ respectively. Similar spessartine-almandine garnets are recorded in the aluminous schist at Aggeneys (Ryan et al., 1982) and at Gamsberg (Rozendaal, 1982). Garnet in the Aggeneys garnet-,anthophyllite quartzite has an average composition of $Alm_{76}Py_{20}Spess_3Gross_1$. Garnet compositions are plotted on a triangular endmember diagram, Figure 8.

Tourmaline

Small quantites of pleochroic orange/yellow tourmaline occur in the brecciated massive sulphide rock. These have a formula of: $Na_{0.5}Ca_{0.03}Mg_{1.5}Fe_{1.6}Mn_{0.3}Ca_{0.2}Al_6B_3Si_{16}O_{27}$ which is equivalent to 44 mol% dravite and 56 mol% schorl endmembers. The total wt% oxides in tourmaline is 85 from which the boron content is estimated at approximately 15 wt% B_2O_3.

Amphibole

The sulphide-rich, amphibole-bearing BIF from Broken Hill contains a Mn-rich amphibole which is described as tirodite by Ryan et al. (1982). The structural formula of the amphibole is $Na_{0.13}Ca_{0.03}Mn_{2.1}Fe_{1.8}Mg_{3.3}Si_8O_{22}$. Garnet-orthoamphibole

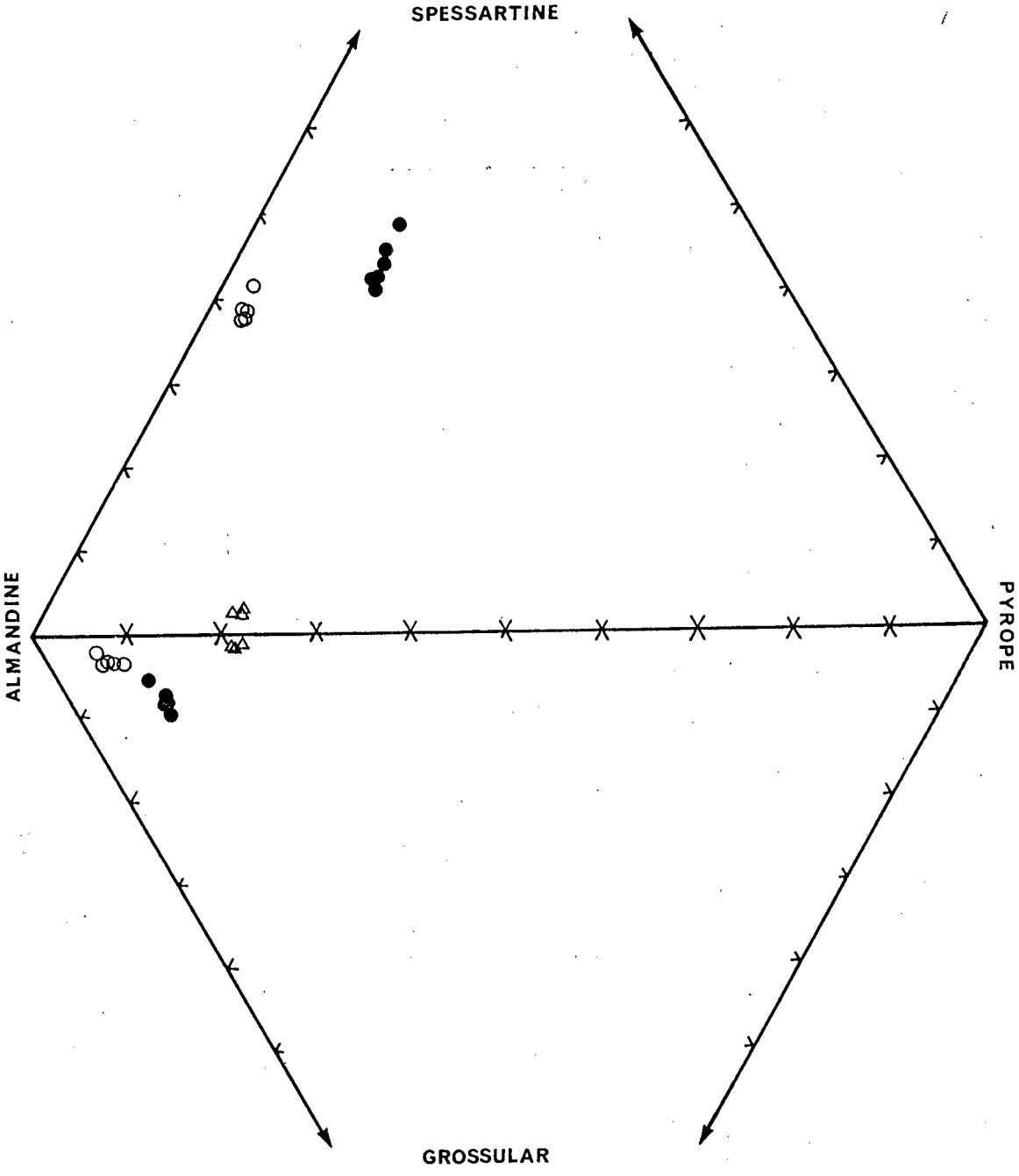

Symbols:
open triangules: sulphide-rich magnetite quartzite
closed circles : brecciated massive sulphide
open circles : metapelitic schist

Figure 8: Garnet compositions (Broken Hill) plotted on a triangular end-member diagram

quartzite from Aggeneys has coexisting anthophyllite and gedrite e.g. Anthophyllite; $Na_{0.08}Ca_{0.01}Mn_{0.04}Fe_{3.12}Mg_{4.1}Al_{0.5}(Si_{7.8}Al_{0.02})O_{22}$ and Gedrite; $Na_{0.31}Ca_{0.02}Mn_{0.04}Fe_{3.3}Mg_{3.1}Al_{1.3}(Si_{6.9}Al_{1.1})O_{22}$.

Pyroxenite

In the magnetite-amphibolite Mn-rich pyroxenite is fairly common. Average analyses yield a structural formula of $Ca_{0.01}Fe_{0.16}Mn_{0.76}Mg_{0.05}SiO_3$.

Magnetite

Magnetite in the BIF contains between 0.2 and 0.5 wt% MnO. In the massive sulphide rocks magnetite contains up to 2.3 wt% MnO.

Gahnite

Average gahnite endmember composition for the BIF is $Ghn_{70.9}Hc_{23.15}Sp_{4.75}Gal_{1.2}$. Zincian hercynite exsolved from magnetite in non-sulphide-bearing magnetite quartzite has a composition of $Hc_{59.6}Ghn_{24.7}Sp_{9.5}Gal_{6.2}$. In the massive sulphide rock, analysed gahnite has the composition $Ghn_{75.4}Hc_{18}Sp_{5.3}Gal_{1.3}$. Gahnite in the amphibole-garnet quartzite has the composition $Ghn_{52.9}Hc_{34.6}Sp_{12.5}$.

Figures 9, 10 show variation in wt% FeO and MgO compared to wt% ZnO in gahnite. Gahnite from Dabiepoort has similar composition to the sulphide-associated gahnite at Broken Hill. However gahnite in the garnet-amphibole quartzite from Aggeneys has lower zinc and higher magnesium content than sulphide-associated gahnite. Zincian hercynite exsolved from magnetite in the BIF has a relatively high Fe content. Compositional differences in gahnite may reflect variation in bulk rock chemistry and thus available components for gahnite formation or alternatively may reflect a sensitivity of gahnite composition to variation in parameters such as metamorphic fluid, temperature, pressure or $f(O)_2$. By accounting for the Fe content of gahnite in these rocks Figure 11 shows that gahnite compositions define separate fields in the different lithologies and thus show sensitivity to variations in bulk rock chemistry despite the dominantly iron-rich character of the surrounding lithologies at Aggeneys.

Analysed gahnite and zincian hercynite from samples studied are plotted on a triangular endmember diagram, Figure 12. Available data on gahnite

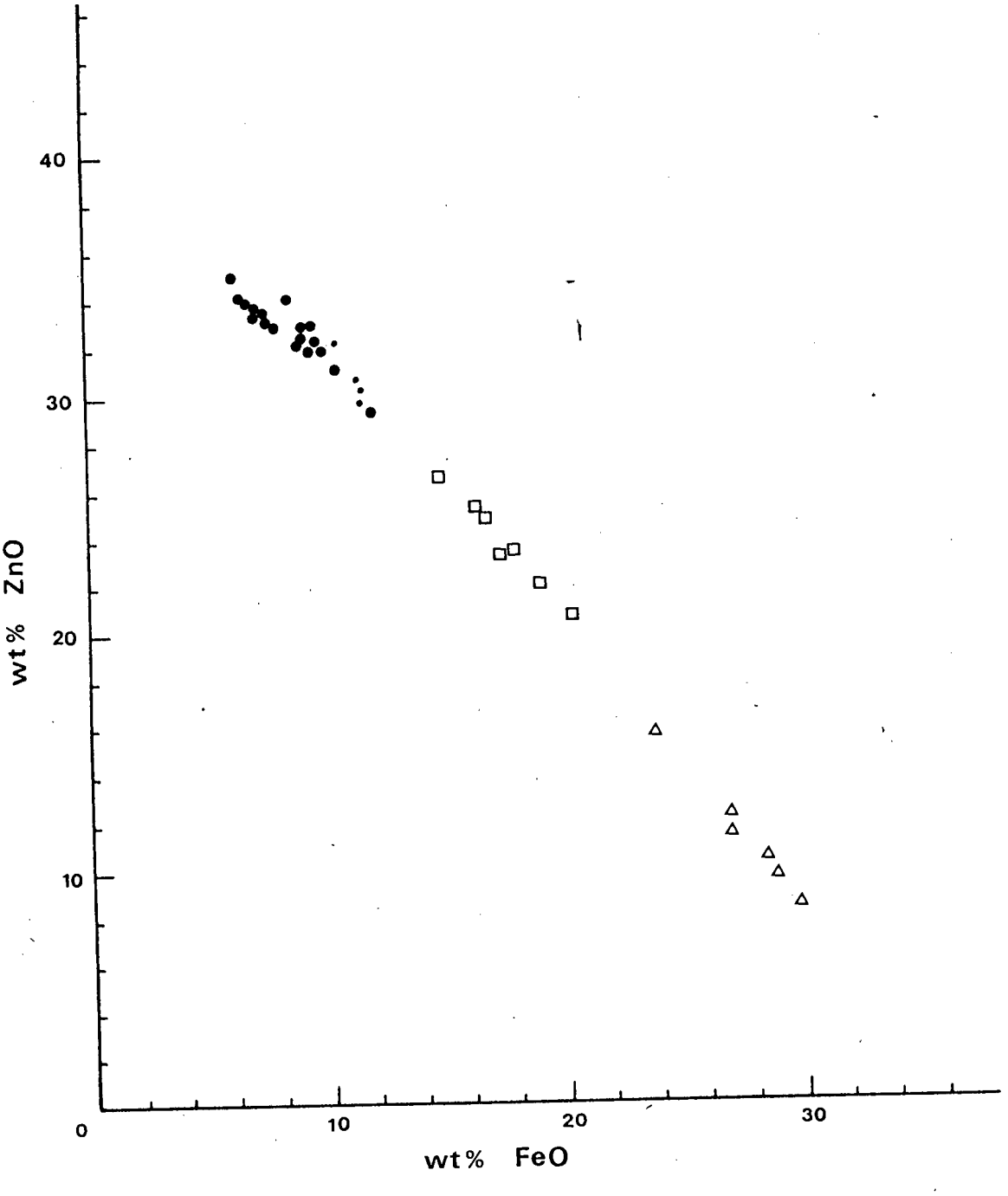

Symbols:
large dots : massive sulphide (Broken Hill)
small dots : gahnite-bearing quartzite (Dabiepoort)
open squares : garnet-orthoamphibole quartzite (Aggeneys)
open triangles: magnetite quartzite (Broken Hill)

Figure 9: Gahnite compositions, (Broken Hill): ZnO/FeO

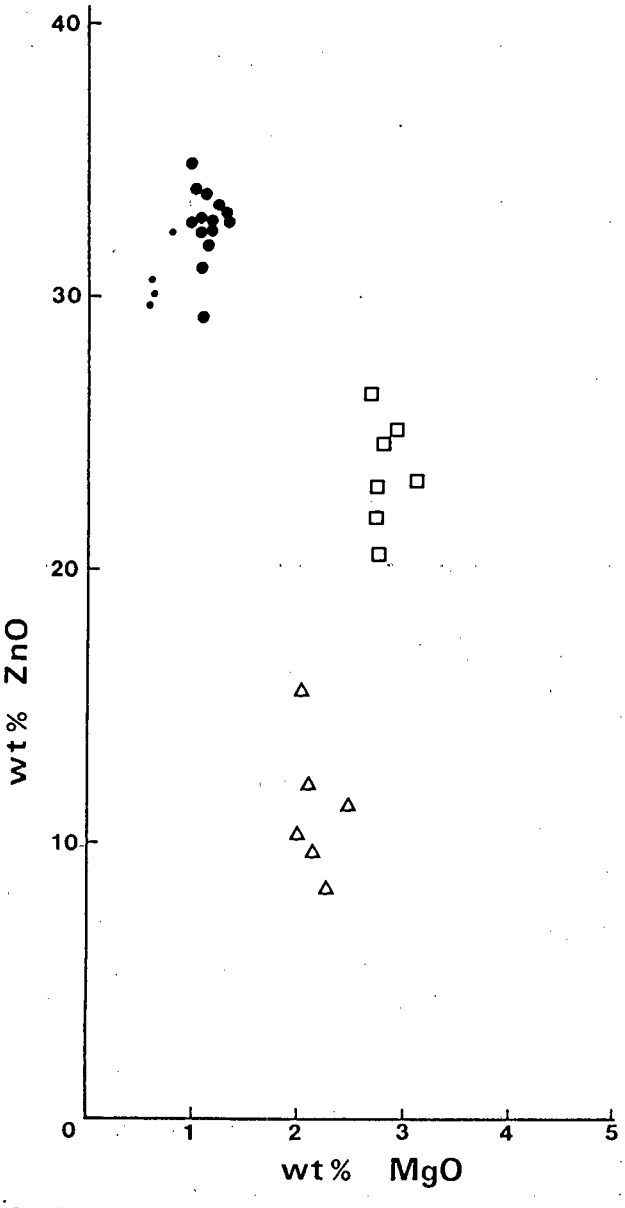

Symbols:
large dots : massive sulphide (Broken Hill)
small dots : gahnite-bearing quartzite (Dabiepoort)
open squares : garnet-orthoamphibole quartzite (Aggeneys)
open triangles: magnetite quartzite (Broken Hill)

Figure 10: Gahnite compositions, (Broken Hill): ZnO/MgO

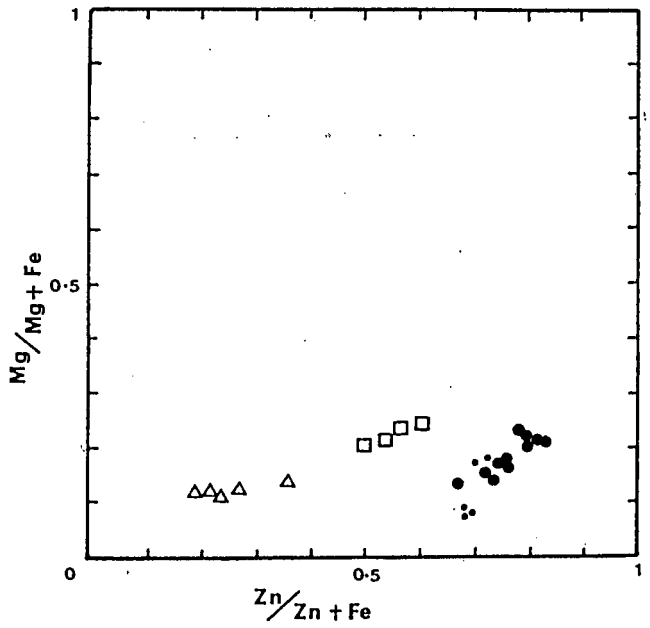

Symbols:
large dots : massive sulphide (Broken Hill)
small dots : gahnite-bearing quartzite (Dabiepoort)
open squares : garnet-orthoamphibole quartzite (Aggeneys)
open triangles: magnetite quartzite (Broken Hill)

Figure 11: Gahnite compositions, (Broken Hill): Mg/Mg+Fe vs. Zn/Zn+Fe

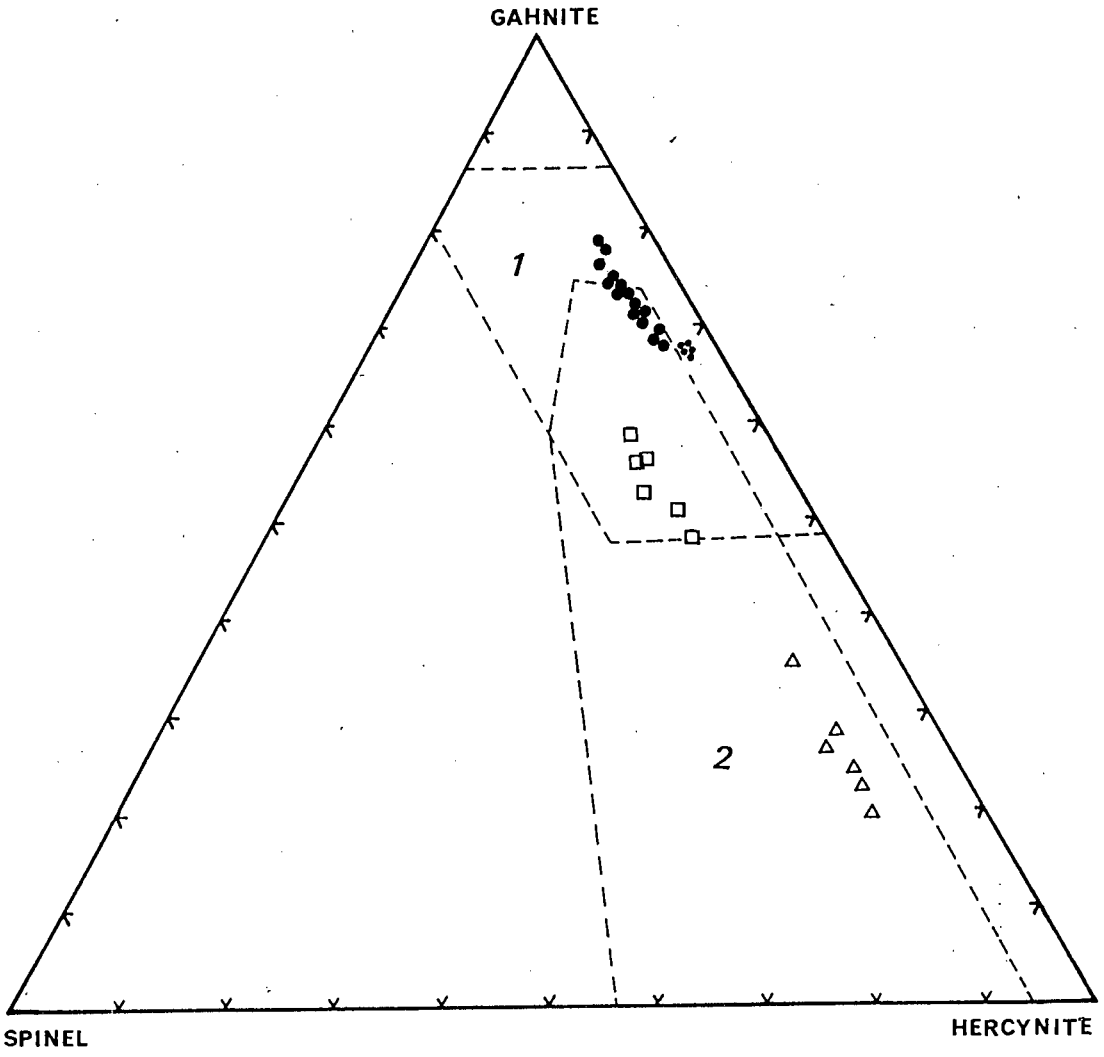

Symbols:
large dots : massive sulphide (Broken Hill)
small dots : gahnite-bearing quartzite (Dabiepoort)
open squares : garnet-orthoamphibole quartzite (Aggeneys)
open triangles: magnetite quartzite (Broken Hill)

Field 1: gahnite associated with metamorphosed massive sulphide deposits (Spry, 1984).
Field 2: gahnite associated with aluminous metasediments (Spry, 1984).

Figure 12: Gahnite compositions (Broken Hill) plotted on a triangular end-member diagram.

associated with sulphide mineralization in other parts of Namaqualand is listed in Table 9, as well as some reported compositions from metamorphosed massive sulphide deposits from other parts of the world. It is apparent that gahnite composition can vary substantially, however, most of those associated with metamorphosed massive sulphide deposits eg. Appalachians (Sandhaus, 1981), Swedish Caledonides (Sundblad, 1982), Quebec (Bernier et al., 1984), Broken Hill, Australia (Plimer, 1977) have high zinc contents and low spinel contents as was suggested by Spry (1984). Included on Figure 12 are the fields proposed by Spry (1984) for gahnite from metamorphosed massive sulphide deposits (field 1) and from aluminous metasediments (field 2).
Table 9 also includes Mg-rich gahnite compositions from high-Mg, aluminous rocks (Essene et al. 1982, Wolter and Siefert 1984, Treloar et al. 1981). Gahnite from the anthophyllite-,garnet-bearing quartzite similarly shows higher Mg contents (11-15 mol% spinel) than the sulphide associated gahnite (3-6 mol% spinel).
The high Zn content of gahnite associated with sulphides (70-80 mol% gahnite), high Mg content of gahnite in the Mg-rich, anthophyllite-,garnet-bearing quartzite and high Fe content of gahnite exsolved from magnetite appear to indicate a sensitivity of spinel composition to bulk rock chemistry.

4.2.3 Metamorphism and $f(O)_2$

Samples obtained from the metapelitic schist at Broken Hill contain the assemblage: quartz-biotite-sillimanite (+ K feldspar, garnet, magnetite). The BAMM Buffer (Zen, 1985) for oxygen fugacity calculation is applicable to this assemblage and the presence of co-existing biotite and garnet enable calculation of metamorphic temperature.

Texturally, biotite and sillimanite define a pervasive schistosity in these rocks. Quartz is strained with grains elongate parallel to the fabric defined by sillimanite and biotite. Biotite is orange-brown to pale brown and is partially corroded along the grain boundaries. The association of biotite, sillimanite and garnet suggest a prograde dehydration reaction involving biotite as a reactant phase. Garnet grains are small (approximately 1 mm in diameter), and mostly occur as inclusions

Table 9. Gahnite compositions from Namaqualand, some massive sulphide deposits and Mg-rich rocks.

Locality:	Reference:	Assemblage:	mol% Gahnite	Hercynite	Spinel	Galaxite
COMPOSITION OF GAHNITE IN NAMAQUALAND						
Gamsberg	Rozendaal, 1982	B member (ore zone)	38	58	3	1
		C member (ore zone)	77	18	<5	<1
Kielder District, Namaqualand	Gorton, 1981	massive sulphide rocks	29	40	31	1
	This study		35	11	53	<1
Kouberg Synform, Namaqualand	Rozendaal 1982	qtz-fsp-sill gneiss	30	56	13	1
		magnetite zones	26	46	20	8
Broken Hill, Black Mountain; Aggeneys	Spry, 1986, 1987a	massive sulphide	65-85			
		garnet quartzites	18-75			
COMPOSITION OF GAHNITE IN MASSIVE SULPHIDE DEPOSITS						
Massive sulphide deposit, Mineral District, Virginia	Sandhaus, 1981	mineralised metapelitic and metavolcanic rocks	70-82	7-24	4-14	
Swedish Caledonides	Sundblad, 1982	mineralised quartz-mica schists	66-82	15-24	3-10	
Bleikvassli ore deposit, Norway	Vokes, 1962	quartz-rich muscovite schist	79	8	11	2
Massive sulphide deposit, Montauben-Les-Mines, Que.	Bernier et al. 1984	biotite-garnet-quartzo-feldspathic gneiss	72	20	8	
Massive sulphide deposit, Broken Hill, Australia	Plimer, 1977	sulphide associated metapelitic rocks	57-78	19-38	4-5	
Massive-sulphide deposit, Fornas, Spain	Williams, 1983	sulphide associated metabasites	72	20	8	
Archean Iron Formation	Appel, 1986	mineralised BIF and associated anthophyllite-gedrite rock	60	26	14	
COMPOSITION OF GAHNITE IN MAGNESIAN-RICH ROCKS						
Massive sulphide deposit, Manitauwadge, Ontario	Essene et al., 1982	spinel-nigerite-hogbomite rock	41	30	29	
Massive sulphide deposit, Falun, Sweden	Wolter and Siefert, 1984	cordierite-anthophyllite rock	50-70	16-50	0-24	
Cu-Co-Zn ore bodies Outokumpu district, Finland	Treloar et al., 1981	spinel-phlogopite schist	13-15	73-78	8-12	<1
		crd-amphibole rock	23-61	23-70	9-19	<1

in biotite. Garnets commonly have a central poikiloblastic region containing tiny quartz and magnetite inclusions and clear rims. In some assemblages biotite is replaced by retrograde chlorite.

Average analysed mineral compositions from the aluminous schist are included in Table 8. The structural formula for muscovite is : $K_{1.24}Na_{0.06}(Fe_{0.2}Mg_{0.07})(Ti_{0.06}Al_{3.7})Si_6Al_2O_{20}(OH)_4$ and
for biotite is
$K_{1.8}Na_{0.03}Fe_3Mg_{1.2}Al_{0.7}Ti_{0.4}(Si_{5.3}Al_{2.7})O_{20}OH_2$.
The compositional range for garnet is $Alm_{74-79}Py_3Spess_{13-20}Gross_{3-4}$.

Ryan et al. (1982) propose three metamorphic episodes in the Bushmanland rocks at Aggeneys, the first, M1, is largely masked by re-equilibration during the slightly lower M2 event. Temperatures of 670 - 695 °C and pressures between 3.5 and 6 kbar have been estimated for the observed maximum metamorphic grade attained in the area (M2) (Ryan et al., 1982) . These estimates are based on the presence of orthoclase, sillimanite and cordierite in the aluminous schist, diopside in the amphibolites, and grossular garnet in calc-silicate rocks at Aggeneys. Retrograde metamorphism to greenschist facies, (M3), result in alteration of garnet to chlorite and epidote, sillimanite to sericite . An estimate of 440 °C at similar or lower pressures is given for this event (Ryan et al., 1982).

In order to calculate P-T conditions of maximum metamorphism, (M2), cores of coexisting garnet-biotite pairs were analysed. Cores were selected to minimise the effects of Fe-Mg re-equilibration during (M3) retrograde metamorphism (Indares and Martingole, 1985b). Results of calculations are listed in Table 10 . Biotite-garnet pairs yield a maximum temperature of 650 °C at 4.5 - 5 kbar, according to the method of Indares and Martingole (1985a). An explanation of this method is outlined in Appendix 2.
Garnet was found to be significantly spessartine-rich in the rocks studied (13-20 mol% spessartine component).

In the magnetite quartzite, small exsolved grains of green spinel occur along the borders of the magnetite grains. Both magnetite and hercynite co-exist with quartz in this assemblage.
The hercynite-quartz stability field has been investigated by Richardson

Table 10: Results of geothermometry on co-existing garnet-biotite pairs in a sample of the aluminous schist from Broken Hill.

analysis nr:	1	2	3	4
Corrections for substitution in Garnet				
X_{Ca}	0.0330	0.0336	0.0332	0.0313
X_{Mn}	0.1962	0.1933	0.1908	0.1922
K_D=Fe/Mg	12.9167	12.1050	12.5398	12.6954
Corrections for substitution in Biotite				
X_{Ti}	0.0761	0.0941	0.0899	0.0810
X_{Al}	0.1195	0.1331	0.1963	0.1218
K_D=Fe/Mg	2.8586	2.2000	2.6271	2.8445
at 5 kbar pressure				
T°K	915	800	843	908
T°C	643	527	570	635

Maximum Temperature = 915 °K or 643 °C

(1968), Hensen and Green (1971), Holdaway and Lee (1977) and Bohlen et al. (1986). Bohlen et al., (1986) did experimental studies in the $Fe\text{-}Al_2O_3\text{-}SiO_2$ system and determined the equilibrium locus of the reaction: $3\ FeAl_2O_4 + 5\ SiO_2 = Fe_3Al_2Si_3O_{12} = 2Al_2SiO_5$ which is located at 5.2 kbar and 865 - 880 °C. However this reaction has a positive dP/dT slope and incorporation of zinc and/or magnetite in hercynite increases the stability field of hercynite-quartz. Zinc, especially may stabilise hercynite to much lower temperatures (Frost 1973, Vielzeuf 1983). In the magnetite quartzite, hercynite has the composition $Hc_{55-69}Ghn_{20-36}Sp_{9-11}$.

Magnetite is able to absorb a limited quantity of zinc into its structure (Wedepohl 1970, Deer et al 1980). The solidus limiting the solid solution between magnetite and hercynite is shown to be dependent on temperature and oxygen fugacity (Turncock and Eugster, 1962). According to their calculated isothermal sections magnetite is able to incorporate less than 5 mol% hercynite in solid solution at 600 °C and $f(O)_2 = -14$. Above 600 °C and at lower $f(O_2)$, the solid solution between magnetite and hercynite increases.

The experiments of Turncock and Eugster (1962) show that magnetite-hercynite solid solution is severely limited at amphibolite grades of metamorphism. Similarly, there is a limit to the stability field of hercynite and quartz at amphibolite facies (Bohlen et al., 1986). However the incorporation of a percentage of zinc into the structure of hercynite may increase the stability field of hercynite-quartz to amphibolite grades and lower (Frost 1973, Vielseuf 1983). In the magnetite quartzite, it is probable that the hercynite-quartz and hercynite-magnetite assemblages coexist by virtue of the zinc content of the original spinel phase. Exsolution of magnetite-hercynite possibly occurred during the post metamorphic cooling stages of the upper amphibolite grade, (M1), event.

Metamorphic $f(O)_2$

Zen (1985), proposed an empirical calculation for $f(O)_2$ based on the assemblage biotite-garnet-muscovite-magnetite-quartz. The aluminous schist contains this assemblage. Table 11 shows results of calculations

Table 11: Results of oxygen fugacity calculations on the aluminous schist and BIF from Broken Hill.

Rock Type:	BIF			Aluminous Schist		
Sample nr:	BH-2	BHWE-1	BHLO-1	BHG156-7	BHG156-5	AG80-195
Correction: biotite						
$-4 \log X_{Si}$	0.15			0.22	0.20	0.24
$-3 \log X_{Fe}$	1.56				0.86	0.83
Correction: garnet						
$-3 \log X_{Fe}$		0.91	0.73	0.40		0.33
Correction: muscovite						
$+2 \log X_{Al}$	-0.15				-0.02	
$+4 \log X_{Si}$	-0.01					-0.05
Average correction biotite	1.71			1.02		
Average correction muscovite	-0.13			-0.07		
Average correction garnet	0.91			0.37		
Total correction	2.47			1.30		

Reference BAMM buffer at 650 °C and 4.5 kb:

$\log f(O)_2 = 10.29 - 26284/T + 0.148(P-1)/T \pm 650/T = -17.5 \pm 0.7$

Corrected $\log f(O)_2$ Aluminous Schist $= -16.02 \pm 0.7$

employing the BAMM buffer system of Zen (1985) and using the calculated temperature of 650 °C and pressure of 4.5 kb. The BAMM Buffer yields a metamorphic log $f(O)_2$ of -17.5 +/- 0.7 without correction for substitution for Fe in biotite and garnet and Al in biotite and muscovite. Corrections for the substitutions yield calculated log $f(O)_2$ = -16.02 +/- 0.7. An attempt was made to apply the buffer to the sulphide-rich BIF, but as the calculation does not take the sulphide phases into account, the results are invalid.

4.2.4 Gahnite Formation

In their study of gahnite at Aggeneys, Spry and Scott (1987a) suggest two reactions for gahnite growth in the sulphide-rich rocks i.e.

1. $Fe_3Al_2Si_3O_{12}$(in garnet) + ZnS + S_2 -> $ZnAl_2O_4$ + 3FeS + $3SiO_2$ + O_2
2. $Fe_3Al_2Si_3O_{12}$ + ZnS + $2.5S_2$ -> $ZnAl_2O_4$ + $3FeS_2$ + $3SiO_2$ + O_2

In the sulphide-free assemblages, e.g. aluminous metasediments, magnetite-barite rocks, garnet-quartzites and magnetite quartzites, they suggest that gahnite-formed during prograde metamorphism of sulphide-bearing sediments i.e.

3. $Al_2Si_2O_5(OH)_4$(kaolinite) + ZnS + $0.5O_2$ -> $ZnAl_2O_4$ + $2SiO_2$ + $2H_2O$ + $0.5S_2$

Gahnite and garnet are observed in a number of sulphide- and non-sulphide-bearing assemblages, although not necessarily in contact, but evidence of garnet breakdown is sparse. Spessartine-rich garnet, as occurs at Aggeneys, is generally accepted as a variety which is stable at relatively low metamorphic grades. Although not observed in the rocks studied, it is more likely that garnet alters to form chlorite than breaks down in an anhydrous reaction to form gahnite.

Gahnite is associated with muscovite and phlogopite in sulphide-bearing rocks, however, the almost insignificant quantities of zinc in mica limits the possibility of gahnite formation from a precursor zinc-bearing phase (Dietvorst, 1980). The common association of gahnite and sphalerite in sulphide-bearing assemblages suggests that gahnite formed early in the paragenetic history as opposed to forming by retrograde alteration of mica or by garnet breakdown.

Ririe (1982) found that coexisting gahnite-magnetite along with ore minerals, in Precambrian sulphide deposits in Colorado, display metamorphic textures which are consistent with a premetamorphic origin. Evidence supports the formation of magnetite and gahnite during prograde metamorphism in response to changes in $f(S)_2$ and $f(O)_2$ by the reactions;

4. $3FeS_2 + 2O_2 \rightarrow Fe_3O_4 + 3S_2$

   $1/2O_2 + Al_2SiO_5 + ZnS \rightarrow ZnAl_2O_4 + SiO_2 + 1/2S_2$

At Aggeneys and Gamsberg there is some dispute as to the origin of the sulphide mineralization with support for a fumarolic exhalative source (Ryan et al., 1982 and Rozendaal, 1982) and a chemogenic sedimentary origin (Moore 1986). It would appear from the metamorphic textures observed in this study that gahnite, sphalerite and magnetite formed during the same prograde metamorphic event and are thus premetamorphic in origin.

Moore and Reid (1988, in press) show that gahnite associated with sphalerite in quartzites in Namaqualand can form from infiltrating metamorphic fluids carrying alkali-Al_2O_3 complexes e.g.

5. $2KH_2 + (Zn,Fe)S \rightarrow (Zn,Fe)Al_2O_4 + H_2S + 2KOH$ or at lower K^+/H^+,

6. $2H_3AlO_3 + (Zn,Fe)S \rightarrow (Zn,Fe)Al_2O_4 + H_2O + H_2S$.

A similar hydrothermal-type reaction was proposed by Hobbs (1975) for gahnite formation in pegmatities and quartz veins at Broken Hill massive sulphide deposit, Australia.

The presence of muscovite rims around gahnite in some rocks appears to support the introduction of a fluid phase into the rocks, possibly associated with the later, retrograde metamorphic event (M3) in this area. The stability of gahnite at amphibolite grades of metamorphism (650 °C, 5 kbar) is indicated by its coexistence with sphalerite, garnet and quartz in sulphide-bearing assemblages. It is therefore suggested that gahnite-formation was initiated during diagenesis and continued during prograde metamorphism of the sulphide-bearing sediments. A reaction such as (3), above is envisaged during diagenesis and during the early metamorphic stages. The abundance of micas and garnet in the rocks indicate an adequate supply of Al throughout the metamorphic paragenesis.

Subsequent to the M1 and M2 metamorphic events, low grade metamorphism accompanied by the introduction of K-bearing fluids into the rocks would account for retrograde breakdown of phlogopite and formation of muscovite in some of the assemblages observed. Reactions such as (5) and (6) are possibly associated with the retrograde event. The presence of sulphides and ubiquitous K-bearing mica phases, in the halo of rocks which surround the ore bodies at Aggeneys, indicate an adequate supply of Zn and K for this type of reaction.

4.3 ACHAB

4.3.1 Petrography

Gahnite-bearing quartzites can be traced as a thin horizon in the aluminous schist from the Namiesberg mountain on Achab farm northwards beyond Tafelberg and towards the Gamsberg in the northwest (Fig.5). In the Namiesberg, gahnite occurs mostly in quartzites and schists at the contact of the aluminous schist and the underlying quartzo-feldspathic gneiss. Gahnite occurs locally in the upper horizons of the aluminous schist at its contact with the metaquarzite unit.

Metapelitic Rocks

Metapelitic rocks sampled for the study of gahnite at this locality include sillimanite and muscovite schists, a cordierite-gedrite rock and biotite-sillimanite-muscovite schists. Gahnite is present in the biotite-sillimanite-muscovite schist which also contains minor ilmenite and rutile. The sillimanite and muscovite schists sampled are almost monomineralic, containing only accessory quantities of zircon. Table 12 lists modal proportions of minerals present in the rocks studied.

Gahnite-bearing biotite-muscovite-sillimanite schists are composed of coarse red-brown biotite, muscovite and fibrolite (Fig.13). Abundant tiny inclusions of zircon occur in coarse biotite laths. Biotite, muscovite and gahnite, sillimanite (Plate 1) or garnet form the major phases present in these rocks (Table 12). Garnet occurs as coarse, euhedral porphyroblasts with a central portion containing many minute quartz inclusions. Occasional grains of biotite and rare green gahnite also occur as inclusions in garnet. Anhedral green gahnite is found interstitially to biotite, sometimes bordering on garnet grains and contains both biotite and sillimanite inclusions (Plate 2). Gahnite occurs as a prograde mineral in these assemblages. No Fe-Ti oxides are present in these samples, although they occur in most other lithologies at this locality.

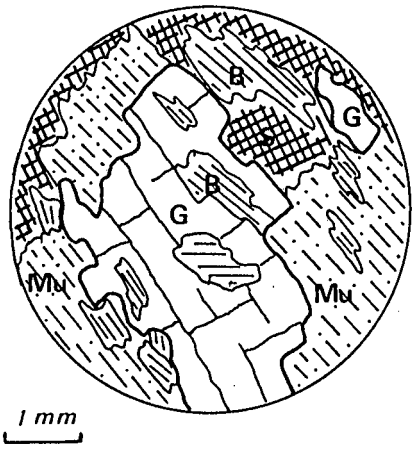

Figure 13: Textural relationship of gahnite in the biotite-muscovite-schist.

Table 12. Estimated modal proportions of minerals present in samples studied at Achab.

SAMPLE	ABN 1	ABN 5	ABN 2	ABN 4	ABN 16	ABN 6	ABN 7
Quartz	10	65				15	60
Biotite				65	15	m	tr
Garnet				15		35	
Cordierite		tr				m	
Sillimanite	85	25		m	35		
Plagioclase						tr	
Muscovite	m		95	15	35		
Sericite			m				
Magnetite	tr	10	tr			m	
Gahnite				tr	15		
Rutile	m						
Zircon	tr			tr			
Gedrite						40	
Tourmaline							40

SAMPLE	ABN 3	ABN 8	ABN 9	ABN 10	ABN 11	ABN 12	ABN 13	ABN 14	ABN 15
Quartz	95	80	80	80	90	75	85	85	95
Biotite	m		m	m		10	tr		tr
Garnet									
Cordierite									
Sillimanite				10		m			
Orthoclase									
Muscovite					tr	tr	m		
Sericite	tr	tr	tr						
Magnetite	m	tr	m	tr	tr	m	tr	tr	tr
Gahnite	tr	20	10	5	10	10	10	15	tr
Rutile		tr		tr	tr	tr	tr	tr	
Zircon									

'm' indicates minerals present in minor proportions (5% or less)
'tr' indicates minerals present in trace quantities (1% or less)

ROCK TYPE

ABN 1,5	sillimanite schist
ABN 2	muscovite schist
ABN 4,16	biotite-muscovite-sillimanite(+garnet, gahnite) schist
ABN 6	garnet-gedrite rock
ABN 7	tourmaline quartzite
ABN 3,8-15	gahnite quartzite

The porphyroblastic garnet-gedrite rock has a matrix composed of quartz and minor cordierite, plagioclase and biotite. Porphyroblasts of gedrite contain inclusions of biotite, quartz, magnetite and cordierite and are bordered by biotite and cordierite. Garnet porphyroblasts contain quartz and magnetite inclusions and are generally surrounded by biotite. Garnet and gedrite comprise in excess of 70 % of constituents of this rock. Rare grains of green zincian spinel are associated with magnetite as inclusions in gedrite.

Gahnite-bearing Quartzites

The gahnite-bearing quartzites contain 5-20 modal% gahnite in a coarsely crystalline quartz martix (Table 12). In some rocks vughs are associated with gahnite-rich laminae. The vughs may be partially infilled with rutile and goethite. The possibility that the vughs are dissolution features resulting from desulphidation of sulphides appears to be supported by trace element analysis. Up to 1.03 wt% Pb and 522 ppm Cu were found in whole rock analyses of some of the gahnite-quartzites. Gahnite in the laminae occurs as coarse, poikiloblastic porphyroblasts concentrated and aligned along bedding planes (Plate 3). Abundant crystallographically orientated inclusions of quartz give the gahnite porphyroblasts a sieve-like appearance. Small, rounded grains of rutile and ilmenite also occur throughout the matrix. In some rocks, gahnite porphyroblasts are associated with cracks and fissures.

Biotite, rutile and muscovite or sillimanite occur as minor phases in the gahnite quartzites (biotite and sillimanite locally up to 10%). Rutile occurs as rounded grains and is closely associated with gahnite. Gahnite-biotite and or gahnite-muscovite associations are fairly common and occassionally rare gahnite grains contain inclusions of needle-like sillimanite. In many of the gahnite quartzites, gahnite is associated with prograde muscovite and biotite.

4.3.2 Mineral Chemistry

The bulk compositions of metapelitic schists and quartzites from this locality indicate high Si, Al and Fe contents and low Mg and K contents (Table 13). Figure 14 gives an indication of the relative proportions of these elements. Relatively high Ti contents (1.3 - 4.9 wt%) are attributed to the presence of trace quantities of ilmenite and minor rutile in the quartzites. Zr contents of 300 - 1300 ppm are attributed to the presence of abundant zircon inclusions in biotite in the metapelitic schists. Significant quantities of Rb (up to 450 ppm) are similarly associated with biotite in the schists. The presence of zinc in the quartzites is attributed to gahnite. Pb contents of 1.03 wt% and Cu up to 522 ppm have been attributed to trace quantities of sulphides (now oxidised) in the quartzites.

Average analyses of minerals in the samples studied are given in Table 14.

Garnet, Plagioclase and Cordierite

The biotite-muscovite-sillimanite schist and the cordierite-anthophyllite rock contain garnet in their assemblages. Endmember garnet compositions are plotted on Figure 15. Average garnet composition in the schists is; $Alm_{70.5}Py_{4.5}Spess_{22}Gross_{3}$. In the porphyroblastic garnet-gedrite rock garnet, co-existing with Mg-rich cordierite and gedrite, has the composition; $Alm_{77.6}Py_{13.5}Spess_{4.9}Gross_{4}$. The composition of plagioclase in this rock is $An_{49}Ab_{51}$.

Biotite and Muscovite

Biotite compositions have been plotted on an endmember diagram (Fig.16) and are shown to be fairly Al-rich (siderophyllite). In zinc-rich lithologies, micas commonly incorporate zinc into their structure (Palache 1935, Frondel and Ito 1966, 1975, Plimer 1977, Stern and Klein 1983). In gahnite-bearing quartzites at Achab muscovite contained less than 0.02 wt% ZnO (lower detection limit = 0.02). However, biotite has ZnO contents of 0.06 - 0.16 wt% and locally up to 0.28 wt%. An altered biotite grain in one of the gahnite quartzites contained 0.7 wt% ZnO. In gahnite-bearing schists biotite contained up to 0.35 wt% ZnO and in the porphyroblastic garnet-gedrite rock 0.09 wt% ZnO.

Table 13. Whole rock analyses of some quartzites and metapelitic schists from Achab.

(analyses by generosity of Dr. J.M. Moore).

Sample:	ABN-1	ABN-2	ABN-3	ABN-4	ABN-5	ABN-6	ABN-7	ABN-8	ABN-9
SiO2	40.67	71.47	95.10	36.33	64.37	49.96	78.00	82.66	74.04
TiO2	2.04	0.87	0.04	1.29	4.85	3.51	0.41	0.41	2.29
Al2O3	54.26	18.91	1.23	36.22	23.74	16.49	11.82	7.85	5.62
FeO	0.89	0.62	2.44	12.95	5.42	14.62	2.65	3.34	9.10
MnO	0.00	0.00	0.00	0.72	0.12	0.36	0.00	0.00	0.13
MgO	0.00	0.00	0.24	3.37	0.21	7.34	2.10	0.00	0.18
CaO	0.06	0.02	0.02	0.39	0.67	1.91	0.33	0.03	0.32
Na2O	0.28	0.35	0.03	0.14	0.25	0.55	0.40	0.14	0.13
K2O	1.54	4.33	0.41	5.02	0.13	1.52	0.10	0.08	0.40
P2O5	0.05	0.03	0.02	0.24	0.43	1.17	0.00	0.05	0.55
H2O+	1.50	3.05	0.56	3.59	0.61	2.53	1.65	0.54	4.34
H2O-	0.10	0.13	0.02	0.16	0.02	0.11	-0.01	0.02	0.10
Total	101.29	99.65	100.09	100.26	100.80	99.96	97.46	95.10	97.10
Trace elements (ppm)									
Rb	76	178	38	457	12	123	5	8	17
Ba	83	583	82	249	112	556	12	88	276
Sr	34	67	2	15	27	31	29	5	115
Th	41	21	<4	37	5	6	10	39	348
U	5	4	<3	5	<4	<5	<3	5	<5
Zr	1310	601	45	739	369	290	384	560	221
Nb	62	20	2	58	26	18	14	9	5
Mo	1	<1	<1	5	4	5	<1	43	78
Sc	28	11	0.8	37	24	25	7.8	4.6	11
Ni	2.3	1.9	7.2	38	3.8	17	24	<2	<2.4
Pb	22	34	<5	26	75	97	9	9	1.03%
Zn	39	3.5	218	1730	182	598	76	3.2%	1.33%
Cu	1.9	<1.1	19	16	38	<2	<1	70	522
Y	33	12	<2	70	32	46	16	22	25
La	43	28	<2	38	39	19	6.2	19	16
Ce	96	61	7	92	103	69	17	44	51
Nd	44	27	<3	41	63	46	8.7	19	30

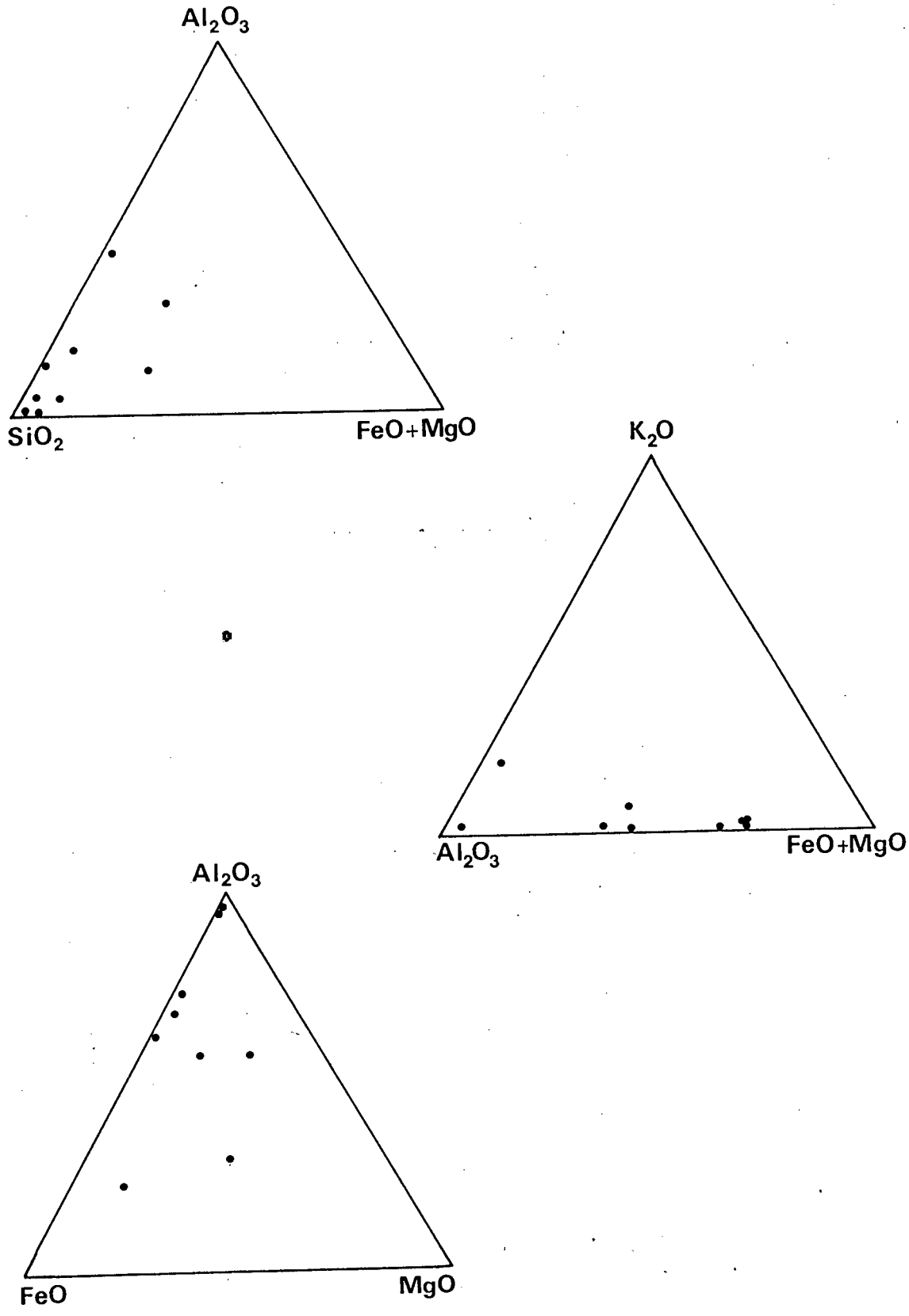

Figure 14: Whole rock compositions of some samples from Achab plotted on triangular diagrams.

Table 14. Average (or Representative) analyses of minerals studied in Achab rocks.

	GARNET				CORDIERITE		PLAGIOCLASE		GEDRITE		SILLIMANITE
n	18		14		6		3		2		1
SAMPLE	ABN 4		ABN 6		ABN 6		ABN 6		ABN 6		ABN 16
		σ		σ		σ		σ		σ	
SiO2	35.89	0.62	37.08	0.54	48.98	0.28	55.66	0.49	43.13	0.84	36.14
TiO2	0.01	0.01	nd		nd		nd		0.23	0.08	nd
Al2O3	21.42	0.25	21.65	0.45	32.97	0.15	27.48	0.31	15.75	0.47	62.67
FeO	30.45	1.26	32.52	1.20	6.08	0.22	nd		23.76	0.05	0.34
MnO	9.51	1.56	2.07	0.36	0.11	0.06	nd		0.55	0.03	nd
MgO	1.94	0.37	5.64	0.63	9.81	0.08	nd		13.33	0.00	nd
CaO	1.29	0.44	1.66	0.11	nd	0.40	9.50	0.40	0.52	0.00	nd
ZnO	nd		nd		nd		nd		0.09	0.00	nd
Na2O	nd		nd		0.35	0.06	5.93	0.20	1.72	0.02	nd
K2O	nd		nd		nd		0.04	0.00	nd		nd
Total	100.51		100.62		98.30		98.61		99.08		99.15

	BIOTITE											
Nr.anal.	4		4		9		4		5		2	
SAMPLE	ABN 3		ABN 4		ABN 6		ABN 9		ABN 10		ABN 13	
		σ		σ		σ		σ		σ		σ
SiO2	36.06	1.23	34.55	0.06	37.15	0.55	35.42	0.43	35.66	0.74	36.65	0.65
TiO2	0.78	0.03	2.22	0.23	1.29	0.18	2.17	0.74	3.10	0.66	3.14	0.18
Al2O3	20.62	0.60	21.00	2.74	17.69	0.25	18.57	0.32	19.53	0.31	19.87	1.10
FeO	18.34	1.20	21.03	1.19	14.69	0.47	14.12	0.50	20.22	0.85	18.59	0.02
MnO	0.29	0.08	0.26	0.09	nd		0.15	0.05	0.29	0.05	0.28	0.03
MgO	8.17	1.31	7.82	0.62	15.32	0.28	12.90	0.98	9.00	0.77	6.92	0.37
CaO	nd		nd		nd		nd		nd		nd	
ZnO	0.16	0.01	0.10	0.09	0.09	0.01	0.06	0.07	0.13	0.08	nd	
Na2O	0.23	0.08	0.28	0.04	0.42	0.05	0.40	0.04	0.31	0.03	0.22	0.09
K2O	7.90	1.45	8.43	0.59	7.79	0.46	7.95	0.13	8.97	0.09	7.72	0.13
Total	92.55		95.69		94.44		91.74		97.21		93.39	

nd: element was not detected or the amount detected was below the detection limit of the analytical method employed.
σ: is a statistical measure of 'n' number of analyses
All Fe is analysed as FeO.

Table 14. Average (or Representative) analyses of minerals studied in Achab rocks.

	BIOTITE		MUSCOVITE							
n	5		1	3		1	1	2		
SAMPLE	ABN 16		ABN 1	ABN 2		ABN 4	ABN 12	ABN 16		
		σ			σ				σ	
SiO2	34.13	0.25	44.28	43.84	0.61	45.51	43.59	45.14	0.17	
TiO2	3.33	0.22	1.71	1.74	0.04	0.66	1.76	1.16	0.11	
Al2O3	19.32	0.23	35.73	34.90	0.26	37.14	34.53	36.47	0.86	
FeO	22.81	0.60	0.95	1.25	0.15	2.10	0.92	1.37	0.18	
MnO	0.23	0.03	nd	nd		0.06	nd	nd		
MgO	6.77	0.15	0.56	0.58	0.06	0.69	0.64	0.49	0.01	
CaO	nd		nd	nd		nd	nd	nd		
ZnO	0.12	0.17	nd	nd		nd	nd	0.02	0.00	
Na2O	0.22	0.02	0.80	0.59	0.02	0.52	0.54	0.67	0.01	
K2O	8.53	0.11	9.24	9.07	0.07	8.30	9.05	10.16	0.12	
Total	95.46		93.27	91.97		94.98	91.03	95.48		

	GAHNITE											
n	6		5		2		11		3		4	
SAMPLE	ABN 3		ABN 4		ABN 6		ABN 8		ABN 9		ABN 10	
		σ		σ		σ		σ				σ
Al2O3	55.42	0.47	56.13	0.37	56.83	0.36	56.06	0.27	58.33	0.52	55.79	0.26
Cr2O3	nd		0.29	0.11	nd		0.04	0.05	nd		nd	
FeO	15.18	1.87	13.48	2.13	22.68	1.58	9.65	0.21	13.82	0.29	11.25	2.45
MnO	0.38	0.12	0.32	0.04	0.14	0.01	0.20	0.04	0.31	0.03	0.36	0.05
MgO	2.15	0.24	1.21	0.22	6.27	0.72	1.36	0.03	3.62	0.24	1.98	0.18
ZnO	25.46	2.15	28.30	2.54	13.22	1.91	32.83	0.21	24.67	0.38	30.16	2.88
Total	98.59		99.73		99.14		100.14		100.75		99.54	

nd: element was not detected or the amount detected was below the detection limit of the analytical method employed.
σ: is a statistical measure of 'n' number of analyses
All Fe is analysed as FeO

Table 14. Average (or Representative) analyses of minerals studied in Achab rocks.

	GAHNITE									
n	13		4		7		7		8	
SAMPLE	ABN 11		ABN 12		ABN 13		ABN 14		ABN 16	
		σ		σ		σ		σ		σ
Al2O3	56.54	0.42	57.20	0.31	56.91	0.29	59.01	0.98	56.50	0.53
Cr2O3	nd		0.11	0.01	0.04	0.05	0.02	0.04	0.06	0.05
FeO	15.08	1.02	12.24	0.26	13.41	1.00	10.27	0.34	14.93	0.20
MnO	0.26	0.03	0.20	0.03	0.42	0.03	0.30	0.03	0.26	0.04
MgO	1.45	0.14	2.04	0.04	1.74	0.03	1.65	0.03	1.41	0.14
ZnO	25.94	0.98	27.86	0.28	27.21	0.52	29.61	0.52	26.87	0.23
Total	99.27		99.65		99.73		100.86		100.03	

nd: element was not detected or the amount detected was below the detection limit of the analytical method employed.
σ: is a statistical measure of 'n' number of analyses
All Fe is analysed as FeO

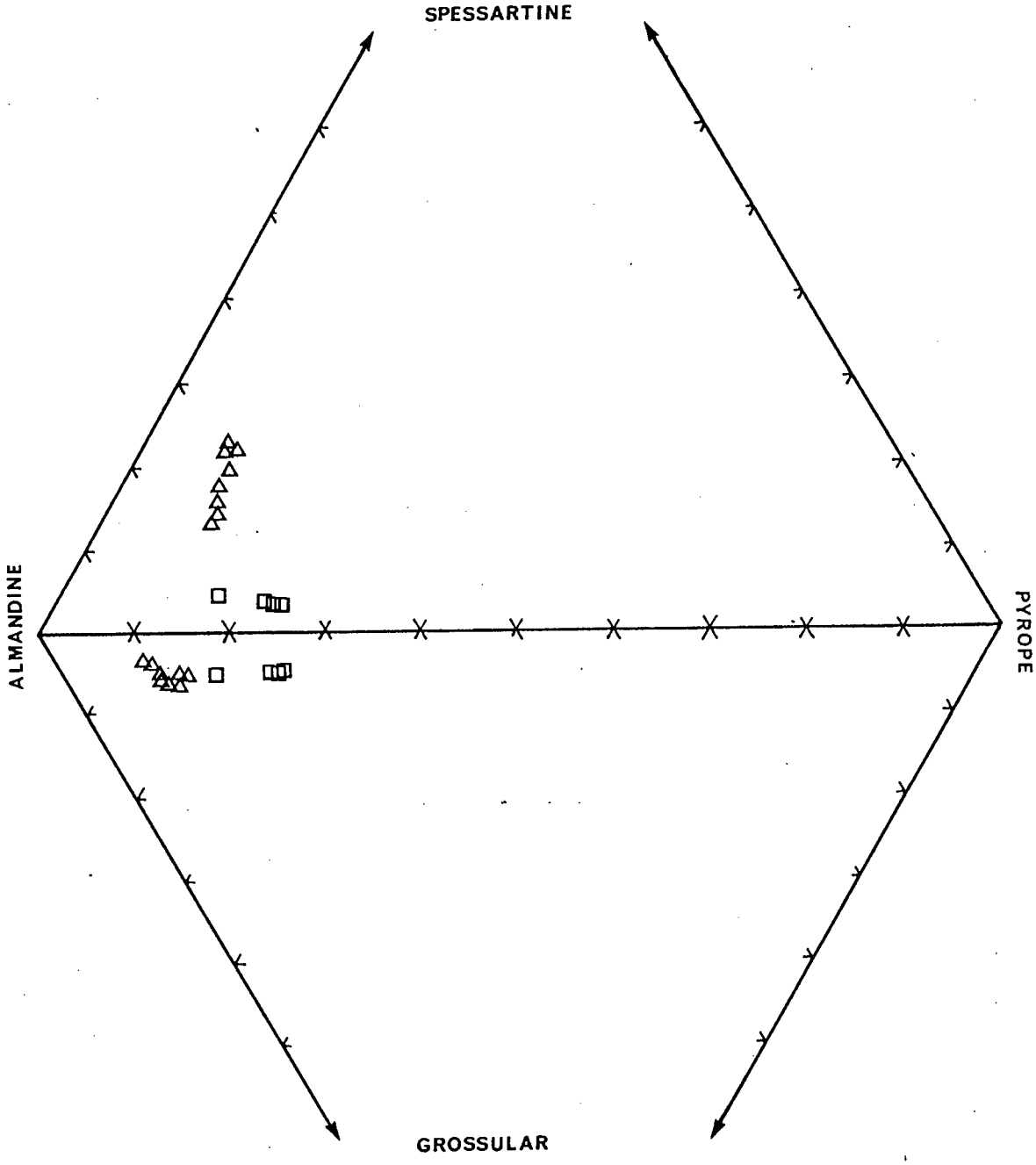

Symbols:
open squares : garnet-gedrite schist
open triangles: biotite-muscovite-sillimanite schist

Figure 15: Garnet compositions (Achab) plotted on a triangular endmember diagram.

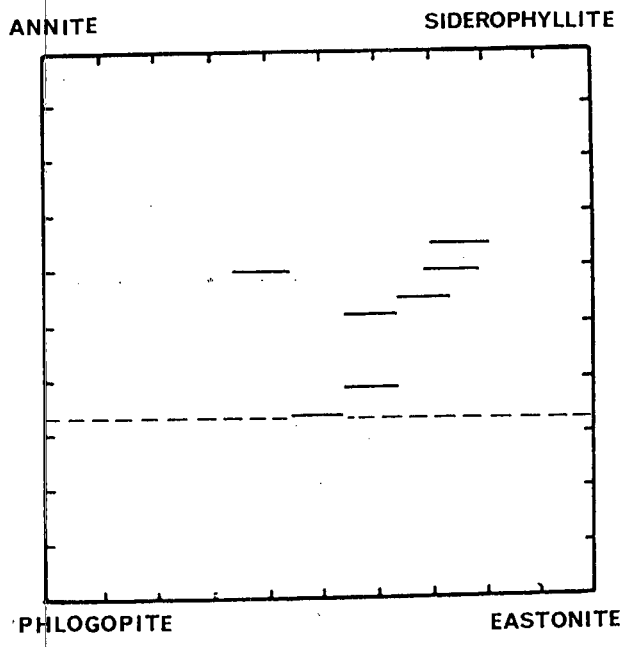

Figure 16: Biotite compositions (Achab) plotted on an endmember diagram.

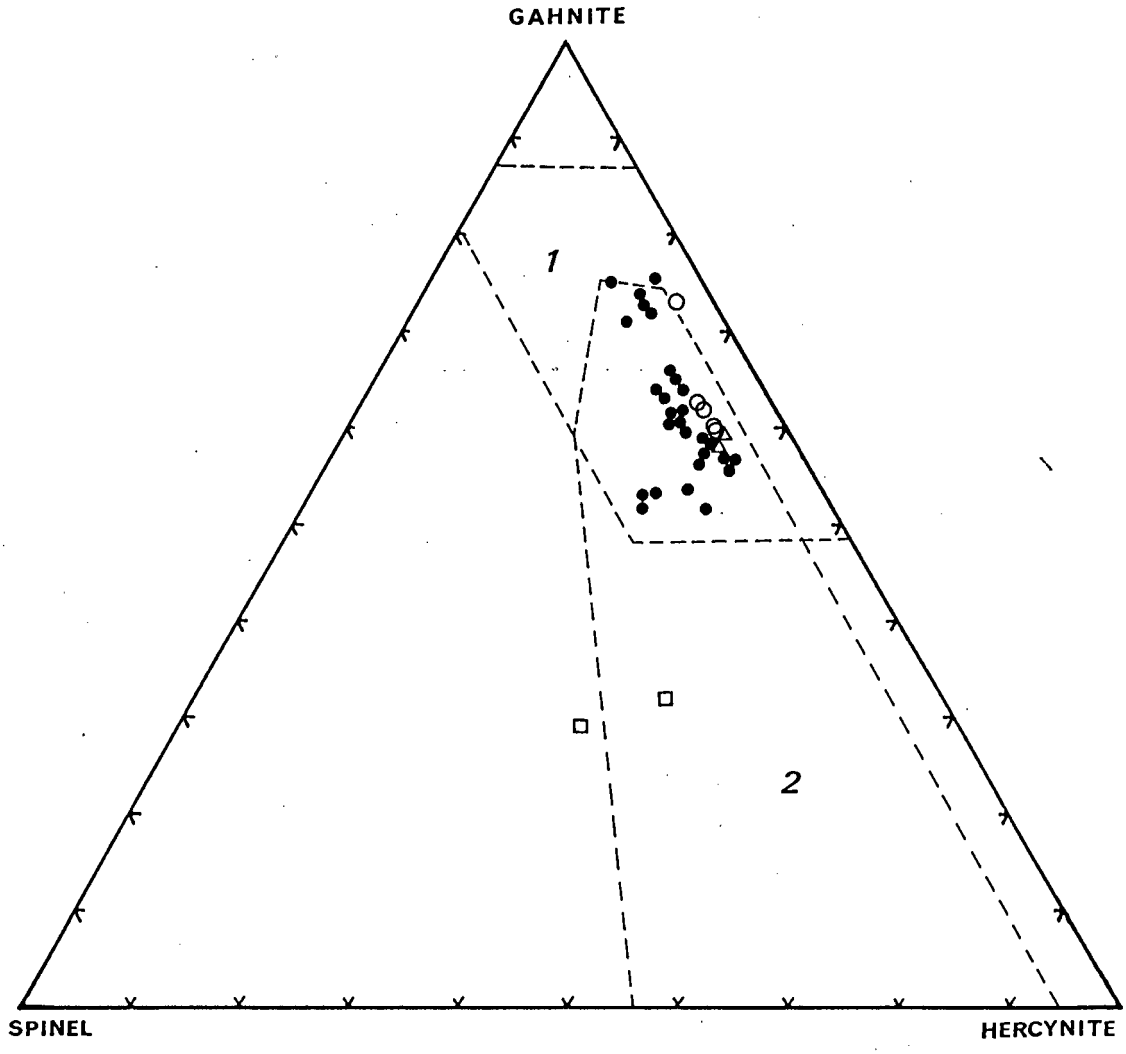

Symbols:
dots : gahnite quartzites
open circles : biotite-muscovite-sillimanite-gahnite schist
open triangles: biotite-muscovite-garnet-sillimanite schist
open squares : garnet-gedrite schist

Field 1: gahnite associated with metamorphosed massive sulphide deposits (Spry, 1984).
Field 2: gahnite associated with aluminous metasediments (Spry, 1984).

Figure 17: Gahnite compositions (Achab) plotted on a triangular endmember diagram.

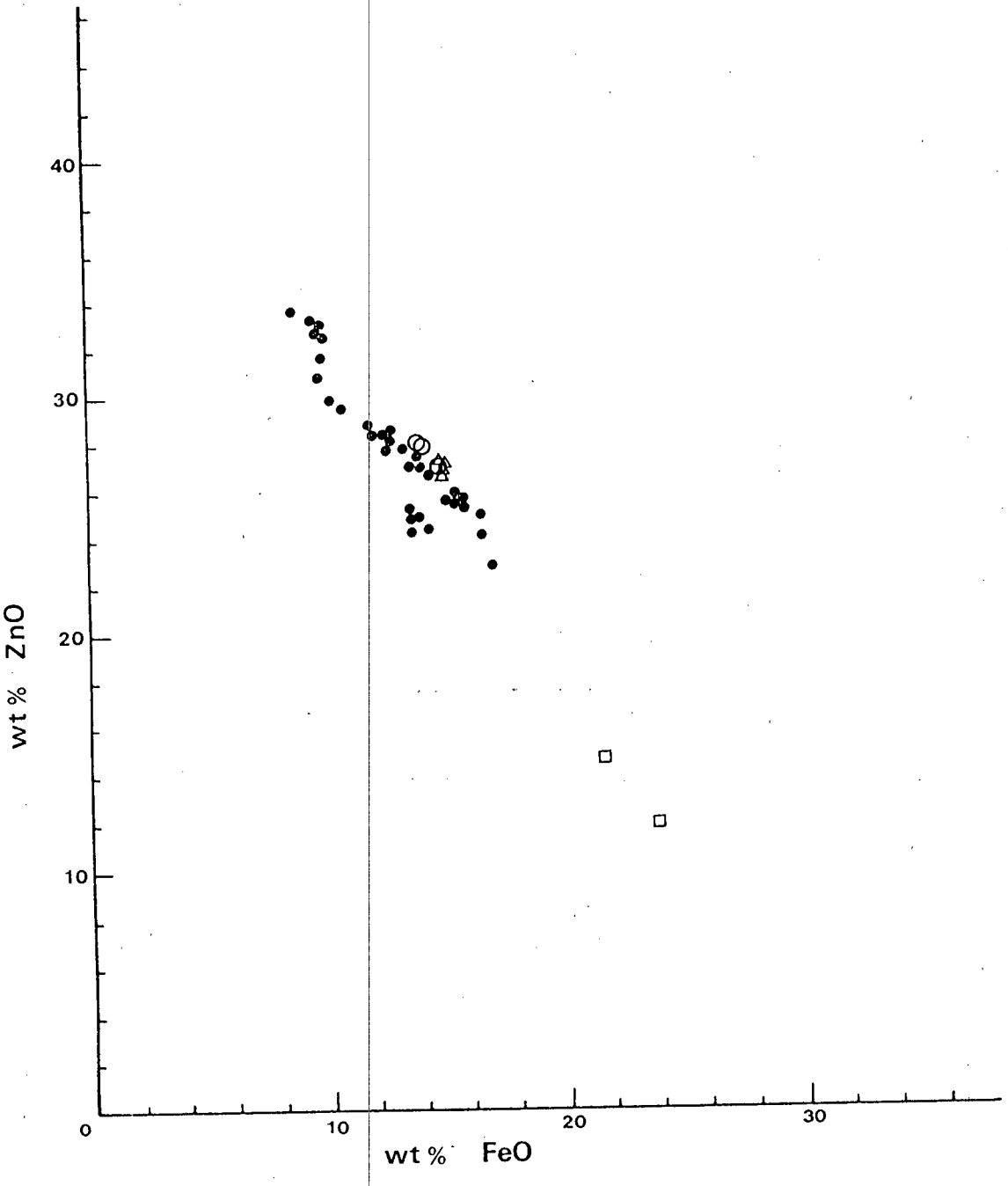

Symbols:
dots : gahnite quartzites
open circles : biotite-muscovite-sillimanite-gahnite schist
open triangles: biotite-muscovite-garnet-sillimanite schist
open squares : garnet-gedrite schist

Figure 18: Gahnite compositions (Achab)., ZnO/FeO.

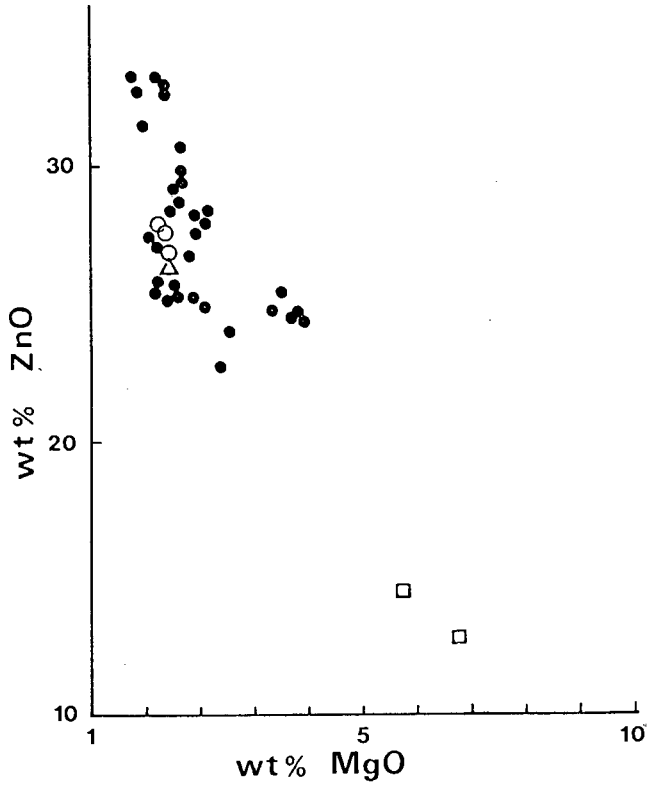

Symbols:
dots : gahnite quartzites
open circles : biotite-muscovite-sillimanite-gahnite schist
open triangles: biotite-muscovite-garnet-sillimanite schist
open squares : garnet-gedrite schist

Figure 19: Gahnite compositions (Achab), ZnO/MgO.

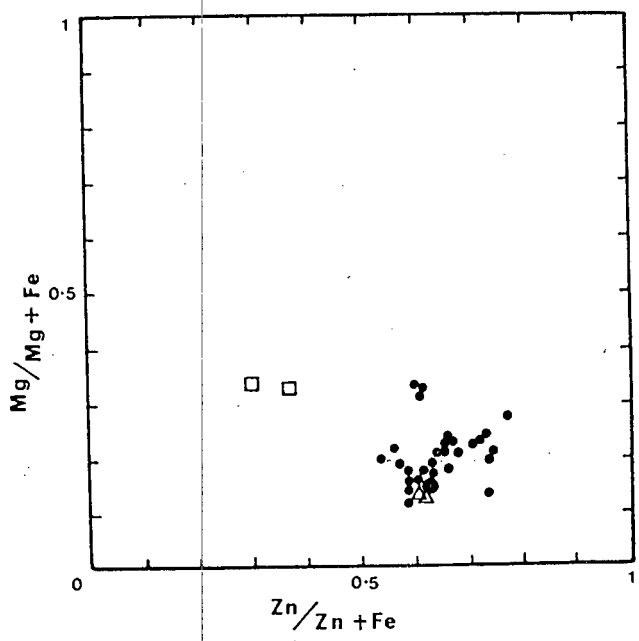

Symbols:
dots : gahnite quartzites
open circles : biotite-muscovite-sillimanite-gahnite schist
open triangles: biotite-muscovite-garnet-sillimanite schist
open squares : garnet-gedrite schist

Figure 20: Gahnite compositions (Achab), Mg/Mg+Fe vs. Zn/Zn+Fe.

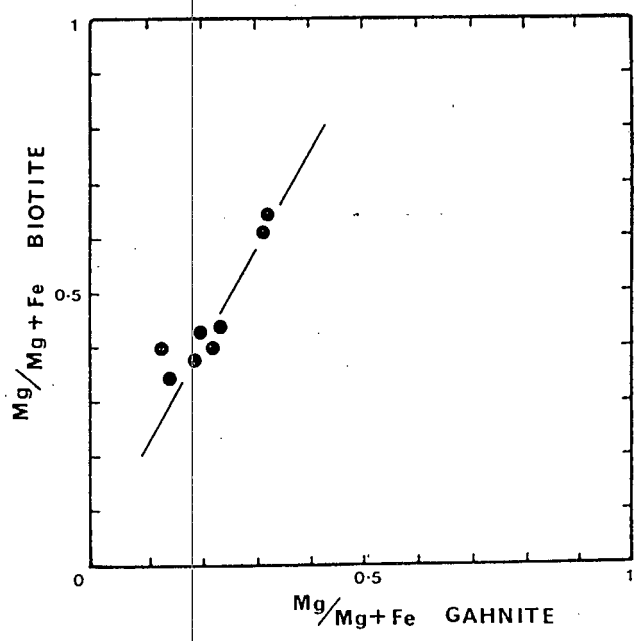

Figure 21: Cation ratios of biotite:gahnite, (Achab).

5 - 3 kbar pressure. Sillimanite is stable throughout the M1 and M2 events. The M3 event is characterised by sericitization and chloritization of feldspars and sillimanite. Moore (1977) estimates that greenschist grade metamorphism with temperatures below 500 °C and pressures below 3 kbar existed during the M3 metamorphic event.

Assemblages observed in the metapelitic rocks at Achab include;
Biotite + muscovite + garnet (+ sillimanite, gahnite)
Sillimanite + muscovite + biotite + gahnite
Garnet + gedrite + quartz + biotite + cordierite + plagioclase (+ilmenite, magnetite, hercynite)
Sillimanite + quartz + rutile + ilmenite
Muscovite + sericite + rutile + ilmenite

The reaction determining the transition from medium to high grade metamorphism in metapelitic rocks is; muscovite + biotite + quartz = K-feldspar + almandine + sillimanite + H_2O (Winkler, 1967). This takes place at around 640-650 °C at between 3.5 and 5 kbar (Winkler op. cit.). The association of biotite, muscovite, sillimanite, almandine and/or gahnite in the pelitic schists indicates that metamorphic conditions close to this transition were reached at this locality.

In the metapelitic biotite-muscovite-sillimanite schists, garnet contains in excess of 20 mol% spessartine indicating possible re-equilibration (during M2 metamorphism) and making it unsuitable for geothermometric calculations. However, the garnet-gedrite rock contains the assemblage: quartz + plagioclase + biotite + cordierite + garnet or gedrite. The presence of plagioclase confirms this assemblage as part of Moore's (1977) upper amphibolite grade facies. This is plotted on an AFM diagram (Fig.22). Garnet-biotite pairs from the garnet-gedrite rock were analysed to determine metamorphic temperatures. Garnet contains approximately 80 mol% almandine in this assemblage. Geothermometry by methods of Holdaway and Lee (1977) and Ferry and Spear (1978) indicate a maximum calculated temperature of 670 °C at 4.5-5 kbar pressure (Table 15). Results employing the method of Thompson (1976) are consistent with those using a recent method by Indares and Martingole (1985a) which takes into account substitution of Ti and Al in biotite and Ca and Mn in garnet. Table 15

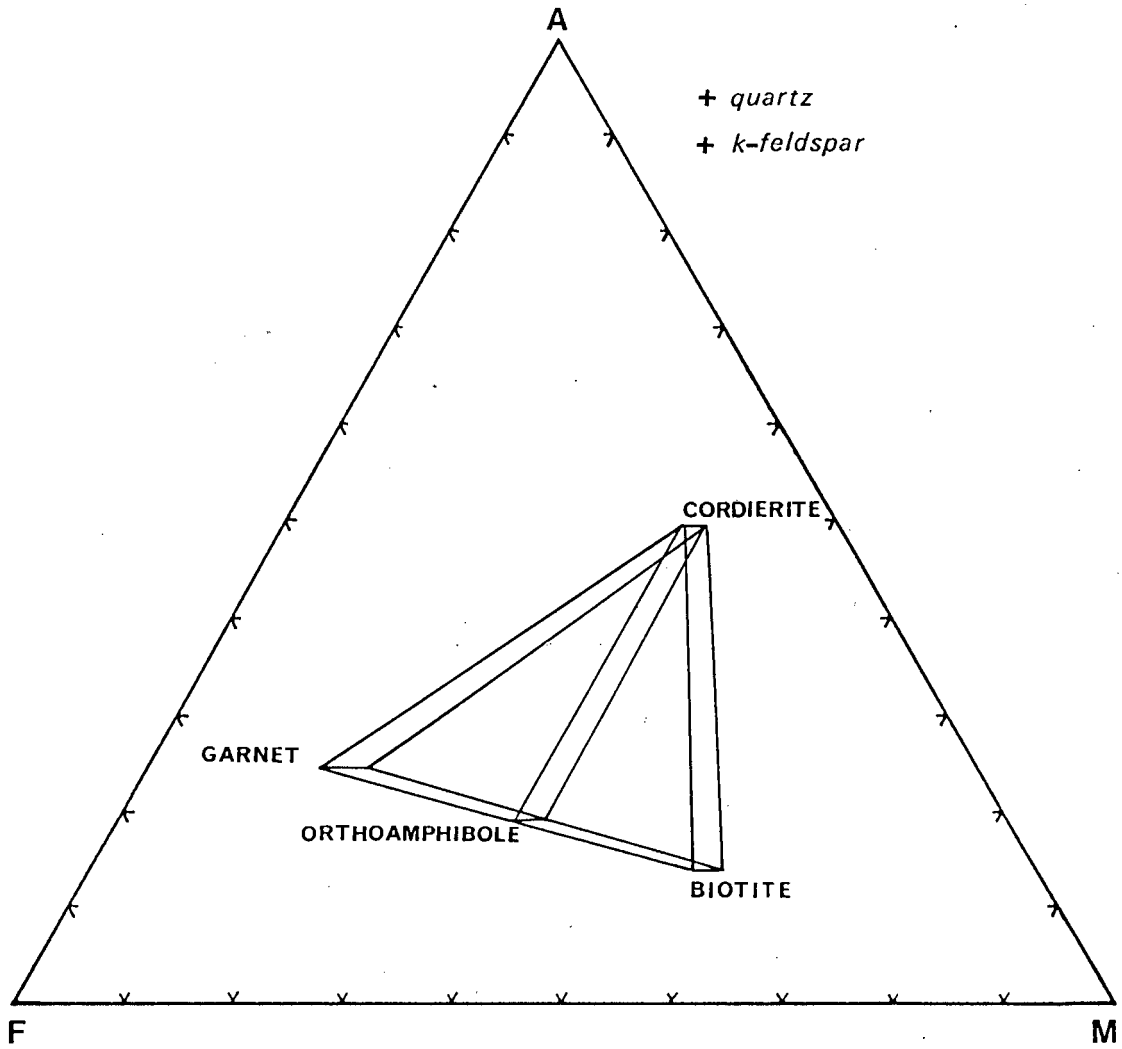

Figure 22: Mineral compositions in the garnet-gedrite schist (Achab), plotted on an AFM diagram (Thompson, 1976).

Table 15: Results of garnet-biotite geothermometry on pelitic rocks from Achab.

Method Employed	Calculated Temperature at 4.5 kbar	
	garnet-biotite (5 mineral pairs)	garnet-cordierite (5 mineral pairs)
Holdaway & Lee (1977)	669°C	
Thompson (1976)	565°C	638°C
Ferry & Spear (1978)	646°C	
Indares & Martingole (1985a)	560°C	

lists results of the calculations. The calculated temperature employing the latter method is 560 °C at 5.5 kb indicating re-equilibration during Moore's (1977) M2 event. The former temperature appears to be more compatible with the observed assemblage and is preferred as an indication of the highest temperature attained during metamorphism of the rocks.

Oxygen fugacities were calculated using the BAMM buffer proposed by Zen (1985). Results of calculations on prograde assemblages in the metapelitic schists and quartzites show that relatively oxidising conditions were associated with the M2 metamorphic event, i.e. $\log f(O)_2 = -15.8$ to -16.4 at 670°C. Table 16 lists results of the calculations.

4.3.4 Gahnite Formation

Gahnite is associated with biotite, sillimanite and garnet in the schists and biotite and muscovite in the quartzites at Achab. No disequilibrium features are observed between gahnite and quartz. It appears that gahnite is stable in the assemblage observed.

Dietvorst (1980) found that small quantities of gahnite formed by breakdown of zinc-bearing biotite (0.14 - 0.24 wt% ZnO), sillimanite and cordierite to form cordierite and spinel. At Achab, biotite contains up to 0.7 wt% ZnO in some cases, but the large quantities of gahnite in these rocks (up to 15%) and the absence of evidence for biotite breakdon preclude gahnite formation by this method alone.

Small quantities of Pb and Cu were found in whole rock analyses of the quartzites and as Gamsberg is situated only 8 km north-west of the sampling locality, it seems probable that the rocks at Achab contained sulphides in their precursor sediments. The gahnite-bearing quartzite horizon appears to be correlated stratigraphically with the sulphide-bearing quartzites which underly the ore horizons at Gamsberg (Moore, pers. comm.). A reasonable method of gahnite formation would be that it formed from ZnS-bearing sediments (shales) along with prograde biotite, sillimanite and garnet during the high grade metamorphic event. It is proposed that zinc entered the structure of biotite during prograde

Table 16: Results of oxygen fugacity calculations on Achab rocks.

Metapelitic Rocks

Assemblages:

(i) Biotite + muscovite + garnet + sillimanite + gahnite + ilmenite + rutile
(ii) Cordierite + plagioclase + biotite + garnet + anthophyllite + ilmenite

Sample nr:	ABN-4	ABN-16	ABN-6	ABN-2	ABN-1
Corrections for substitution in Biotite					
-4 log X_{Si}	0.22	0.23	0.15		
-3 log X_{Fe}	1.02	0.93	1.56		
Corrections for substitution in Garnet					
-3 log X_{Fe}	0.47		0.37		
Corrections for substitution in muscovite					
+2 log X_{Al}	-0.04			0.14	-0.08
+4 log X_{Si}	0.01			0.15	
Total correction	1.66	1.16	2.08	0.30	-0.12

Average Correction = 1.75

Reference BAMM buffer at 670 °C and 5.5 kbar:
Log $f(O)_2$ = 10.29 - 26284/T + 0.148(P-1)/T ± 650/T = -17.58 ± 0.7

Corrected log $f(O)_2$ = -15.83 ± 0.7

Quartzites

Assemblage:

Quartz + gahnite + sillimanite + biotite + muscovite + rutile

Sample nr:	ABN-3	ABN-12	ABN-9	ABN-10	ABN-13
Corrections for substitution in Biotite					
-4 log X_{Si}	0.17		0.18	0.25	0.13
-3 log X_{Fe}	1.03		1.56	1.01	1.21
Corrections for substitution in muscovite					
+2 log X_{Al}		-0.08			-0.06
+4 log X_{Si}		-0.01			-0.01
Total correction	1.20	-0.07	1.74	1.26	1.29

Average Correction = 1.21

Reference BAMM buffer at 670 °C and 5.5 kbar:
Log $f(O)_2$ = 10.29 - 26284/T + 0.148(P-1)/T ± 650/T = -17.58 ± 0.7

Corrected log $f(O)_2$ = -16.37 ± 0.7

metamorphism. Dietvorst (1980 and Plimer (1977) document prograde biotite, associated with mineralization, containing small quantities of zinc. Dietvorst (op. cit.) found that gahnite formed as a reaction product of the breakdown of biotite to chlorite during retrograde metamorphism. Evidence of Fe-Mg exchange between gahnite and biotite (Fig.21.) is interpreted to result from Zn-Fe-Mg exchange initiated by overstepping the zinc saturation level of biotite during subsequent low grade metamorphism (Moore's M2 event).

Thus initial gahnite formation is the same as that which is suggested at Aggeneys i.e.;
$ZnS + Al_2Si_2O_5(OH)_4$ (kaolinite in argillaceous sediments) $+ 0.5\ O_2 \rightarrow ZnAl_2O_4 + 2SiO_2 + 0.5S_2 + H_2O$ ....(Spry, 1987a).

In the garnet-gedrite rock small quantities of gahnite occur as inclusions in the gedrite porphyroblasts. Williams (1983) proposed that gahnite formed as inclusions in gedrite associated with sphalerite by reaction; gedrite + sphalerite + O_2 -> gahnite + SiO_2 + H_2O (+ S in fluid). However there is no evidence of gedrite breakdown to form gahnite in the garnet-gedrite rock. It would seem thus, that gahnite in this assemblage has also formed as a prograde mineral. The relatively Mg-rich, Zn-poor composition (Fig.17) of gahnite in this assemblage is attributed to the bulk chemistry of the rock in which it formed.

In some of the gahnite quartzites, poikiloblastic gahnite occurs along fractures. It appears that the fractures or cracks acted as conduits whereby fluids carrying the components necessary for gahnite formation could enter the rock. Although biotite is commonly altered in these rocks it is not necessarily associated with fractures (or gahnite) and the biotite breakdown is interpreted to result from a weathering process. Moore and Reid (1988 in press) have suggested that aluminium may be carried in alkali complexes by metamorphic fluids. It is proposed that retrograde breakdown of prograde aluminous mineral phases in the underlying sediments resulted in fluids carrying Al-alkali and Zn-Fe oxide complexes which permeated the overlying rocks i.e.;
$2KH_2AlO_3 + (Zn,Fe)O + O \rightarrow (Zn,Fe)Al_2O_4 + 2H_2O + 2KOH$ ...(Moore and Reid, 1988 in press). This resulted in re-equilibration and addition to pre-existing gahnite and accounts for some of the variation in gahnite composition observed at this locality (Fig.17).

4.4 SWARTKOPPIES

Massive gahnite and porphyroblastic fibrolite-gahnite rocks occur in the economically exploited, sillimanite-corundum rocks at Swartkoppies, on the farm Pella Mission in northern Namaqualand (Fig.1). The regional geology of this locality is described in chapter 3.3.3.

4.4.1 Petrography

Gahnite-bearing rocks from Swartkoppies include a massive, crystalline gahnite rock, a porphyroblastic gahnite-fibrolite rock, a gahnite-fibrolite rock and a gahnite-sillimanite rock. Modal proportions of the minerals present in the samples studied from this locality are listed in Table 17.

The massive gahnite rock is composed almost entirely of medium grained, dark, blue-green, crystalline gahnite. Gahnite grain size is bimodal, with the majority of grains euhedral to subhedral and between 0.5 and 3 mm in size.
In patches gahnite is subhedral to anhedral and fine grained (0.1 mm), (Plate 4). Round, 0.4 mm, vugh-like structures infilled with rutile needles and corundum occur throughout. Rutile occasionally forms small, 0.1 mm, reddish-brown inclusions in gahnite. Much of the coarser gahnite grains are colour-zoned with darker green cores and pale, almost colourless rims
(Plate 4). Locally yellow-orange goethite infills intergranular spaces and crosscuts gahnite grains.

The porphyroblastic fibrolite-gahnite rock contains isolated, 3.5 - 8 mm, dark green, euhedral gahnite crystals in a massive white fibrolite matrix (Fig.23a). Fibrolite comprises in excess of 90% of this assemblage. Gahnite porphyroblasts contain inclusions of corundum, occasional goethite blebs and fine, needle-like fibrolite. Crystalline gahnite comprises approximately 5% of the rock's constituents. Pale muscovite commonly borders gahnite grains and similarly to gahnite, contains inclusions of fibrolite. Goethite and fine grained rutile occur as minor constituents associated with recrystallized, coarse sillimanite in the matrix. Rare, fine quartz veins transect this rock.

Table 17. Estimated modal proportions of minerals present in samples studied from Swartkoppies.

SAMPLE	SK 2	SK 10	SK 3	SK 4
Sillimanite		95	70	70
Gahnite	95	m	15	25
Biotite			10	m
Rutile	m	m		m
Goethite	m			
Corundum	tr			
Ilmenite			5	

'm' indicates minerals present in minor proportions (5% or less).
'tr' indicates minerals present in trace quantities (1% or less).

ROCK TYPES:

SK 2 : Massive gahnite rock
SK 10 : Porphyroblastic fibrolite-gahnite rock
SK 3 : Sillimanite-gahnite-biotite rock
SK-4 : fibrolite-gahnite rock

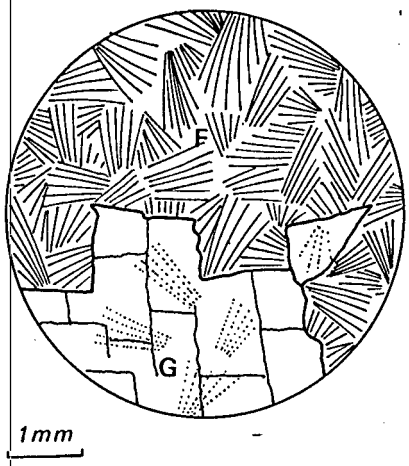

b. Relationship of gahnite to sillimanite and biotite in the sillimanite-gahnite-biotite rock.

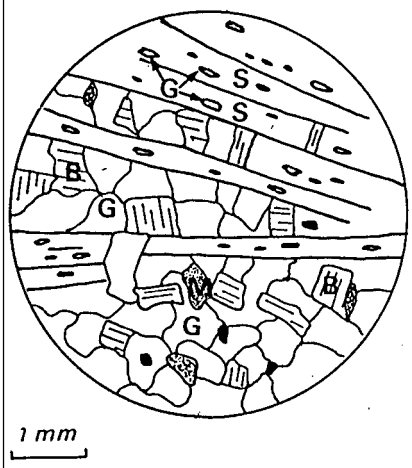

a. Anhedral gahnite porphyroblasts in the fibrolite-gahnite rock.

Abbreviations:
B - biotite, M - magnetite, G - gahnite, S - sillimanite.

Figure 23: Textural relationships of gahnite in samples from Swartkoppi

A sillimanite-gahnite-biotite rock has a matrix composed of recrystallised radiating sillimanite laths and fibrolite. This rock contains approximately 70 mol% sillimanite and 15 mol% gahnite (Fig.23b). Biotite is the only other major mineral phase and comprises approximately 10% of the rock. The presence of sillimanite crystals along with fibrolite probably indicates recrystallization in response to changing metamorphic conditions.

Gahnite aggregates are composed of 0.06 - 0.4 mm, subhedral, bright green grains associated with the coarsely crystalline sillimanite. Anhedral gahnite and magnetite blebs also occur as numerous inclusions along cleavage planes in sillimanite (Fig.23b).

Locally biotite rich areas occur in the matrix. The biotite is orange-brown to pale brown and similar to sillimanite, contains inclusions of gahnite and magnetite. Biotite grains are interrupted and broken up by the coarse sillimanite laths. Larger gahnite grains also contain segments of disrupted biotite laths. Magnetite occasionally occurs as coarse 0.6 mm grains associated with gahnite but no gahnite exsolution is observed in magnetite. Minute grains of rutile occur in association with magnetite. It appears that biotite, sillimanite, magnetite, gahnite and rutile have crystallized as part of the same prograde assemblage.

The fibrolite-gahnite rock is composed of fibrous sillimanite and aggregates of gahnite grains. In contrast to the previous lithology, this rock contains very little biotite and fibrolite is not recrysallized to form sillimanite.

Gahnite aggregates are composed of 0.1 - 0.4 mm, fractured, gahnite grains. Common sillimanite and magnetite inclusions and rare orange-brown biotite occur in the aggregates. Occasional rutile grains are associated with magnetite and spinel. Veins composed of fine grained, polygonal quartz transect the rock. Some of the coarser gahnite grains are colour zoned similar to the massive gahnite rock. No spinel exsolution was observed in magnetite.

4.4.2 Mineral Chemistry

Mineral analyses of biotite and gahnite are given in Table 18.

Biotite

Biotite is annite with approximately 17 wt% FeO and 10 - 13wt% MgO. Average biotite composition (Table 18) is : $K_{1.5}Na_{0.1}Mg_3Fe_2Al_{0.8}(Si_{5.3}Al_{2.7})O_{20}OH)_4$. The zinc content in biotite is below the detection limit of the microprobe for this element (0.02 wt%).

Qualitative analysis for zinc in magnetite and fibrolite similarly indicated a concentration level below the detection limit of the microprobe.

Gahnite

In the samples studied gahnite exhibits a marked range in Zn-content considering the small sampling area. Compositions vary between 0.13 - 0.35 wt% MnO, 1.7 - 3.5 wt% MgO, 15.7 - 25 wt% FeO, 13.2 - 25 wt% ZnO, and range from zincian hercynite to gahnite.

Molecular proportions of Zn, Fe and Mg in gahnite were recalculated as end-member gahnite, hercynite and spinel. The normalised values are plotted on a triangular diagram (Fig.24). The galaxite molecule is insignificant (< 0.4 wt% MnO) and is not included.

Gahnite compositions vary from a zincian hercynite in the sillimanite-gahnite-biotite rocks to gahnite in the massive gahnite rock and porphyroblastic fibrolite-gahnite rock. All spinel compositions plot on the Fe-rich (hercynite) side of the diagram and show very limited variation in Mg content. The compositional range of gahnite studied from this locality falls within the area indicated by Spry (1984) for gahnite occurring in aluminous metasediments (Fig.24). In the aluminous rocks at Swartkoppies, gahnite exhibits a far greater range in Zn content than the sulphide associated gahnite at Broken Hill or gahnite in quartzites at Achab.

Table 18. Average (or representative) analyses of biotite and gahnite from Swartkoppies.

BIOTITE

n	4		1
SAMPLE	SK 3		SK 4
		σ	
SiO2	35.42	0.44	35.35
TiO2	1.53	0.37	2.41
Al2O3	19.72	0.22	19.78
FeO	16.60	0.48	17.83
MnO	0.14	0.02	0.09
MgO	12.60	0.48	10.23
CaO	nd		nd
ZnO	nd		nd
Na2O	0.32	0.06	0.33
K2O	8.25	0.16	8.23
Total	94.58		94.20

GAHNITE

n	13		12		11		2	
SAMPLE	SK 2		SK 3		SK 4		SK 10	
		σ		σ		σ		σ
Al2O3	58.28	0.45	57.76	0.28	57.64	0.54	56.32	0.02
Cr2O3	0.05	0.05	0.24	0.03	0.11	0.03	nd	
FeO	15.68	0.48	25.02	0.35	20.86	0.65	15.98	0.48
MnO	0.13	0.06	0.35	0.03	0.26	0.03	0.19	0.03
MgO	2.01	0.07	3.49	0.11	2.82	0.11	1.73	0.08
ZnO	24.31	0.38	13.24	0.28	18.40	0.34	25.02	0.96
Total	100.46		100.10		100.09		99.24	

nd: element was not detected or the amount detected was below the detection limit of the analytical method employed.
σ: is a statistical measure of the range of 'n' number of analyses.
All Fe is analysed as FeO.

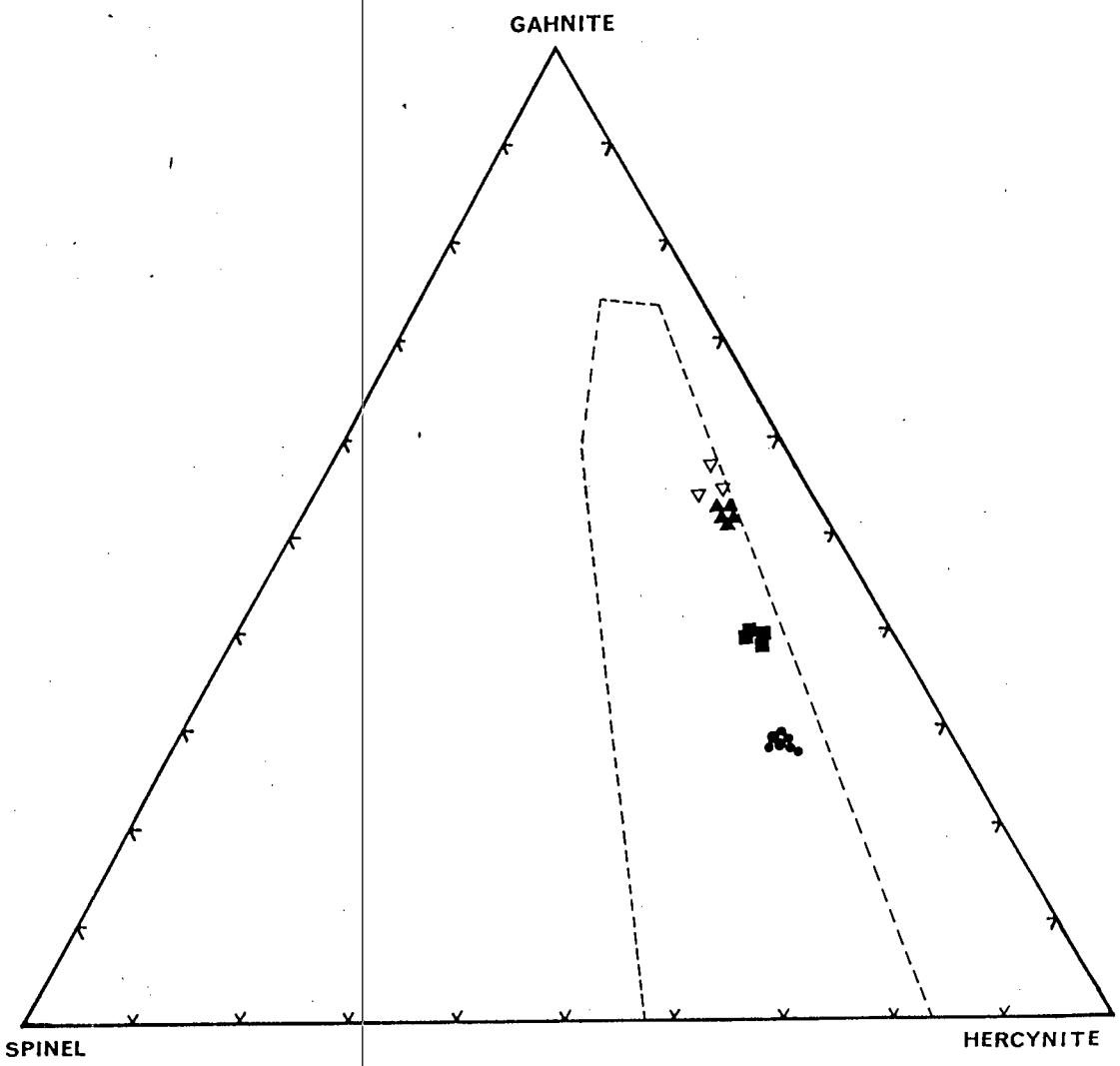

Symbols:
open triangles : porphyroblastic fibrolite-gahnite rock
closed triangles: massive gahnite rock
closed squares : fibrolite-gahnite rock
dots : sillimanite-gahnite-biotite rock

demarcated field: gahnite associated with aluminous metasediments (Spry, 1984).

Figure 24: Gahnite compositions (Swartkoppies) plotted on a triangul endmember diagram.

The zinc-rich gahnite in the porphyroblastic fibrolite-gahnite rock has the compositional range $Ghn_{54-58}Hc_{35-38}Sp_{7-10}$ and in the massive gahnite rock $Ghn_{51-55}Hc_{36-40}Sp_{8-10}$. Zincian hercynite from the fibrolite-gahnite fibrolite rock has a compositional range of $Ghn_{38-41}Hc_{49}Sp_{13}$. In the recrystallised sillimanite-gahnite-biotite rock, zincian hercynite has the compositional range; $Ghn_{27-30}Hc_{54-58}Sp_{14-17}$.
Plotting gahnite compositions in terms of their cation variability indicates an inverse relationship between Fe and Zn (Fig.25), and between Mg and Zn (Fig.26). On both diagrams compositions of gahnite in the massive gahnite and porphyroblastic gahnite-fibrolite rocks overlap to some extent and contain the highest zinc contents. A plot of the Mg/Mg+Fe vs. Zn/Zn+Fe ratio of gahnite (Fig.27) indicates little variation in Mg/Fe ratio in gahnite from Swartkoppies.

Zoning in gahnite

Minor compositional zoning occurs in colour zoned gahnite grains. In the porphyroblastic gahnite-fibrolite rock this is shown by an increase of 0.5 - 2 wt% ZnO and a similar decrease in iron content from core to rim, corresponding to the colour variation of dark green cores and pale to colourless rims. Zoning is discussed in more detail in chapter 5.3.

4.4.3 Metamorphism

The sillimanite-corundum rocks at this locality are hosted in a sillimanite-biotite-garnet metapelitic schist. No geothermometric estimations or calculations have been applied to Swartkoppies rocks in previous studies and unfortunately none of the metapelitic schist samples were available for this study. Similar sillimanite-corundum rocks are, however, found in the aluminous schist at Achab and Aggeneys (Moore 1977, 1980, 1986) and the metapelitic schist at Swartkoppies is correlated with the Namies schist at Achab (Moore, 1977) and the Aluminous schist at Aggeneys (Joubert, 1970) by SACS (1980). At the two last named localities three metamorphic events have been determined (Moore 1977, SACS 1980, Ryan et al., 1982) with a maximum grade of upper amphibolite facies.

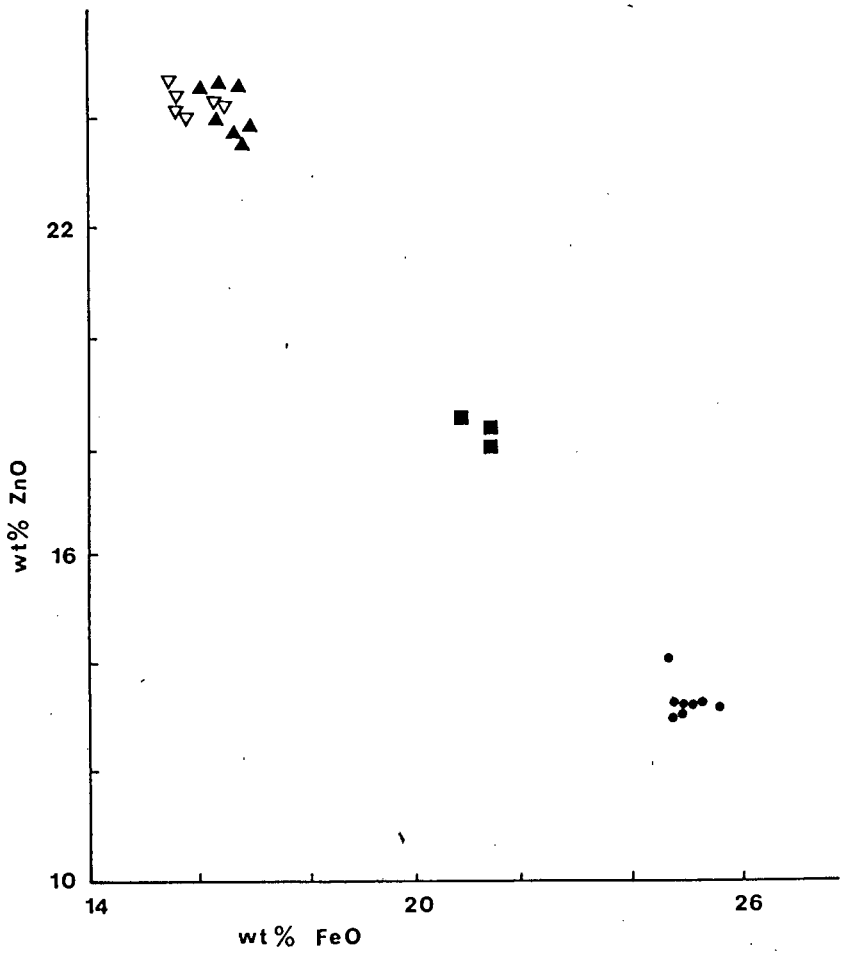

Symbols:
open triangles : porphyroblastic fibrolite-gahnite rock
closed triangles: massive gahnite rock
closed squares : fibrolite-gahnite rock
dots : sillimanite-gahnite-biotite rock

Figure 25: Gahnite compositions (Swartkoppies), ZnO/FeO.

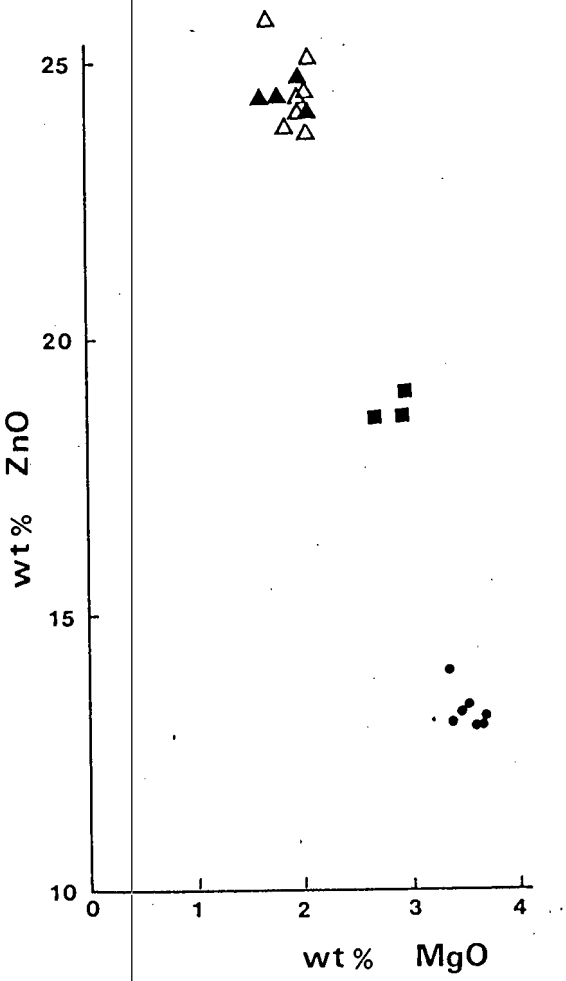

Figure 26: Gahnite compositions (Swartkoppies), ZnO/MgO.

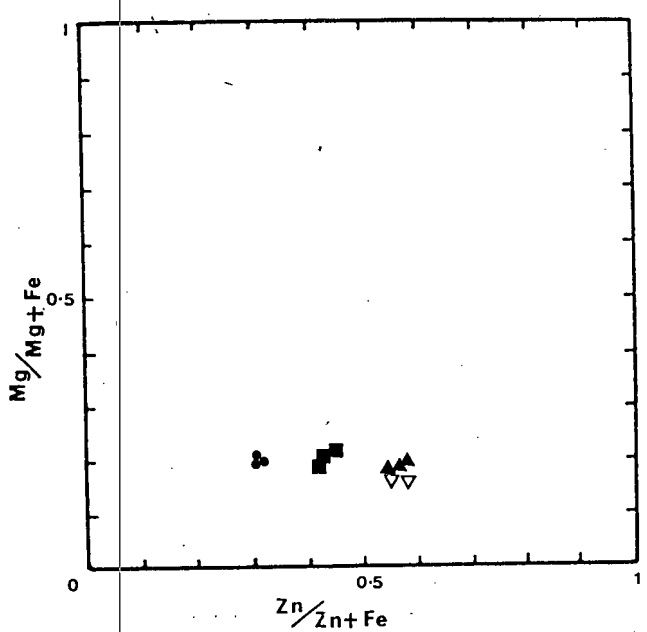

Symbols:
open triangles : porphyroblastic gahnite-fibrolite rock
closed triangles: massive gahnite rock
closed squares : gahnite-fibrolite rock
dots : gahnite-sillimanite-biotite rock

Figure 27: Gahnite compositions (Swartkoppies), Zn/Zn+Fe vs. Mg/Mg+F

Co-existing sillimanite-biotite-garnet at Swartkoppies indicates that similar metamorphic grades were attained in the area. Regional metamorphism of amphibolite to upper amphiblite grade is assumed in the Swartkoppies area with temperatures of 650 ±50 °C and pressures of 4 - 5 kbar, based on the calculations made in chapters 4.2.3 and 4.3.3.

4.4.4 Gahnite Formation

Similar gahnite-bearing, garnet-sillimanite schists and gneisses to those at Swartkoppies, are associated with the metamorphosed massive sulphide deposit at Broken Hill, Australia (Plimer 1977, Segnit 1961). Segnit (1961) proposed that the garnet-sillimanite rocks formed as a result of metamorphism of argillaceous (kaolinite-rich) sediments and that gahnite formed, during metamorphism, from zinc absorbed onto clay minerals e.g.; $Al_2Si_2O_5(OH)_4 + ZnO(\text{in kaolinite}) = ZnAl_2O_4 + SiO_2 + 2H_2O$.

The absence of a zinc-bearing aluminous phase at Swartkoppies (sillimanite, biotite and magnetite did not contain zinc) reduce the probability of gahnite formation by breakdown of a zinc-bearing precursor mineral phase, but do not necessarily exclude it. However, the porphyroblastic and massive habit of gahnite, the similarity of the stratigraphic column with that at Achab and Aggeneys (Fig.2) and the presence of concentrations of sulphides in Bushmanland Sequence rocks at a number of localities in Namaqualand (Rozendaal 1982, Moore 1986) suggests that sphalerite might be the precursor Zn phase at this locality. At Aggeneys and Gamsberg small quantities of sulphides occur in the rocks surrounding the ore body (Ryan et al. 1982, Rozendaal 1982) and there is evidence for sulphides occuring in more than one stratigraphic horizon in these ore bodies (Moore, 1986). It is proposed that, similar to the Aggeneys and Achab localities, gahnite formed during prograde metamorphism from ZnS-bearing shales. The presence of magnetite in the sillimanite-biotite-gahnite assemblage indicates oxidising conditions during metamorphism and supports the formation of gahnite and zincian hercynite by a reactions such as;
$2Al_2Si_2O_5(OH)_4 \rightarrow Al_2SiO_5 + Al_2O_3 + 3SiO_2 + 4H_2O$ and
$2Al_2Si_2O_5(OH)_4 + ZnS + 4FeS_2 + 4O_2 \rightarrow 2(Fe,Zn)Al_2O_4 + Fe_3O_4 + 4SiO_2 + 4H_2O + 3/2S_2$.

The host sillimanite-corundum rock contains very little Si in the form of free quartz and it is unlikely that the compositional variation (Fe, Zn) of gahnite between samples can be explained in terms of disequilibrium of gahnite-sillimanite. Rather, it is proposed that limited mobilization of Zn and Al species resulted in the formation of gahnite in an essentially closed-system metamorphic environment. Hence the variation of Zn and Fe components of gahnite at this locality is largely a function of the availability of components (i.e bulk chemistry).

4.5 ORANJEFONTEIN

At Oranjefontein, on Vioolskraalberg, gahnite occurs in small quantities in almost all lithological types overlying the quartzo-feldspathic gneiss. For the purpose of description these rocks are divided into rocks in which gahnite occurs mainly as an accessory phase; the aluminous schist, metapelitic rocks and glassy quartzites, and where blue and green gahnite occurs as major phases; the quartzites and garnet-rich rocks occuring at the interface between the aluminous schist horizon and the overlying massive quartzite unit.
This locality formed part of the investigation into mineralogic anomalies in the Namaqualand Metamorphic Province supported by the CSIR as part of the National Geoscience Programme. The Oranjefontein gahnite occurrence is described in a paper by Hicks et al. (1985) and much of the information contained therein results from this study and that which formed part of an unpublished honours project (Hicks, 1983).

4.5.1 Petrography

A geological map of Vioolskraalberg is shown in Figure 6 and the description of the stratigraphic succession at this locality is given in chapter 3.3.4. A petrographic description of the lithologies, as they appear in the stratigraphic column, is given below. Estimated modal proportions of minerals present in the samples studied at this locality are given in Table 19.

Quartzo-feldspathic gneiss

As these rocks are not of particular relevance to this study, they are only mentioned briefly. The biotite-rich, quartzo-feldspathic rock crops out locally as a nodular pink-weathering leucogneiss. The leucogneiss owes its distinctive pink colour to the presence of K-feldspar (>90 mol% orthoclase). Lens-shaped sillimanite segregations weather positively and give the rock a nodular appearance. Locally these rocks contain some garnet and amazonite.

Table 19. Estimated modal proportions of minerals present in samples studied at Oranjefontein.

	PINK GNEISS		ALUMINOUS SCHIST						
SAMPLE	JE 10	JE 12	JE 76	JE 30	JE 27	JE 11	JE 13	JE 28	JE 29
Quartz	75	55	75	60	60	65	85	75	60
Biotite		m	10	m	10	10	m	m	m
Chlorite				m	m			m	
Muscovite									
Hercynite				tr	tr			tr	
Magnetite				m	m	m		m	m
Cordierite			10	30	20	20	m	m	10
Orthoclase			m				10	m	15
Sillimanite		5							
Garnet	m	m							m
Sericite	20	30	m	m	m	m			
Zircon	tr	tr			tr	tr	tr		
Goethite	tr	tr				tr			
Epidote									
Hematite	tr								
Rutile		tr		tr					

	ALUMINOUS SCHIST		BIOTITE-GARNET-CORDIERITE SCHIST		MASSIVE GARNET ROCK	ALTERED GARNET-BIOTITE ROCKS			
SAMPLE	JE 33	JE 34	JE 31	JE 32	JE 44	JE 36	JE 35	JE 82	JE 50
Quartz	60	75	45	m	10				
Biotite	m	m	30	50		50	30	45	10
Chlorite									
Muscovite									m
Green gahnite					m		10	m	
Blue gahnite									
Hercynite									
Magnetite	m	m			m	m	m	10	
Hematite									
Cordierite	25	10	m	30					
Orthoclase	m								
Sillimanite				m					
Garnet			15	15	80	55	50	30	45
Sericite		m			m		m		45
Zircon	tr		tr	tr		tr			
Goethite			tr	tr	tr	tr		m	tr
Epidote									
Rutile					tr				tr

'm' refers to minerals present in minor proportions (5% or less)
'tr' refers to minerals present in trace quantities (1% or less)

Table 19. Estimated modal proportions of minerals present in samples studied at Oranjefontein.

	ALTERED GARNET–BIOTITE ROCKS					GARNET–BEARING METAQUARTZITES	
SAMPLE	JE 7	JE 9	JE 16	JE 19	JE 18	JE 14	JE 15
Quartz		30	m				
Biotite				60	50	90	90
Chlorite	65		m	10	m	m	m
Muscovite							
Green gahnite				15	20		
Blue gahnite					10	m	m
Hercynite			tr				
Magnetite			m				
Hematite	m						
Cordierite							
Orthoclase							
Sillimanite							
Garnet	15			m	m	tr	tr
Sericite		10					
Zircon							
Goethite	m			m	m		
Epidote	15	60					
Rutile				m	m	m	m
Tourmaline							
Galena			m				m

	METAQUARTZITE					
SAMPLE	JE 20	JE 21	JE 17	JE 38	JE 37	JE 39
Quartz	75	95	95	95	95	95
Biotite					m	m
Chlorite	m	m	m			
Muscovite						
Hercynite						tr
Magnetite						tr
Hematite	m					
Cordierite						
Orthoclase						
Sillimanite						
Garnet	20	tr	tr			
Sericite		tr	tr			
Zircon				tr		
Goethite						
Epidote						
Rutile				tr		
Tourmaline			m	m		
Galena			tr			tr

'm' refers to minerals present in minor proportions (5% or less)
'tr' refers to minerals present in trace quantities (1% or less)

Table 19. Estimated modal proportions of minerals present in samples studied at Oranjefontein.

GAHNITE (+PHLOGOPITE, GARNET) QUARTZITES

SAMPLE	JE 1	JE 2	JE 3	JE 4	JE 6	JE 74	JE 5
Quartz	75	70	55	75	90	90	95
Biotite ...altered	10	10	10	10	m	m	m
Chlorite							
Muscovite							
Green gahnite	m	m	20	m		m	m
Blue gahnite	m	10	10	10	m	m	m
Hercynite							
Magnetite							
Hematite	m	m	m	m			m
Garnet	tr	tr	tr	tr	tr	tr	tr
Rutile	tr	tr	tr	tr	tr	tr	tr
Sericite	tr	tr	tr	tr	tr	tr	tr
Goethite	tr	tr	tr	tr	tr		tr
Galena	m						

SAMPLE	GAHNITE(+PHLOGOPITE,GARNET) QUARTZITES JE 78	JE 51	OF 3	JE 88	GAHNITE QUARTZITES JE 22	JE 23	JE 24	JE 25	JE 26
Quartz	45	65	65	50	50	75	55	80	75
Biotite				m					
...altered	15	15	m						
Chlorite				m					
Muscovite									
Green gahnite	m	15	10	20	20	10	20		
Blue gahnite	25		10	m	25	10	10	10	20
Hercynite									
Magnetite									
Hematite	10	m	10	20	m	m	10	10	m
Garnet									
Rutile	tr		tr		tr	tr	tr		
Sericite	tr	tr	tr	tr	tr	tr	tr	tr	tr
Goethite	tr	m	tr	tr					
Galena									

'm' refers to minerals present in minor proportions (5% or less)
'tr' refers to minerals present in trace quantities (1% or less)

Metapelitic Schist

Cordierite-bearing metapelitic schist forms the major stratigraphic horizon between the quartzo-feldspathic gneiss and overlying quartzites. Biotite, quartz, cordierite and sillimanite form the major constituents of this rock (Table 19). Assemblages observed include; quartz + feldspar + biotite + sillimanite (± garnet, magnetite) and quartz + cordierite + sillimanite + biotite (± magnetite, green spinel, feldspar). The feldspar is untwinned albite ($Ab_{94}An_4Or_2$).

The majority of the matrix is composed of medium grained interlocking quartz grains. Magnesium-rich cordierite occurs interstitially, commonly with circular inclusions of quartz. Most of the cordierite is altered to pinnite. Feldspar does not occur in direct contact with cordierite, and is invariably sericitised. Quartz generally constitutes in excess of 50% of the rock, while cordierite and feldspar comprise between 15 and 30%. The remaining major constituents are sillimanite and biotite which are aligned within the foliation plane. Biotite is orange-brown and generally occurs as blunt laths. Alteration of biotite produces narrow, lens-shaped inclusions of quartz parallel to the biotite cleavage which is outlined by minute blebs of haematite, goethite and rutile. Garnet is present in minor quantities (< 3%). Garnet grains are euhedral, commonly fractured and less than 0.5 mm in diameter. Magnetite, containing inclusions of exsolved green hercynite, is a common, accessory phase generally associated with cordierite.

Narrow horizons of more resistant biotite-garnet-cordierite schists occur locally within the aluminous schist. Minor quantities of quartz, sillimanite and green spinel form part of the assemblage. Garnet occurs as 2.5 mm fractured grains and contains inclusions of biotite and quartz. Cordierite and biotite are coarse grained, the cordierite invariably pinitised. Biotite constitutes the most abundant phase and is pleochroic, dark brown to green-brown. Minute grains of quartz are occasionally found in association with biotite or cordierite.

Massive Garnet and Garnet-biotite Rocks

Within the aluminous schist horizon, below and at the interface between the schist and the quartzite, pod-like bodies of garnet-biotite, massive garnet and garnet-biotite-gahnite rocks occur. These are restricted in extent and are preserved within the major synformal fold closure (Fig.5).
In the garnet-biotite rocks, garnet constitutes 60 - 70% of the rock with up to 40% biotite and rare green gahnite. The green gahnite invariably occurs as inclusions in garnet. Garnet occurs as subhedral 0.3 to 0.5 mm grains. Blue gahnite, when present, is associated with biotite alteration. Most biotite is altered by retrograde metamorphism and replaced by chlorite and rutile in non-gahnite-bearing assemblages. Epidote-chlorite-garnet rocks within the same stratigraphic horizon as the garnet-biotite rocks are interpreted as altered equivalents of the latter.

In gahnite-bearing, garnet-biotite rocks biotite is replaced by quartz, sericite, oxides and blue gahnite (Fig.28a). The alteration products mimic the biotite grain shape with minute blebs of hematite, goethite and rutile outlining the grain border and cleavage traces and blue gahnite infilling the spaces between the traces. In massive garnet rocks, blue gahnite may comprise a substantial proportion of the assemblage. It occurs as narrow rims around garnet grains or infills fractures in garnet (Fig.28b). In these rocks fractured garnet grains are eroded and possibly act as a nucleation site for blue gahnite. Green gahnite occurs as rare inclusions in garnet in the massive garnet rocks and is invariably surrounded by blue gahnite.

Locally an outcrop of garnet-biotite-gahnite-quartz rock contains 10 - 20 % green gahnite. Green gahnite and garnet occur as coexisting porphyroblastic phases with interstitial altered biotite and fine grained, recrystallised quartz (Fig.28c). Blue gahnite, if present, is associated with altered biotite and quartz (Plate 5). Where blue gahnite is not present, quartz appears to form part of a retrograde chlorite-quartz assemblage. It appears that these rocks, like the epidote chlorite rocks (above), are the altered equivalents of garnet-biotite rocks.

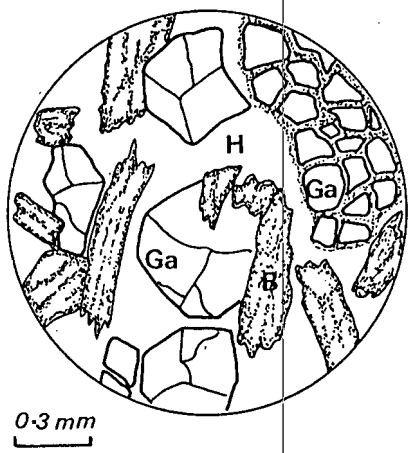

a. Garnet-biotite rock.

The matrix is composed mostly of hematite. Blue gahnite, quartz and hematite replace biotite. Hematite infills fractures in garnet.

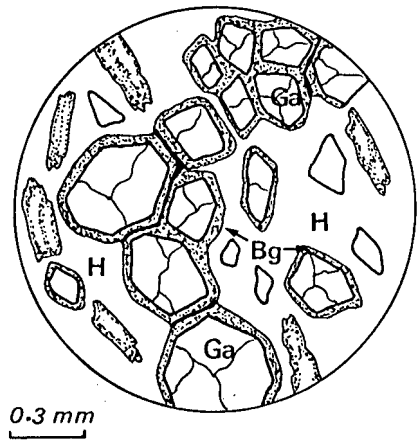

b. Massive garnet rock.

Blue gahnite surrounds garnet grai
The matrix is composed mostly of hematite.

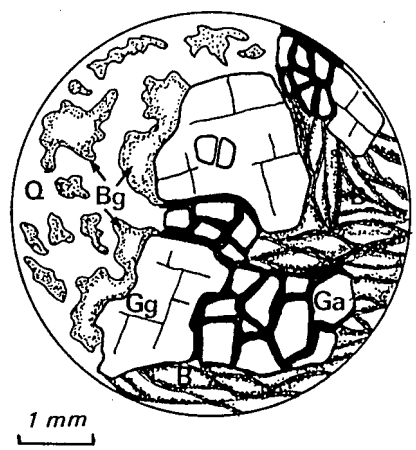

c. Garnet-biotite-gahnite-quartz rock.

Blue gahnite, biotite and garnet surround green gahnite. Hematite infills fractures in garnet. Biotite is replaced by hematite and blue gahnite and appears as elogate, ellipsoid shapes, defined by the cleavage traces.

Abbreviations:
B - biotite, Bg - blue gahnite, Ga - garnet, Gg - green gahnite, H - hematite, Q - quartz.

Figure 28: Textures in the garnet-rich lithologies at Oranjefontein.

A distinctive green coloured, galena-bearing rock occurs in the upper layers of the aluminous schist on the south facing side of Vioolskraalberg. Epidote, sericite, chlorite and galena form the major constituents with disseminated galena making up approximately 5% of the rock. Occasional grains of magnetite, green spinel and rare, highly corroded garnet grains occur as minor constituents. The texture of this rock suggests complete replacement of a precurser garnet-biotite assemblage similar to the piemontite-chlorite rocks which occur at the same horizon on the western limits of the syncline. The different mineralogies of the altered garnet-biotite rocks are explained in terms of retrograde metamorphism of garnet-rich rocks with slightly different bulk chemistries.

Summary
Textural evidence indicates the presence of both a prograde and retrograde assemblage in the garnet-biotite and massive garnet rocks. Green spinel, garnet, and biotite are associated with the prograde assemblage whereas blue gahnite, quartz and iron oxides are associated with biotite alteration as a retrograde assemblage. In non-gahnite-bearing assemblages epidote and chlorite replace garnet-biotite assemblages or chlorite replaces biotite.

In the massive garnet rocks, garnet is corroded and infilled by blue gahnite. In the gahnite-rich garnet-biotite-quartz rocks, quartz occurs as a late stage mineral phase associated with retrograde minerals such as chlorite or blue gahnite. Green gahnite appears to be out of equilibrium with the assemblage and is rimmed by garnet, altered biotite or blue gahnite. Blue gahnite is associated with altered biotite which appears to be replaced by blue gahnite, iron oxides and quartz.

Green spinel is generally rare in the massive garnet rocks, but where it occurs is always associated with the prograde garnet-biotite assemblage.

Gahnite-bearing Quartzites

These rocks generally contain 10% or more gahnite and crop out between the aluminous schist and massive quartzites on the southern and western sides of Vioolskraalberg. Although they occur in a stratigraphically equivalent horizon to the massive garnet and garnet-biotite rocks, they have far greater lateral extent (Fig.6). On the western flank of Vioolskraalberg the assemblage is quartz + blue gahnite + green gahnite + phlogopite (+ rutile, garnet, galena). To the south, the gahnite quartzites contain a higher proportion of gahnite and no garnet or mica. Texturally the rocks to the west display evidence of a precursor pelitic component in the assemblage whereas this is either absent or masked by retrograde overprinting in the gahnite quartzites on the southern flank of the Vioolskraalberg.

Gahnite (+ phlogopite, garnet) quartzites

The matrix of these rocks is composed of coarse grained, interlocking quartz grains. Anhedral, green gahnite grains comprise 5 - 7% of the rock, have an average grain size of 0.5 mm and commonly are embayed to quartz. Blue gahnite comprises up to 10% of the assemblage and forms <0.1 mm grains which are dispersed throughout the matrix and also occur in aggregates. Altered phlogopite and tiny garnet grains occur throughout these rocks (Plate 6). Blue gahnite also commonly occurs as rim to green gahnite porphyroblasts (Plate 7). Haloes composed of tiny blebs of iron oxides surround blue gahnite aggregates and are believed to be the remains of altered phlogopite (Plate 8). The phlogopite "ghosts" are recognised as concentrations of fine hematite along original grain boundaries and cleavage traces whereas blue gahnite and quartz crosscut the former grain boundaries (Plate 6). Rounded grains of rutile and tiny garnet grains occur in minor to trace quantities throughout the matrix of these rocks. Rare unaltered phlogopite grains occur as inclusions in quartz but most phlogopite appears to have been replaced by quartz, iron oxides, rutile and blue gahnite.
One sample contained approximately 5% galena in the form of coarse (~10mm) crystals and as fine grained, disseminate inclusions in quartz. The galena is partially replaced by anglesite.

Gahnite Quartzites

In these rocks coarse, crystalline green gahnite occurs as poikiloblastic porphyroblasts with abundant, fine-grained quartz inclusions. Blue gahnite comprises more than 20% of the rock and generally forms large aggregates made up of small (~0.1 mm), euhedral grains. The matrix of these rocks is composed of fine grained recrystallised quartz, commonly exhibiting a mortar texture. Webbed masses of hematite needles comprise up to 10% of some rocks and are associated with aggregates of blue gahnite. The characteristic biotite outlines and rutile found in the west facing rocks are absent and instead, extremely fine-grained iron oxides define elongate, wavey, lens-shaped outlines (Plate 7). These may represent the last traces of a coarse-grained precusor phase such as occurs in the garnet-biotite rocks but the effects of retrograde metamorphism mask most of the confirming evidence for this.
An unusual feature in some rocks is the presence of euhedral blue gahnite grains containing a central, circular portion defined by a rim of very fine-grained, red coloured, hematite (Plate 9).

Summary
Green and blue gahnite are major mineral phases in these rocks. Green gahnite is coarser grained, commonly porphyroblastic and surrounded by a narrow rim of blue gahnite. Blue gahnite is finer grained and commonly occurs as aggregates composed of euhedral (~0.1 mm) grains or as rims to green gahnite. Hematite and blue gahnite are associated with retrograde replacement of biotite and green gahnite. Retrograde alteration of phlogopite results in in situ replacement by quartz, blue gahnite, iron oxides and rutile. The retrograde overprint is more pervasive on the southern limits of the syncline where green gahnite is ubiquitously rimmed by blue gahnite and traces of any precursor assemblage has all but disappeared. On the western limits of the syncline, green gahnite contains quartz inclusions and appears to be stable with respect to quartz.

Massive Glassy Quartzites

White, glassy, coarse-grained, metaquartzites overly the metapelitic schist, forming a prominent capping to Vioolskraalberg. These contain local concentrations of tourmaline, biotite, Fe and Fe-Ti opaques and garnet. Towards the base of the quartzite unit in the south, concentrations of garnet comprise up to 20% of the rock. Blue gahnite occurs in cracks and fissures in the lower horizons of the quartzite. In a few instances a central core of green gahnite is surrounded by a radiating corona of blue gahnite which occupies fissures in the rock and forms a network of veins up to 30 cm from the green gahnite core.

4.5.2 Mineral Chemistry

Bulk rock analyses of a gahnite quartzite and gahnite-bearing, garnet-biotite rock are listed in Table 20 (analyses by courtesy of Dr. J.M. Moore). Trace quantities of galena and chalcopyrite were observed toward the base of the metaquartzite unit and minor proportions of galena occur locally in the underlying gahnite quartzites and an epidote-chlorite rock. Thus the presence of up to 5000 ppm Pb and trace quantities of Cu in the whole rock analyses are taken to indicate the presence of minor sulphides, now oxidised. Table 21 lists average analyses of the minerals in the samples.

Garnet

Average endmember garnet compositions in the assemblages studied are listed in Appendix 3 and are plotted on an endmember diagram, Figure 29.

Garnet composition and habit vary considerably throughout the stratigraphic column at Vioolskraalberg. The variation probably reflects differences in bulk rock chemistry and varying degrees of the retrograde metamorphic overprint.

Almost all garnets are of the Fe-Mg-Mn series. Garnet in the quartzo-feldspathic gneiss is the one exception with an endmember composition of $Alm_{37}Spess_{40}Py_{12}Gross_{11}$. In the metapelitic garnet-

Table 20. Whole rock analyses of two gahnite-bearing rocks from Oranjefontein.

Sample:	OF-7	OF-8
SiO2	95.71	38.13
TiO2	0.04	1.01
Al2O3	1.21	22.07
FeO	1.33	16.68
MnO	0.15	4.20
MgO	0.47	5,95
CaO	0.03	0.81
Na2O	0.04	0.18
K2O	0.00	0.04
P2O5	0.00	0.30
H2O+	0.57	3.44
H2O-	0.11	0.29
Total	99.55	92.81
Trace elements (ppm)		
Rb	<2	<3
Ba	8.3	297
Sr	<2	7
Th	21	91
U	<3	<5
Zr	36	559
Nb	<1	18
Mo	<1	6
Sc	1	14
Ni	1.7	6.6
Pb	4270	6165
Zn	1305	4.19%
Cu	52	78
Y	4	44
La	<2	81
Ce	6.8	154
Nd	<3	69

Rock Types:
OF-7: Gahnite(+phlogopite,garnet) quartzite
OF-8: Garnet-biotite-gahnite rock

Table 21. Average (or representative) analyses of minerals from samples studied at Oranjefontein.

	GARNET											
n	4		6		2		4		3		2	
SAMPLE	JE 2	σ	JE 3	σ	JE 7	σ	JE 10	σ	JE 14	σ	JE 19	σ
SiO2	39.22	0.19	38.64	0.26	37.56	0.26	36.86	0.20	37.23	0.09	38.11	0.51
TiO2	nd		0.04	0.00	nd		0.07	0.02	0.14	0.01	0.05	0.01
Al2O3	22.08	0.05	22.04	0.23	21.08	0.20	21.41	0.14	21.03	0.19	22.15	0.11
FeO	18.41	0.67	18.85	0.93	20.05	0.90	17.11	0.22	8.59	0.13	15.49	0.10
MnO	9.59	0.11	10.10	0.52	13.84	0.41	18.80	0.10	22.94	0.28	12.35	0.60
MgO	9.11	0.34	8.42	0.90	5.07	0.73	3.05	0.10	4.08	0.13	8.92	0.42
CaO	2.12	0.04	2.27	0.22	1.93	0.06	3.76	0.04	4.98	0.01	2.23	0.04
Na2O	nd		nd		nd		nd		nd		nd	
K2O	nd		nd		nd		nd		nd		nd	
Total	100.53		100.36		99.53		101.06		98.99		99.30	

	GARNET											
n	4		3		3		3		3		7	
SAMPLE	JE 20	σ	JE 29	σ	JE 31	σ	JE 32	σ	JE 35	σ	JE 36	σ
SiO2	38.90	0.10	37.73	0.16	37.41	0.46	37.31	0.58	38.36	0.23	37.39	0.26
TiO2	0.06	0.01	nd		nd		nd		nd		0.07	0.02
Al2O3	22.00	0.08	22.28	0.20	21.79	0.30	22.02	0.23	21.87	0.18	20.86	0.37
FeO	12.68	0.11	28.02	0.33	29.85	0.77	30.34	0.66	14.47	0.04	18.09	0.36
MnO	15.50	0.20	2.26	0.02	3.18	0.27	4.80	0.40	14.77	0.79	17.29	0.17
MgO	8.91	0.04	8.38	0.43	6.22	0.84	5.86	0.70	7.79	0.66	3.54	0.20
CaO	2.13	0.03	1.62	0.04	1.61	0.02	0.64	0.05	2.69	0.15	2.34	0.04
Na2O	nd		nd		nd		nd		nd		nd	
K2O	nd		nd		nd		nd		nd		nd	
Total	100.18		100.29		100.06		100.97		99.95		99.58	

nd: element was not detected or the amount detected is below the detection limit of the analytical method employed.
σ: is a statistical measure of the range of 'n' number of analyses.
All Fe is analysed as FeO.

Table 21. Average (or representative) analyses of minerals from samples studied at Oranjefontein.

	GARNET							
n	2		1		2		2	
SAMPLE	JE 18		JE 74		JE 82		OF 7	
		σ				σ		σ
SiO2	39.06	0.13	38.05		37.99	0.07	37.69	0.17
TiO2	nd		nd		nd		0.06	0.01
Al2O3	22.78	0.01	21.70		21.62	0.01	21.98	0.16
FeO	15.96	0.01	15.70		16.78	0.29	18.37	0.52
MnO	10.85	0.01	14.04		11.62	0.12	9.52	0.72
MgO	9.74	0.08	8.56		9.15	0.11	9.05	0.79
CaO	2.17	0.01	1.58		1.69	0.16	2.10	0.09
Na2O	nd		nd		nd		nd	
K2O	nd		nd		nd		nd	
Total	100.56		99.63		98.85		98.77	

	CORDIERITE				PLAGIOCLASE			ORTHOCLASE
n	4		3		1	2		1
SAMPLE	JE 29		JE G		JE 29	JE 10		JE 10
		σ		σ			σ	
SiO2	48.83	0.17	50.97	0.43	66.23	66.56	0.23	62.80
TiO2	nd		nd		nd	nd		0.04
Al2O3	33.72	0.35	34.20	0.10	20.31	19.84	0.35	18.72
FeO	5.59	0.22	2.45	0.05	0.11	nd		nd
MnO	0.20	0.02	nd		nd	nd		nd
MgO	10.15	0.32	12.22	0.21	nd	nd		nd
CaO	nd		nd		0.63	0.31	0.11	nd
Na2O	0.09	0.02	0.15	0.05	7.55	11.20	0.08	0.91
K2O	nd		nd		0.11	0.06	0.02	14.41
Total	98.58		99.99		94.94	97.97		96.88

nd: element was not detected or the amount detected is below the detection limit of the analytical method employed.
σ: is a statistical measure of the range of 'n' number of analyses.
All Fe is analysed as FeO.

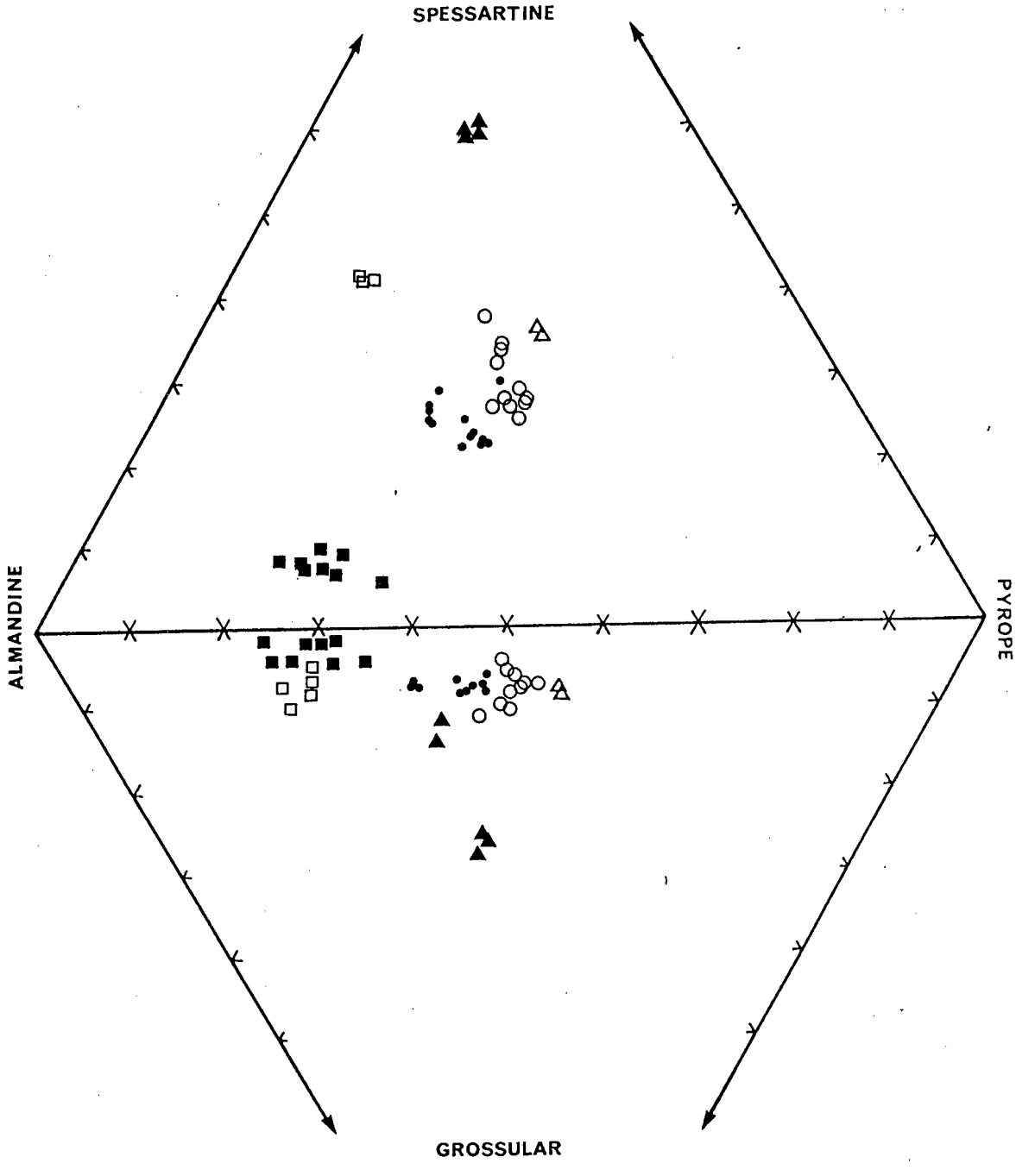

Symbols:

dots	: gahnite(+phlogopite, garnet) quartzites
circles	: gahnite-biotite-gahnite-quartz rocks and garnet-biotite rocks
closed triangles	: garnet-, gahnite-bearing metaquartzite
open triangles	: garnet-bearing metaquartzite
closed squares	: metapelitic schists
open squares	: garnet-biotite rocks

Figure 29: Garnet compositions from Oranjefontein plotted on a triangular endmember diagram.

Table 21. Average (or representative) analyses of minerals from samples studied at Oranjefontein.

BIOTITE

n	6		6		3		3		2	
SAMPLE	JE 2		JE 29		JE 31		JE 32		JE74	
		σ		σ		σ		σ		σ
SiO2	37.40	1.71	35.54	0.56	36.61	0.26	35.99	0.35	38.24	0.04
TiO2	4.82	0.68	3.31	1.07	3.14	0.12	3.25	0.09	0.74	0.35
Al2O3	16.05	0.32	17.72	0.56	16.52	0.13	16.19	0.19	16.15	0.91
FeO	9.89	0.59	13.63	2.00	12.28	0.79	13.45	0.47	5.81	0.83
MnO	0.25	0.03	0.13	0.05	nd		nd		0.22	0.13
MgO	17.69	0.67	14.50	2.03	15.86	0.50	15.59	0.19	21.30	0.26
CaO	nd		nd		nd		nd		nd	
ZnO	0.35	0.07	nd		nd		nd		0.34	0.25
Na2O	0.22	0.05	0.10	0.06	0.21	0.03	0.23	0.02	0.35	0.01
K2O	8.95	1.19	9.33	0.21	9.41	0.18	9.26	0.17	8.60	0.12
Total	95.62		94.26		94.03		93.96		91.75	

nd: element was not detected or the amount detected is below the detection limit of the analytical method employed.
σ: is a statistical measure of the range of 'n' number of analyses.
All Fe is analysed as FeO.

Table 21. Average (or representative) analyses of minerals from samples studied at Oranjefontein.

CHLORITE

n	5		4		3		7		5		3	
SAMPLE	JE 7		JE 14		JE 16		JE 18		JE 19		JE 20	
		σ		σ		σ		σ		σ		σ
SiO2	31.32	1.24	24.05	0.73	27.17	1.39	27.09	1.67	27.06	1.89	25.86	0.19
TiO2	nd		nd		nd		0.18	0.10	nd		nd	
Al2O3	21.10	0.40	21.71	0.55	19.55	0.54	20.09	0.92	21.68	0.83	20.58	0.47
FeO	7.04	1.28	26.86	0.93	19.98	0.19	18.34	1.26	23.68	1.57	21.63	0.21
MnO	1.62	0.13	2.05	0.20	2.21	0.10	2.11	0.12	1.71	0.22	2.49	0.08
MgO	24.52	1.24	11.08	0.97	18.32	0.10	15.69	1.28	11.73	0.37	14.82	0.20
CaO	0.06	0.01	nd		nd		nd		0.13	0.04	0.05	0.01
ZnO	0.81	0.06	1.95	1.19	1.51	0.12	3.42	0.95	2.12	0.49	2.60	0.05
Na2O	nd		nd		nd		0.04	0.02	0.08	0.04	0.03	0.01
K2O	0.08	0.03	nd		nd		0.03	0.02	0.13	0.05	nd	
Total	86.55		87.70		88.74		86.99		88.32		88.06	

CHLORITE

n	11		5	
SAMPLE	JE 36		OF 7	
		σ		σ
SiO2	27.41	0.25	24.96	1.04
TiO2	nd		nd	
Al2O3	19.25	0.21	20.66	1.32
FeO	10.19	0.84	24.31	2.74
MnO	3.35	0.34	1.67	0.15
MgO	21.95	0.22	13.25	1.88
CaO	0.04	0.03	0.04	0.02
ZnO	5.04	0.52	1.05	0.29
Na2O	0.04	0.02	nd	
K2O	nd		nd	
Total	87.27		85.94	

nd: element was not detected or the amount detected is below the detection limit of the analytical method employed.
σ: is a statistical measure of the range of 'n' number of analyses.
All Fe is analysed as FeO.

Table 21. Average (or representative) analyses of minerals from samples studied at Oranjefontein.

	AMPHIBOLE				PYROXENE			
n	2		1		3		2	
SAMPLE	JE A		JE G		JE A		JE G	
		σ				σ		σ
SiO2	41.49	0.62	42.39		52.36	0.52	50.39	0.27
TiO2	1.52	0.18	0.53		0.12	0.02	0.09	0.01
Al2O3	15.75	0.23	19.02		5.59	0.33	7.99	0.64
FeO	9.55	0.06	14.59		15.15	0.10	17.85	0.33
MnO	0.72	0.02	0.17		1.61	0.08	0.16	0.01
MgO	14.80	0.33	18.49		26.38	0.47	24.87	0.37
CaO	11.22	0.00	0.62		0.24	0.03	0.10	0.03
Na2O	2.16	0.01	2.08		nd		nd	
K2O	0.64	0.05	nd		nd		nd	
Total	97.85		97.89		101.45		101.45	

All Fe is analysed as FeO.

REPRESENTATIVE ANALYSES OF EPIDOTE

n	4		5	
SAMPLE	JE 16		JE 7	
		σ		σ
SiO2	37.94	1.09	35.97	2.09
TiO2	nd		nd	
Al2O3	25.18	0.70	22.47	2.25
Fe2O3	12.23	0.76	8.96	3.25
MnO	0.77	0.45	5.11	4.31
MgO	nd		0.15	0.13
CaO	22.79	0.65	21.95	1.46
Na2O	nd		nd	
K2O	nd		nd	
Total	98.91		94.61	

Fe was analysed as FeO and has been recalculated to Fe2O3.

nd: element was not detected or the amount detected is below the detection limit of the analytical method employed.
σ: is a statistical measure of the range of 'n' number of analyses.

Table 21. Average (or representative) analyses of minerals from samples studied at Oranjefontein.

GAHNITE

n	5		4		1		2		10		3	
SAMPLE	JE 2		JE 2		JE 3		JE 3		JE 15		JE 14	
COLOUR	blue		green		blue		green		blue		blue	
		σ		σ		σ		σ		σ		σ
Al2O3	55.32	0.27	58.32	0.38	55.05	0.12	58.22	0.01	55.18	0.57	56.32	0.33
Cr2O3	nd		0.24	0.04	nd		0.13	0.02	nd		nd	
FeO	2.08	0.12	7.01	0.38	2.27	0.04	8.60	0.43	1.83	0.16	1.24	0.14
MnO	nd		0.19	0.04	0.05	0.01	0.20	0.02	nd		nd	
MgO	0.08	0.01	4.92	0.09	0.11	0.03	5.64	0.04	0.09	0.09	0.07	0.04
ZnO	41.99	0.35	28.72	1.37	42.67	0.45	27.75	0.19	43.31	0.93	41.25	0.38
Total	99.47		99.40		100.15		100.54		100.41		98.88	

GAHNITE

Nr.anal.	6		2		9		4		8		1	
SAMPLE	JE 18		JE 18		JE 19		JE 23		JE 23		JE 26	
COLOUR	blue		green		green		blue		green		blue	
		σ		σ		σ		σ		σ		
Al2O3	55.38	0.19	58.58	0.01	58.61	0.61	56.33	0.52	60.44	0.25	55.39	
Cr2O3	nd		nd		0.08	0.05	nd		nd		nd	
FeO	2.38	0.29	8.74	0.11	8.01	0.64	1.22	0.34	4.98	0.20	1.68	
MnO	nd		0.45	0.04	0.40	0.10	0.08	0.05	0.31	0.04	0.04	
MgO	0.13	0.06	6.02	0.01	7.01	0.16	0.14	0.08	7.65	0.16	0.08	
ZnO	41.99	0.25	27.02	0.03	25.50	0.80	41.91	0.56	26.69	0.31	43.31	
Total	99.88		100.81		99.61		99.68		100.07		100.50	

nd: element was not detected or the amount detected is below the detection limit of the analytical method employed.
σ: is a statistical measure of the range of 'n' number of analyses.
All Fe is analysed as FeO.

Table 21. Average (or representative) analyses of minerals from samples studied at Oranjefontein.

	GAHNITE										
n	3		1		4		2		3		1
SAMPLE	JE 35		JE 39		JE 74		JE 74		JE 82		JE 82
COLOUR	blue		blue		blue		green		blue		green
		σ		σ		σ		σ		σ	
Al2O3	55.12	0.20	54.32		56.31	0.26	59.45	0.38	53.41	0.32	59.22
Cr2O3	0.07	0.04	nd		nd		nd		nd		nd
FeO	2.19	0.32	2.02		1.37	0.54	7.62	0.37	3.63	0.30	7.11
MnO	0.20	0.09	0.08		0.10	0.00	0.35	0.00	0.10	0.02	0.27
MgO	0.12	0.01	0.13		0.11	0.01	5.91	0.42	0.14	0.03	6.00
ZnO	42.26	0.12	42.16		42.75	0.61	27.32	0.81	41.13	0.38	26.99
Total	99.96		98.71		100.64		100.65		98.41		99.59

	GAHNITE				ZINCIAN HERCYNITE					
n	3		2		1		5		4	
SAMPLE	OF 7		JE 16		JE 29		JE A		JE G	
COLOUR	green									
		σ		σ		σ		σ		σ
Al2O3	58.30	0.16	60.45	0.23	54.68		61.55	0.68	61.21	0.16
Cr2O3	nd		nd		0.67		0.09	0.04	0.93	0.46
FeO	10.01	1.16	12.58	1.82	27.37		21.62	0.79	21.63	1.79
MnO	0.49	0.10	1.22	0.18	0.39		0.83	0.06	nd	
MgO	5.86	0.76	12.75	0.54	6.23		14.72	0.39	13.76	0.59
ZnO	24.73	2.20	12.79	2.42	8.31		0.48	0.24	0.30	0.52
Total	99.39		99.79		97.65		99.29		97.83	

nd: element was not detected or the amount detected is below the detection limit of the analytical method employed.
σ: is a statistical measure of the range of 'n' number of analyses.
All Fe is analysed as FeO.

biotite-cordierite schists garnet has the composition $Alm_{59-66}Spess_{5-11}Py_{21-31}Gross_{1.5-4}$ and is relatively almandine-rich compared to garnet occuring over the rest of Vioolskraalberg. In the massive garnet and garnet-biotite rocks, garnet is spessartine-rich i.e. $Alm_{30-40}Spess_{23-39}Py_{14-37}Gross_{3.5-7}$. Garnet in the altered piemontite-chlorite rock is also relatively spessartine-rich and has an average composition of $Alm_{44}Spess_{31}Py_{20}Gross_{4}$.

Garnet in the metaquartzite has an average composition of $Alm_{27}Spess_{33}Py_{34}Gross_{6}$. In a garnet-bearing metaquartzite, where garnet is partially replaced by chlorite and blue gahnite, garnet has a compositional range of $Alm_{19-22}Spess_{51-55}Py_{15-16}Gross_{6-13}$

Variation of garnet composition with metamorphic grade is a fairly well established phenomena. With increasing metamorphic grade Fe and ultimately Mg contents increase whereas Ca and Mn contents decrease (Miyashiro 1973, Winkler 1967). This probably accounts for some of the variation observed. However the alteration of biotite-garnet assemblages to garnet-gahnite-quartz- hematite assemblages in some cases and in other cases to epidote-chlorite or piemontite-garnet-chlorite must also necessarily affect the composition of the garnet. It is apparent that small scale variation in bulk rock chemistry has produced a wide array of mineral assemblages which may be the main factor in the compositional variation observed in minerals such as spinel, garnet and epidote at this locality.

Fe - Ti Oxides

Abundant hematite and goethite associated with blue gahnite are an observed feature of the gahnite quartzites. Hematite occurs as haloes surrounding small aggregates of blue gahnite in some rocks and as webbed masses composed of tiny needles in other rocks. Hematite + goethite + rutile partially replace biotite throughout the gahnite-bearing lithologies. Ilmenite, magnetite and titanomaghemite occur as coarse blebs in the aluminous schist, generally in association with cordierite or sillimanite. Local concentrations of ilmenite and magnetite occur in the massive quartzite unit. Magnetite occurs in association with green gahnite in some of the gahnite quartzites.

Micas

The composition of biotite in the aluminous schist is annite with 4.5 wt% TiO_2. In the metapelitic garnet-biotite-cordierite schist the mica is phlogopite with 3.5 wt% TiO_2. Although biotite is a common constituent of all rock types in the study area, the pervasive affects of retrograde metamorphism have resulted in its replacement by chlorite or hematite, goethite, rutile, blue gahnite and quartz. In the gahnite quartzites, biotite armoured by quartz contained up to 0.4wt% ZnO (detection limit is 0.02 wt% ZnO). Prograde biotite from the Broken Hill massive sulphide deposit, Australia contained up to 5350 ppm zinc (Plimer, 1977). Frost (1973) found up to 0.5 wt% ZnO in biotite associated with sulphides. Zinc-bearing biotites containing 0.24 wt% ZnO are believed to be the precursor mineral to gahnite formed during retrograde metamorphism (Dietvorst, 1980).

Chlorite occurs in the garnet-biotite rocks as a replacement of biotite and in the quartzites, associated with blue gahnite as a partial replacement of garnet. In terms of Hey's (1954) classification (Fig.30) Oranjefontein chlorites are ripidolites and pycnochlorites. High manganese (2.8 - 4.4 wt% MnO) and zinc (0.8 - 5.4 wt% ZnO) contents are associated with blue gahnite-bearing assemblages. Similar Zn-,Mn-rich chlorites, containing up to 10 wt% ZnO and a similar quantity of MnO are associated with low temperature, hydrothermal veins at Franklin, New Jersey by Frondel and Ito (1975). They suggest that Fe and Mg can be more or less completely replaced by other divalent ions including Mn, Co, Ni and Zn.

Epidote

In the galena-bearing, epidote-chlorite rock epidote is pleochroic pale yellow-green to colourless and has the structural formula $Ca_{1.9}Fe_{0.7}Mn_{0.05}Al_{0.2}Al_2O(OH)[Si_2O_7][SiO_4]$. The endmember composition is clinozoisite (75 - 78 mol%), epidote (22 - 25 mol%) and piemontite (1 - 3 mol%), (Fig.31).

In a maroon coloured, garnet-piemontite-chlorite rock associated with the massive garnet rocks, piemontite has a wide range of compositon (Fig.31).

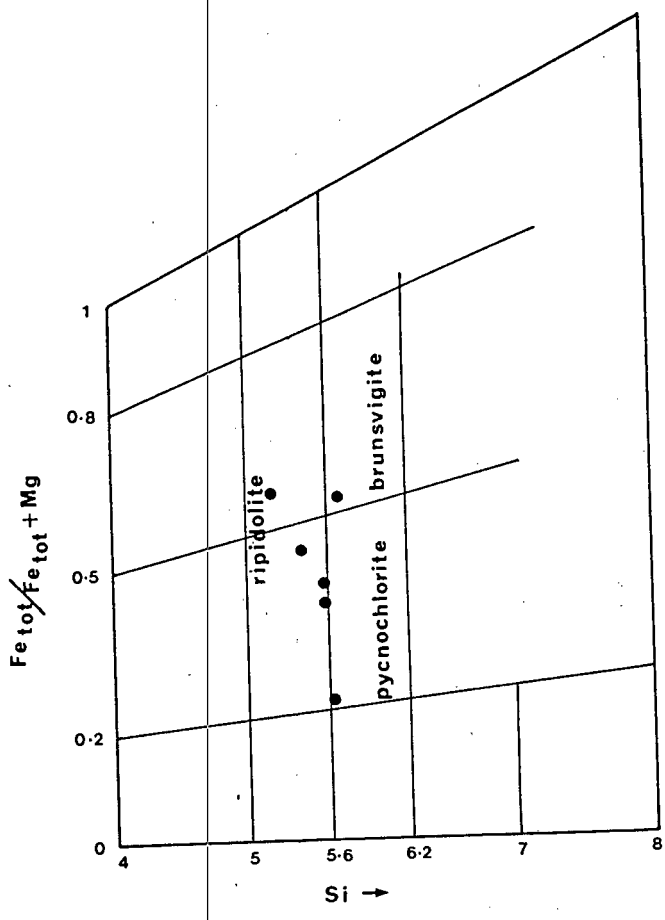

Figure 30: Chlorite compositions plotted as a function of Si and Fe content (after Hey, 1954).

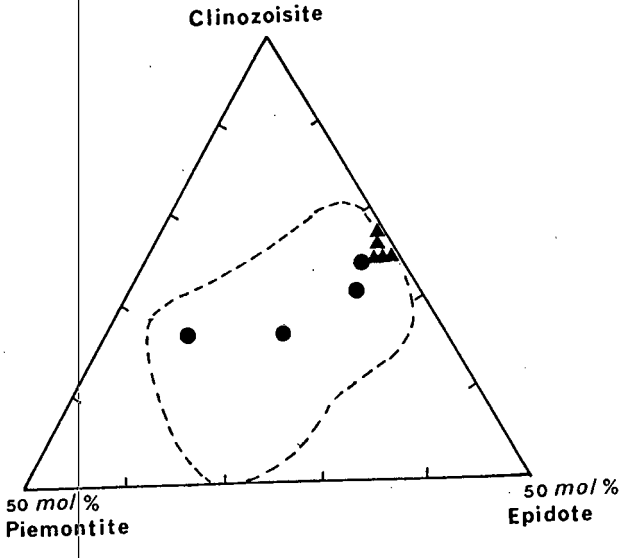

Figure 31: Epidote plotted on a triangular endmember diagram (after Ashley 1984). The staggered line outlines the field of natural piemontites (from Keskinen and Liou, 1979).

The structural formula is:
$Ca_{1.9}Fe_{0.69-0.24}Mn_{0.85-0.06}Mg_{0-0.03}Al_{0.2-0.02}Al_2OH[Si_2O_4][SiO_4]$.
Garnet in this assemblage is similarly Mn-rich (17 wt% MnO) and chlorite contains 1.5 - 1.75 wt% MnO.

A massive epidote rock containing only minor quantities of quartz and chlorite was found on the western face of Vioolskraalberg at a similar stratigraphic level to the garnet-piemontite-chlorite rock. However, epidote in this rock is greenish yellow to colourless and exhibits the distinctive high interference colours of epidote (clinozoisite has low interference colours). The absence of any pink colouration indicates negligable manganese (Deer et al., 1080). It appears thus that the manganese rich lithology is limited in extent within this stratigraphic horizon.

According to Deer et al. (1980), piemontite occurs in rocks of the greenschist facies. In general, higher oxygen fugacity conditions are required for the formation of Mn^{3+} than Fe^{3+}, and the presence of both (Mn^{3+} in piemontite and Fe^{3+} in hematite) in association with retrograde assemblages implies high oxygen fugacity conditions during the rerograde metamorphic event.

Gahnite, Zincian Spinel, and Hercynite

Several varieties of green-coloured spinel with widely differing compositions are associated with different assemblages at Vioolskraalberg. Analysed spinels are plotted on a triangular endmember diagram (Fig.32). Figures 33, 34 and 35 show gahnite compositions in terms of cation content on two axis diagrams.

Green gahnite in the gahnite(+ phlogopite, garnet) quartzites has an average composition of $Ghn_{64}Sp_{25}Hc_{16}$ and in the gahnite quartzites, where the effects of retrograde metamorphism are more pervasive, $Ghn_{57}Sp_{32}Hc_{11}$. In the garnet-biotite-gahnite-quartz rocks, green gahnite has the composition $Ghn_{59}Sp_{26}Hc_{15}$. In gahnite-rich garnet-biotite-quartz rocks gahnite has the composition $Ghn_{55}Sp_{30}Hc_{15}$.

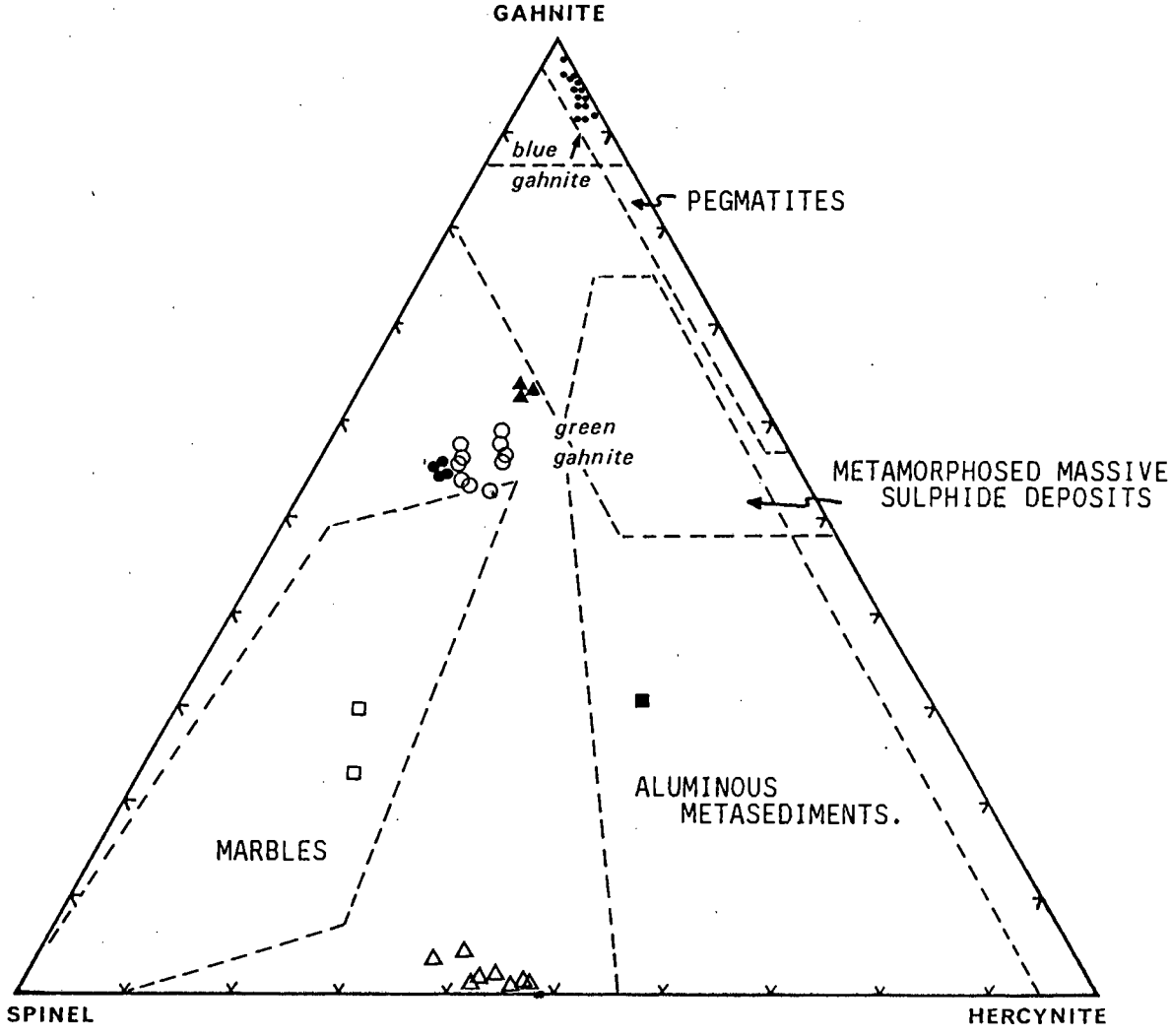

Symbols:

small dots	: blue gahnite
closed triangles	: gahnite(+phlogopite, garnet) quartzites
open circles	: garnet-biotite rocks
large dots	: gahnite quartzites
closed squares	: aluminous schist
open squares	: calc silicate (altered garnet-biotite rock)
open triangles	: amphibolite and granulite rocks

Demarcated fields refer to gahnite associated with particular lithologies (from Spry, 1984).

Figure 32: Gahnite composition from Oranjefontein plotted on a triangular endmember diagram.

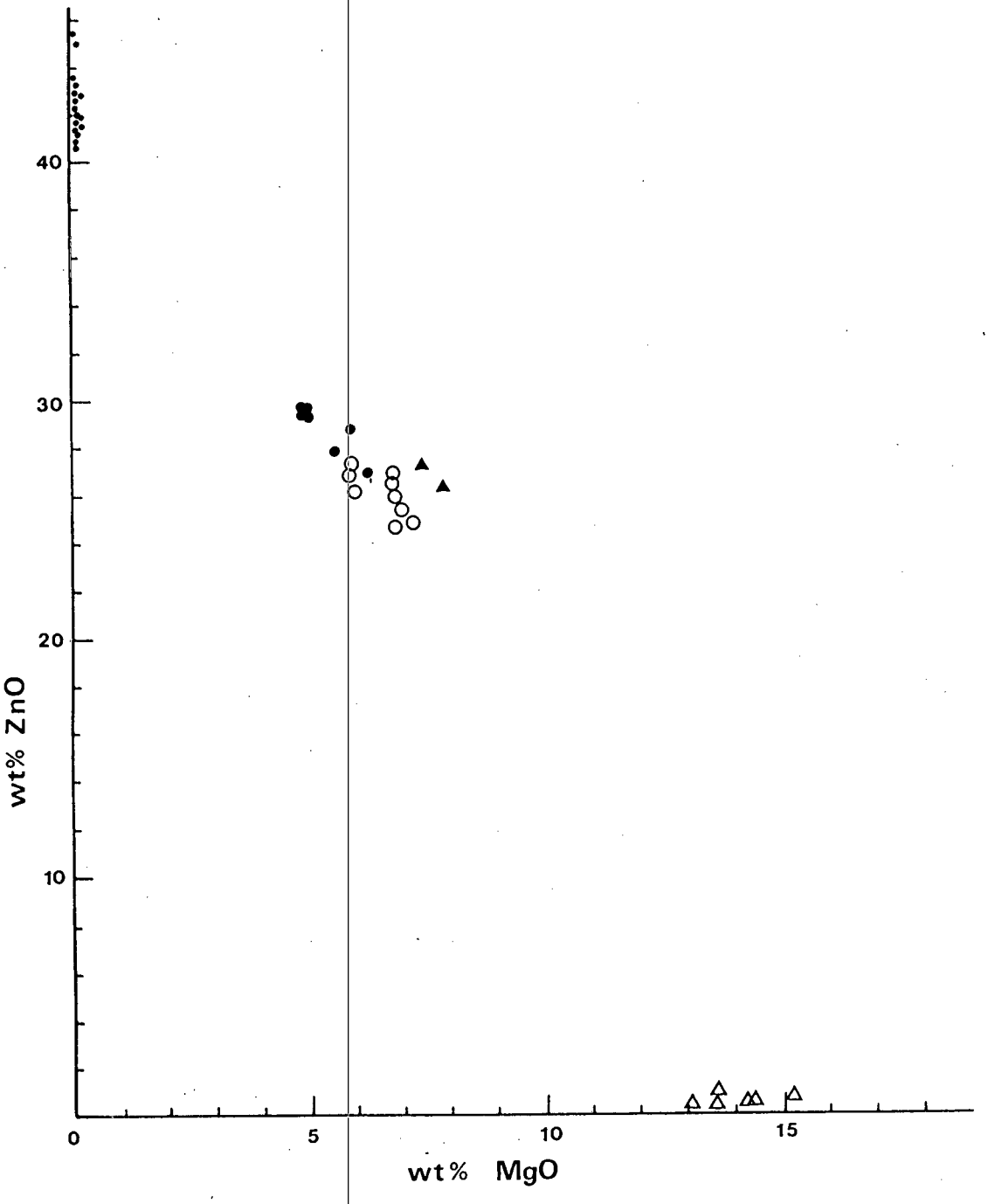

Symbols:
small dots : blue gahnite
closed triangles: gahnite(+phlogopite, garnet) quartzites
open circles : garnet-biotite rocks
large dots : gahnite quartzites
open triangles : amphibolite and granulite rocks

Figure 33: Gahnite compositions (Oranjefontein), ZnO/MgO.

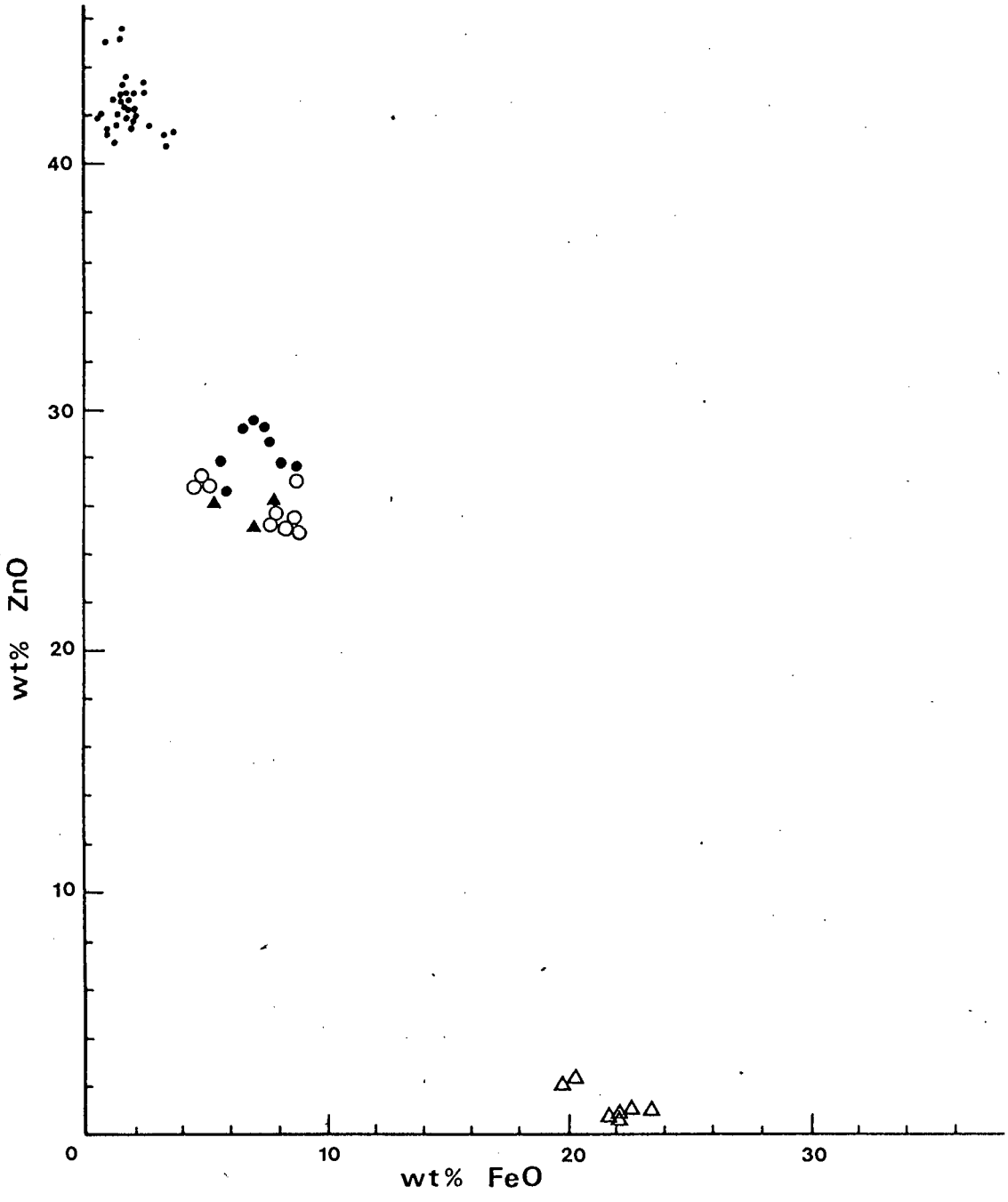

Symbols:
small dots : blue gahnite
closed triangles: gahnite(+phlogopite, garnet) quartzites
open circles : garnet-biotite rocks
large dots : gahnite quartzites
open triangles : amphibolite and granulite rocks

Figure 34: Gahnite compositions (Oranjefontein), ZnO/FeO.

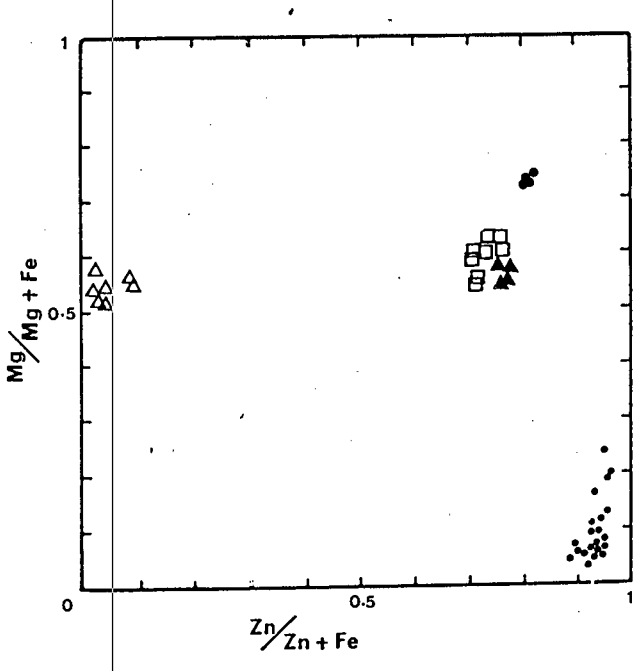

Symbols:
small dots : blue gahnite
closed triangles: gahnite(+phlogopite, garnet) quartzites
open squares : garnet-biotite rocks
large dots : gahnite quartzites
open triangles : amphibolite and granulite rocks

Figure 35: Gahnite compositions (Oranjefontein), Mg/Mg+Fe vs. Zn/Zn+Fe.

Green gahnite occurring as a minor phase in the epidote-chlorite rocks has a compositional range of $Ghn_{50-60}Sp_{22-29}Hc_{20}$ in the piedmontite rock and $Ghn_{23-31}Sp_{53-57}Hc_{16-19}$ in the galena-bearing, clinozoisite-chlorite rock. In both assemblages, green gahnite is surrounded by chlorite. Bright green zincian hercynite occurs as exsolved grains in magnetite in the aluminous schist. This spinel has an average composition of $Ghn_{32}Sp_{26}Hc_{42}$.

According to Spry's (1984) research, gahnite with high Mg contents are generally associated with marbles (Fig.40). However, gahnite with similar Zn contents to that occurring at Oranjefontein are reported from cordierite-anthophyllite rocks associated with mineralization at Montauben-Les-Mines, Quebec i.e. $Ghn_{58-66}Hc_{18-21}Sp_{15-21}$ (Bernier et al., 1984) and at Falun, Sweden i.e. $Ghn_{50-70}Hc_{16-50}Sp_{0-24}$ (Wolter and Siefert, 1984).

On the neighbouring farm, on the northern flanks of Vioolskraalberg, at a similar horizon, quartz-cordierite-two pyroxene granulites contain coarse intergrowths of magnetite and pleonaste (Fe-Mg spinel). The range of composition in these spinels is $Ghn_{1-5}Sp_{50-60}Hc_{36-47}$ and it is interesting to observe that even in these rocks spinel contains detectable quantities of zinc (0.5 - 2.3 wt% ZnO). Cordierite-anthophyllite or cordierite-orthopyroxene assemblages are frequently reported as containing small proportions of spinel. Where these rocks are associated with mineralization the spinels commonly contain a component of zinc. Similar zinc-bearing pleonastes as are found at Oranjefontein are reported by Treloar et al. (1981), Teale (1980), Schreurs and Westra (1985) and Coolen (1981).

The blue gahnite on Vioolskraalberg is close to endmember gahnite and compared to green gahnite, shows a relatively small range in compositon i.e. $Ghn_{91-98}Sp_{0-3}Hc_{1-7}$. Almost endmember gahnite is rare and generally occurs in low temperature, quartz-bearing rocks and pegmatites (Spry, 1984). Kramm (1977) records gahnite with composition, $Ghn_{88}Sp_{10}Gal_2$ in low grade viridine-braunite-muscovite schists from Belgium and gem quality, blue spinel ($Ghn_{88}Hc_{10}Sp_1Gal_1$) associated with mineralized pegmatites in Nigeria are reported by Batchelor and

Kinnaird (1984). In the rocks studied here, blue gahnite is associated with a late-stage, retrograde metamorphic event and is commonly associated with quartz. Reported occurrences of blue coloured gahnite are like-wise rare, the only documentation of these found, being those of Batchelor and Kinnaird (above) and the gem quality, Mg-Zn spinels from Sri Lanka (Anderson et al. 1937, Schmetzer and Bank 1985). Batchelor and Kinnaird ascribe the blue colour to the absence of ferric (Fe^{3+}), which commonly substitutes for Al, in the spinel structure.

4.5.3 Zoning in gahnite

Green gahnite porphyroblasts surrounded by rims of polycrystalline blue gahnite provide a striking colour difference in these rocks (cover plate). The colour change is abrupt and is matched by an equally abrupt change in composition (Fig.36). Individually the two spinels are, however, compositionally homogenous and cannot be considered as a single zoned mineral. If the blue gahnite is derived from green gahnite breakdown during a distinct, low temperature, retrograde metamorphic event, there is very little evidence for re-equilibration between the two spinel phases. The high zinc content of blue gahnite is in part explained in terms of zinc introduced into the rocks during retrograde metamorphism. It appears that the kinetics of new mineral growth combined with the disequilibrium of green gahnite-quartz, resulted in the formation of the blue gahnite overgrowths.

4.5.4 Metamorphism and $f(O)_2$

In central Namaqualand, to the south of Oranjefontein, metapelitic rocks are dominated by granulite-facies assemblages. A commonly observed assemblage in these rocks is quartz + k-feldspar + garnet + cordierite (Joubert 1971, Moore 1983). To the north of the area, at Aggeneys and Gamsberg, amphibolite-grade metamorphism is characterised by quartz + biotite + muscovite + sillimanite in metapelitic schists (Rozendaal 1978, Moore 1977). Calculations based on garnet-biotite geothermometry at Broken Hill and Achab (this study) provide temperatures compatible with M2 metamorphism at these localities viz. 650 °C at 4.5 - 5 kbar. Albat (1984) estimated pressure-temperature conditions of 700 - 900 °C and

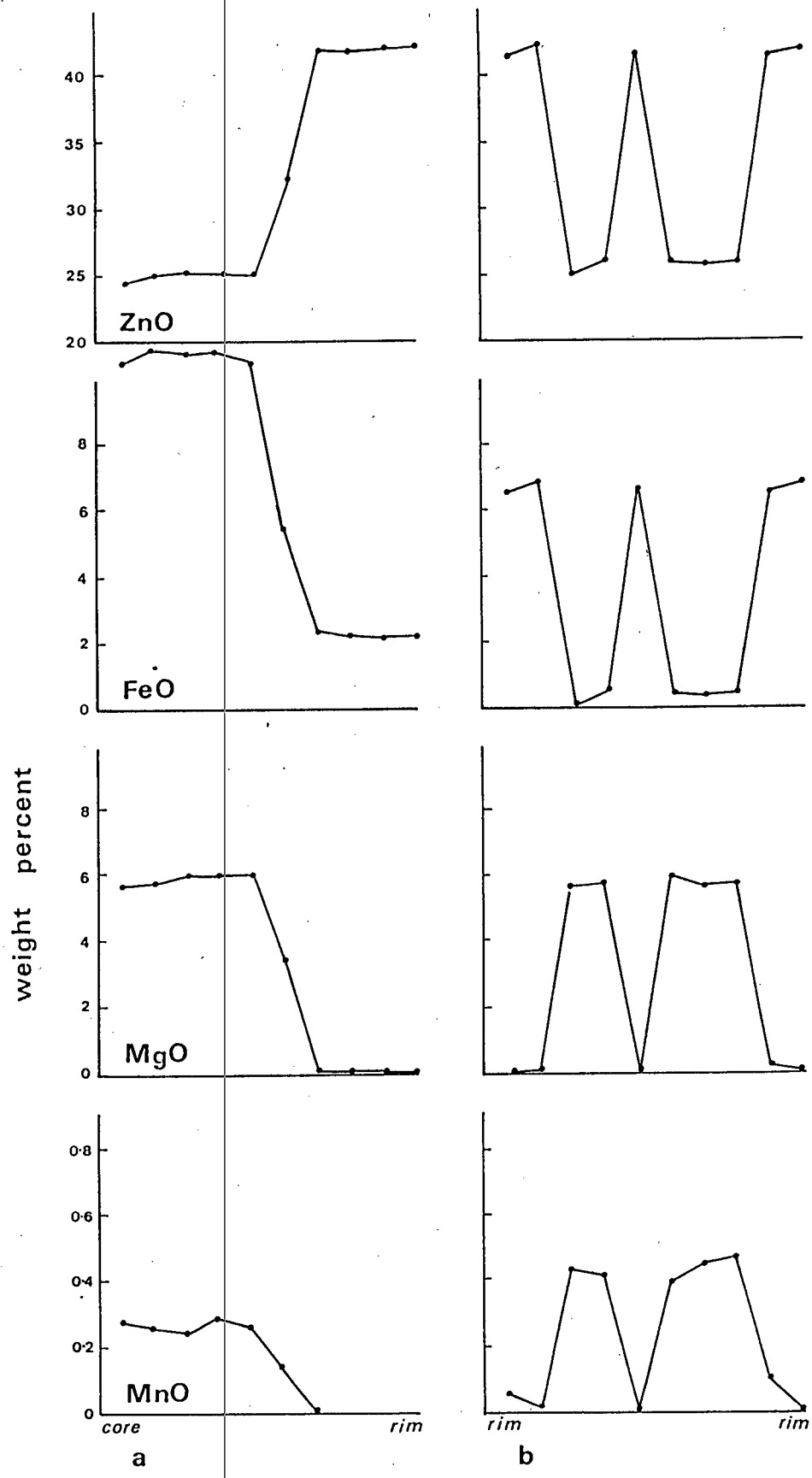

Figure 36: Zoned profiles across gahnite grains. (a: from centre to rim, b: from rim, accross central vein of blue gahnite, to rim) Distance between individual analyses, (dots on diagram), is equivalent to 50 um.

5 - 6 kbar in the granulite-facies terrane in the south. At Oranjefontein the the quartz + k-feldspar + cordierite + sillimanite ± garnet and garnet + biotite + cordierite assemblages in the metapelitic rocks indicate that higher metamorphic grades were attained than at Aggeneys and Achab.

Garnet compositions are plotted as functions of their cation variability according to a method proposed by Sturt (1962) (Fig.37). Sturt (1962) showed that Fe and Mg content of garnet increases with increasing metamorphic grade. On Figure 37, it is apparent that garnet in the garnet-cordierite-biotite rock and the aluminous schist have similar Ca+Mn/Fe+Mg ratios and are representative of Sturt's (1962) sillimanite zone. Garnet associated with green gahnite in garnet-biotite rocks has similarly high Fe and Mg content whereas garnet occurring in blue gahnite-bearing assemblages and garnet partially replaced by retrograde chlorite are correlated with Sturt's (1962) biotite zone.

Analysed coexisting garnet-biotite and cordierite-biotite pairs from the metapelitic assemblages are plotted on an AFM diagram, (Fig.38). The crossing tie lines are explained in terms of a difference in bulk rock compositions of the two lithologies.

Geothermometric calculations were applied to the co-existing garnet-biotite and biotite-cordierite mineral pairs from the aluminous schist and metapelitic garnet-cordierite-biotite rock. Using the methods of Thompson (1976), Holdaway and Lee (1977), Ferry and Spear (1978) and Indares and Martingole (1985a) and a pressure of 4.5 - 5 kbar, based on the Mg/Fe ratio of cordierite, temperatures of 530 - 720 °C were calculated. Results are given in Table 22.

Mafic rocks on the northern side of Vioolskraalberg, at the same stratigraphic horizon contain orthopyroxene-clinopyroxene assemblages. Geothermometric calculations based on coexisting orthopyroxene- , clinopyroxene pairs yield temperatures of 750 °C at 4.5 - 5 kbar (J. Mc Stay, pers. comm.). The mineral assemblages observed in the metapelitic rocks indicate upper-amphibolite- to granulite-facies metamorphism but temperatures obtained from biotite-garnet-cordierite geothermometry are variable (530 - 720 °C). The range of calculated temperatures suggests

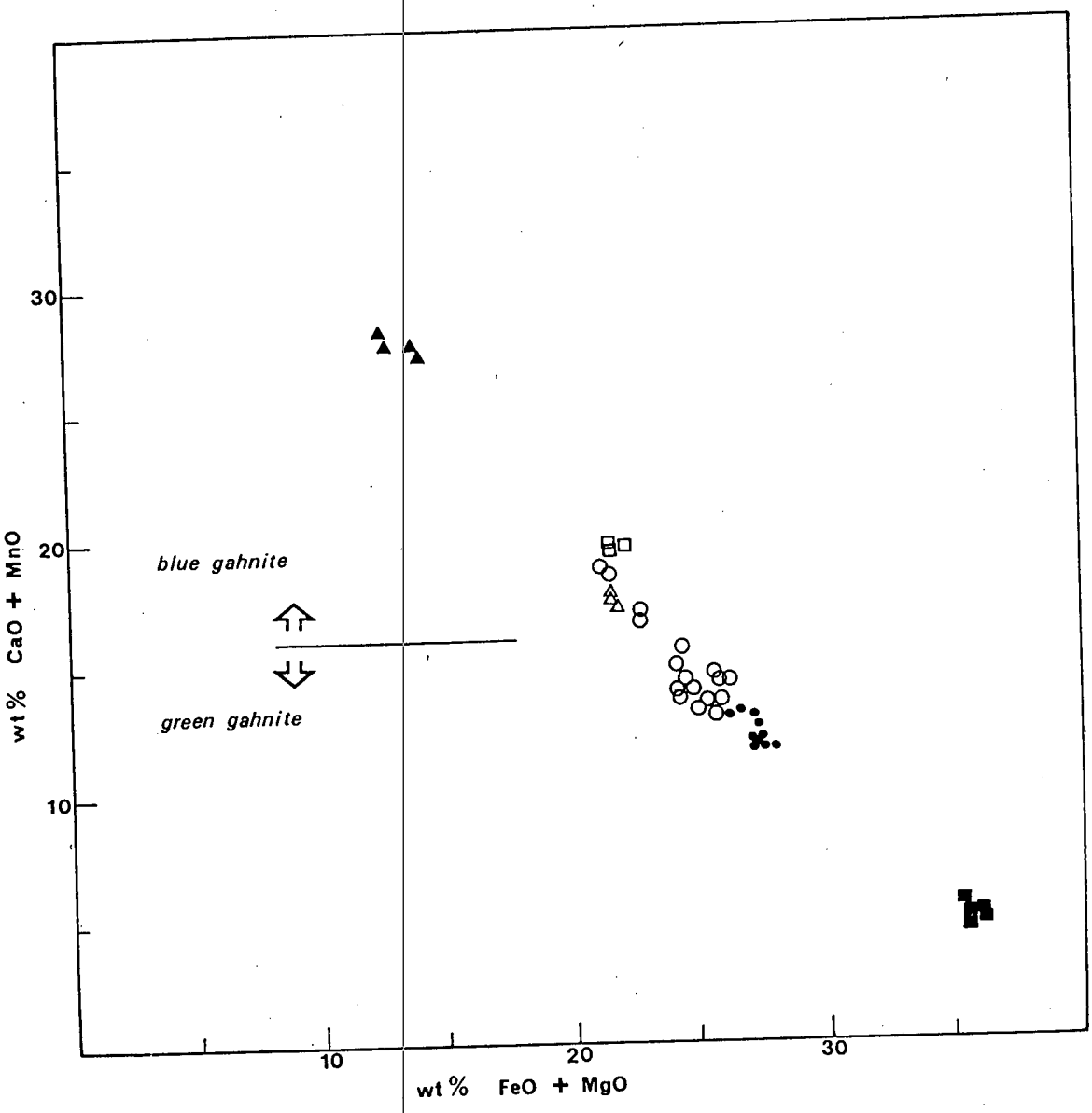

Symbols:

dots	:	gahnite(+phlogopite, garnet) quartzites
circles	:	gahnite-bearing, garnet-biotite rocks
closed triangles	:	garnet-, gahnite-bearing metaquartzite
open triangles	:	garnet-bearing metaquartzite
closed squares	:	garnet-biotite-cordierite schist
open squares	:	garnet-biotite rocks

Figure 37: Garnets plotted as wt% CaO+MnO vs. wt% FeO+MgO (after Sturt, 1962).

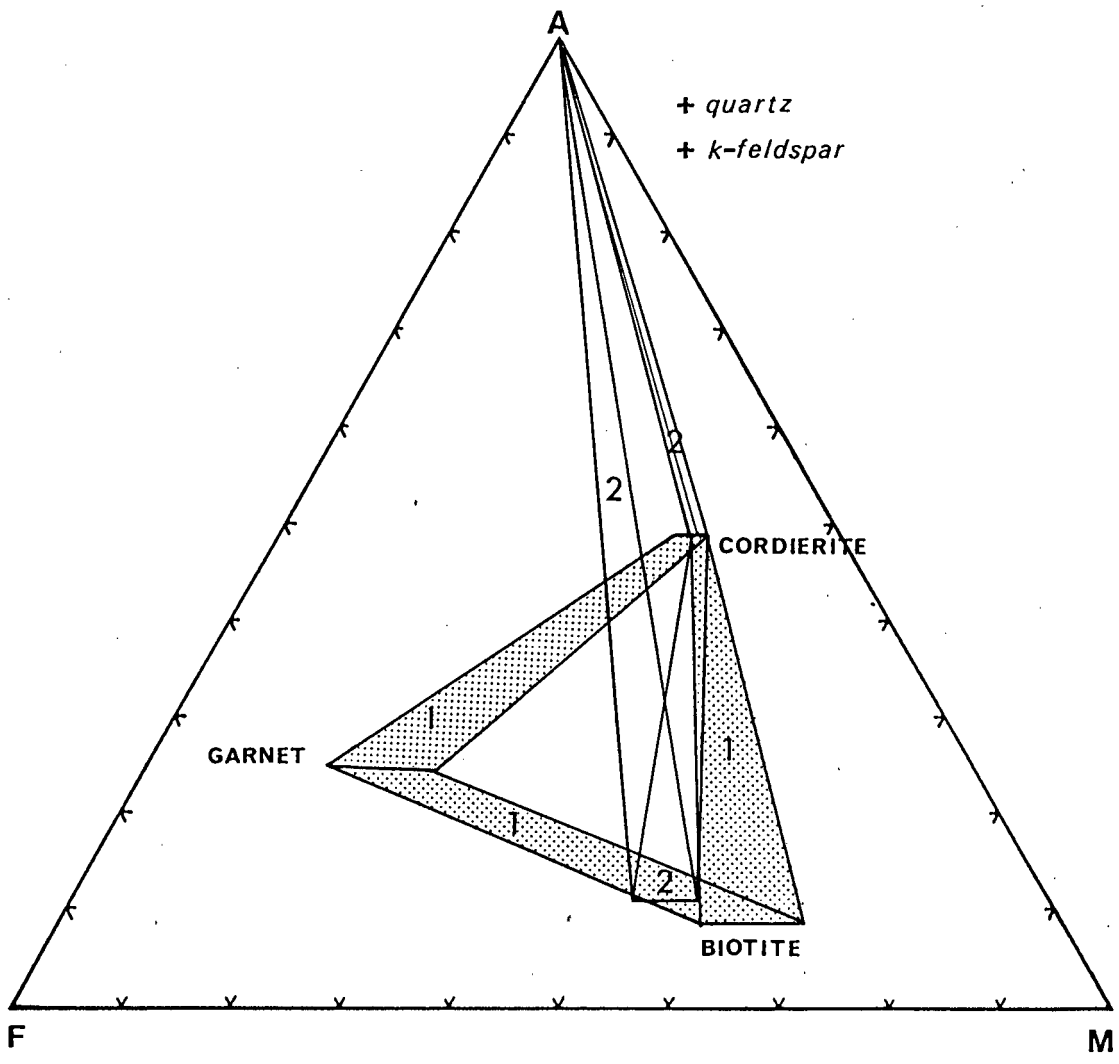

Figure 38: The aluminous schist (1) and metapelitic schist (2) plotted on an AFM diagram.

Table 22: Results of garnet-biotite geothermometry on metapelitic rocks from Oranjefontein.

Method Employed		Thompson (1976)	Holdaway & Lee (1977)	Ferry & Spear (1978)	Indares & Martingole (1985a) *
Sample	Analysis No.				
JE 31 biotite-garnet	1	587	574	560	581
	2	627	609	527	516
	3	641	621	517	502
	4	594	580	553	
JE 32 biotite-garnet	1	642	622	516	474
	2	631	612	525	584
	3	670	646	495	471
	4	628	719	526	
	5	559	550	584	
	6	640	620	517	
JE 29 biot-gar	1				568
	2				577
JE 29 biotite-cordierite	1		541		
	2		507		
	3		510		
	4		633		
	5		599		
JE 30 biotite-cordierite	1		616		
	2		698		
	3		632		

MAXIMUM TEMPERATURES

JE 31,32	670 ±30 °C
JE 29,30,31,32	719 ±50 °C
JE 31,32	560 ±30 °C
JE 29,31,32	580 ±50 °C

* Calculations employing the method of Indares and Martingole were done on a different set of analyses.

that the retrograde metamorphic event resulted in some re-equilibration between Fe-Mg minerals in the metapelitic rocks. Temperatures of 650 - 750 °C at 4.5 - 5 kbar, are compatible with the high-grade metamorhpic assemblages observed in the metapelitic rocks.

The presence of epidote-chlorite replacing garnet-biotite assemblages, chloritized biotite, garnet and widespread seritization/pinitization of feldspar and cordierite are evidence of a later low temperature, retrograde metamorphic event. Blue gahnite formation, in intergrowths with rutile, hematite and quartz replacing biotite, and in intergrowths with hematite and chlorite replacing garnet, is associated with this event. Quartz pegmatites associated with shearing at Vioolskraalberg are associated with this event (Joubert, 1971). Metamorphic conditions of greenschist facies are estimated (based on the presence of chlorite and epidote) with temperatures of less than 500 °C at pressures equal to or lower than that of the main metamorphic event at this locality.

The quartz-magnetite associations in the aluminous schist generally indicate fairly oxidising conditions during prograde metamorphism and hematite, (associated with blue gahnite) even higher $f(O)_2$ conditions during retrograde metamorphism.

Quartz-magnetite-garnet-biotite assemblages in the metapelitic schist enable the application of Zen's (1985) BAMM buffer. Application of the buffer calculations indicate an average log $fO_2 = -16.5 \pm 0.7$ during upper amphibolite-granulite grade metamorphism (Table 23).

4.5.5 Gahnite Formation

Blue gahnite is fine-grained, occurring as aggregates of euhedral grains whereas green gahnite is porphyroblastic and may contain inclusions of quartz or biotite. Green gahnite is restricted in its occurrence to rocks at the contact of the aluminous schist and the overlying metaquartzite, whereas blue gahnite mineralization extends into the metaquartzite and garnet-rich rocks. Green gahnite is associated with prograde assemblages and it is proposed that green gahnite formed during the upper amphibolite grade metamorphic event.

Table 23: Results of oxygen fugacity calculations on Oranjefontein rocks.

Sample nr:	JE 31 (3 analyses)	JE 32 (3 analyses)	JE 29 (6 analyses)
Corrections for substitution in Biotite			
-4 log X_{Si}	0.17	0.19	0.19
	0.18	0.18	0.21
	0.18	0.17	0.24
			0.24
			0.18
			0.20
-3 log X_{Fe}	1.77	1.59	1.64
	1.71	1.66	1.42
	1.89	1.70	1.66
			1.64
			2.03
			1.48
Corrections for substitution in Garnet			
-3 log X_{Fe}	0.50	0.57	0.63
	0.59	0.53	0.67
	0.55	0.49	0.65
Average correction Biotite (Si)	0.18	0.17	0.21
Average correction Biotite (Fe)	1.79	1.65	1.65
Average correction Garnet (Fe)	0.55	0.53	0.65
Total correction	2.52	2.35	2.51

Average Correction = 2.46

Reference BAMM buffer at 650 °C and 4.5 kb:

Log $f(O)_2$ = 10.29 - 26284/T + 0.148(P-1)/T ± 650/T = -18.97 ± 0.7

Corrected log $f(O)_2$ = -16.51 ± 0.7

The local presence of disseminated galena and rare chalcopyrite in the quartzites and presence of trace quantities of Pb and Cu in the bulk chemical analyses is supporting evidence for the presence of sulphides in the precursor sediments at Oranjefontein. The moblity of the Zn^{2+} ion and its tendency to form colloids with Fe^{2+} and OH (Wedepohl 1972) would result in desulphidation of sphalerite more readily than galena, which would account for the continued presence of galena in these rocks whereas only trace quantities of chalcopyrite and no sphalerite remain. It is proposed that the original sediments included a thin sulphide-bearing horizon between the precursor sediments of the metapelitic schist and the overlying quartzite horizons. The sulphide-bearing horizon was associated with unusually Mn, Mg, Fe and Al-rich sediments which under prolonged metamorphism to uppper amphibolite grades led to the formation of garnet, biotite, cordierite and green gahnite. A suggested prograde reaction is (Hicks et al. 1985):

sphalerite + Mg-clay minerals -> green gahnite + biotite + garnet + quartz + S_2 + H_2O

Minor but significant amounts of zinc were taken up by biotite during this reaction (ZnO up to 0.5 wt%).

Segnit (1961) and Sandhaus and Craig (1986) proposed that, gahnite located in the peripheral regions of metamorphosed sulphide deposits and within metapelitic rocks where there is no association with sphalerite, may have formed by reactions involving zinc species adsorbed onto clay minerals or Fe/Mn oxides (Vine and Tourtelot 1970, Coveney 1979, Helios and Rybicke 1985). The presence of postulated clay minerals and significant concentrations of manganese in the proposed precursor lithologies at Oranjefontein may indicate that some zinc initially occurred adsorbed onto these components. The high levels of zinc, relative to iron, manganese and magnesium, in the gahnite-bearing quartzites, however, make it unlikely that all zinc could have been accomodated in this manner (Hicks et al., op. cit.).

Mineralogical and textural evidence for the formation of near end-member blue gahnite indicate that it formed during a period of retrograde metamorphism of greenschist grade subsequent to the formation of green gahnite. Low-temperature metamorphism accompanied by a fluid phase resulted in the breakdown of garnet and biotite and resulted in the formation of blue gahnite, chlorite, epidote and sericite.

Dietvorst (1980) proposed the formation of gahnite during retrograde breakdown of zinc-bearing biotite to form chlorite. In this process zinc is transferred from biotite to gahnite and does not enter the chlorite structure. At Oranjefontein, retrograde chlorite contains more zinc than biotite (3.9 wt% as opposed to 0.4 wt%) and this process cannot apply to blue gahnite formation. It is proposed that biotite, garnet and green gahnite participated in the retrograde, blue gahnite-forming reaction. The proposed retrograde reaction is;

(Zn,Mg)green gahnite + Mg-biotite + garnet + quartz + H20 -> blue gahnite + chlorite + rutile + hematite + sericite ...Hicks et al. (op. cit.).

The retrograde blue gahnite assemblages generally contain abundant quartz and very little sericite, which suggests this reaction was accompanied by addition of SiO_2 to and removal of K from the system.

Chapter 5. CONCLUSIONS

5.1 Gahnite Mineralogy

Figure 2 showed that the stratigraphic successions at Swartkoppies, Broken Hill and Oranjefontein are similar and are correlated with the Bushmanland rocks of the NMC.
At Swartkoppies and Achab, gahnite is associated with aluminous rocks and schists. At Oranjefontein, green gahnite occurs in garnet-biotite rocks in the uppermost horizons of the aluminous schist. Gahnite occurs in greater quantities in the metaquartzites at Achab and Oranjefontein. At Broken Hill gahnite occurs in the sulphide-bearing BIF rocks which occur below the massive quartzites.

Figures 39, 41, 42 and 43 summarise the analytical data on gahnite and spinels in the study areas.

Figure 40 (from Spry, 1984), results from a compilation of gahnite compositions as related to host rock lithology. Results of this study indicate that close to endmember blue gahnite from Oranjefontein is associated with a low grade metamorphic overprint which was associated with shearing and the emplacement of quartz veins (pegmatites) at this locality. Spry's diagram shows that gahnite of this composition generally occurs in association with pegmatities. Mg-rich gahnite is generally associated with marbles, however the Zn, Mg-rich composition of green gahnite at Oranjefontein is attributed to formation from ZnS-bearing, Mg-rich precursor clays. Gahnite composition from Achab and the massive sulphide deposit at Aggeneys is typical of gahnite associated with metamorphosed massive sulphide deposits (Fig.40). Achab is geographically close to the Aggeneys-Gamsberg ore body and it is proposed that gahnite formed in these rocks during prograde metamorphism of precursor ZnS-bearing metasediments. Gahnite in the highly aluminous rocks at Swartkoppies has a compositional range typical of those occurring in aluminous metasediments (Fig.40).

From Figure 39, it is apparent that gahnite compositions vary significantly between the study localities. Gahnite from Aggeneys is

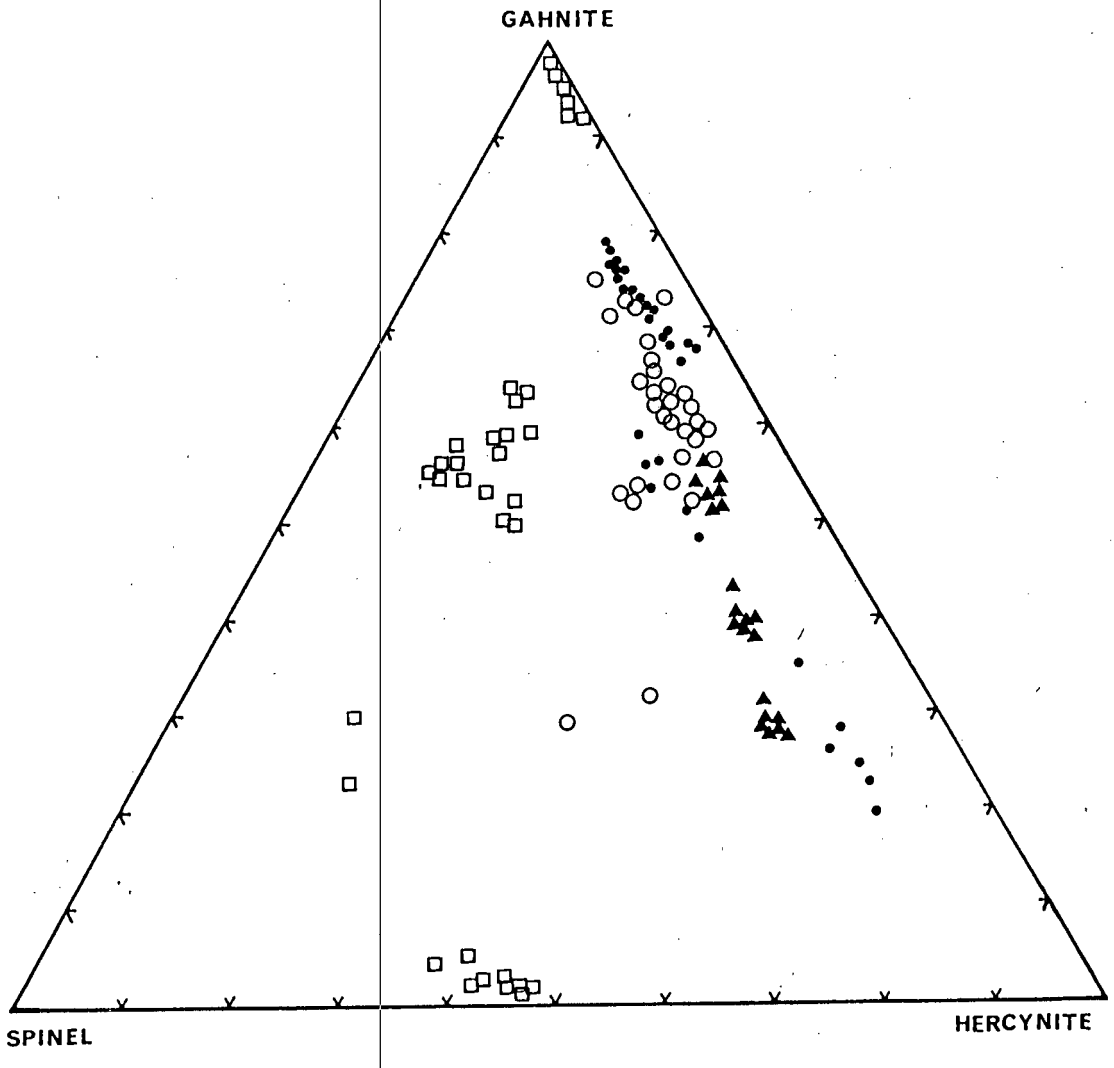

Symbols:
squares : Oranjefontein
dots : Aggeneys/Broken Hill
circles : Achab
triangles: Swartkoppies

Figure 39: Gahnite from the study localities plotted on a triangular endmember diagram.

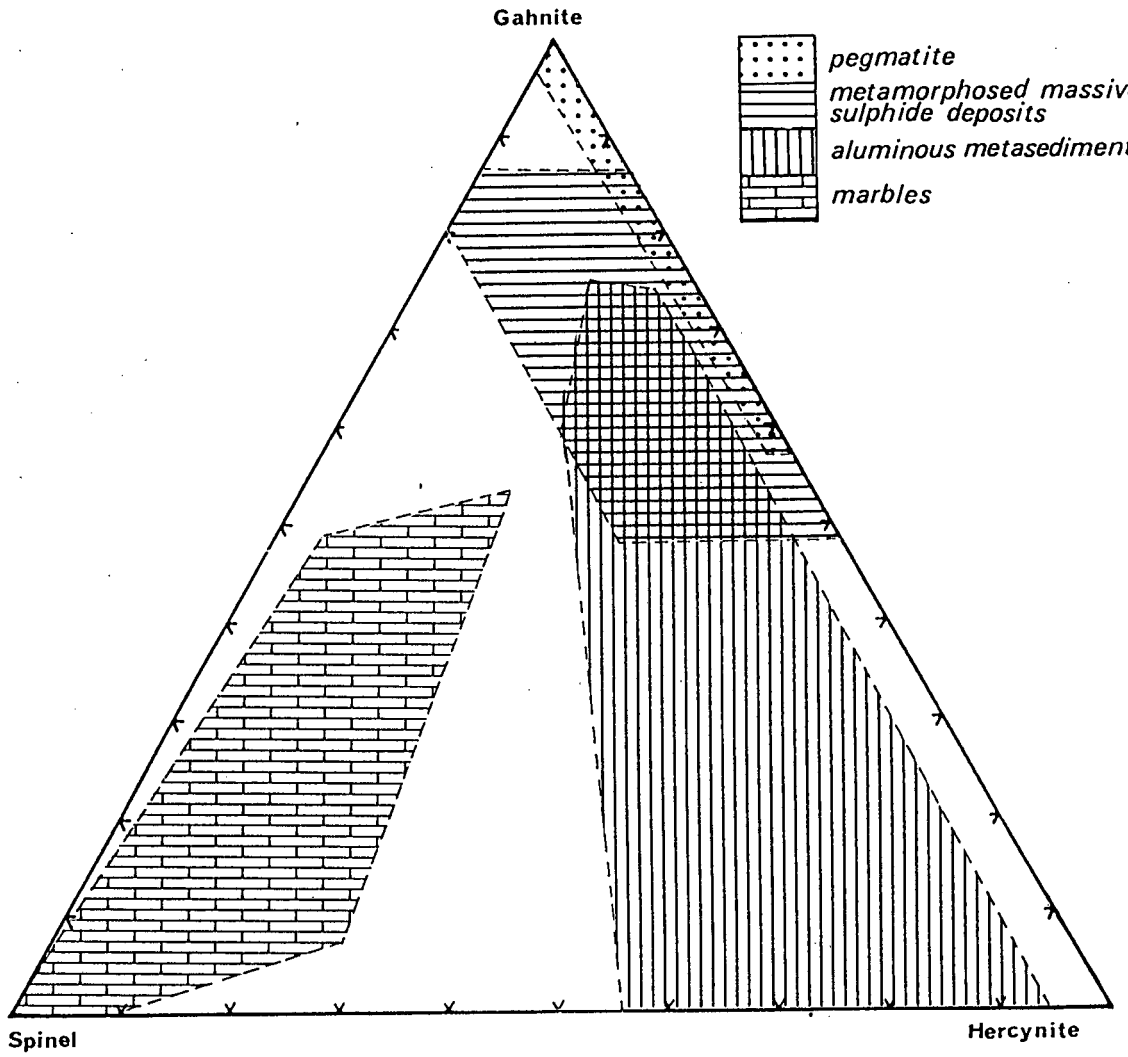

Figure 40: Compositional fields of gahnite according to host rock lithology (from Spry, 1984).

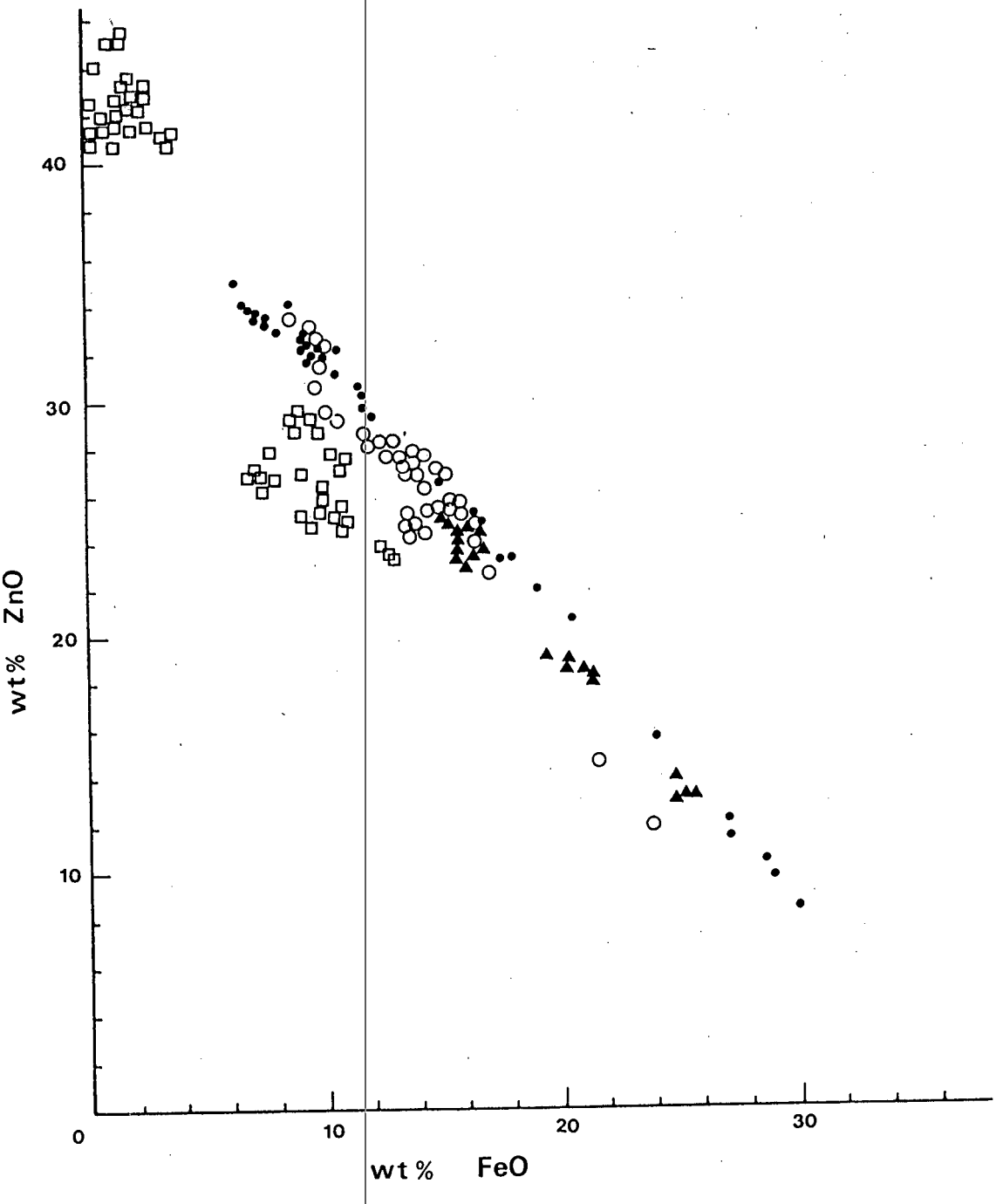

Symbols:
squares : Oranjefontein
dots : Aggeneys/Broken Hill
circles : Achab
triangles: Swartkoppies

Figure 41: Gahnite compositions from the study localities, ZnO/FeO.

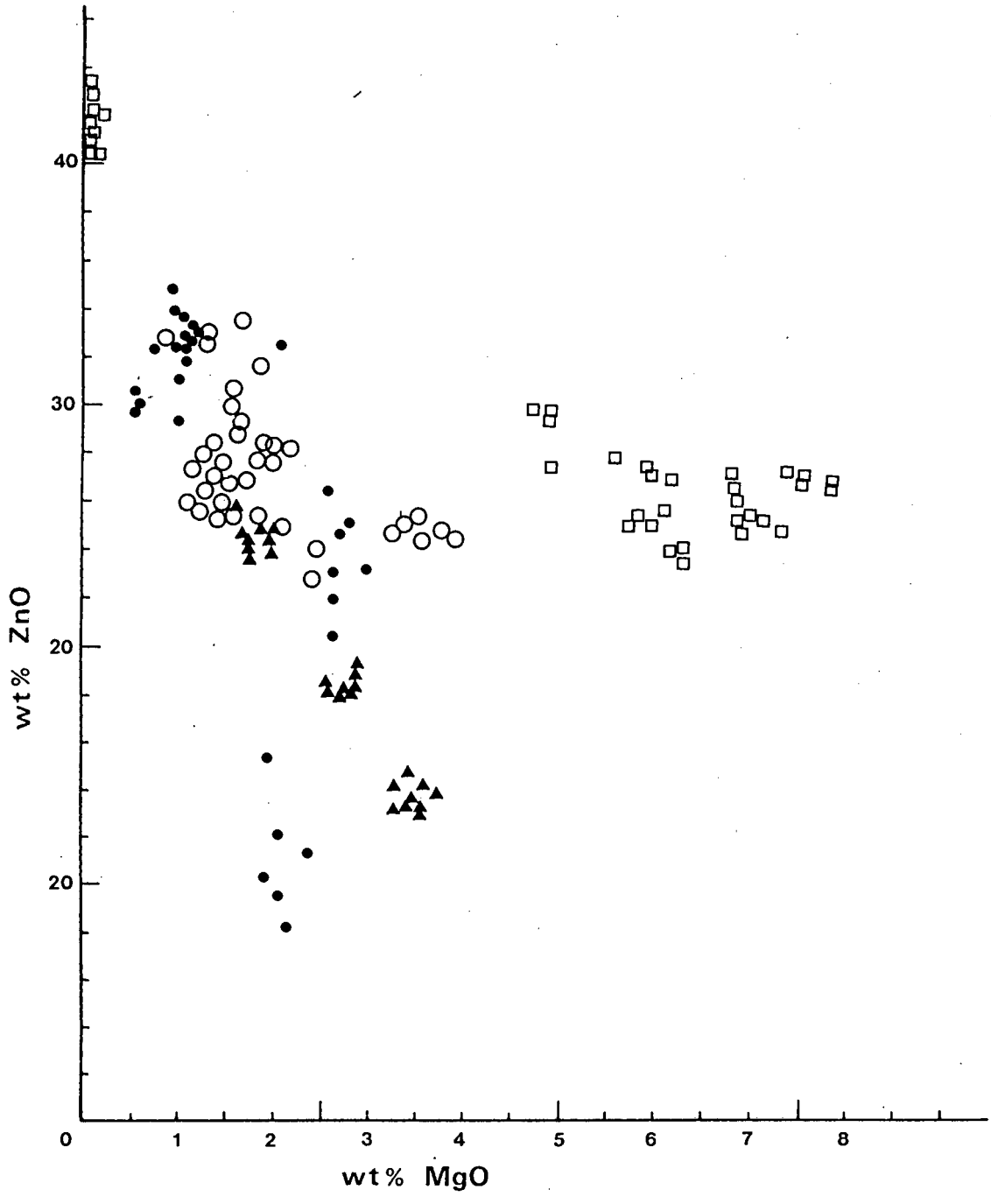

Symbols:
squares : Oranjefontein
dots : Aggeneys/Broken Hill
circles : Achab
triangles: Swartkoppies

Figure 42: Gahnite compositions from the study localities, ZnO/MgO.

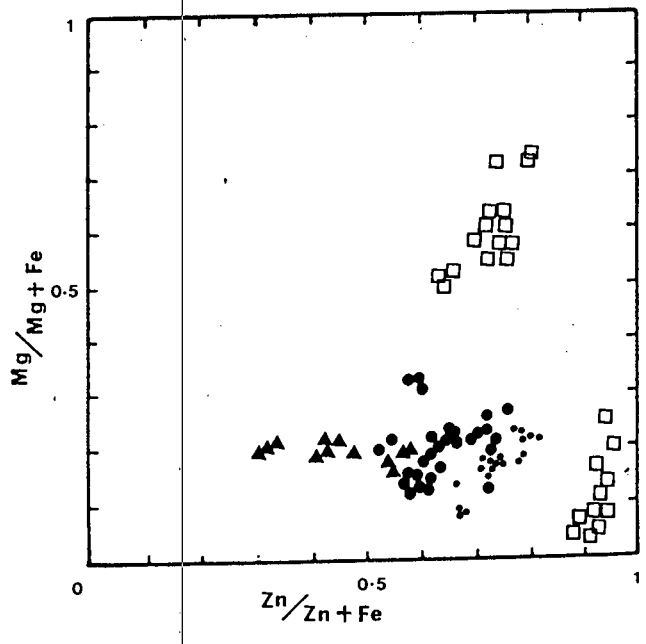

Symbols:
squares : Oranjefontein
small dots: Aggeneys/Broken Hill
large dots: Achab
triangles : Swartkoppies

Figure 43: Gahnite compositions from the study localities, Mg/Mg+Fe vs. Zn/Zn+Fe.

Zn-rich, Swartkoppies is Fe-rich and from Achab has a composition intermediate between these two. Green gahnite from Oranjefontein is relatively Mg-rich compared to Achab, but has similar Zn content. Blue gahnite from Oranjefontein is extremely Zn-rich and has almost no Mg component. Figures 39, 41 and 42 show almost complete solid solution between Zn, Fe and Mg components in spinel. Most of this is attributed to variation in bulk chemistry of the precursor sediments. At Aggeneys and Achab, Mg-rich gahnite occurs in the amphibole-,garnet-bearing quartzite and garnet-gedrite schist whereas hercynite and Fe-gahnite occur in the magnetite quartzite and aluminous schist. Variation in zinc content of gahnite appears to be controlled by $f(O)_2$, $f(S)_2$ and temperature during gahnite formation. This is shown by the relatively high Zn content of the sulphide associated gahnite and extremely high Zn content in the retrograde blue gahnite.

5.2 Appraisal of zinc in minerals associated with gahnite

In metamorphosed rocks close to mineralised terranes staurolite is commonly cited as a zinc-bearing mineral and possible precursor to gahnite formation e.g. Atkin (1978), Stoddard (1979), Spry (1982a), Schumacher (1985). To a lesser extent zinc-bearing micas such as muscovite (Frondel and Ito, 1975), biotite (Frost 1973, Plimer 1977, Dietvorst 1980) and chlorite (Frondel and Ito 1975, Dietvorst 1980) are reported.
In gahnite-bearing lithologies in Namaqualand staurolite is uncommon although it is reported to occur in association with gahnite at Gamsberg (Spry and Scott, 1986b). However, muscovite, biotite and chlorite are common in gahnite-bearing assemblages in all lithologies. All of the micas were analysed for zinc and also sillimanite, garnet and magnetite in view of their possible participation in gahnite-forming reactions. No zinc was found to occur in garnet or sillimanite and is attributed to the tendency for zinc to prefer four-fold co-ordination with oxygen in minerals.

Zinc in mica

The open structure of mica allows a fairly free range of substitution into octahedral sites and due to similarity in ionic radii it is possible that zinc may substitute for iron, magnesium or manganese in the structure. A

zinc-bearing muscovite, hendricksite, containing in excess of 20 mol% ZnO is described by Frondel and Ito (1975).
Prograde and retrograde muscovite was analysed in gahnite-bearing assemblages from Broken Hill and Achab. However, none contained significant zinc
(> 0.2 wt% ZnO).

Zinc-bearing biotites are mentioned by Plimer (1977) in association with sulphide mineralization at Broken Hill, Australia and in the Scandinavian Caledonides at Kemiö by Dietvorst (1980). Dietvorst (op. cit.) suggests that biotite, at amphibolite grades, is able to absorb small quantities of zinc, but that at lower temperaratures, zinc is less stable in the biotite structure.
At Achab, amphibolite-facies biotite contains up to 0.35 wt% ZnO. In the gahnite quartzites at Oranjefontein small biotite laths, armoured by quartz, and containing up to 0.4 wt% ZnO formed during prograde metamorphism of upper amphibolite grade.

Although chlorite is a common constituent in rocks associated with metamorphosed massive sulphide deposits it has seldom been analysed as a potential zinc-bearing mineral (Frondel and Ito, 1975). At Oranjefontein, pervasive retrograde metamorphism has caused the alteration of biotite and garnet to chlorite in many of the rocks. Extensive analyses made on chlorites indicate a percentage of zinc in most chlorites. In garnet-bearing quartzites and garnet-biotite rocks containing blue gahnite, retrograde chlorite contains an average of 1.4 wt% ZnO and locally up to 3.5 wt% ZnO.

Zinc in magnetite
In magnetite, zinc and aluminium may substitute for Fe^{2+} and Fe^{3+} respectively (Wedepohl 1970, Deer et al. 1980). In rocks of the NMC magnetite-hercynite$_{ss}$ is common, and at the gahnite-bearing localities the hercynite commonly incorporates a minor gahnite component. It is probable that at the high metamorphic grades which prevailed in the NMC, a small amount of zinc was contained in the original magnetite-hercynite$_{ss}$ phase.

5.3 Compositional zoning in spinels

Zoning in gahnite in quartzitic rocks

Compositional zoning in gahnite in quartz rich environments has been reported from some localities and is generally accepted to result from re-equilibration of spinel in response to changes in temperature (Dietvorst 1980, Tulloch 1981, Sandhaus 1981, Treloar et al. 1981, Spry 1984, 1986, 1987b). Increasing zinc and decreasing iron and to a lesser extent magnesium, from core to rim, is the most commonly reported pattern and is attributed to gahnite formation under conditions of decreasing temperatures (e.g. Dietvorst 1980, Tulloch 1981, Spry 1984, 1986, 1987b). The opposite trend of decreasing zinc from core to rim is less common (Sandhaus 1981). Several workers (e.g. Frost 1973, Dietvorst 1980, Tulloch 1981, Hicks et al. 1985) observe that hercynite, unstable in the presence of quartz below 750°C, is stabilized at lower temperatures by increased incorporation of zinc into its structure.

Gahnite-bearing quartzites occur at Aggeneys, Achab and Oranjefontein. At Aggeneys the gahnite-bearing quartzite contained amphibole and garnet but gahnite is very fine grained and is not compositionally zoned. Similarly in the Dabiepoort quartzites, gahnite is fine grained and homogeneous. Gahnite-bearing quartzites at Achab contain coarse, poikiloblastic gahnite with numerous inclusions of quartz and these too are not zoned. Green gahnite in Oranjefontein quartzites occurs as coarse porphyroblasts, is commonly embayed to quartz and occasionally has quartz inclusions. Blue gahnite commonly occurs as a rim surrounding the green gahnite and also as tiny euhedral grains in the quartz matrix. A compositional profile across a rimmed gahnite grain (Fig.36), shows the sharp compositional break between green gahnite and blue gahnite. The compositional break coincides with an abrupt change in colour from a green central core to the blue rim, but individually the two varieties of gahnite are homogeneous. This compositional change is not considered to be a growth zonation but represents an overgrowth in response to widely differing metamorphic conditions which result in the original green gahnite being out of equilibrium in the quartzites. Many of the gahnite-bearing rocks contain garnet and analysis of core - rim compositions of garnet in gahnite- and non-gahnite-bearing lithologies did not reveal a consistent zonation pattern.

Zoning in gahnite associated with Fe - Mg aluminosilicate minerals

Zoning in spinels in aluminous metasediments has been attributed to the partitioning of zinc, iron and magnesium between spinels and adjacent ferromagnesium aluminosilicate (Spry 1984, 1987b).

At Oranjefontein, in garnet-biotite-gahnite-quartz rocks, green gahnite occurs in direct contact with all three phases. However, even in this case the gahnite was homogeneous. Occasional grains of green gahnite in massive garnet rocks and garnet-biotite rocks were similarly unzoned. At Achab gahnite in contact with biotite and garnet in metapelitic schists did not show any zonation pattern. Gahnite in the massive gahnite rock at Swartkoppies and to a lesser extent, in the gahnite- and biotite-bearing fibrolite rocks at this locality showed some colour zonation, with dark green cores and pale green rims. The massive gahnite rock showed the most obvious colour zonation and this corresponds with an increase of 2.2 mol% gahnite and decrease of 1.7 mol% hercynite and 0.5 mol% spinel from core to rim (Fig.44). The gahnite-, biotite-bearing fibrolite rock showed the least compositional zoning at this locality. None of the biotite in rocks from Swartkoppies contained zinc and it is unlikely that the slight compositional zoning results from Fe-Mg exchange. It is also difficult to explain why the most dramatic zoning at this locality should occur in the massive gahnite rocks. In the absence of any suitable mineral for Fe-Mg exchange and the absence of sulphides for $f(S)_2$ - $f(O)_2$ controlled equilibria between gahnite and sphalerite, the zoning is attributed to gahnite growth during a period of decreasing metamorphic temperatures.

Zoning in gahnite associated with sulphide minerals

In metamorphosed massive sulphide deposits, Spry (1984, 1987b) has observed compositional zoning in gahnite and associated sphalerite. This he attributed to the partitioning of Zn and Fe in response to changing $f(O)_2$ - $f(S)_2$ conditions between the two phases and associated pyrite/pyrrhotite. In this study coexisting gahnite and sphalerite were observed in the massive sulphide rocks and sulphide-bearing BIF from Broken Hill.

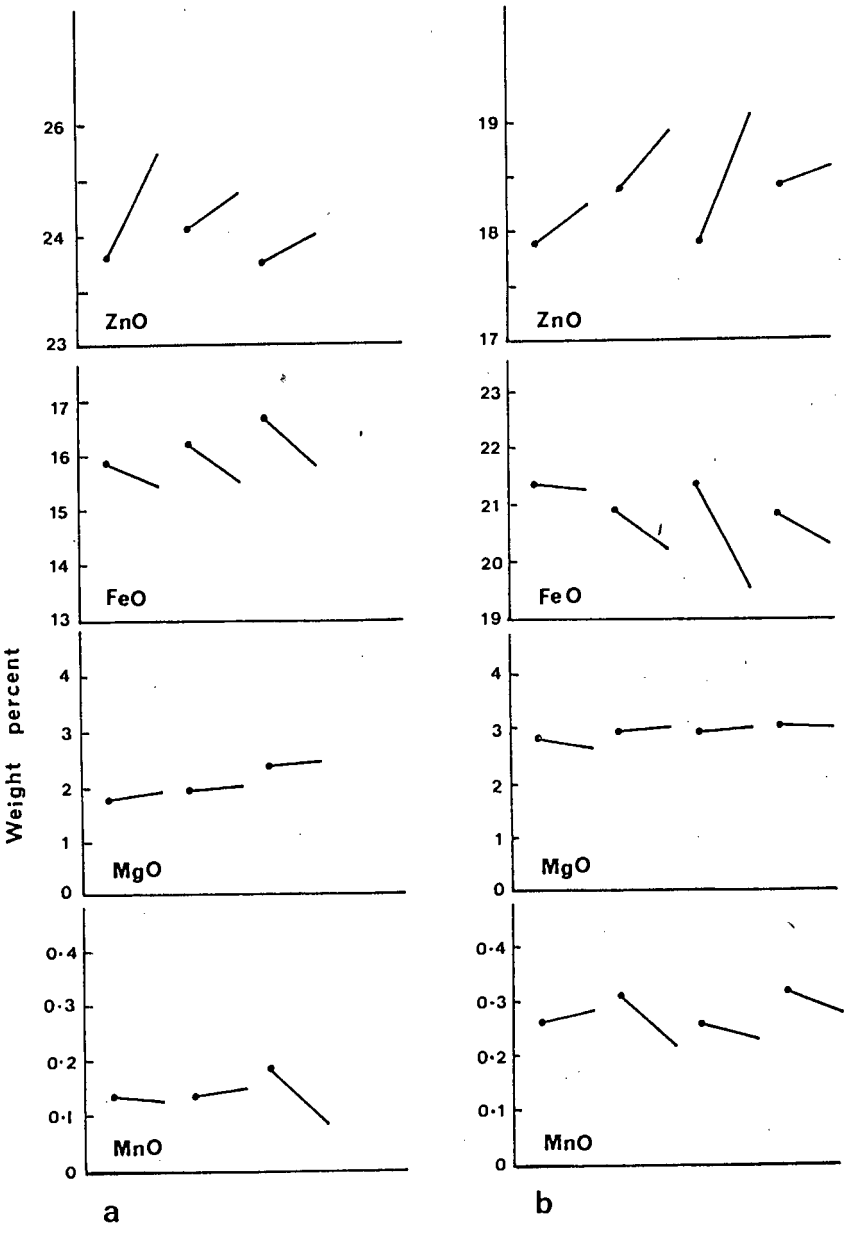

Figure 44: Core-rim analyses of gahnite from Swartkoppies in a; the massive gahnite rock and b; the gahnite-biotite-fibrolite rock.

Spry (1987a) observes that gahnite from Aggeneys is commonly colour zoned, this being attributed to the fine inclusions of secondary sphalerite, but only observed compositional zoning in gahnite enclosed in magnetite in the quartz-magnetite lithology. Here gahnite showed up to 18 mol% decrease in gahnite content with a corresponding increase of 14 mol% hercynite, 3 mol% galaxite and 2 mol% spinel. He attributed this to depletion in zinc during gahnite growth. In this study it was found that gahnite in the massive sulphide rocks from Broken Hill is generally fairly fine grained and most commonly unzoned, however, one exception does occur. In a quartz-rich massive sulphide rock, gahnite coexists with quartz and muscovite in the gangue and sphalerite in the massive ore. Figure 45 shows an increase of 0.7 wt% ZnO and decrease of 0.5 wt% FeO and 0.2 wt% MgO between core and rim in two of the coarsest gahnite grains. The associated muscovite did not contain zinc and the association of gahnite and sphalerite suggest that Zn/Fe partitioning between the phases has resulted in minor zoning.

It appears that there are various possibilities for gahnite zonation. Some of these are summarised below:

1. Re-equilibration of gahnite in quartz-rich rocks in response to changing metamorphic temperatures due to the incompatibility of iron-rich spinels and quartz below granulite grades of metamorphism.
2. Zn-Fe-Mg exchange between gahnite and associated Fe-Mg aluminosilicate minerals at amphibolite grades of metamorphism.
3. Zn/Fe partitioning, controlled by $f(S)_2$ - $f(O)_2$ equilibria between gahnite and sphalerite, pyrite/pyrrhotite in metamorphosed massive sulphide deposits.
4. A further possibility is the apparent sensitivity of gahnite composition to changes in metamorphic $f(O)_2$. Moore and Reid (1987 in press) observed that fine-grained, disseminate gahnite in a gahnite-bearing quartzite shows significant compositional changes which can be related to its proximity to oxidising metamorphic fluid pathways.

Results from this study are thus not entirely consistent with documented occurrences of zoned gahnite. In this study it was found that gahnite in quartzites and quartz-rich rocks are generally not zoned, however this may be due in part to either fine grain size of gahnite or the extremely

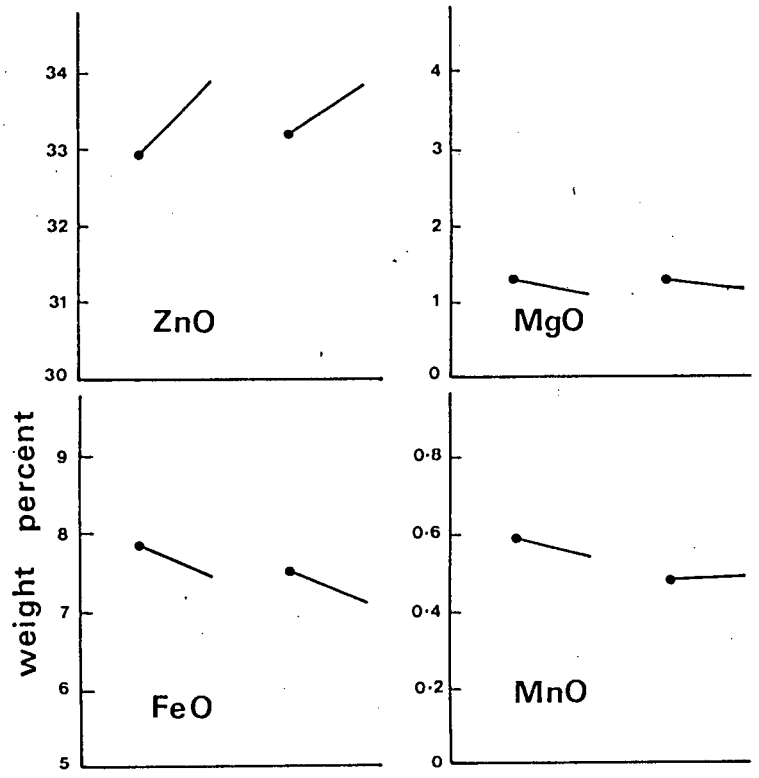

Figure 45: Core-rim compositions of gahnite from Broken Hill.

poikiloblastic habit. In association with ferromagnesiun aluminosilicate minerals such as garnet or biotite, no consistent compositional zonation was observed in gahnite. At Swartkoppies, in massive gahnite rocks, colour zonation is associated with minor but consistent compositional zoning exhibited by increasing zinc and decreasing iron and magnesium from core to rim. This is attributed to a re-equilibration in response to changing metamorphic temperatures during the growth of gahnite. Compositional zoning, although present, was less obvious in the gahnite-, biotite-bearing fibrolite rocks from Swartkoppies. In the metamorphosed massive from Broken Hill only one rock contained zoned gahnite and in this rock gahnite is in contact with quartz and sphalerite. Here the zoning is attributed to Fe/Zn exchange between gahnite and sphalerite as proposed by Spry (1984, 1987a).

5.4 Gahnite in relation to Pressure, Temperature, and $f(O)_2$

Wall and England (1979) suggest that the hercynite content of zincian spinels is buffered by equilibria such as; $3FeAl_2O_4 + 5SiO_2 = Fe_3Al_2Si_3O_{12} + 2Al_2SiO_5$ and suggest that this reaction may be useful as a sliding geothermometer in conjunction with accurate geobarometry. Bohlen et al. (1986) did experimental reversals on this reaction and found that the equilibrium is located at 5.2 - 5.4 kbar at 880 °C and that it shifts to higher pressures with increasing temperatures. The incorporation of additional components of Zn or Fe^{3+}, in hercynite broadens the stability field of hercynite-quartz and shifts the equilibrium to higher pressures.

Gahnite-quartz associations are found in granulite-, amphibolite- and greenschist facies parageneses in Namaqualand, indicating stability over a range of metamorphic conditions. Frost (1973), Kramm (1977) and Spry (1984) observe that gahnite in quartz-rich terranes is stabilised by increased incorporation of zinc into its structure under decreasing metamorphic temperatures. This theory is supported to some extent by the study of gahnite in Namaqualand. Figure 46 shows gahnite compositions in the quartzites. Gahnite in quartz-rich assemblages at Oranjefontein contains 50 - 65 mol% gahnite at upper amphibolite to granulite grades and

in excess of 90 mol% gahnite at greenschist grades. Gahnite in quartz-rich assemblages at Achab and Aggeneys contains 50 - 75 mol% gahnite at upper amphibolite grades (Fig.46).

Siefert and Schumacher (1986) suggest that the composition of the ($Mg-Zn-Fe^{2+}$) spinel coexisting with cordierite and quartz may be sensitive to changes in pressure and investigated a geobarometer based on the reaction; $Mg_2Al_2Si_5O_{18} = 2MgAl_2O_4 + 5SiO_2$. No such assemblages occur in the study area and this reaction could not have taken place. There does, however, appear to be some correlation of Mg content of gahnite with pressure and temperature. Figure 39 shows that gahnite and pleonaste in the granulite facies at Oranjefontein has in excess of 20 - 35 mol% spinel and 50 - 60 mol% spinel respectively (T = 650 - 750 °C, P = 4.5 - 5 kbar). Gahnite and zincian hercynite from Aggeneys, Achab and Swartkoppies at upper amphibolite grade metamorphism has between 5 and 20 mol% spinel (T = 650 - 670 °C, P = 4.5 - 5 kbar). The composition of blue gahnite from which Oranjefontein formed during low temperature retrograde metamorphism contains less than 1 mol% spinel. The variation in gahnite-bearing assemblages does not support a spinel-quartz-aluminosilicate reaction, in which case the increase in mol% spinel content of gahnite with metamorphic temperature and pressure should be viewed with caution. However additional data may well yield more conclusive results in Namaqualand.

In some assemblages in the rocks studied, gahnite and garnet coexist stably although quartz and aluminosilicate are not necessarily part of the same paragenesis. Spry (1984, 1987a) and Spry and Scott (1986a) have suggested that gahnite may form by garnet breakdown in a solid-solid reaction i.e $Fe_3Al_2Si_3O_{12} + ZnS + S_2 \rightarrow ZnAl_2O_4 + 3FeS + 3SiO_2 + O_2$. Using the diagram suggested by Sturt (1962), garnet compositions were plotted as a function of Ca+Mn/Fe+Mg, (Fig.48). The hercynite content of gahnite associated with particular garnet-bearing rocks has been added to the diagram. Figure 48 shows an increase in hercynite content of gahnite with increasing Fe+Mg of garnet. There is, however no conclusive evidence for garnet-gahnite type reactions and Fe-Mg exchange is the most likely cause for this correlation between mineral phases.

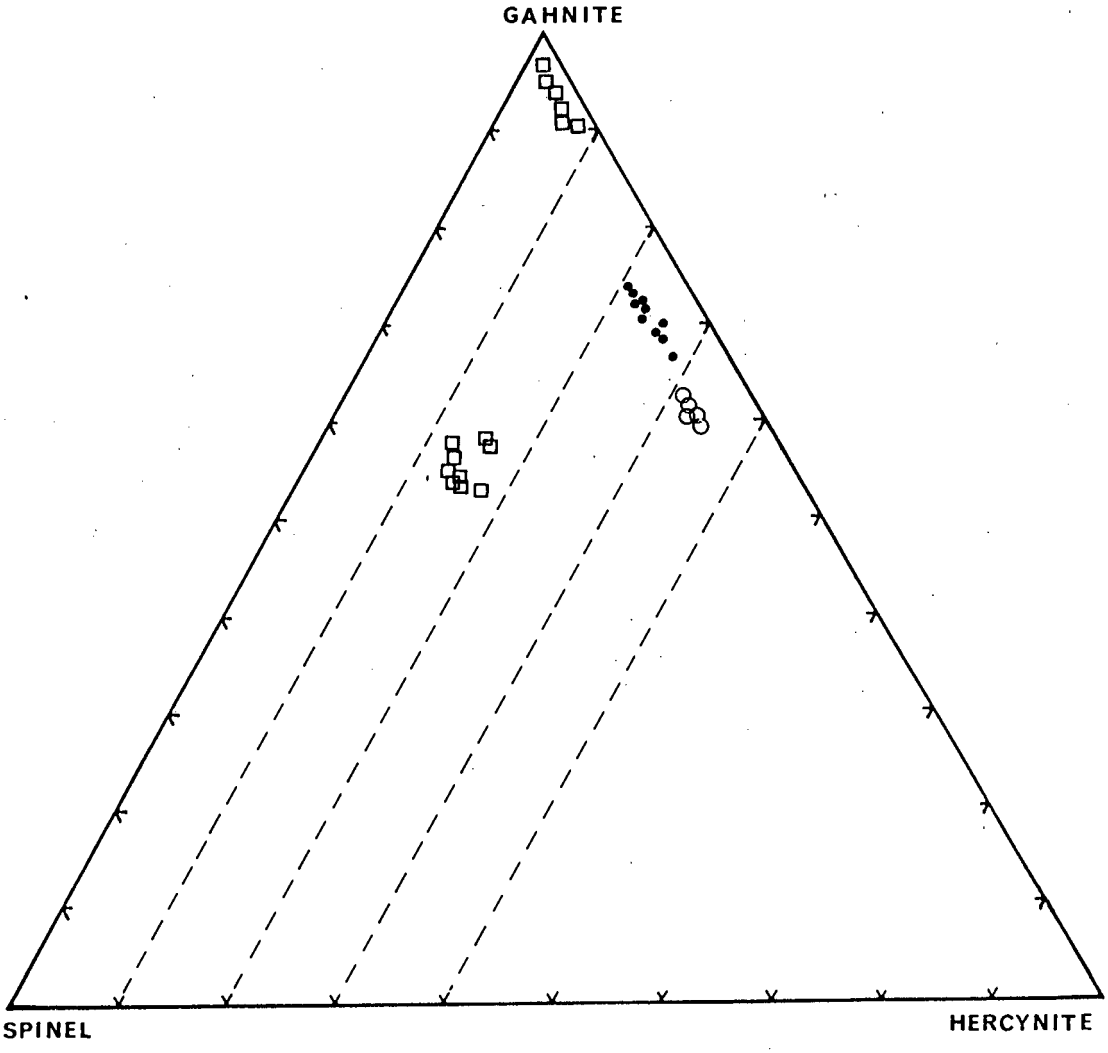

Figure 46: Gahnite compositions from gahnite quartzites at Oranjefontein (squares), Aggeneys (dots) and Achab (circles), plotted on an endmember diagram.

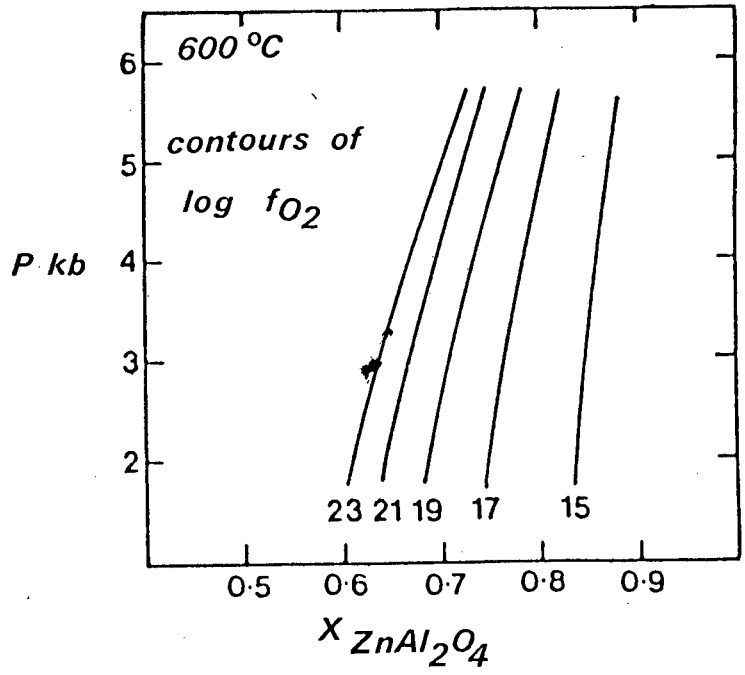

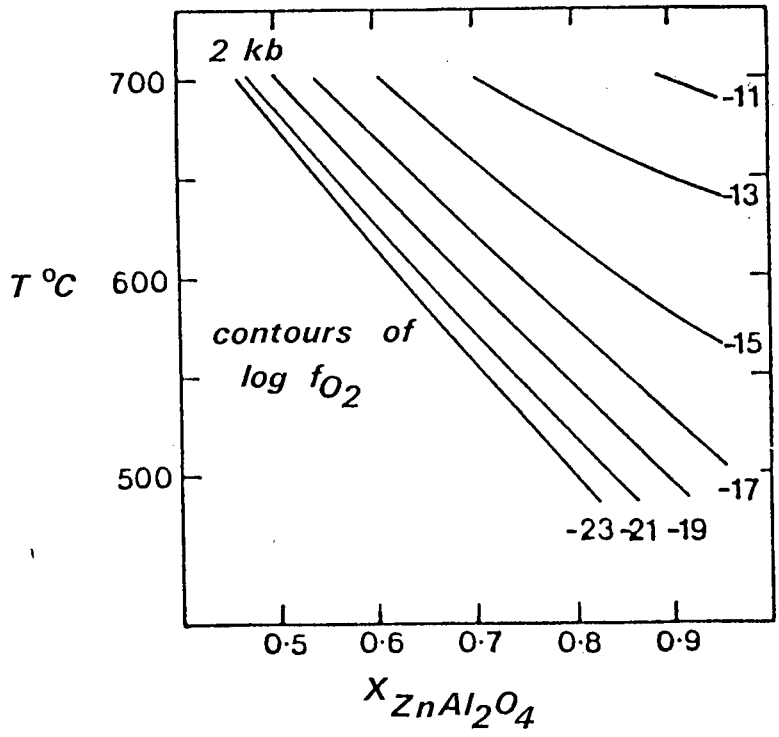

Figure 47: Variation of gahnite composition with pressure and temperature (from Spry, 1984).

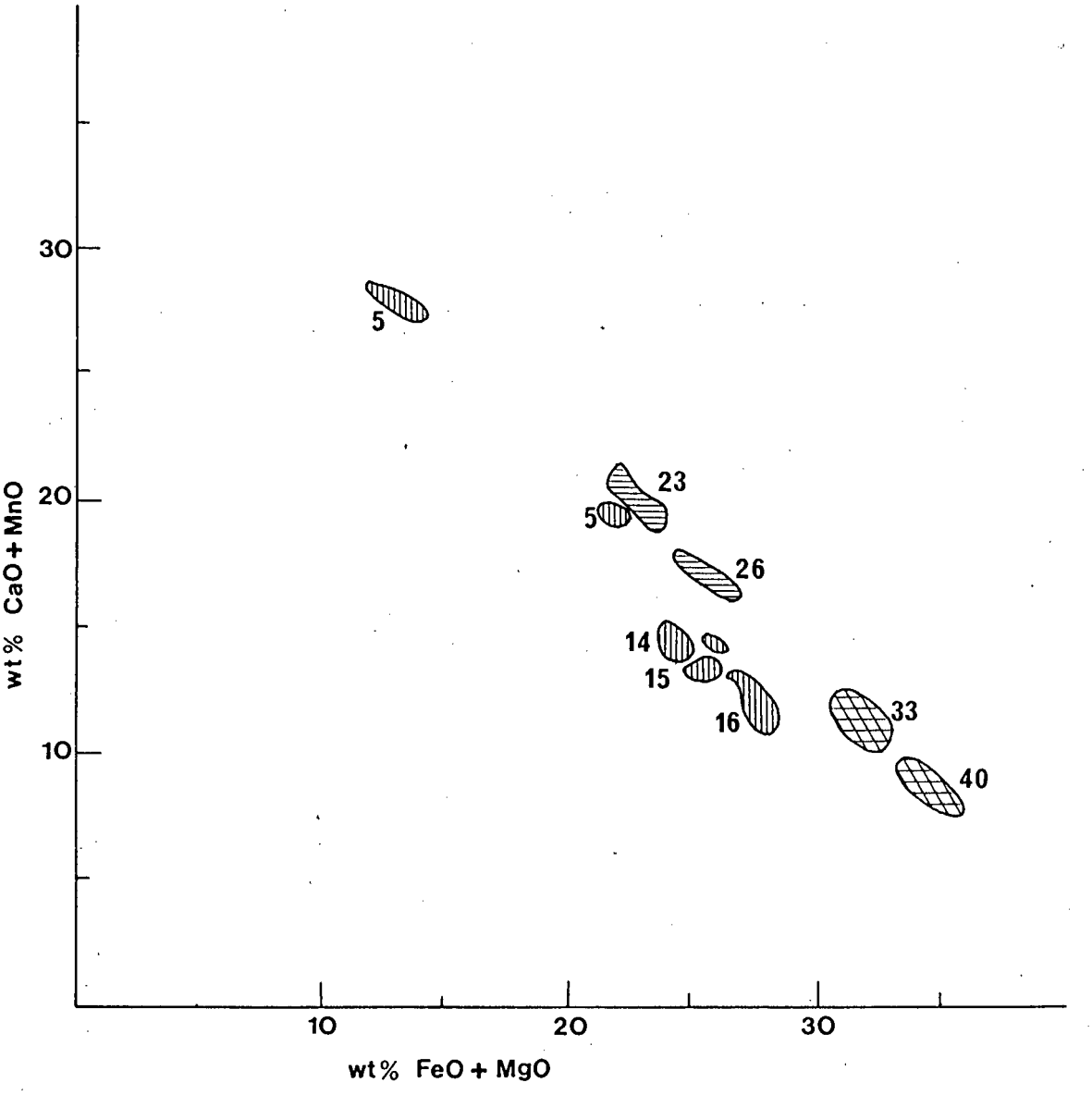

Figure 48: The average hercynite content of gahnite (numbers) plotted alongside garnet from Aggeneys (horizontal stripe), Achab (cross hatch), and Oranjefontein (vertical stripe). Diagram after Sturt, 1962).

Spry and Scott (1986a) found that the composition of spinels in equilibrium with sphalerite and pyrite/pyrrhotite become more Zn-enriched with increasing $f(O)_2$ and $f(S)_2$ and can be used as a measure of $f(O)_2$ during metamorphism (Fig.47). This, most probably is the cause for variation in Zn content of gahnite in the massive sulphide rocks and sulphide-associated BIF's at Aggeneys (Fig.39). A similar variation was observed in gahnite in sulphide-bearing rocks in the Mineral District, Virginia (Sandhaus 1981, Craig 1983) and Broken Hill, Australia (Plimer, 1977).

The variation in Fe-Mg content of gahnite (Fig.39) may in part be attributed to variation in bulk rock composition ie. Mg-rich rocks at Oranjefontein, Fe-rich rocks at Aggeneys, Achab and relatively Fe-rich rocks at Swartkoppies. In garnet-biotite rocks at Oranjefontein and the metapelitic schists at Achab, gahnite composition may be further affected by Fe-Mg exchange between gahnite and garnet or biotite. Hercynite-quartz reacts to form garnet and sillimanite i.e.
$3FeAl_2O_4 + 5SiO_2 = Fe_3Al_2Si_3O_{12} + 2Al_2SiO_5$ as shown by Richardson (1968), Wall and England (1979) and Bohlen et al. (1986). Along with oxidising metamorphic fluids, the instability of (Zn-)Fe-Mg green gahnite and quartz caused formation of almost endmember blue gahnite in quartzites at Oranjefontein.
Moore and Reid (1988 in press) have shown that gahnite composition may vary substantially even on the scale of centimeters according to its relative proximity to oxidising metamorphic fluid pathways. Gahnite-quartzites at Oranjefontein compared to Achab have undergone relatively higher grade metamorphism at similar oxygen fugacities, (calculated log $f(O)_2$ is -16.02+/-0.7 in metapelitic rocks at Achab and -16.51+/-0.7 at Oranjefontein), yet have similar Fe and Zn content (Fig.40), so it would seem that prevailing metamorphic $f(O)_2$ rather than temperature is the determining factor for gahnite composition in similar rock types where Zn-Fe-S equilibria and Fe-Mg exchange can be discounted. At Swartkoppies the 30 mol% variation in gahnite component is also attributed to changes in $f(O)_2$ rather than temperature. In these rocks, despite the presence of biotite, there is very little variation in Mg-Fe content of gahnite. It appears that gahnite exhibits a range of compositions in the amphibolite grades, whereas in the greenschist facies, e.g. the blue gahnite at Oranjefontein it has a narrow compositional range.

It is concluded by this study that spinel composition is affected by bulk composition, Fe,Mg,Zn exchange between gahnite and co-existing silicate, sulphide or oxide minerals, metamorphic $f(O)_2$ and temperature. In different lithologies which have been subjected to any one or a combination of these parameters, gahnite composition will be dependent on the dominant parameter or a dominant combination of parameters. The affect of bulk rock composition and mineralogy will determine gahnite composition during initial growth. However, $f(O)_2$ and temperature apply strong constraints on gahnite composition in gahnite-quartz assemblages and $f(O)_2$ - $f(S)_2$ conditions in gahnite-sphalerite-pyrite assemblages.

5.5 Gahnite in exploration

One factor which emerges from this study of gahnite is that on a regional scale gahnite may have substantially variable composition in rocks of the same genetic sequence and occurring at similar stratigraphic levels. Similar studies of gahnite associated with sulphide mineralization in the Mineral District, Virginia (Sandhaus 1981, Craig 1983 and Sandhaus and Craig 1986) and Broken Hill, Australia (Plimer, 1977) show a far more restricted range of gahnite composition. This has significant implications on the use of gahnite composition as a guide to mineralization in Namaqualand. Sheridan and Raymond (1977), Karlsson et al. (1980) and Craig (1983) have commented on the association of gahnite with zinc mineralization and its potential for use in exploration. Spry (1984, 1986) and Spry and Scott (1986 a,b) found that gahnite associated with metamorphosed massive sulphide deposits has high zinc and iron contents and low magnesium contents. Bernier et al. (1984) found that the Zn/Zn+Fe+Mg ratio of gahnite associated with staurolite could be related to their proximity to mineralised zones and similarly Ririe and Foster (1984) suggested that the association of gahnite and sillimanite could be used as a directional indicator for sulphide mineralization.

The results of this study indicate that gahnite forms in aluminous terranes during regional metamorphism if zinc is present in the form of sulphides or as a constituent of the precursor sediments. According to Figures 39 and 40, there is some confirmation for Spry's (op. cit.) theory, in that gahnite occurring in aluminous sediments has more variable composition than gahnite associated with sulphides which tends to be richer in zinc and iron and has low magnesium contents. However this study does indicate a potential for compositional variation in gahnite which can be attributed to factors other than Zn-Fe-S equilibria. This must be taken into account if gahnite composition or gahnite-bearing assemblages are to be used as indicators for sulphide mineralization.

5.6 Implications for mineralization in the Bushmanland rocks

It is generally considered that rocks of the Bushmanland sequence at Aggeneys and Gamsberg are sedimentary and reflect a continental, shallow marine depositional environment (Moore 1977, 1980, Rozendaal 1982). The Namies Schist is considered to have formed by deposition of (illitic and kaolinitic) clays and clastic material in shallow water in a large basin (Moore 1977, 1980, Rozendaal 1982). The overlying massive quartzite unit is thought to represent mature, quartz-rich sediment deposited in a shallow water, near shore, high energy environment (Rozendaal 1982). Reducing conditions are inferred by the presence of pyrite and pyrrhotite, while the presence of Pb, Zn and Ba in the quartzites suggest the influx of hydrothermal fluids (Rozendaal 1982). The iron formation at Aggeneys and Gamsberg is considered to have a submarine exhalative origin by Ryan et al. (1982) and Rozendaal (1982). However Moore (1977, 1986) interprets the siliceous, ferruginous and manganiferous rocks to result from chemogenic precipitation under hypersaline conditions in a restricted basin. Metamorphic textures exhibited by gahnite in relation to other minerals in gahnite-bearing assemblages in Namaqualand indicate that gahnite is metamorphic in origin. It is concluded that the precursor sphalerite was originally a costituent of the precursor sediments (e.g. black shales) and gahnite formed as a prograde mineral from sphalerite-bearing sediments in response to changing $f(O)_2$ - $f(S)_2$ conditions during diagenesis and metamorphism.

An implication from the presence of similar Mn-rich, sulphide-bearing sediments at Oranjefontein is that similar basins existed elsewhere in Namaqualand. This may have implications for wide spread mineralization in the Bushmanland rocks.

If economic mineralization in Bushmanland rocks occurs in small basins, it may be necessary to exercise caution if the presence of gahnite in used as an indicator of sulphide mineralization. Gahnite appears to have formed readily where sulphides were part of the precursor sediments in a number of quartzites, metapelitic rocks and sulphide-bearing BIF in Bushmanland rocks in Namaqualand. However, gahnite is stable at the metamorphic grades which have affected Namaqualand rocks on a regional scale and persists in assemblages where all but traces of the precursor sulphides have disappeared.

REFERENCES

Albat, H.M. (1984). The proterozoic granulite facies terrane around Kliprand, Namaqualand Metamorphic Complex. Bull. Precambrian. Res. Unit, Univ. Cape Town, 33, 382p.

Andersen, B.W., Payne, C.J. and Hey, M.H. (1937). Magnesium-zinc-spinels from Ceylon. Mineralog. Mag., 24, 547-554.

Appel, U.P.W. (1986). Gahnite in an Archean iron-formation, west Greenland. Mineralog. Mag., 50, 175-177.

Ashley, P.M. (1984). Piemontite-bearing rocks from the Olary District, South Australia. Australian J. Earth Sci., 31, 203-216.

Atkin, B.P. (1978). Hercynite as a breakdown product of staurolite from within the aureole of the Ardara Pluton, Co. Donegal, Eire. Mineralog. Mag., 42, 237-239.

Batchelor, R.A. and Kinnaird, J.A. (1984). Gahnite compositions compared. Mineralog. Mag., 48, 425-429.

Bence, A.E., and Albee, A.L. (1968). Empirical correction factors for the electron microanalysis of silicates and oxides. J. Geol. 76, 382-403.

Bernier, L., Pouliot, G. and Trzcienski, W.E. (1984). Gahnite and zincian staurolite in the north zone of the metamorphosed Pb-Zn-(Cu-Ag-Au) deposit of Montauben-Les-Mines, Que. Geol. assoc. Canada; Mineralog. assoc. Canada Progm. Abstr., 9, p46.

Bohlen, S.R., Dollase, W.A., and Wall, V.J. 1986. Calibration and application of spinel equilibria in the system FeO-Al_2O_3-SiO_2. J. Petrol., 27 (5), 1143-1156.

Blignault, H.J., van Aswegen, G., van der Merwe, S.W. and Colliston, W.P. (1983). The Namaqualand geotraverse and environs: part of the Proterozoic Namaqua Mobile Belt. Spec. Publ. Soc. S. Afr., 10, 1-29.

Clifford, T.N., Gronow, J., Rex, D.C., Burger, A.J. (1975). Geochronological and petrogenic studies of high-grade metamorphic rocks and intrusives in Namaqualand, South Africa. J. Petrol., 16 (1), 154-188.

Clifford, T.N., Stumpfl, E.F. and McIver, J.R. (1975). A sappirine-cordierite-bronzite-phlogopite paragenesis fron Namaqualand, South Africa. Mineralog. Mag., 40, 347-356.

Coetzee, C.B. (1941). Sillimanite-corundum rock: a metamorphosed bauxite in Namaqualand. Trans. geol. Soc. S. Afr., 28, 199-205.

Coetzee, C.B. (1958). Manganiferous iron ore, hematite, barite and sillimanite on Gams (portion 1), Namaqualand. Bull. geol. Surv. S. Afr., 28, 29pp.

Coolen, J.J.M.M.M. (1981). Högbomite and aluminium spinel from some metamorphic rocks and Fe-Ti ores. N. Jb. Miner. Mh., 8, 374-384.

Coveney, R.M. (1979). Sphalerite concentrations in mid-continent Pennsylvanian black shales of Missouri and Kansas. Econ. Geol., 74 (1), 131-140.

Craig, J.R. (1983). Metamorphic features in Appalachian massive sulphides. Mineralog. Mag., 47, 515-525.

Deer, W.A., Howie, R.A. and Zussman, J. (eds.) (1980). An Introduction to the Rock-Forming Minerals. Longman Group Limited, London, 528pp.

De Jager, D.H. (1963). Sillimanite in Namaqualand: review of reserves and report on some low grade deposits. Bull. geol. Surv. S. Afr., 40, 42pp.

De Jager, D.H. and von Backstrom, J.W. (1961). The sillimanite deposits in Namaqualand near Pofadder. Bull. geol. Surv. S.Afr., 33, 49p.

De Waal, S.A. (1981). Neoformed supergene sphalerite and possible precipitation control by gahnite. Soc. Francaise Mineralogie Christallographie Bull., 104, 732-736.

Dietvorst, E.J.L. (1980). Biotite breakdown and the formation of gahnite in metapelitic rocks from Kemiö, southwest Finland. Contrib. Mineral. Petrol., 75, 327-337.

Eskola, P. (1914). An occurrence of gahnite in pegmatite near Träskböle in Perniö, Finland. Geol. Fören. Förhandl., 36 (1), 25-30.

Essene, E.J., Petersen, E.U. and Peacor, D.R. (1982). Nigerite-högbomite-spinel assemblages from Manitouwadge, Ontario and their significance. American Geophys. Union Trans. (EOS), 63 (18), p456.

Feenstra, A. (1985). Metamorphism of bauxites on Naxos, Greece. Geologica Ultraiectina, 39, 206p.

Ferry, J.M. and Spear, F.S. (1978). Experimental calibration of the partitioning of Fe and Mg between biotite and garnet. Contrib. Mineral. Petrol., 66, 113-117.

Field, S.W. and Haggerty, S.E. (1984). Gahnite from the Davis Mine, Rowe, Massachusetts. Trans. Am. Geophys. Union. (EOS), 65(16), p293.

Frick, C and Coetzee, C.B. (1974). The mineralogy and the petrology of the sillimanite deposits west of Pofadder, Namaqualand. Trans. geol. Soc. S. Afr., 77, 169-176.

Friedman, G.M. (1954). The spinel-silica reaction succession: a study of incompatible mineral phases. J. Geology, 62, 365-374.

Frondel, C. and Baum, J.L. (1974). Structure and mineralogy of the Franklin zinc-iron-manganese deposit, New Jersey. Econ. Geol., 69, 157-180.

Joubert, P. (1971). The regional tectonism of the gneisses of part of Namaqualand. Bull. Precambrian Res. Unit, Univ. Cape Town, 10, 220pp.

Joubert, P. (1974). The gneisses of Namaqualand and their deformation. Trans. geol. Soc. S. Afr., 77, 339-345.

Karlsson, K.L., Rickard, D. and Vivallo, W. (1980). The Precambrian sulphide deposits of Colorado: Report from a field study. Ore Research Group Ann. Rpt., Stokholm Univ., 45-53.

Keskinen, M. and Liou, J.G. (1979). Synthesis and stability relations of Mn-Al piemontite $Ca_2MnAl_2Si_3O_{12}(OH)$. Am. Miner., 64, 317-328.

Kramm, U. (1977). Gahnite in the Venn-Stavelot Massif and its petrologic significance. Geol. Soc. Belgique Annales., T.100, 199-201.

Lipson, R.D. (1978). Some aspects of the geology of part of the Aggeneysberge and surrounding gneisses, Namaqualand. Unpubl. M. Sc. thesis, Univ. Witwatersrand.

Mathias, M. (1941). The occurrence of barite in an iron ore deposit in Namaqualand. Trans. R. Soc. S. Afr., 28, 207-217.

Moore, J.M. (1974). Some aspects of the geology of the Nuniepoort base metal occurrence, Zuurwater, Namaqualand. Broken Hill Project. Black Mountain Mineral Development Company Limited.

Moore, J.M. (1977). The geology of the Namiesberg, Northern Cape. Bull. Precambrian Res. Unit, Univ. Cape Town, Bull.20, 69pp.

Moore, J.M. (1980). Paleo-environmental implications of the origin of sillimanite-rich rocks in the north-west cape, South Africa, and their relation to the sulphide deposits of the area. In: J.D. Ridge (ed.). Proceedings of the Fifth Quadrennial IAGOD Symposium.E. Schweizerbart'sche Verlagsbuchhandlung, Stuttgart. 210-215.

Moore, J.M. (1983). Investigations of and for 'Aggeneys type' Zn-Pb-Cu-Ag ore deposits in Namaqualand, South Africa - past and present. Soc. Min. Engrs. Aime, preprint 83-12, 6p.

Moore, J.M. (1986). A comparitive study of metamorphosed supracrustal rocks from the western Namaqualand Metamorphic complex. Unpubl. PhD thesis. Univ. Cape Town.

Moore, J.M. and Reid, A.M., (1988 in press). Sphalerite inclusions in gahnite fronm the Namaqualand Metamorphic Complex. Can. Miner.

Miyashiro, A. (ed.)(1973). Metamorphism and metamorphic belts. Allen & Unwin, London, 492pp.

Nèmec, D. (1972). Das vorkommen der Zn-spinelle in der Böhmischen Masse. Tschermaks Mineralog. Petrog. Mitt., 19, 95-109.

Palache, C., (1935). The minerals of Franklin and Sterling Hill, Sussex County, New Jersey. U.S. Geol. Surv. Prof. Paper 180.

Pehrman, G. (1948). Gahnit von Rozendal auf Kimoto, S.W. Finland. Bull. Geol. Inst. Univ. Upsala , 32, 329-336.

Plimer, I.R. (1977). The mineralogy of the high-grade matamorphic rocks enclosing the Broken Hill orebodies, Australia. N. Jb. Miner. Abh., 131, 115-139.

Plimer, I.R. (1984). Tha mineralogical history of the Broken Hill Lode, NSW. Australian J. Earth Sci., 31, 379-402.

Praekelt, H.E., Colliston, W.P., and Schoch, A.E. (1983). The stratigraphic interpretation of a highly deformed Proterozoic region in central Bushmanland, South Africa: first correlation of structurally separated metaseiments of the Aggeneys Subgroup. Precambrian Res., 23, 177-185.

Rankin, G.A. and Merwin, H.E. (1918). The ternary system $MgO-Al_2O_3-SiO_2$. Amer. Jour. Sci., 45, 301-325.

Richardson, S.W. (1968). Staurolite stability in a part of the system Fe-Al-Si-O-OH. J. Petrol., 9(3), 467-488.

Ririe, G.T. and Foster, C. (1984). Zinc ratios in gahnite associated with a massive sulphide deposit. Geol. Soc. Am. Abstr. Progr., 16(6), p635.

Ririe, G.T. (1982). A model for gahnite and magnetite formation during metamorphism of sulphide-rich rocks. Geol. Soc. Am. Abstr. Progr., 14, 227-228.

Rumble III, D. (1976). Oxide minerals in metamorphic rocks. In: A.E. Gorensy, S.E. Haggerty, J.S. Heubner, D.H. Lindsley, D. Rumble III (eds.). Oxide Minerals. Mineralog. Soc. Am. Short Course Notes, Volume 3. Southern printing Company, Blacksburg, Virginia. R1-R24.

Rozendaal, A. (1978). The Gamsberg zinc deposit, Namaqualand, 235-265. In: Vervoerd, W.J. (ed.). Mineralization in metamorphic terranes. Spec. Publ. geol. Soc. S. Afr., 4, 552p.

Rozendaal, A. (1980). The Gamsberg zinc deposit, South Africa: A banded stratiform base-metal deposit. In: J.D. Ridge (ed.). Proceedings of the Fifth Quadrennial IAGOD Symposium. E. Schweizerbart'sche Verlagsbuchhandlung, Stuttgart, 619-633.

Rozendaal, A. (1982). The petrology of the Gamsberg zinc deposit and Bushmanland iron formations with special reference to their relationships and genesis. Unpubl. PhD thesis. Univ. Stellenbosch. 349pp.

Ryan, P.J. (1982). The geology of the Broken hill ore deposit, Aggeneys, South Africa. Proc., 12th CMMI Congress. H.W. Glen (Ed.). Johannesburg, S. Afr. Inst. Min. Metall. (or Geol. Soc. S. Afr.), 181-220.

Ryan, P.J., Lawrence, A.L., Lipson, R.D., Moore, J.M., Paterson, A., Stedman, D.P. and van Zyl, D. (1982). The Aggeneys base metal deposits, Namaqualand, South Africa. Econ. Geol. Research Unit, Univ. Witwatersrand, Information Circular, 160, 33p.

SACS (1980). South African Committee for Stratigraphy (S A C S), (1980). Stratigraphy of South Africa, Part 1 (comp. L.E. Kent). Lithostratigraphy of the Republic of South Africa, South West Africa/Namibia, and the Republics of Bophuthatswana, Transkei and Venda. Handb. geol. Surv. S. Afr., 8.

Salotti, C.A. (1965). Mineralogy and paragenesis of the Cotopaxi, Colorado, Cu-Zn skarn deposit. Am. Miner., 50, 1179-1212.

Sandhaus, D.J. (1981). Gahnite in metamorphosed volcanogenic massive sulphides of the Mineral District, Virginia. Unpub. M.Sc. thesis, Virginia Polytech. Inst. and State Univ., 164pp.

Sandhaus, D.J. and Craig J.R. (1986). Gahnite in the metamorphosed stratiform massive sulphide deposits of the Mineral District, Virginia, U.S.A. Tshermaks Min. Petr. Mitt., 35, 77-98.

Schmetzer, K. and Bank, H. (1985). Crystal chemistry of zincian spinels (gahnospinels) from Sri Lanka. N. Jb. Miner. Mh.,8, 353-356.

Schreurs, J. and Westra, L. (1985). Cordierite-orthopyroxene rocks: the granulite facies equivalents of the Orijärvi cordierite-anthophyllite rocks in West Uusimaa, southwest Finland. Lithos, 18, 215-228.

Schumacher, R. (1985). Zincian staurolite in Glen Doll, Scotland. Mineral. Mag., 49, 561-571.

Segnit, E.R. (1961). Petrology of the zinc lode, New Broken Hill Consolidated Ltd, new South Wales. Inst. Min. Metall. Proc., 199, 87-112.

Sheridan, D.M. and Raymond, W.H. (1977). Preliminary data on some Precambrian deposits of zinc-copper-lead sulphides and zinc spinel (gahnite) in Colorado. U.S. Geol. Surv. Open File Rpt., 77-607, 27pp.

Sheridan, D.M. and Raymond, W.H. (1984). Precambrian deposits of zinc-copper-lead sulphides and zinc spinel (gahnite) in Colorado. U.S. Geol. Surv. Bull., 1550, 31pp.

Siefert, F. and Schumacher, J.C. (1986). Cordierite-spinel-quartz assemblages: a potential geobarometer. Geol. soc. Finlande, 58, 95-108.

Simpson, E.S. (1930). Contributions to the mineralogy of Western Australia.
Jour. Roy. Soc. W. Aust., 16, 25-40.

Simpson, E.S. (1931). Contributions to the mineralogy of Western Australia.
Jour. Roy. Soc. W. Aust., 17, 137-148..

Simpson, E.S. (1937). Contributions to the mineralogy of Western Australia.
Jour. Roy. Soc. W. Aust., 23, 17-35.

Spry, P.G. (1982a). Zincian spinels as indicators of metamophosed base metal deposits. Geol. Ass. Can. Progm. Abstr., 7, p82.

Spry, P.G. (1982b). An unusual gahnite-forming reaction, Geco base-metal deposit, Manitouwadge, Ontario. Can. Miner., 20, 549-553.

Spry, P.G. (1983). Zincian spinels in the Appalachian-Caledonide orogen. Progr. & Abstr. Symp. on Stratabound sulphides of the Appalachian-Caledonide orogen, p26.

Spry, P.G. (1984). The synthesis, stability, origin and exploration significance of zincian spinels. Unpubl. PhD. thesis, Univ. Toronto, 158pp.

Spry, P.G. (1986). The composition of zincian spinels as a guide to metamorphosed ore deposits: the Aggeneys example, Namaqualand, South Africa. Geol. Soc. Am. Abstr. Progr., p760.

Spry, P.G. (1987a). The chemistry and origin of zincian spinels associated with the Aggeneys Cu-Pb-Zn-Ag deposits, Namaqualand, South Africa. Mineral. Deposita, 22, 262-268.

Spry, P.G. (1987b). Compositional zoning in zincian spinel. Can. Miner., 25, 97-104.

Spry, P.G. and Scott, S.D. (1986a). The stability of zincian spinels in sulphide systems and their potential as exploration guides for metamorphosed Massive Sulphide Deposits. Econ. Geol., 81, 1446-1463.

Spry, P.G. and Scott, S.D. (1986b). Zincian spinel and staurolite as guides to ore in the Appalachian and Scandinavian Caledonides. Can. Miner., 24, 147-163.

Stern, W.P. and Klein, H.H. (1983). Inconsistent chemical data on phlogopite: analyses and genesis of phlogopites from Madagascar. Schweiz. mineral. petrogr. Mitt., 63, 187-202

Stevenson, R.K. (1985). An occurrence of amazonite, gahnite, and sphalerite near Portman Lake, Northwest Territories. In: M.J. Kiel, D. Busby (eds). Current Research Part A. Geol. Surv. Can. Paper 85-1A.

Stoddard, E.F. (1976). Sillimanite-spinel segregations in granulite-facies metapelites and a possible breakdown reaction of staurolite. Geol. Soc. Amer. Abstr. Progr., 8, p1125.

Stoddard, E.F. (1979). Zinc-rich hercynite in high-grade metamorphic rocks: a product of the dehydration of staurolite. Am. Miner., 64, 736-741.

Stumpfl, E.F., Clifford, T.N., Burger, A.J. and Van Zyl, D. (1976). The copper deposits of O'Okiep District, S.A.: New Data and concepts. Mineral. Deposita, 11, 46-70.

Sturt, B.A. (1962). The composition of garnets from pelitic schists in relation to the grade of regional metamorphism. J. Petrol., 3 (2), 181-191.

Sundblad, K. (1982). Distribution of gahnite-bearing sulphide deposits in the Scandinavian Caledonides. Trans. Instn. Min. Metall., 91, 214-218.

Tankard, A.J., Jackson, M.P.A., Erikson, K.A., Hobday, D.K., Hunter, D.R., Minter, W.E.L. (eds.) (1982) . Crustal Evolution of Southern Africa - 3.8 Billion Years of Earth History. Springer-Verlag New York, Heidelberg, Berlin., 523pp.

Teale, G.S. (1980). The occurrence of högbomite and taffeite in a spinel-phlogopite schist from the Mount Painter Province of South Australia. Mineralog. Mag., 43, 575-577.

Thompson, A.B. (1976). Mineral reactions in pelitic rocks: II. Calculation of some P-T-X (Fe-Mg) phase relations. Am. J. Sc., 276, 425-454.

Treloar, P.J., Koistinen, T.J., Bowes, D.R. (1981). Metamorphic development of cordierite-amphibolie rocks and mica schists in the vicinity of the Outokumpu ore deposit, Finland. Trans. Roy. Soc. Edinburgh: Earth Sciences, 72, 201-215.

Tulloch, A.J. (1981). Gahnite and columbite in an alkali-feldspar granite from New Zealand. Mineralog. Mag., 44, 275-278.

Turncock, A.C. and Eugster, H.P. (1962). Fe-Al oxides: Phase relationships below 1000 °C. J. Petrol., 3, 533-565.

Vielzeuf F.D. (1983). The spinel and quartz associations in high grade xenoliths from Tallente (S.E. Spain) and their potential use in geothermometry and barometry. Contrib. Mineral. Petrol., 82, 301-311.

Vine, J.D. and Tourtelot, E.B. (1970). Geochemistry of black shale deposits - a summary report. Econ. Geol., 65, 253-273.

Vokes, F.M. (1962). Contributions to the mineralogy of Norway, No. 15, Gahnite in the Bleikvassli ore. Norsk. Geol. Tidsskr., 42, 317-329.

Von Gehlin, K. Nielsen, H., Chunnett, I. and Rozendaal, A. (1983). Sulphur isotopes in metamorphosed Precambrian Fe-Pb-Zn-Cu sulphides and baryte at Aggeneys and Gamsberg, South Africa. Mineralog. Mag., 47, 481-486.

Von Knorring, D. and Dearnley, R. (1960). The Lewisian pegmatites of South Harris, Outer Hebrides. Mineralog. Mag., 32, 366-378.

Wall, V.J. and England R.N. (1979). Zn-Fe spinel-silicate-sulphide reactions as sensors of metamorphic intensive variables and processes. Geol. Soc. Am. Abstr. with Progr., 11 (7), p534.

Waters, D.J. (1986). Metamorphic zonation and thermal history of pelitic gneisses from western Namaqualand, South Africa. Trans. geol. Soc. S. Afr., 89, 97-102.

Waters, D.J. and Whales C.J. (1984). Dehydration melting and the granulite transition in metapelites from southern Namaqualand, S. Africa. Contr. Miner. Petrol., 88, 269-275.

Waters, D.J. and Moore, J.M. (1985). Kornerupine in Mg-Al-rich gneisses from Namaqualand, South Africa: mineralogy and evidence for late-metamorphic fluid activity. Contrib. Mineral. Petrol., 91, 369-382.

Wedepohl, K.H. (exec. ed.) (1970). Zinc. In: Handbook of geochemistry. Springer-Verlag Berlin, Heidelberg, New York.

Williams, P.J. (1983). The mineralogy and metamorphism of some gahnite-bearing silicate inclusions in massive sulphides from Fornas, north-west Spain. Min. Mag., 47, 233-235.

Winkler, H.G.F. (1967) (ed.). Petrogenesis of metamorphic rocks. Springer-Verlag New York, Heidelberg, Berlin. 334pp.

Wolter, H.U. and Siefert.F. (1984). Mineralogy and genesis of cordierite-anthophyllite rocks from the sulphide deposit of Falun, Sweden., Lithos, 17, 147-152.

Zelt, G.A.D. Granulite facies metamorphism in Namaqualand, South Africa. Precambr. Res., 13, 253-274.

Zen, E-An. (1985). An oxygen buffer for some peraluminous granites and metamorphic rocks. Am. Miner., 70, 65-73.

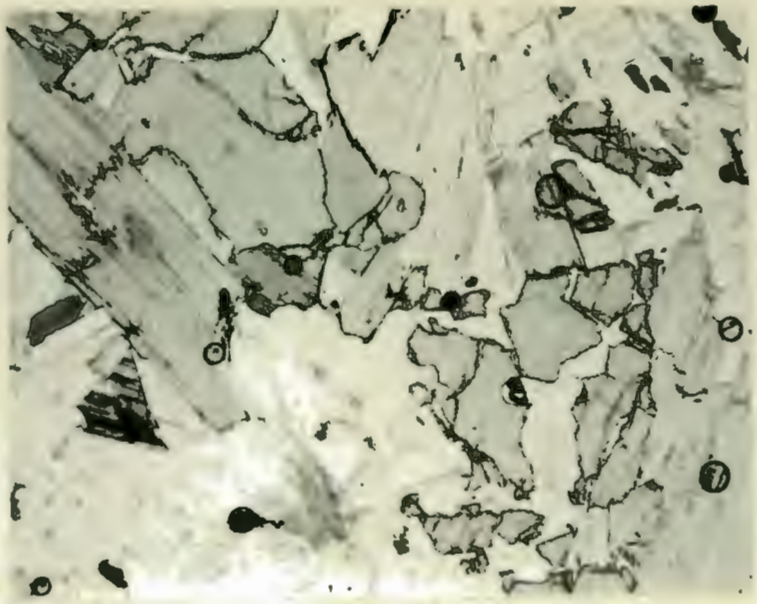

Plate 1. x25
Biotite-muscovite-sillimanite-gahnite schist, Achab. Prograde gahnite (G) is associated with biotite (B), quartz (Q) and sillimanite (S).

Plate 2. x25
Biotite-muscovite-garnet-sillimanite schist, Achab. Small grains of gahnite (G) are associated with garnet (Ga) or occur as inclusions in biotite (B).

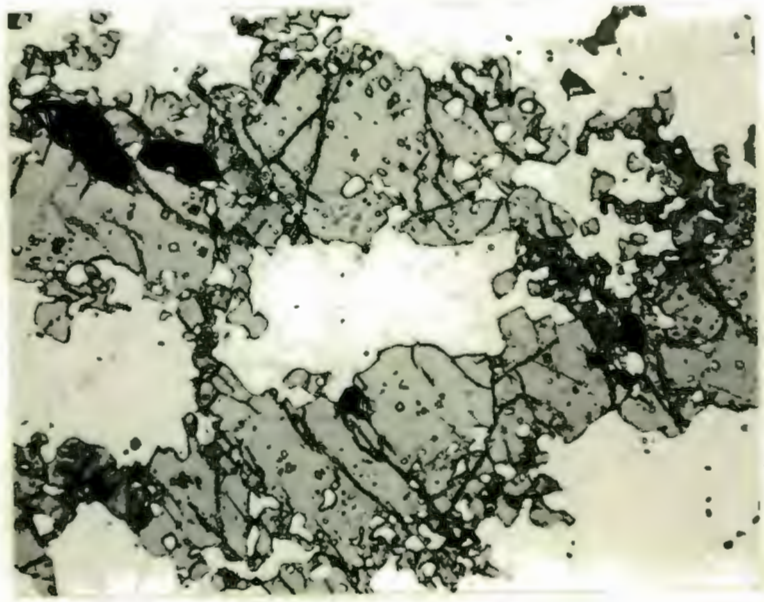

Plate 3. x25
Gahnite quartzite, Achab. Poikiloblastic porphyroblasts of gahnite (G) in a banded gahnite quartzite.

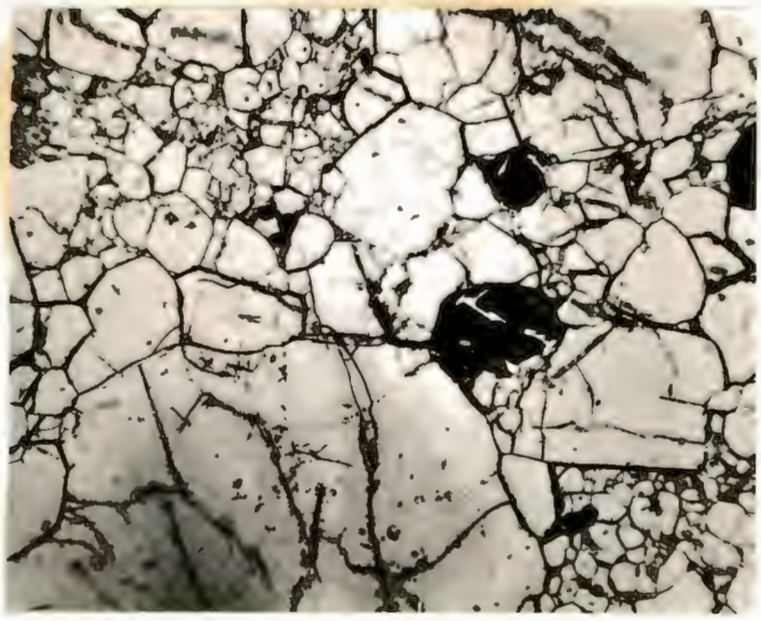

Plate 4. x25.
Massive gahnite rock, Swartkoppies.
Note that the centre of the large grain is darker coloured than the rim.

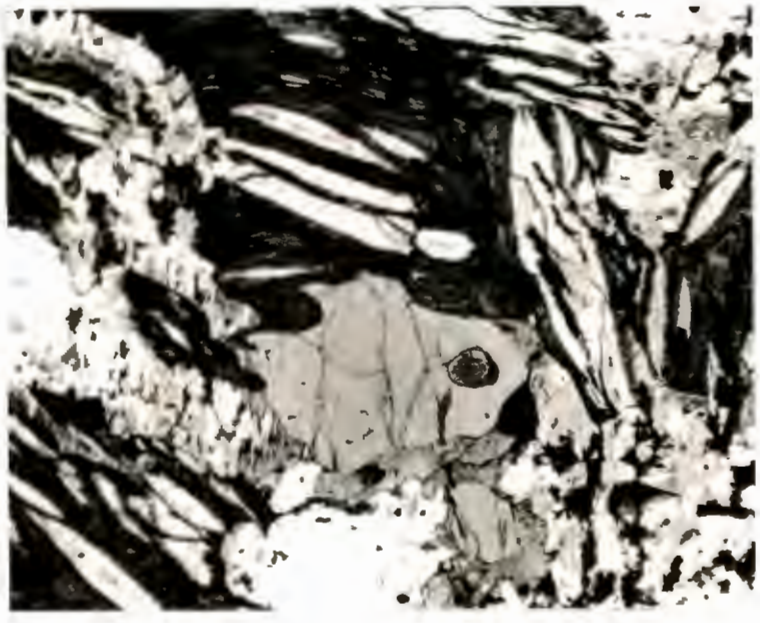

Plate 5. x25.
Garnet-biotite-gahnite-quartz rock, Oranjefontein.
Green gahnite (Gg) is rimmed by blue gahnite (Bg). Biotite (dark area) is replaced by hematite, quartz and blue gahnite.

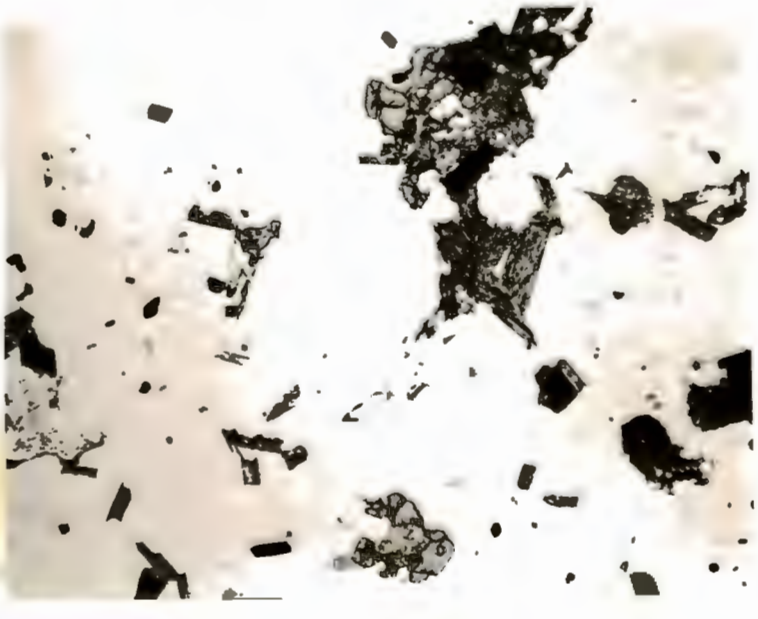

Plate 6. x25.
Gahnite (+phlogopite, garnet) quartzite, Oranjefontein.
Green gahnite (Gg) and biotite (laths) breakdown to form blue gahnite (Bg).

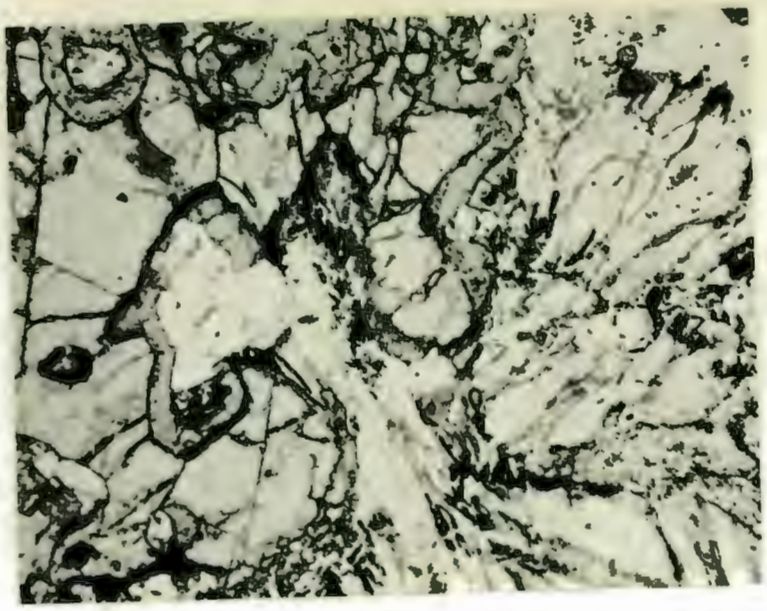

Plate 7. x25.
Gahnite quartzite,
Oranjefontein.
Green gahnite (Gg) with blue gahnite (Bg) rims. Specks of hematite outline shapes, indicating a precursor mineral assemblage.

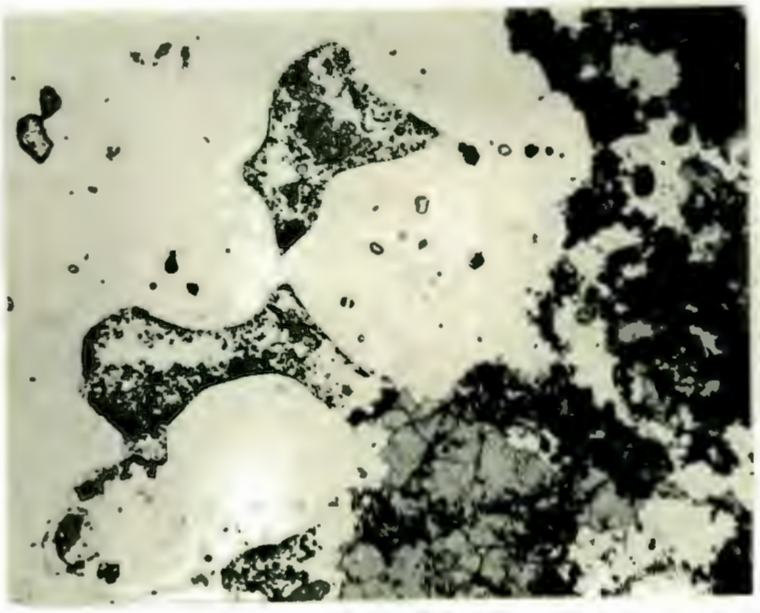

Plate 8. x25.
Gahnite quartzite,
Oranjefontein.
'Haloes' composed of specks of hematite outline the former grain boundaries of phlogopite. Blue gahnite (Bg) occurs in the haloes and also as aggregates associated with webbed hematite (dark mineral).

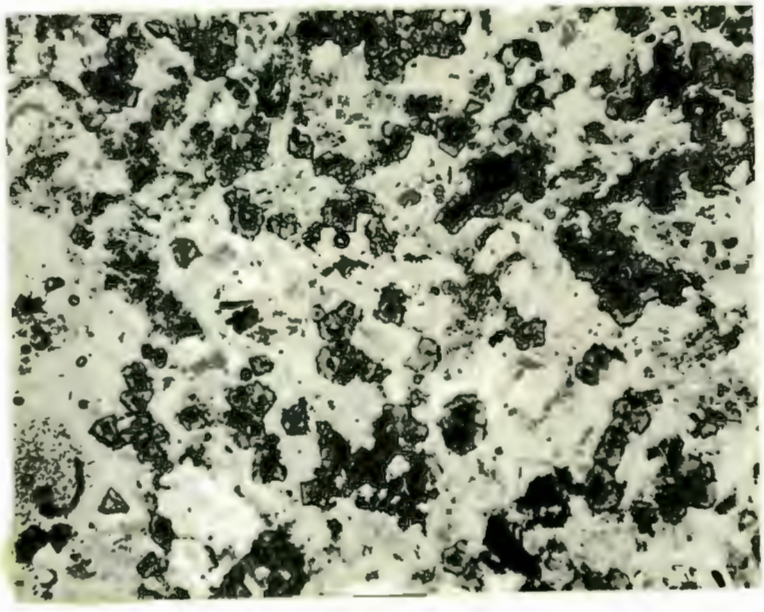

Plate 9. x25.
Gahnite quartzite,
Oranjefontein.
Euhedral blue gahnite crystals with a central circular area defined by a rim of hematite specks.

APPENDIX 1

ANALYTICAL METHODS AND PROCEDURES

All mineral analyses were done on the Cameca microprobe owned by the Geochemistry department of the University of Cape Town. The microprobe unit provides an online reduction of analytical data by the ZAF method. This was found to be inadequate for analyses of silicate minerals with high Fe contents e.g almandine, hercynite and so a method was built into the program whereby these analyses could be corrected for by the Bence Albee (1968) method.

Operating conditions are outlined below:

Accelerating Voltage: 15 kV
25 kV for analysis of trace quantities of Zn in micas.

Beam Current: 40 nA
20 nA for micas.
The beam was focussed for analysis of all minerals except micas, for which it was defocussed.

Counting Time: 10 sec
20 sec for Zn in micas.

Standards used: Most of the standards are natural, IUGS approved standards. Zn (in sphalerite) and Cr were analysed on sphalerite and chrome metal respectively. These standards have been tested by the Geochemistry Department at U.C.T. and are acceptable. Listed below are the standards used for analysis of minerals.

MINERAL	ELEMENT	STANDARD
Spinel, Magnetite	Si	Diopside
	Al	Chrome, Gahnite
	Ti	Rutile
	Mg, Cr	Chrome
	Fe	Chrome, Ilmenite
	Mn	Rhodonite
	Zn	Gahnite
Micas, Amphibole	Na, K, Si, Fe	Kakanui hornblende
	Ti	Rutile
	Al, Mg, Ca	Kakanui pyrope,hornblende
	Mn	Rhodonite
	Zn	Zinc
Epidote	Si	Diopside
	Ti	Rutile
	Al, Cr, Fe, Mg	Chrome
	Mn	Rhodonite
	Zn	Zinc
Tourmaline	Si,Al,Fe,Mg,Ca,Na,K	Kakanui hornblende
	Ti	Rutile
	Cr	Chrome
	Mn	Rhodonite
Garnet	Si, Al, Mg, Ca	Kakanui pyrope
	Ti	Rutile
	Cr	Chrome
	Mn	Rhodonite
	Na	Kakanui hornblende
Cordierite	Si, Mg, Ca	Diopside
	Ti	Rutile
	Al, Fe	Kakanui pyrope
	Mn	Rhodonite
	Na, K	Kakanui hornblende
Feldspar	Na, Si, Al	Nunu
	K	Or-1
	Fe, Mg	Kakanui hornblende
	Ca	Laco
Sphalerite	Zn	Sphalerite
	Fe, S	Sm-3
	Mn	Rhodonite

Average lowest detection limit (LLD) of the elements in the analyses are listed below.

	Sp	Mt	Gt	Biot	Musc	Chl	Crd
SiO_2	0.04	0.03	0.04	0.03	0.03	0.04	0.04
TiO_2	0.04	0.04	0.04	0.02	0.02	0.04	0.04
Al_2O_3	0.04	0.05	0.04	0.03	0.03	0.03	0.04
Cr_2O_3	0.05	0.04	0.05	0.04	0.04		0.05
FeO	0.08	0.07	0.08	0.04	0.03	0.10	0.08
MnO	0.07	0.07	0.06	0.03	0.03	0.07	0.06
MgO	0.03	0.04	0.03	0.03	0.02	0.03	0.03
CaO				0.07		0.03	0.03
ZnO	0.17	0.16	0.03	0.02	0.02	0.16	0.02
Na_2O			0.03	0.03	0.03	0.04	0.02
K_2O				0.03	0.02	0.03	
F				0.12			

	Fsp	Amphi	Tourm	Epi	Pyxm
SiO_2	0.06	0.04	0.04	0.04	0.05
TiO_2			0.04	0.04	0.05
Al_2O_3	0.04	0.03	0.04	0.03	0.04
Cr_2O_3		0.05	0.04	0.04	0.05
FeO		0.08	0.07	0.03	0.07
MnO		0.07	0.05	0.03	0.06
MgO	0.03	0.03	0.02	0.03	0.03
CaO	0.03	0.03	0.03	0.03	0.03
ZnO					
Na_2O	0.04	0.03	0.03	0.04	0.04
K_2O	0.03	0.02	0.02	0.03	

	Sphalerite
Zn	0.05
Fe	0.03
Mn	0.03
S	0.03

The electron microprobe is unable to distinguish between Fe^{2+} and Fe^{3+} and all Fe is analysed as FeO (ie. Fe^{2+}). This results in stoichiometric irregularities in minerals which incorporate significant quantities of Fe^{3+} in their structure. A method based on the stoichiometry of individual minerals has been included in the data reduction program to account for this, but it was found to be inadequate for iron-rich spinels and iron oxides. The most commonly used methods for recalculation of total FeO to FeO and Fe_2O_3 are based on mineral structure, stoichiometry or charge balance. The method used here was suggested by Haggerty (pers. comm.) and does not require site occupancy assumptions. An example of a gahnite calculation is outlined below:

	Wt% oxide	Atomic props.	Mol props.	No. Cations	No. Anions	Anions x1.7131	Cations x1.7131	Wt% oxide
SiO_2		60.08						
TiO_2		79.90						
Al_2O_3	58.70	101.96	0.5757	1.1514	1.7271	2.9587	1.9725	58.70
Cr_2O_3	0.05	151.85	0.0003	0.0007	0.0010	0.0017	0.0012	0.05
FeO	7.75	71.85	0.1079	0.1079	0.1079	0.1848	0.1848	6.63
Fe_2O_3		159.69						1.18
MnO	0.38	70.94	0.0054	0.0054	0.0054	0.0093	0.0093	0.38
MgO	7.01	40.31	0.1739	0.1739	0.1739	0.2979	0.2979	7.01
CaO		56.08						
ZnO	25.38	81.38	0.3119	0.3119	0.3119	0.5343	0.5343	25.38
Total	99.27			1.7512		3.9867	3.0000	99.33

Nr cations in gahnite = 3/1.7512 = 1.7131
Nr anions in gahnite = 4
4 - 3.9867 = 0.0133
0.0133 x 2 = 0.0266 ....Fe_2O_3 in formula
0.1848 - 0.0266 = 0.1582 ....FeO in formula
Recalculate wt% FeO = 0.1582/1.7131 = 0.0923
0.0923 x 71.85 = 6.6351
Recalculate wt% Fe_2O_3 = 0.0266/1.7131 = 0.0155
0.0155 x 159.69 = 2.3553
2.3553/2 = 1.1777

APPENDIX 2

EXPLANATION OF GEOTHERMOMETRIC AND OXYGEN FUGACITY CALCULATIONS

GEOTHERMOMETRY

On the basis of predicted phase relations in the system K_2O-FeO-MgO-Al_2O_3-SiO_2-H_2O and available experimental and thermochemical data, Thompson (1976) provides a method to calculate isobaric T - X(Fe-Mg) sections. Predicted reactions involving garnet - biotite - cordierite - sillimanite - quartz with muscovite or K-feldspar are compared with available experimental data and compositions of co-existing phases in natural assemblages. The equation:

$n \ln K_D + \Delta\bar{V}\Delta P/RT = \Delta\bar{S}/R + \Delta\bar{H}/R \cdot 1/T$

provides a means of calculating temperature based on Fe - Mg exchange between garnet - cordierite and garnet - biotite pairs

($\ln K_D = Fe^{gar}/Mg^{gar}.Mg^{biot}/Fe^{biot}$ or $Fe^{gar}/Mg^{gar}.Mg^{crd}/Fe^{crd}$

$\Delta\bar{S}/R$, $\Delta\bar{H}/R$ for the exchange reactions are obtained from experimentally investigated reactions in pure Fe and Mg systems, $\Delta\bar{V}/R$ is obtained from available thermochemical data.

	$\Delta\bar{V}/R$ (deg bar^{-1})	$\Delta\bar{S}/R$	$\Delta\bar{H}/R$ (deg)
gar-biot	-0.0234	-1.560	2739.646
Gar-Crd	-0.0155	-1.896	2724.948

Ferry and Spear (1978) did experimental investigations on the exchange reaction : $Fe_3Al_2Si_3O_{12}$(almandine) + $KMg_3AlSi_3O_{10}(OH)_2$(phlogopite) = $Mg_3AL_2Si_3O_{12}$(pyrope) + $KFe_3AlSi_3O_{10}(OH)_2$(biotite).

They determined the partitioning of Fe and Mg between sythetic garnet and biotite at 2.07 kbar in the range 550 - 800 °C.

At equilibrium $\Delta\bar{G} = \Delta\bar{H} - T\Delta\bar{S} + P\Delta\bar{V} + 3RT \ln K = 0$.

Estmates of $\Delta\bar{H}$ and $\Delta\bar{S}$ are obtained from their experiments (4.662 e.u. and 12.454 cal) and $\Delta\bar{V}$ is obtained from thermochemical data (0.057 cal/bar).

It was found that at 2.07 Kbar and between 550 and 800 °C,

ln (Mg/Fe gar / Mg/Fe biot) = -2109/T(K) + 0.782. The equation has a

resolution of ± 50 °C and provides a geothermometer without correction for components, (other than Fe and Mg), of up to 0.2 Ca+Mn/Ca+Mn+Fe+Mg in garnet and 0.15 $(Al^{v1}+Ti)/Al^{v1}+Ti+Fe+Mg$ in biotite.

Departures from ideality in garnet due to substitution of Ca and Mn for Fe and Mg and in biotite due substitution of Al^{v1} for Al^{iv}, cause inconsistancies in geothermometric calculations in high grade (granulite facies) metamorphic rocks which are not present in the middle amphibolite facies. Using the experimental results of Ferry and Spear (1978), Indares and Martingole (1985a) provide a new calibration which incorporates correction for substitutions in garnet and biotite. Two models, (model A, calculated with available thermodynamic data and model B, compiled from empirical data), are proposed to account for deviations from ideality. The calibration

$$T(K) = [12454 - 0.057P(bar) + 3(mX_{Al} + nX_{Ti}\ biot) - (w_{Ca}X_{Ca} + w_{Mn}X_{Mn}\ gar)]/\ 4.662 - 5.9616 \ln K_D$$

where $m = (w_{FeAl} - w_{MgAl}\ biot) = -4.464$ (model A)
$= -1590$ (model B) and
$n = (w_{FeTi} - w_{MgTi}\ biot) = -6767$ (model A)
$= -1451$ (model B)

is based on Ferry and Spear's (1978) experimental method and gives results comparable with those of Thompson's (1976) calibration. Indares and Martingole (1985b) found that inconsistencies in geothermometric calculations in granulite facies rocks can be attributed to local variations in K_D values on the scale of a thin section, caused by late Fe - Mg exchange during cooling. This can be avoided by obtaining analyses from garnet cores and matrix biotite. In contrast, adjacent garnet - biotite grains or inclusions of biotite in garnet provide K_D values representative of some stage during cooling.

GEOBAROMETRY

The stability field of cordierite in high-grade metapelitic rocks was determined experimentally by Holdaway and Lee (1977). The equations:

(1) 1.26 Fe crd + 0.84 K-fsp + (1-1.26n)H_2O = 2.08 sill + 4 qtz
(2) 2.52 Mg biot + 3 alm = 2.52 Fe biot + 3 py
(3) 3 Fe crd = 2 alm + 4 sill + 5 qtz + 3n H_2O

provide the basis for a geobarometer. Equation (1) takes place at 640 °C at 2 kbar and 710 °C at 2.7 kbar. Equation 2 takes place at 650 °C at 3.4 kbar and 760 °C at 2.9 kbar. At the temperature and f(H_2O) of interest the molar content of cordierite is given by n. The barometer is based on the relation
P V = -RT ln (X_{Fe} products/X_{Fe} reactants). Results of the experiments using this relation are:

P V = -2.52 RT ln [X_{Fe} biot/X_{Fe} crd] for reaction (1) (V = -1.1519)
and P V = -6 Rt ln [X_{Fe}alm/X_{Fe} crd] for reaction (2) (V = -2.7805)

OXYGEN FUGACITY CALCULATIONS

Zen (1985) developed an oxygen fugacity buffer curve based on the assemblage biotite - garnet - muscovite - magnetite - quartz which is applicable to peraluminous granites, schists and gneisses. The reaction:
$KFe_3AlSi_3O_{12}H_2O$ (annite) + $Fe_3Al_2Si_3O_{12}$ (almandine) + O_2
<-> $KAl_2AlSi_3O_{12}H_2$ + $2Fe_3O_4$ (magnetite) + $3SiO_2$ (quartz)
provides the base for the buffer system.
Using thermochemical data and the equilibrium oxygen fugacity equation
2.303 RT log $f(O)_2$ = $G_s(T_c,1)$ + $V(P_e-1)$....where G_s, V_s = sum of G/V for the reaction phases.
The equation applicable to endmember phases is
log $f(O)_2$ = 10.29 - 26284/T + 0.148(P-1)/T ± 650/T = Reference buffer curve.

Compositional corrections are necessary to account for:

(i) annite - phlogopite solid solution and excess aluminium on tetrahedral and octahedral sites in biotite,

(ii) aluminium distribution over the tetrahedral and octahedral sites and excess Si in tetrahedral sites in muscovite,

(iii) components of spessartine, pyrope and grossular in garnet.

Taking into account the departures of biotite, garnet, and muscovite from their endmember formulae the BAMM buffer equation is:

$$\log f(O)_2 = 10.29 - 26284/T + 0.148(P-1)/T(K) - 4\log X_{Si}(biot) - 3\log X Fe^{2+}(biot) - 3\log X Fe^{2+}(gar) + 2\log X Al^{VI}(musc) + 4\log X Si(musc) \pm (650/T - 1)$$

This provides a buffer curve located between the hematite - magnetite and the magnetite-quartz-fayalite curves. Absence of biotite or almandine in the assemblage indicates higher oxygen fugacity and absence of muscovite or magnetite, lower oxygen fugacity than the buffer value. A biotite-garnet rock should not be stable with hematite.

APPENDIX 3

ENDMEMBER COMPOSITIONS OF GAHNITE
(After stoichiometric recalculation for Fe 3+ and subtraction of magnetite component.)

Symbols:
c : centre of grain
r : rim of grain
bl : blue gahnite (Oranjefontein
gr : green gahnite (Oranjefontein)

	Hercynite	Spinel	Gahnite		Hercynite	Spinel	Gahnite
ABN 12	30.17	8.84	61.00	ABN 13	33.04	7.59	59.37
ABN 12	29.19	9.05	61.76	ABN 13	28.29	7.63	64.08
ABN 12	29.55	9.17	61.29	ABN 13	32.61	7.69	59.70
ABN 12	30.61	9.04	60.35	ABN 13	32.14	8.20	59.66
ABN 13	33.93	7.19	58.88	ABN 13	32.26	8.22	59.52

	Hercynite	Spinel	Gahnite		Hercynite	Spinel	Gahnite
ABN 13	29.33	8.29	62.39	ABN 14	26.10	7.66	66.24
ABN 14	26.97	7.50	65.52	ABN 14	25.80	7.36	66.83
ABN 14	24.46	7.46	68.08	ABN 14	25.82	7.30	66.87
ABN 14	27.18	7.65	65.18	ABN 16	33.43	5.62	60.95
ABN 14	26.34	7.49	66.17	ABN 16	34.09	5.31	60.60

	Hercynite	Spinel	Gahnite		Hercynite	Spinel	Gahnite
ABN 16	33.15	6.90	59.94	ABN 16	33.77	6.84	59.38
ABN 16	34.26	6.08	59.66	ABN 3	33.83	11.48	54.69
ABN 16	33.12	6.86	60.02	ABN 3	29.27	8.76	61.89
ABN 16	34.03	6.62	59.36	ABN 3	25.25	9.93	64.82
ABN 16	33.72	6.61	59.67	ABN 3	33.45	9.62	56.93

	Hercynite	Spinel	Gahnite		Hercynite	Spinel	Gahnite
ABN 3	36.78	10.96	52.27	ABN 4	31.39	5.77	62.83
ABN 3	33.22	8.66	58.13	ABN 4	32.17	6.11	61.72
ABN 4	23.26	3.30	73.43	ABN 6	42.29	25.61	32.09
ABN 4	33.96	5.90	60.14	ABN 6	36.43	34.03	29.54
ABN 4	34.67	5.83	59.50	ABN 6	19.64	6.14	74.23

	Hercynite	Spinel	Gahnite
ABN 8	21.13	6.11	72.76
ABN 8	20.65	6.22	73.13
ABN 8	20.15	6.13	73.73
ABN 8	19.57	6.15	74.28
ABN 8	20.29	6.25	73.46

	Hercynite	Spinel	Gahnite
ABN 8	19.38	6.21	74.41
ABN 8	19.45	6.30	74.24
ABN 8	19.84	5.89	74.26
ABN 8	21.54	6.09	72.37
ABN 8	20.23	6.27	73.50

	Hercynite	Spinel	Gahnite
ABN 9	29.89	16.76	53.35
ABN 9	30.66	17.12	52.22
ABN 9	30.46	15.46	54.07
ABN 9	31.47	14.65	53.88
ABN 9	31.03	14.95	54.03

	Hercynite	Spinel	Gahnite
ABN 9	31.20	15.90	52.90
ABN 10	28.57	9.38	62.06
ABN 10	25.85	10.08	64.07
ABN 10	16.47	8.01	75.52
ABN 10	19.87	8.73	71.40

	Hercynite	Spinel	Gahnite
ABN 11	32.21	6.71	61.08
ABN 11	35.43	7.05	57.53
ABN 11	34.89	6.39	58.72
ABN 11	36.77	5.75	57.48
ABN 11	30.06	6.36	63.58

	Hercynite	Spinel	Gahnite
ABN 11 c	36.57	7.05	56.38
ABN 11 r	36.88	7.05	56.07
ABN 11 c	36.44	7.34	56.21
ABN 11 r	36.52	7.13	56.36
ABN 11	36.83	5.92	57.25

	Hercynite	Spinel	Gahnite
ABN 11	37.03	5.28	57.69
SK 2 c	39.66	8.13	52.21
SK 2 r	37.95	8.62	53.44
SK 2	37.86	9.17	52.97
SK 2	38.55	8.76	52.68

	Hercynite	Spinel	Gahnite
SK 2 c	38.89	8.59	52.52
SK 2 r	38.33	8.82	52.85
SK 2 c	37.93	8.78	53.29
SK 2 r	38.31	9.13	52.57
SK 2	37.12	9.16	53.72

	Hercynite	Spinel	Gahnite
SK 2	36.67	9.01	54.33
SK 2	38.47	8.70	52.84
SK 2 c	39.33	8.97	51.70
SK 2 r	38.90	8.94	52.15
SK 2	55.68	15.86	28.46

	Hercynite	Spinel	Gahnite
SK 3	56.41	14.98	28.61
SK 3	55.98	15.09	28.93
SK 3 c	56.49	15.54	27.97
SK 3 r	56.47	14.91	28.62
SK 3 c	56.15	15.03	28.82

	Hercynite	Spinel	Gahnite
SK 3 r	58.01	14.30	27.69
SK 3 c	56.30	14.57	29.14
SK 3 r	55.39	15.45	29.16
SK 3 c	55.84	15.97	28.19
SK 3 r	54.98	16.10	28.92

	Hercynite	Spinel	Gahnite
SK 3	55.67	15.39	28.94
SK 4	49.22	12.06	38.72
SK 4 c	48.29	11.54	40.17
SK 4 r	48.35	12.33	39.32
SK 4 c	47.22	12.76	40.02

	Hercynite	Spinel	Gahnite
SK 4 r	46.82	12.81	40.38
SK 4 c	46.56	12.58	40.86
SK 4 r	48.44	12.48	39.09
SK 4 c	47.12	12.66	40.22
SK 4 r	46.65	13.00	40.35

	Hercynite	Spinel	Gahnite
SK 4 c	47.55	12.34	40.11
SK 4 r	46.80	11.98	41.22
SK 4 c	35.06	7.53	57.41
SK 4 r	37.52	8.08	54.40
SK 4	36.92	8.14	54.94

	Hercynite	Spinel	Gahnite
BH 2 c	19.91	5.86	74.27
BH 2 r	18.92	4.95	76.13
BH 2	16.91	4.67	78.42
BH 2	18.24	5.47	76.28
BH 2	17.86	4.96	77.48

	Hercynite	Spinel	Gahnite
BH 2	18.89	5.76	75.36
BH 2	18.99	5.77	75.25
BH 2 c	19.27	5.63	75.10
BH 2 r	18.23	5.09	76.68
BH 2	18.84	5.59	75.58

	Hercynite	Spinel	Gahnite
BH 2	15.79	4.35	79.85
BH WE 1	22.10	4.92	72.98
BH WE 1	21.58	5.11	73.31
BH WE 1	24.27	4.38	71.35
BH WE 1	22.63	4.51	72.85

	Hercynite	Spinel	Gahnite
BH WE 1	22.04	5.17	72.80
BH WE 1	23.48	5.00	71.53
BH WE 1	20.81	4.72	74.46
BH WE 1	23.57	5.00	71.43
BH WE 1	23.07	4.64	72.29

	Hercynite	Spinel	Gahnite
BH WE 2	25.79	4.72	69.49
BH WE 2	23.27	5.05	71.68
BH WE 2	22.67	4.40	72.93
BH WE 2	26.26	4.83	68.91
BH WE 2	28.41	4.76	66.83

	Hercynite	Spinel	Gahnite
BH WE 2	22.97	4.53	72.49
BH WE 2	22.92	4.54	72.54
BH WE 2	22.64	5.05	72.31
BH WE 2	21.79	4.58	73.63
BH WE 2	22.51	4.95	72.54

	Hercynite	Spinel	Gahnite
BHG 302	54.96	9.28	35.75
BHG 302	65.90	9.48	24.62
BHG 302	62.21	9.67	28.12
BHG 302	69.43	10.79	19.78
BHG 302	62.05	11.52	26.43

	Hercynite	Spinel	Gahnite
BHG 302	67.22	10.03	22.76
240 AG 56	36.77	11.95	31.28
240 AG 56	39.39	12.02	48.69
240 AG 56	42.15	12.09	45.76
240 AG 56	28.07	11.97	56.96

	Hercynite	Spinel	Gahnite
240 AG 56	30.75	12.94	56.31
240 AG 56	31.81	12.45	55.73
240 AG 56	32.95	13.99	53.05
DPB 1	29.62	2.53	67.85
DPB 1	28.68	2.58	68.74

	Hercynite	Spinel	Gahnite
DPB 1	29.51	2.70	67.79
JE 2 bl	5.21	0.30	94.49
JE 2 bl	4.92	0.30	94.78
JE 2 bl	4.31	0.30	95.39
JE 2 bl	4.12	0.30	95.58

	Hercynite	Spinel	Gahnite
JE 2 bl	3.92	0.40	95.68
JE 2 gr	15.18	21.26	63.56
JE 2 gr	16.65	21.12	62.37
JE 2 gr	15.10	21.28	63.63
JE 2 gr	16.25	20.38	63.37

	Hercynite	Spinel	Gahnite
JE 3 bl	3.54	0.61	95.86
JE 3 bl	3.12	0.40	96.48
JE 3 gr	17.02	23.81	59.17
JE 3 gr	16.62	24.29	59.59
JE 15 bl	0.00	0.30	99.70

	Hercynite	Spinel	Gahnite
JE 15 bl	4.79	0.27	94.95
JE 15 bl	4.23	0.36	95.41
JE 15 bl	4.84	0.26	94.90
JE 15 bl	5.30	0.97	93.73
JE 15 bl	4.43	0.57	95.00

	Hercynite	Spinel	Gahnite
JE 15 bl	3.94	0.31	95.75
JE 15 bl	3.80	0.27	95.93
JE 15 bl	4.23	0.31	95.45
JE 15 bl	3.96	0.00	96.04
JE 14 bl	3.70	0.50	95.80

	Hercynite	Spinel	Gahnite
JE 14 bl	3.01	0.30	96.69
JE 14 bl	3.10	0.20	95.80
JE 18 bl	4.25	0.30	95.45
JE 18 bl	6.21	1.12	92.67
JE 18 bl	4.92	0.10	94.98

	Hercynite	Spinel	Gahnite
JE 18 bl	4.52	0.60	94.87
JE 18 bl	4.73	0.30	94.96
JE 18 bl	3.73	1.11	95.16
JE 18 gr	16.52	25.90	57.58
JE 18 gr	16.62	25.85	57.54

	Hercynite	Spinel	Gahnite
JE 19 gr	15.32	30.87	53.81
JE 19 gr	10.96	33.45	55.59
JE 19 gr	17.13	29.59	53.28
JE 19 gr	14.51	31.14	54.35
JE 19 gr	14.88	30.44	54.68

	Hercynite	Spinel	Gahnite
JE 19 gr	13.38	30.70	55.91
JE 19 gr	13.32	30.29	56.39
JE 19 gr	13.46	29.83	56.70
JE 19 gr	12.29	29.69	58.01
JE 23 bl	2.70	0.70	96.60

	Hercynite	Spinel	Gahnite
JE 23 bl	3.61	1.10	95.29
JE 23 bl	2.10	0.50	97.40
JE 23 bl	3.90	0.21	95.90
JE 23 gr	12.42	32.52	54.15
JE 23 gr	12.25	32.48	54.51

	Hercynite	Spinel	Gahnite
JE 23 gr	11.60	32.88	54.86
JE 23 gr	11.24	32.19	55.89
JE 23 gr	11.71	31.76	55.81
JE 23 gr	11.40	32.00	55.84
JE 23 gr	11.42	31.56	56.26

	Hercynite	Spinel	Gahnite
JE 23 gr	11.72	31.17	56.37
JE 26 bl	2.22	0.10	97.68
JE 35 bl	3.83	0.60	95.57
JE 35 bl	3.76	0.41	95.83
JE 35 bl	4.26	0.41	95.33

	Hercynite	Spinel	Gahnite
JE 39 bl	2.73	0.61	96.66
JE 74 bl	3.44	0.55	96.01
JE 74 bl	4.36	0.49	95.15
JE 74 bl	3.33	0.45	96.22
JE 74 bl	16.92	26.52	56.56

	Hercynite	Spinel	Gahnite
JE 74 bl	1.62	0.00	98.38
JE 74 gr	16.28	24.18	59.54
JE 82 bl	1.46	0.52	98.03
JE 82 bl	3.19	0.77	96.04
JE 82 bl	3.18	0.66	96.16

	Hercynite	Spinel	Gahnite
JE 84 gr	16.73	25.78	57.48
OF 7 gr	21.14	28.15	50.71
OF 7 gr	18.94	21.88	59.18
OF 7 gr	21.05	27.19	51.76
JE 16	16.29	52.94	30.77

	Hercynite	Spinel	Gahnite
JE 16	19.29	56.91	23.80
JE 29	42.76	25.77	31.47
JE A	41.97	56.85	1.18
JE A	46.12	52.99	0.89
JE A	44.97	53.82	1.22

	Hercynite	Spinel	Gahnite
JE A	45.18	53.89	0.93
JE A	45.22	53.55	1.23
JE G	39.54	55.73	4.72
JE G	43.48	53.97	2.55
JE G	36.62	59.32	4.06

	Hercynite	Spinel	Gahnite
JE G	41.75	56.07	2.17

AVERAGE ENDMEMBER COMPOSITIONS Of ORANJEFONTEIN GARNET

Sample	JE 32	JE 31	JE 29	JE 10	JE 36	JE 35	JE 7	JE 74	JE 19
UV	0.09	0.03	0.14	0.02	0.09	0.07	0.10	0.00	0.02
AD	0.03	0.05	0.04	0.23	1.81	0.12	1.40	0.77	0.09
GROSS	1.66	4.38	4.26	10.06	4.70	7.12	3.90	3.52	5.93
PYR	21.28	23.81	31.62	11.72	14.06	29.69	19.80	32.32	34.03
SPESS	10.98	7.03	4.87	40.07	39.03	32.03	30.80	30.13	26.77
ALM	65.97	64.72	59.08	36.91	40.32	30.96	43.80	33.25	33.17

Sample	JE 18	JE 82	JE 20	JE 14	JE 15	JE 3	JE 2	OF 7
UV	0.00	0.01	0.03	0.03	0.11	0.02	0.03	0.00
AD	0.07	0.96	0.63	1.09	2.04	0.12	0.70	0.10
GROSS	5.80	3.94	5.08	12.77	5.65	6.02	5.02	5.59
PYR	36.88	34.67	33.78	16.01	15.38	31.92	34.50	34.46
SPESS	23.34	24.95	33.41	51.17	54.94	21.79	20.63	20.61
ALM	33.92	35.48	27.07	18.93	22.00	40.14	33.54	39.27

List of rock types

JE 31, 32	Metepelitic schists
JE 29	Aluminous schist
JE 10	Quartzo-feldspathic gneiss
JE 36	Garnet-biotite rock
JE 35, 7	Altered garnet-biotite rocks
JE 74	Gahnite quartzite
JE 19, 18	Garnet-biotite-gahnite-quartz rocks
JE 82	Gahnite-bearing massive garnet rock
JE 20	Garnet-bearing metaquartzite
JE 7	Piemontite-garnet rock
JE 14, 15	Garnet-,gahnite-bearing metaquartzite
JE 3, 2	Gahnite quartzites

Abbreviatons:

UV	uvarovite
AD	andradite
GROSS	grossular
PYR	pyrope
SPESS	spessartine
ALM	almandine

APPENDIX 4.

Mineral Analyses

Electron microprobe analyses of minerals are listed in this section. All Fe was analysed as FeO. Calculated Fe^{3+} is included in the spinel analyses.

MUSCOVITE

SIO2	42.55	42.74	42.76	43.17	42.68	42.33	43.08	43.71	42.98	44.24
TIO2	1.62	1.60	1.47	1.57	1.59	1.33	1.37	1.24	1.48	1.33
AL2O3	32.34	31.91	31.81	32.27	31.79	31.94	32.64	31.88	31.88	32.30
CR2O3	-	3.37	-	-	-	-	-	-	-	-
FEO	2.92	3.37	4.04	2.60	3.10	2.97	2.82	2.66	2.57	2.41
MNO	.09	.09	.07	.05	.05	.07	.05	.14	.09	.05
MGO	1.70	1.71	1.55	1.70	1.70	1.63	1.58	1.44	1.32	1.38
CAO	.17	-	.23	-	-	-	-	-	-	-
NA2O	9.08	.23	.23	.21	.21	.17	.23	.43	.43	.48
K2O	-	9.38	9.22	9.42	9.23	9.20	9.23	9.63	9.47	9.81
ZNO	-	.04	ND	.15	.07	.13	.36	-	-	-
TOTAL	90.47	94.44	91.40	91.14	90.42	89.77	91.36	91.13	90.22	92.00

** ATOMIC PROPORTIONS BASED ON SELECTED NO. OF OXYGENS **

OXYGEN	22	22	22	22	22	22	22	22	22	22
SI	5.897	5.877	6.027	6.056	6.047	6.038	6.034	6.137	6.092	6.143
TI	.169	.165	.156	.166	.169	.143	.144	.131	.158	.139
AL	5.283	5.172	5.285	5.336	5.309	5.370	5.389	5.276	5.327	5.287
CR	-	.366	-	-	-	-	-	-	-	-
FE2+	.338	.388	.476	.305	.367	.354	.330	.312	.305	.280
MN	.011	.010	.008	.006	.006	.008	.006	.017	.011	.006
MG	.351	.350	.326	.355	.359	.347	.330	.301	.279	.286
CA	.025	-	.035	-	-	-	-	-	-	-
NA	2.440	.061	.063	.057	.058	.047	.062	.117	.118	.129
K	-	1.646	1.658	1.686	1.668	1.674	1.649	1.725	1.713	1.738
ZN	-	.004	-	.016	.007	.014	.037	-	-	-
SUM	14.513	14.041	14.035	13.982	13.992	13.995	13.983	14.016	14.002	14.008

**** SAMPLE DIRECTORY ****

SAMPLE NO.	DESCRIPTION	SAMPLE NO.	DESCRIPTION
1	BH-2	6	BH-2
2	BH-2	7	BH-2
3	BH-2	8	BH LO-1
4	BH-2	9	BH LO-1
5	BH-2	10	BH LO-1

MUSCOVITE

SIO2	44.00	45.30	44.27	44.32	43.16	44.04	45.51	43.59	45.72	45.26
TIO2	.11	.59	1.71	1.72	1.71	1.79	.66	1.76	1.32	1.08
AL2O3	35.23	35.50	35.73	34.67	34.83	35.19	37.14	34.53	36.34	37.08
CR2O3	-	-	-	.05	.07	-	.05	.06	-	-
FEO	1.05	1.83	.94	1.27	1.09	1.38	2.10	.92	1.40	1.24
MNO	ND	-	-	-	-	-	.06	ND	.04	-
MGO	.79	.34	.56	.62	.50	.65	.69	.64	.58	.48
CAO	-	-	-	-	-	-	-	-	-	-
NA2O	.72	.22	.80	.58	.62	.58	.52	.54	.62	.67
K2O	9.40	7.13	9.24	9.15	9.04	9.03	8.30	9.05	9.23	10.07
ZNO	-	-	-	.07	ND	.05	-	.14	-	ND
TOTAL	91.32	90.91	93.25	92.45	91.04	92.71	95.03	91.25	95.25	95.90

** ATOMIC PROPORTIONS BASED ON SELECTED NO. OF OXYGENS **

OXYGEN	22	22	22	22	22	22	22	22	22	22
SI	6.080	6.188	5.991	6.055	5.987	6.000	6.018	6.028	6.051	5.979
TI	.011	.061	.174	.177	.178	.183	.066	.183	.131	.107
AL	5.738	5.716	5.699	5.583	5.695	5.651	5.789	5.628	5.669	5.773
CR	-	-	-	.005	.008	-	.005	.007	-	-
FE2+	.121	.209	.106	.145	.126	.157	.232	.106	.155	.137
MN	-	-	-	-	-	-	.007	-	.004	-
MG	.163	.069	.113	.126	.103	.132	.136	.132	.114	.094
CA	-	-	-	-	-	-	-	-	-	-
NA	.193	.058	.210	.154	.167	.153	.133	.145	.159	.172
K	1.657	1.243	1.595	1.595	1.600	1.570	1.400	1.597	1.558	1.697
ZN	-	-	-	.007	-	.005	-	.014	-	-
SUM	13.965	13.544	13.888	13.848	13.867	13.852	13.786	13.842	13.842	13.962

**** SAMPLE DIRECTORY ****

SAMPLE NO.	DESCRIPTION	SAMPLE NO.	DESCRIPTION
11	BH LO-1	16	ABN-2
12	BH 156-5	17	ABN-4
13	ABN-1	18	ABN-12
14	ABN-2	19	ABN-13
15	ABN-2	20	ABN-16

MUSCOVITE

SIO2	45.02
TIO2	1.24
AL2O3	35.86
CR2O3	-
FEO	1.49
MNO	-
MGO	.50
CAO	-
NA2O	.66
K2O	10.24
ZNO	ND
TOTAL	95.03

** ATOMIC PROPORTIONS BASED ON SELECTED NO. OF OXYGENS **

OXYGEN	22
SI	6.021
TI	.125
AL	5.653
CR	-
FE2+	.167
MN	-
MG	.100
CA	-
NA	.171
K	1.747
ZN	-
SUM	13.986

**** SAMPLE DIRECTORY ****

SAMPLE NO.	DESCRIPTION	SAMPLE NO.	DESCRIPTION
21	ABN-16		

BIOTITE

SIO2	41.22	40.32	37.01	36.81	35.16	35.06	35.11	33.64	34.13	33.99
TIO2	.08	.06	1.91	1.77	3.44	3.95	3.29	2.96	3.85	3.73
AL2O3	12.98	13.12	17.18	12.77	18.67	19.43	19.24	19.00	19.98	18.96
CR2O3	-	-	-	-	-	-	-	.07	.08	-
FEO	9.91	10.49	14.55	14.58	25.13	23.23	24.52	26.94	24.84	26.12
MNO	.51	.42	.98	1.00	.35	.31	.29	.25	.23	.24
MGO	21.32	20.07	14.48	14.03	5.43	5.53	5.32	5.90	5.30	5.15
CAO	-	-	-	-	-	-	-	-	-	-
NA2O	1.02	1.08	.12	.08	.08	.11	.09	.11	.10	-
K2O	7.33	6.84	8.79	8.68	9.60	9.54	9.73	7.66	7.55	9.06
ZNO	-	-	.13	.18	-	-	-	-	-	-
TOTAL	94.37	92.40	95.15	89.90	97.86	97.16	97.59	96.53	96.06	97.25

** ATOMIC PROPORTIONS BASED ON SELECTED NO. OF OXYGENS **

OXYGEN	22	22	22	22	22	22	22	22	22	22
SI	5.979	5.978	5.514	5.845	5.368	5.336	5.358	5.214	5.242	5.243
TI	.009	.007	.214	.211	.395	.452	.378	.345	.445	.433
AL	2.219	2.293	3.017	2.390	3.359	3.486	3.461	3.471	3.617	3.447
CR	-	-	-	-	-	-	-	.009	.010	-
FE2+	1.202	1.301	1.813	1.936	3.208	2.957	3.129	3.492	3.190	3.370
MN	.063	.053	.124	.134	.045	.040	.037	.033	.030	.031
MG	4.609	4.435	3.215	3.320	1.235	1.254	1.210	1.363	1.213	1.184
CA	-	-	-	-	-	-	-	-	-	-
NA	.287	.310	.035	.025	.024	.032	.027	.033	.030	-
K	1.356	1.294	1.671	1.758	1.870	1.853	1.894	1.515	1.479	1.783
ZN	-	-	.014	.021	-	-	-	-	-	-
SUM	15.724	15.671	15.616	15.641	15.504	15.411	15.494	15.475	15.255	15.492

**** SAMPLE DIRECTORY ****

SAMPLE NO.	DESCRIPTION	SAMPLE NO.	DESCRIPTION
1	BH WE-2	6	BHG 156-5
2	BH WE-2	7	BHG 156-5
3	BH-2	8	AG 80 195
4	BH-2	9	AG 80 195
5	BHG 156-5	10	BHG 156-7

BIOTITE

SIO2	36.11	33.71	33.88	34.89	35.93	34.54	34.63	34.48	34.57	37.33
TIO2	4.22	3.96	4.53	.82	.78	2.31	2.33	2.36	1.89	1.30
AL2O3	20.23	18.96	19.44	20.53	20.41	20.08	19.49	19.34	25.09	17.51
CR2O3	-	-	.07	-	-	-	-	.04	-	-
FEO	20.57	25.72	24.09	19.35	19.38	20.44	21.25	22.59	19.85	13.95
MNO	.17	.24	.17	.34	.37	.18	.21	.39	.25	.05
MGO	5.25	5.05	5.18	8.86	9.60	8.09	8.39	7.87	6.94	15.37
CAO	-	-	-	-	-	-	-	-	-	-
NA2O	.04	.09	.09	.30	.30	.31	.25	.32	.25	.53
K2O	9.78	8.76	9.15	9.09	9.18	8.87	8.69	8.65	7.57	8.39
ZNO	-	-	-	.15	.17	.22	.11	.07	-	.08
TOTAL	96.37	96.49	96.60	94.33	96.12	95.04	95.35	96.11	96.41	94.51

** ATOMIC PROPORTIONS BASED ON SELECTED NO. OF OXYGENS **

OXYGEN	22	22	22	22	22	22	22	22	22	22
SI	5.449	5.230	5.214	5.361	5.406	5.296	5.307	5.283	5.119	5.545
TI	.479	.462	.524	.095	.088	.266	.269	.272	.210	.145
AL	3.598	3.467	3.526	3.718	3.620	3.629	3.521	3.493	4.379	3.066
CR	-	-	.009	-	-	-	-	.005	-	-
FE2+	2.596	3.337	3.100	2.486	2.439	2.621	2.724	2.895	2.458	1.733
MN	.022	.032	.022	.044	.047	.023	.027	.051	.031	.006
MG	1.181	1.168	1.188	2.029	2.153	1.849	1.916	1.797	1.532	3.402
CA	-	-	-	-	-	-	-	-	-	-
NA	.012	.027	.027	.089	.088	.092	.074	.095	.072	.153
K	1.883	1.734	1.796	1.782	1.762	1.735	1.699	1.691	1.430	1.590
ZN	-	-	-	.017	.019	.025	.012	.008	-	.009
SUM	15.220	15.455	15.406	15.621	15.621	15.537	15.550	15.589	15.232	15.648

**** SAMPLE DIRECTORY ****

SAMPLE NO.	DESCRIPTION	SAMPLE NO.	DESCRIPTION
11	BHG 156-7	16	ABN-4
12	BHG 156-7	17	ABN-4
13	BHG 156-7	18	ABN-4
14	ABN-3	19	ABN-4
15	ABN-3	20	ABN-6

BIOTITE

SIO2	38.39	37.42	37.67	36.24	37.05	36.74	36.46	34.85	35.85	35.58
TIO2	1.40	1.38	1.34	.84	1.22	1.20	1.37	2.63	1.43	1.65
AL2O3	17.18	17.71	17.95	17.67	17.61	17.42	17.76	18.36	18.88	18.79
CR2O3	-	-	-	-	-	-	-	-	-	-
FEO	13.47	14.16	14.22	14.67	14.18	14.62	14.93	14.26	13.45	14.14
MNO	-	-	-	-	-	-	-	.14	.09	.19
MGO	16.53	15.21	15.34	15.83	15.09	15.46	15.42	12.48	14.09	13.24
CAO	-	-	-	-	-	-	-	-	-	-
NA2O	-	.51	.38	.38	.40	.42	.41	.43	.39	.43
K2O	7.70	7.97	7.55	7.19	7.77	7.67	7.18	7.97	7.77	8.00
ZNO	.10	-	-	-	-	-	-	-	-	.15
TOTAL	94.77	94.36	94.45	92.82	93.32	93.53	93.53	91.12	91.95	92.17

** ATOMIC PROPORTIONS BASED ON SELECTED NO. OF OXYGENS **

OXYGEN	22	22	22	22	22	22	22	22	22	22
SI	5.625	5.551	5.561	5.468	5.554	5.512	5.463	5.389	5.443	5.428
TI	.154	.154	.149	.095	.138	.135	.154	.306	.163	.189
AL	2.967	3.096	3.123	3.143	3.111	3.080	3.137	3.347	3.379	3.379
CR	-	-	-	-	-	-	-	-	-	-
FE2+	1.651	1.757	1.756	1.851	1.778	1.834	1.871	1.844	1.708	1.804
MN	-	-	-	-	-	-	-	.018	.012	.025
MG	3.610	3.362	3.375	3.560	3.371	3.456	3.443	2.876	3.188	3.010
CA	-	-	-	-	-	-	-	-	-	-
NA	-	.147	.109	.111	.116	.122	.119	.129	.115	.127
K	1.439	1.508	1.422	1.384	1.486	1.468	1.373	1.572	1.505	1.557
ZN	.011	-	-	-	-	-	-	-	-	.017
SUM	15.457	15.575	15.494	15.613	15.554	15.608	15.560	15.482	15.514	15.536

**** SAMPLE DIRECTORY ****

SAMPLE NO.	DESCRIPTION	SAMPLE NO.	DESCRIPTION
21	ABN-6	26	ABN-6
22	ABN-6	27	ABN-6
23	ABN-6	28	ABN-9
24	ABN-6	29	ABN-9
25	ABN-6	30	ABN-9

BIOTITE

SIO2	35.39	35.11	35.80	36.86	35.49	35.02	37.11	36.19	34.57	33.96
TIO2	2.94	3.55	3.82	3.18	2.81	2.13	3.01	3.27	3.45	3.42
AL2O3	18.24	19.51	19.18	19.85	19.28	19.85	20.64	19.09	19.73	19.28
CR2O3	-	-	-	-	-	-	-	-	-	-
FEO	14.64	21.39	20.53	20.36	19.61	19.19	18.57	18.59	23.19	21.96
MNO	.20	.35	.31	.29	.26	.23	.30	.26	.19	.22
MGO	11.81	8.53	8.05	8.85	9.81	9.77	6.66	7.18	6.71	6.57
CAO	-	-	-	-	.21	-	-	-	-	-
NA2O	.36	.34	.27	.30	.31	.35	.29	.16	.21	.25
K2O	8.06	9.07	8.94	9.04	8.95	8.83	7.81	7.63	8.50	8.46
ZNO	-	.07	.09	.12	.10	.28	-	-	-	.27
TOTAL	91.64	97.92	96.99	98.85	96.83	95.65	94.39	92.37	96.55	94.39

** ATOMIC PROPORTIONS BASED ON SELECTED NO. OF OXYGENS **

OXYGEN	22	22	22	22	22	22	22	22	22	22
SI	5.446	5.250	5.368	5.399	5.317	5.302	5.584	5.586	5.267	5.286
TI	.340	.399	.431	.350	.317	.243	.341	.380	.395	.400
AL	3.309	3.439	3.390	3.427	3.405	3.542	3.661	3.473	3.543	3.537
CR	-	-	-	-	-	-	-	-	-	-
FE2+	1.884	2.675	2.575	2.494	2.457	2.430	2.337	2.400	2.955	2.859
MN	.026	.044	.039	.036	.033	.029	.038	.034	.025	.029
MG	2.709	1.901	1.799	1.932	2.190	2.204	1.493	1.652	1.524	1.524
CA	-	-	-	-	.034	-	-	-	-	-
NA	.107	.099	.079	.085	.090	.103	.085	.048	.062	.075
K	1.582	1.730	1.710	1.689	1.711	1.705	1.499	1.502	1.652	1.680
ZN	-	.008	.010	.013	.011	.031	-	-	-	.031
SUM	15.404	15.546	15.400	15.425	15.564	15.589	15.037	15.074	15.423	15.422

**** SAMPLE DIRECTORY ****

SAMPLE NO.	DESCRIPTION	SAMPLE NO.	DESCRIPTION
31	ABN-9	36	ABN-10
32	ABN-10	37	ABN-13
33	ABN-10	38	ABN-13
34	ABN-10	39	ABN-16
35	ABN-10	40	ABN-16

BIOTITE

SIO2	33.99	34.04	34.08	35.60	35.68	35.66	34.77	35.35	33.97	37.64
TIO2	3.53	3.25	2.98	1.83	1.06	1.39	1.83	2.41	3.44	5.11
AL2O3	19.22	19.18	19.19	19.64	19.95	19.85	19.45	19.73	16.61	15.74
CR2O3	-	-	-	-	-	-	-	-	-	-
FEO	22.43	23.05	23.41	16.03	16.37	16.91	17.08	17.83	11.03	9.91
MNO	.27	.25	.22	.12	.13	.15	.15	.09	.30	.27
MGO	6.81	6.79	6.99	12.62	13.19	12.51	12.02	10.23	18.84	17.06
CAO	-	-	-	-	-	-	-	-	-	-
NA2O	.22	.20	.21	.28	.30	.41	.29	.33	.32	.22
K2O	8.68	8.61	8.40	8.02	8.26	8.32	8.38	8.23	6.55	9.43
ZNO	.35	.12	-	-	-	-	-	-	.47	.36
TOTAL	95.50	95.49	95.48	94.14	94.94	95.20	93.97	94.20	91.53	95.74

** ATOMIC PROPORTIONS BASED ON SELECTED NO. OF OXYGENS **

OXYGEN	22	22	22	22	22	22	22	22	22	22
SI	5.251	5.264	5.268	5.350	5.331	5.332	5.289	5.363	5.159	5.476
TI	.410	.378	.346	.207	.119	.156	.209	.275	.393	.559
AL	3.500	3.496	3.497	3.479	3.513	3.499	3.487	3.528	2.973	2.699
CR	-	-	-	-	-	-	-	-	-	-
FE2+	2.898	2.981	3.027	2.015	2.046	2.115	2.173	2.262	1.401	1.206
MN	.035	.033	.029	.015	.016	.019	.019	.012	.039	.033
MG	1.568	1.565	1.610	2.827	2.937	2.788	2.725	2.313	4.264	3.699
CA	-	-	-	-	-	-	-	-	-	-
NA	.066	.060	.063	.082	.087	.119	.086	.097	.094	.062
K	1.711	1.699	1.657	1.538	1.575	1.587	1.626	1.593	1.269	1.750
ZN	.040	.014	-	-	-	-	-	-	.053	.039
SUM	15.478	15.489	15.497	15.513	15.624	15.615	15.614	15.443	15.644	15.522

**** SAMPLE DIRECTORY ****

SAMPLE NO.	DESCRIPTION	SAMPLE NO.	DESCRIPTION
41	ABN-16	46	SK-3
42	ABN-16	47	SK-3
43	ABN-16	48	SK-4
44	SK-3	49	JE-2
45	SK-3	50	JE-2

BIOTITE

SIO2	38.38	38.05	38.40	37.98	35.73	35.25	34.48	35.37	36.57	35.36
TIO2	5.16	5.17	5.00	5.01	3.05	3.93	3.40	4.14	1.30	4.03
AL2O3	16.19	15.99	15.81	15.95	17.34	17.62	18.57	17.83	18.02	16.96
CR2O3	-	-	-	-	.07	-	-	-	-	-
FEO	9.44	9.76	9.45	9.76	13.48	15.96	13.29	13.59	10.19	15.24
MNO	.21	.23	.23	.26	.08	.09	.19	.20	.10	.14
MGO	17.87	17.26	17.93	17.16	14.78	12.56	13.97	14.01	18.35	13.32
CAO	-	-	.33	-	-	-	-	-	-	-
NA2O	.16	.19	.23	.21	.14	.08	.08	.08	.15	.09
K2O	8.92	9.55	9.56	9.69	9.08	9.39	9.49	9.57	9.05	9.37
ZNO	.27	.34	.33	.34	-	-	-	-	-	-
TOTAL	96.60	96.54	97.27	96.36	93.75	94.88	93.47	94.79	93.73	94.51

** ATOMIC PROPORTIONS BASED ON SELECTED NO. OF OXYGENS **

OXYGEN	22	22	22	22	22	22	22	22	22	22
SI	5.487	5.480	5.485	5.487	5.381	5.320	5.227	5.290	5.406	5.345
TI	.555	.560	.537	.544	.345	.446	.388	.466	.145	.458
AL	2.728	2.714	2.662	2.716	3.078	3.134	3.318	3.143	3.140	3.022
CR	-	-	-	-	.008	-	-	-	-	-
FE2+	1.129	1.176	1.129	1.179	1.698	2.014	1.685	1.700	1.260	1.927
MN	.025	.028	.028	.032	.010	.012	.024	.025	.013	.018
MG	3.807	3.705	3.817	3.694	3.317	2.825	3.156	3.123	4.043	3.001
CA	-	-	.051	-	-	-	-	-	-	-
NA	.044	.053	.064	.059	.041	.023	.024	.023	.043	.026
K	1.627	1.755	1.742	1.786	1.745	1.808	1.835	1.826	1.707	1.807
ZN	.029	.036	.035	.036	-	-	-	-	-	-
SUM	15.430	15.507	15.550	15.533	15.623	15.583	15.656	15.597	15.755	15.603

**** SAMPLE DIRECTORY ****

SAMPLE NO.	DESCRIPTION	SAMPLE NO.	DESCRIPTION
51	JE-2	56	JE-29
52	JE-2	57	JE-29
53	JE-2	58	JE-29
54	JE-2	59	JE-29
55	JE-29	60	JE-29

BIOTITE

SIO2	36.62	36.34	36.86	35.59	36.11	36.26	38.26	38.21
TIO2	3.02	3.10	3.30	3.33	3.27	3.16	.49	.99
AL2O3	16.58	16.38	16.61	15.98	16.29	16.31	16.79	15.51
CR2O3	.06	-	.05	-	-	-	-	-
FEO	12.44	12.97	11.42	13.98	13.40	12.98	4.98	6.64
MNO	-	-	-	.10	-	-	.13	.31
MGO	15.65	15.47	16.46	15.37	15.65	15.74	21.11	21.48
CAO	-	-	-	-	-	-	-	-
NA2O	.21	.21	.24	.23	.23	.25	.36	.35
K2O	9.40	9.25	9.60	9.06	9.32	9.39	8.68	8.51
ZNO	-	-	-	-	-	-	.52	.16
TOTAL	93.98	93.72	94.54	93.64	94.27	94.09	91.32	92.16

** ATOMIC PROPORTIONS BASED ON SELECTED NO. OF OXYGENS **

OXYGEN	22	22	22	22	22	22	22	22
SI	5.477	5.464	5.459	5.395	5.418	5.439	5.651	5.640
TI	.340	.351	.368	.380	.369	.357	.054	.110
AL	2.923	2.903	2.900	2.855	2.881	2.884	2.923	2.698
CR	.007	-	.006	-	-	-	-	-
FE2+	1.556	1.631	1.414	1.772	1.681	1.628	.615	.820
MN	-	-	-	.013	-	-	.016	.039
MG	3.488	3.467	3.633	3.472	3.499	3.519	4.647	4.725
CA	-	-	-	-	-	-	-	-
NA	.061	.061	.069	.068	.067	.073	.103	.100
K	1.794	1.774	1.814	1.752	1.784	1.797	1.636	1.603
ZN	-	-	-	-	-	-	.057	.017
SUM	15.646	15.651	15.662	15.707	15.699	15.697	15.702	15.752

**** SAMPLE DIRECTORY ****

SAMPLE NO.	DESCRIPTION	SAMPLE NO.	DESCRIPTION
61	JE-31	66	JE-32
62	JE-31	67	JE-74
63	JE-31	68	JE-74
64	JE-32		
65	JE-32		

CHLORITE

SIO2	29.68	31.86	29.73	31.09	31.67	33.28	30.37	30.20	25.10	23.45
TIO2	-	-	-	ND	.07	ND	.11	ND	.05	-
AL2O3	9.95	8.42	10.32	21.25	21.05	21.64	21.02	20.53	22.29	22.21
CR2O3	-	-	-	-	-	-	-	-	-	-
FEO	43.66	43.47	44.27	7.93	6.41	6.08	5.94	8.85	25.59	26.85
MNO	2.02	2.08	2.03	1.52	1.55	1.52	1.78	1.74	1.81	2.28
MGO	2.41	1.80	2.22	24.10	25.20	22.95	26.22	24.15	11.31	9.79
CAO	.14	.24	.06	.06	.06	.08	.06	ND	ND	ND
NA2O	.20	.14	.06	-	.04	.02	-	.02	.04	.04
K2O	.32	.39	.25	.05	.11	.52	.05	.09	.34	-
ZNO	-	.15	-	.74	.84	.76	.83	.87	1.25	3.73
TOTAL	88.38	88.55	88.94	86.77	87.00	86.87	86.38	86.51	87.80	88.38

** ATOMIC PROPORTIONS BASED ON SELECTED NO. OF OXYGENS **

OXYGEN	28	28	28	28	28	28	28	28	28	28
SI	6.965	7.424	6.935	6.034	6.087	6.364	5.892	5.940	5.378	5.131
TI	-	-	-	-	.010	-	.016	-	.008	-
AL	2.752	2.313	2.837	4.861	4.769	4.878	4.807	4.759	5.630	5.728
CR	-	-	-	-	-	-	-	-	-	-
FE2+	8.569	8.472	8.636	1.287	1.030	.972	.964	1.456	4.586	4.913
MN	.402	.411	.401	.250	.252	.246	.293	.290	.329	.423
MG	.843	.625	.772	6.971	7.218	6.540	7.581	7.079	3.612	3.192
CA	.035	.060	.015	.012	.012	.016	.012	-	-	-
NA	.091	.063	.027	-	.015	.007	-	.008	.017	.017
K	.096	.116	.074	.012	.027	.127	.012	.023	.093	-
ZN	-	.026	-	.106	.119	.107	.119	.126	.198	.603
SUM	19.752	19.509	19.697	19.538	19.540	19.261	19.695	19.691	19.854	20.014

**** SAMPLE DIRECTORY ****

SAMPLE NO.	DESCRIPTION	SAMPLE NO.	DESCRIPTION
1	BH WE-2	6	JE-7
2	BH WE-2	7	JE-7
3	BH WE-2	8	JE-7
4	JE-7	9	JE-14
5	JE-7	10	JE-14

CHLORITE

SIO2	23.93	23.71	26.33	28.78	26.40	26.17	30.12	26.26	25.42	27.92
TIO2	ND	ND	.10	-	-	.26	.27	.15	2.51	-
AL2O3	21.05	21.29	19.93	18.93	19.80	19.61	19.76	20.10	18.71	19.82
CR2O3	-	-	-	-	-	-	-	-	-	-
FEO	27.18	27.80	20.19	19.83	19.92	19.33	16.89	19.10	18.73	16.56
MNO	2.00	2.10	2.23	2.11	2.30	2.29	1.97	2.09	2.14	1.95
MGO	11.73	11.47	17.44	19.37	18.15	17.28	15.68	16.56	16.26	16.12
CAO	.04	.04	ND	.10	.04	-	-	-	ND	.09
NA2O	-	.02	.06	-	-	.03	.03	.08	.02	.04
K2O	-	-	-	-	-	-	.04	.04	ND	.06
ZNO	1.40	1.41	1.41	1.65	1.48	3.26	3.87	2.81	3.64	5.25
TOTAL	87.35	87.86	87.72	90.77	88.09	88.23	88.63	87.19	87.48	87.81

** ATOMIC PROPORTIONS BASED ON SELECTED NO. OF OXYGENS **

OXYGEN	28	28	28	28	28	28	28	28	28	28
SI	5.231	5.174	5.504	5.773	5.492	5.481	6.126	5.533	5.386	5.814
TI	-	-	.016	-	-	.041	.041	.024	.400	-
AL	5.424	5.476	4.911	4.476	4.855	4.841	4.737	4.992	4.673	4.865
CR	-	-	-	-	-	-	-	-	-	-
FE2+	4.969	5.073	3.530	3.327	3.466	3.386	2.873	3.366	3.319	2.884
MN	.370	.388	.395	.358	.405	.406	.339	.373	.384	.344
MG	3.821	3.730	5.433	5.790	5.627	5.393	4.753	5.200	5.134	5.003
CA	.009	.009	-	.021	.009	-	-	-	-	.020
NA	-	.008	.024	-	-	.012	.012	.033	.008	.016
K	-	-	-	-	-	-	.010	.011	-	.016
ZN	.226	.227	.218	.244	.227	.504	.581	.437	.570	.807
SUM	20.054	20.089	20.037	19.989	20.081	20.064	19.475	19.969	19.886	19.769

**** SAMPLE DIRECTORY ****

SAMPLE NO.	DESCRIPTION	SAMPLE NO.	DESCRIPTION
11	JE-14	16	JE-18
12	JE-14	17	JE-18
13	JE-16	18	JE-18
14	JE-16	19	JE-18
15	JE-16	20	JE-18

CHLORITE

SIO2	27.97	25.79	26.21	25.56	29.00	29.21	25.34	25.65	25.91	26.01
TIO2	-	.05	-	-	.04	ND	.06	-	ND	ND
AL2O3	21.72	20.59	22.85	21.39	21.74	20.55	21.88	20.62	20.09	21.02
CR2O3	-	-	-	-	-	-	-	-	-	-
FEO	17.90	19.86	23.77	24.93	21.55	22.78	25.38	21.66	21.41	21.82
MNO	2.13	2.21	1.83	1.95	1.46	1.48	1.83	2.51	2.40	2.55
MGO	13.91	14.01	11.46	11.31	12.08	11.65	12.16	14.73	15.05	14.67
CAO	.08	.06	.15	.12	.16	.15	.06	.04	.06	.04
NA2O	.06	.05	.13	.06	.05	.06	-	.02	.04	-
K2O	.04	ND	.13	.09	.13	.21	.07	-	ND	-
ZNO	2.55	2.58	1.74	1.78	2.61	2.71	1.78	2.56	2.65	2.58
TOTAL	86.36	85.23	88.27	87.19	88.82	88.83	88.56	87.79	87.66	88.71

** ATOMIC PROPORTIONS BASED ON SELECTED NO. OF OXYGENS **

OXYGEN	28	28	28	28	28	28	28	28	28	28
SI	5.849	5.578	5.519	5.511	5.971	6.066	5.384	5.445	5.504	5.458
TI	-	.008	-	-	.006	-	.010	-	-	-
AL	5.354	5.249	5.671	5.436	5.276	5.031	5.480	5.159	5.030	5.199
CR	-	-	-	-	-	-	-	-	-	-
FE2+	3.130	3.592	4.186	4.496	3.711	3.957	4.510	3.845	3.803	3.829
MN	.377	.405	.326	.356	.255	.260	.329	.451	.432	.453
MG	4.335	4.516	3.596	3.635	3.707	3.606	3.851	4.660	4.764	4.588
CA	.018	.014	.034	.028	.035	.033	.014	.009	.014	.009
NA	.024	.021	.053	.025	.020	.024	-	.008	.016	-
K	.011	-	.035	.025	.034	.056	.019	-	-	-
ZN	.394	.412	.271	.283	.397	.416	.279	.401	.416	.400
SUM	19.492	19.804	19.690	19.795	19.412	19.453	19.876	19.980	19.990	19.939

**** SAMPLE DIRECTORY ****

SAMPLE NO.	DESCRIPTION	SAMPLE NO.	DESCRIPTION
21	JE-18	26	JE-19
22	JE-18	27	JE-19
23	JE-19	28	JE-20
24	JE-19	29	JE-20
25	JE-19	30	JE-20

CHLORITE

SIO2	27.08	27.23	27.84	27.23	27.64	27.49	27.30	27.34	27.26
TIO2	.04	ND	ND	ND	-	.04	ND	ND	-
AL2O3	19.26	19.15	19.73	19.15	19.29	19.29	18.93	19.14	19.23
CR2O3	-	-	-	-	-	-	-	-	-
FEO	10.93	10.70	10.53	10.70	9.08	10.08	11.81	9.04	10.03
MNO	3.29	3.08	3.58	3.08	3.76	3.43	2.77	3.81	3.38
MGO	21.82	22.22	21.90	22.22	21.98	22.10	21.57	21.68	21.82
CAO	.06	ND	ND	ND	.06	ND	ND	.08	.05
NA2O	.06	.06	.02	.05	.06	.03	.06	.04	.03
K2O	-	-	ND	ND	-	ND	ND	-	ND
ZNO	4.72	4.60	5.34	4.60	5.67	5.12	4.03	5.73	4.88
TOTAL	87.26	87.10	89.02	87.11	87.54	87.64	86.54	86.89	86.70

** ATOMIC PROPORTIONS BASED ON SELECTED NO. OF OXYGENS **

OXYGEN	28	28	28	28	28	28	28	28	28
SI	5.562	5.585	5.604	5.585	5.640	5.607	5.639	5.628	5.613
TI	.006	-	-	-	-	.006	-	-	-
AL	4.663	4.629	4.681	4.629	4.639	4.638	4.609	4.644	4.667
CR	-	-	-	-	-	-	-	-	-
FE2+	1.877	1.835	1.773	1.835	1.549	1.719	2.040	1.556	1.727
MN	.572	.535	.610	.535	.650	.593	.485	.664	.589
MG	6.679	6.792	6.570	6.792	6.684	6.718	6.640	6.651	6.696
CA	.013	-	-	-	.013	-	-	.018	.011
NA	.024	.024	.008	.020	.024	.012	.024	.016	.012
K	-	-	-	-	-	-	-	-	-
ZN	.716	.697	.794	.697	.854	.771	.615	.871	.742
SUM	20.113	20.108	20.057	20.109	20.053	20.078	20.068	20.053	20.062

**** SAMPLE DIRECTORY ****

SAMPLE NO.	DESCRIPTION	SAMPLE NO.	DESCRIPTION
		36	JE-36
32	JE-36	37	JE-36
33	JE-36	38	JE-36
34	JE-36	39	JE-36
35	JE-36	40	JE-36

CHLORITE

SIO2	27.79	27.35	25.12	25.18	25.10	23.28	26.14
TIO2	ND	-	-	-	-	-	2.42
AL2O3	19.51	19.09	21.45	20.49	21.34	21.58	18.43
CR2O3	-	-	-	-	-	-	-
FEO	9.85	9.43	23.95	24.44	24.22	28.33	20.61
MNO	3.48	3.68	1.66	1.78	1.75	1.75	1.41
MGO	22.19	21.98	12.48	13.19	14.04	10.74	15.82
CAO	.05	.06	.04	ND	-	.05	.06
NA2O	.03	.04	.06	.04	-	-	-
K2O	ND	-	ND	-	-	ND	.09
ZNO	5.39	5.39	1.18	1.50	.81	.81	.97
TOTAL	88.34	87.02	85.97	86.65	87.26	86.57	85.95

** ATOMIC PROPORTIONS BASED ON SELECTED NO. OF OXYGENS **

OXYGEN	28	28	28	28	28	28	28
SI	5.620	5.619	5.444	5.450	5.357	5.150	5.572
TI	-	-	-	-	-	-	.388
AL	4.651	4.623	5.480	5.227	5.368	5.627	4.631
CR	-	-	-	-	-	-	-
FE2+	1.666	1.620	4.341	4.424	4.323	5.242	3.674
MN	.596	.640	.305	.326	.316	.328	.255
MG	6.688	6.729	4.031	4.254	4.466	3.541	5.026
CA	.011	.013	.009	-	-	.012	.014
NA	.012	.016	.025	.017	-	-	-
K	-	-	-	-	-	-	.024
ZN	.805	.818	.189	.240	.128	.132	.153
SUM	20.058	20.078	19.833	19.945	19.959	20.040	19.737

**** SAMPLE DIRECTORY ****

SAMPLE NO.	DESCRIPTION	SAMPLE NO.	DESCRIPTION
41	JE-36	46	OF-7
42	JE-36	47	OF-7
43	OF-7		
44	OF-7		
45	OF-7		

GARNET

SIO2	36.72	36.60	36.73	36.50	36.45	36.97	36.97	36.43	36.03	36.21
TIO2	-	-	-	-	-	-	-	-	ND	ND
AL2O3	21.02	21.00	20.80	20.58	20.70	20.99	20.86	21.47	21.60	21.49
CR2O3	-	-	-	-	-	-	-	ND	-	ND
FEO	21.05	22.14	22.11	21.28	20.53	21.86	22.04	25.32	24.79	25.13
MNO	18.95	16.92	17.51	18.07	19.50	17.66	17.50	15.99	16.50	15.82
MGO	1.32	1.52	1.50	1.46	1.31	1.52	1.52	.96	.92	1.02
CAO	.86	1.86	1.59	1.42	.88	1.57	1.44	.57	.60	.63
NA2O	-	-	-	-	-	-	-	-	.02	-
K2O	-	-	-	-	-	-	-	-	-	-
TOTAL	99.92	100.04	100.24	99.31	99.37	100.57	100.33	100.76	100.49	100.35

** ATOMIC PROPORTIONS BASED ON SELECTED NO. OF OXYGENS **

OXYGEN	12	12	12	12	12	12	12	12	12	12
SI	2.995	2.979	2.988	2.996	2.994	2.993	3.000	2.962	2.940	2.954
TI	-	-	-	-	-	-	-	-	-	-
AL	2.020	2.015	1.995	1.991	2.004	2.003	1.995	2.057	2.078	2.066
CR	-	-	-	-	-	-	-	-	-	-
FE2+	1.436	1.507	1.504	1.461	1.410	1.480	1.496	1.722	1.692	1.715
MN	1.309	1.167	1.207	1.256	1.357	1.211	1.203	1.101	1.141	1.093
MG	.160	.184	.182	.179	.160	.183	.184	.116	.112	.124
CA	.075	.162	.139	.125	.077	.136	.125	.050	.052	.055
NA	-	-	-	-	-	-	-	-	.003	-
K	-	-	-	-	-	-	-	-	-	-
SUM	7.995	8.014	8.014	8.008	8.004	8.006	8.003	8.009	8.020	8.011

**** SAMPLE DIRECTORY ****

SAMPLE NO.	DESCRIPTION	SAMPLE NO.	DESCRIPTION
1	BH WE-1	6	BH WE-1
2	BH WE-1 CORE	7	BH WE-1
3	BH WE-1 RIM	8	BH LO-1 CORE
4	BH WE-1 CORE	9	BH LO-1 RIM
5	BH WE-1 RIM	10	BH LO-1 CORE

GARNET

SIO2	36.15	36.15	36.41	36.33	37.25	37.29	37.49	37.56	37.27	36.99
TIO2	-	.09	ND	ND	-	-	-	-	-	-
AL2O3	21.40	21.52	21.57	21.53	21.61	21.89	22.01	21.92	21.12	21.08
CR2O3	-	ND	-	-	-	-	-	-	-	-
FEO	25.13	23.83	24.60	25.07	35.95	35.33	34.73	35.34	34.71	34.92
MNO	15.93	17.59	16.33	15.91	1.25	1.21	1.24	1.29	5.80	5.72
MGO	.93	.81	1.04	1.06	5.18	5.29	5.42	5.45	1.42	1.38
CAO	.57	.29	.59	.59	.33	.34	.35	.30	1.95	1.93
NA2O	-	.03	.03	-	-	-	.02	-	-	-
K2O	-	-	-	-	-	-	-	-	-	-
TOTAL	100.11	100.33	100.60	100.52	101.57	101.35	101.26	101.86	102.27	102.02

** ATOMIC PROPORTIONS BASED ON SELECTED NO. OF OXYGENS **

OXYGEN	12	12	12	12	12	12	12	12	12	12
SI	2.958	2.953	2.960	2.957	2.943	2.942	2.951	2.947	2.981	2.971
TI	-	.006	-	-	-	-	-	-	-	-
AL	2.064	2.072	2.067	2.066	2.012	2.036	2.042	2.027	1.991	1.995
CR	-	-	-	-	-	-	-	-	-	-
FE2+	1.720	1.628	1.672	1.707	2.375	2.331	2.286	2.319	2.322	2.345
MN	1.104	1.217	1.124	1.097	.084	.081	.083	.086	.393	.389
MG	.113	.099	.126	.129	.610	.622	.636	.637	.169	.165
CA	.050	.025	.051	.051	.028	.029	.030	.025	.167	.166
NA	-	.005	.005	-	-	-	.003	-	-	-
K	-	-	-	-	-	-	-	-	-	-
SUM	8.010	8.007	8.007	8.008	8.051	8.040	8.030	8.040	8.023	8.032

**** SAMPLE DIRECTORY ****

SAMPLE NO.	DESCRIPTION	SAMPLE NO.	DESCRIPTION
11	BH LO-1 RIM	16	240 AG 56 RIM
12	BH LO-1	17	240 AG 56 CORE
13	BH LO-1	18	240 AG 56 RIM
14	BH LO-1	19	AG 80 195
15	240 AG 56 CORE	20	AG 80 195

GARNET

SIO2	37.32	36.99	36.89	37.16	36.74	37.10	36.91	36.79	37.09	36.39
TIO2	-	-	ND	-	-	-	.06	-	-	.04
AL2O3	21.28	21.08	21.28	21.25	21.12	21.28	21.11	21.15	21.26	21.31
CR2O3	-	-	-	-	-	-	-	-	-	ND
FEO	34.96	32.19	33.09	32.84	33.05	33.08	33.01	32.84	33.04	29.45
MNO	5.67	8.71	8.82	8.78	8.88	8.67	8.80	8.66	8.76	10.22
MGO	1.29	1.40	1.35	1.53	1.32	1.48	1.27	1.45	1.37	1.88
CAO	1.90	1.16	1.16	1.21	1.10	1.19	1.77	1.11	1.28	1.76
NA2O	-	-	-	-	-	-	-	-	-	-
K2O	-	-	-	-	-	-	-	-	-	-
TOTAL	102.42	101.53	102.61	102.77	102.21	102.80	102.93	102.00	102.80	101.07

** ATOMIC PROPORTIONS BASED ON SELECTED NO. OF OXYGENS **

OXYGEN	12	12	12	12	12	12	12	12	12	12
SI	2.980	2.981	2.954	2.965	2.956	2.962	2.951	2.960	2.963	2.940
TI	-	-	-	-	-	-	.004	-	-	.002
AL	2.003	2.003	2.009	1.999	2.003	2.002	1.989	2.006	2.002	2.030
CR	-	-	-	-	-	-	-	-	-	-
FE2+	2.335	2.170	2.216	2.192	2.224	2.209	2.207	2.210	2.207	1.990
MN	.384	.595	.598	.594	.605	.586	.596	.590	.593	.699
MG	.154	.168	.161	.182	.158	.176	.151	.174	.163	.226
CA	.163	.100	.100	.103	.095	.102	.152	.096	.110	.152
NA	-	-	-	-	-	-	-	-	-	-
K	-	-	-	-	-	-	-	-	-	-
SUM	8.018	8.017	8.040	8.035	8.042	8.037	8.051	8.037	8.037	8.042

**** SAMPLE DIRECTORY ****

SAMPLE NO.	DESCRIPTION	SAMPLE NO.	DESCRIPTION
21	AG 80 195	26	BHG 156-7 CORE
22	BHG 156-7 CORE	27	BHG 156-7 RIM
23	BHG 156-7 RIM	28	BHG 156-7 CORE
24	BHG 156-7 CORE	29	BHG 156-7 RIM
25	BHG 156-7 RIM	30	ABN-4 CORE

GARNET

SIO2	36.41	36.40	37.02	35.54	36.22	36.34	34.75	36.10	36.21	36.21
TIO2	-	-	-	-	-	-	-	-	-	ND
AL2O3	21.90	21.31	21.64	21.69	21.80	21.25	21.09	21.72	21.37	21.23
CR2O3	ND	-	.05	-	-	-	-	-	.04	ND
FEO	32.95	32.91	29.47	29.31	29.54	29.89	29.68	32.42	29.87	31.49
MNO	10.98	6.15	10.27	10.01	9.80	9.34	11.11	6.53	10.72	7.10
MGO	1.58	2.64	1.78	1.89	1.80	2.11	1.59	2.71	1.57	2.45
CAO	.77	1.52	1.55	.73	1.58	1.58	.93	1.54	.93	1.61
NA2O	-	-	-	-	-	-	-	-	-	-
K2O	-	-	-	-	-	-	-	-	-	-
TOTAL	104.61	100.93	101.78	99.17	100.74	100.51	99.15	101.02	100.71	100.13

** ATOMIC PROPORTIONS BASED ON SELECTED NO. OF OXYGENS **

OXYGEN	12	12	12	12	12	12	12	12	12	12
SI	2.882	2.936	2.961	2.921	2.930	2.947	2.888	2.909	2.943	2.941
TI	-	-	-	-	-	-	-	-	-	-
AL	2.043	2.026	2.040	2.101	2.078	2.031	2.066	2.063	2.047	2.033
CR	-	-	.003	-	-	-	-	-	.003	-
FE2+	2.181	2.220	1.971	2.014	1.998	2.027	2.063	2.185	2.030	2.139
MN	.736	.420	.696	.697	.671	.641	.782	.446	.738	.489
MG	.186	.317	.212	.231	.217	.255	.197	.325	.190	.297
CA	.065	.131	.133	.064	.137	.137	.083	.133	.081	.140
NA	-	-	-	-	-	-	-	-	-	-
K	-	-	-	-	-	-	-	-	-	-
SUM	8.096	8.051	8.017	8.029	8.031	8.038	8.079	8.060	8.032	8.041

**** SAMPLE DIRECTORY ****

SAMPLE NO.	DESCRIPTION	SAMPLE NO.	DESCRIPTION
31	ABN-4 RIM	36	ABN-4 CORE
32	ABN-4 CORE	37	ABN-4 RIM
33	ABN-4 RIM	38	ABN-4 CORE
34	ABN-4 CORE	39	ABN-4 RIM
35	ABN-4 RIM	40	ABN-4 CORE

GARNET

SIO2	35.86	35.94	34.85	37.36	37.74	37.44	37.53	37.34	35.86	36.45
TIO2	-	-	-	-	-	ND	-	ND	-	-
AL2O3	21.55	21.23	20.96	21.53	21.79	21.75	21.31	20.63	21.45	21.68
CR2O3	ND	ND	-	-	-	-	-	-	-	-
FEO	29.82	29.83	29.50	30.43	31.84	31.74	32.44	31.96	33.35	32.17
MNO	10.81	8.70	10.51	3.14	1.97	2.00	1.96	1.93	1.98	1.70
MGO	1.71	2.10	1.75	6.05	6.04	5.83	5.52	5.91	5.16	6.37
CAO	1.00	1.70	1.53	1.94	1.68	1.69	1.63	1.69	1.59	1.63
NA2O	-	-	-	-	-	-	-	-	-	-
K2O	-	-	-	-	-	-	-	-	-	-
TOTAL	100.78	99.52	99.10	100.45	101.06	100.47	100.39	99.48	99.39	100.00

** ATOMIC PROPORTIONS BASED ON SELECTED NO. OF OXYGENS **

OXYGEN	12	12	12	12	12	12	12	12	12	12
SI	2.916	2.940	2.893	2.950	2.958	2.954	2.973	2.984	2.896	2.900
TI	-	-	-	-	-	-	-	-	-	-
AL	2.065	2.047	2.051	2.004	2.013	2.023	1.990	1.943	2.042	2.033
CR	-	-	-	-	-	-	-	-	-	-
FE2+	2.028	2.041	2.048	2.009	2.087	2.094	2.149	2.136	2.252	2.141
MN	.745	.603	.739	.210	.131	.134	.132	.131	.135	.115
MG	.207	.256	.216	.712	.706	.685	.652	.704	.621	.755
CA	.087	.149	.136	.164	.141	.143	.138	.145	.138	.139
NA	-	-	-	-	-	-	-	-	-	-
K	-	-	-	-	-	-	-	-	-	-
SUM	8.050	8.036	8.082	8.049	8.036	8.034	8.033	8.043	8.084	8.083

**** SAMPLE DIRECTORY ****

SAMPLE NO.	DESCRIPTION	SAMPLE NO.	DESCRIPTION
41	ABN-4 RIM	46	ABN-6
42	ABN-4 CORE	47	ABN-6
43	ABN-4 RIM	48	ABN-6
44	ABN-6	49	ABN-6
45	ABN-6	50	ABN-6

GARNET

SIO2	37.08	36.88	39.47	39.04	39.25	39.12	38.87	38.75	38.76	38.81
TIO2	ND	-	.04	ND	ND	ND	ND	.04	.04	.04
AL2O3	20.99	21.64	22.09	22.14	22.03	22.06	22.22	22.29	22.16	22.13
CR2O3	ND	-	-	-	ND	-	-	-	-	-
FEO	32.86	31.51	18.10	19.41	18.01	18.12	18.38	18.11	17.98	18.61
MNO	2.17	1.97	9.50	9.49	9.71	9.64	9.50	9.85	9.77	10.03
MGO	5.07	6.43	9.21	8.61	9.28	9.34	9.11	9.11	9.11	8.65
CAO	1.69	1.78	2.10	2.09	2.17	2.13	2.38	2.39	2.42	2.43
NA2O	-	-	-	-	-	-	.03	.02	.02	-
K2O	-	-	-	-	-	-	-	-	-	-
TOTAL	99.90	100.21	100.51	100.81	100.49	100.44	100.52	100.56	100.26	100.70

** ATOMIC PROPORTIONS BASED ON SELECTED NO. OF OXYGENS **

OXYGEN	12	12	12	12	12	12	12	12	12	12
SI	2.966	2.921	3.013	2.991	3.001	2.994	2.978	2.969	2.977	2.978
TI	-	-	.002	-	-	-	-	.002	.002	.002
AL	1.979	2.020	1.987	2.000	1.985	1.990	2.006	2.013	2.006	2.002
CR	-	-	-	-	-	-	-	-	-	-
FE2+	2.198	2.087	1.155	1.244	1.152	1.160	1.178	1.160	1.155	1.194
MN	.147	.132	.614	.616	.629	.625	.616	.639	.636	.652
MG	.604	.759	1.048	.983	1.057	1.065	1.040	1.040	1.043	.989
CA	.145	.151	.172	.172	.178	.175	.195	.196	.199	.200
NA	-	-	-	-	-	-	.004	.003	.003	-
K	-	-	-	-	-	-	-	-	-	-
SUM	8.042	8.069	7.991	8.007	8.005	8.010	8.020	8.024	8.020	8.018

**** SAMPLE DIRECTORY ****

SAMPLE NO.	DESCRIPTION	SAMPLE NO.	DESCRIPTION
51	ABN-6	56	JE-2
52	ABN-6	57	JE-3
53	JE-2	58	JE-3
54	JE-2	59	JE-3
55	JE-2	60	JE-3

GARNET

SIO2	38.46	38.19	37.37	37.74	36.56	36.89	36.96	37.01	37.30	37.14
TIO2	.04	ND	ND.	ND	.08	.05	.07	.09	.13	.14
AL2O3	21.86	21.69	20.94	21.22	21.46	21.20	21.44	21.53	21.20	20.82
CR2O3	-	-	.04	ND	-	-	-	-	ND	-
FEO	19.99	20.05	19.41	20.68	17.21	16.79	17.18	17.26	8.72	8.46
MNO	10.80	10.67	13.55	14.13	18.74	18.94	18.72	18.78	22.80	23.26
MGO	7.29	7.27	5.58	4.55	3.02	3.05	2.95	3.18	4.00	4.00
CAO	2.14	1.87	1.89	1.97	3.78	3.75	3.71	3.80	4.98	4.97
NA2O	.02	-	-	-	-	-	-	-	-	.02
K2O	-	-	-	-	-	-	-	-	-	-
TOTAL	100.60	99.76	98.80	100.35	100.85	100.67	101.03	101.65	99.15	98.81

** ATOMIC PROPORTIONS BASED ON SELECTED NO. OF OXYGENS **

OXYGEN	12	12	12	12	12	12	12	12	12	12
SI	2.984	2.987	2.992	2.995	2.925	2.951	2.946	2.934	2.980	2.983
TI	.002	-	-	-	.005	.003	.004	.005	.008	.008
AL	1.999	2.000	1.976	1.985	2.024	1.999	2.015	2.012	1.996	1.971
CR	-	-	.003	-	-	-	-	-	-	-
FE2+	1.297	1.312	1.300	1.372	1.151	1.123	1.145	1.144	.583	.568
MN	.710	.707	.919	.950	1.270	1.284	1.264	1.261	1.543	1.583
MG	.843	.848	.666	.538	.360	.364	.350	.376	.476	.479
CA	.178	.157	.162	.167	.324	.321	.317	.323	.426	.428
NA	.003	-	-	-	-	-	-	-	-	.003
K	-	-	-	-	-	-	-	-	-	-
SUM	8.016	8.011	8.018	8.010	8.059	8.046	8.042	8.055	8.013	8.024

**** SAMPLE DIRECTORY ****

SAMPLE NO.	DESCRIPTION	SAMPLE NO.	DESCRIPTION
61	JE-3	66	JE-10
62	JE-3	67	JE-10
63	JE-7	68	JE-10
64	JE-7	69	JE-14
65	JE-10	70	JE-14

GARNET

SIO2	37.27	39.15	37.14	37.27	39.15	38.96	38.47	37.75	38.95	39.00
TIO2	.14	.13	.14	.14	.06	ND	.04	.06	.05	.07
AL2O3	21.06	21.20	20.82	21.06	22.78	22.77	22.23	22.07	21.91	22.02
CR2O3	-	ND	-	-	-	-	-	-	ND	-
FEO	8.60	8.72	8.46	8.60	15.95	15.97	15.56	15.42	12.69	12.62
MNO	22.75	22.80	23.26	22.75	10.85	10.84	11.92	12.77	15.22	15.67
MGO	4.23	4.01	4.00	4.23	9.79	9.68	9.21	8.62	8.96	8.87
CAO	4.99	4.98	4.97	4.99	2.16	2.18	2.20	2.25	2.09	2.16
NA2O	-	-	.02	-	-	-	-	-	-	-
K2O	-	-	-	-	-	-	-	-	-	-
TOTAL	99.04	101.01	98.81	99.04	100.74	100.42	99.63	98.94	99.89	100.41

** ATOMIC PROPORTIONS BASED ON SELECTED NO. OF OXYGENS **

OXYGEN	12	12	12	12	12	12	12	12	12	12
SI	2.980	3.052	2.983	2.980	2.972	2.968	2.969	2.950	2.999	2.992
TI	.008	.008	.008	.008	.003	-	.002	.004	.003	.004
AL	1.985	1.948	1.971	1.985	2.038	2.045	2.022	2.033	1.989	1.991
CR	-	-	-	-	-	-	-	-	-	-
FE2+	.575	.569	.568	.575	1.012	1.018	1.004	1.008	.817	.810
MN	1.541	1.506	1.583	1.541	.698	.700	.779	.845	.993	1.018
MG	.504	.466	.479	.504	1.107	1.099	1.059	1.004	1.028	1.014
CA	.427	.416	.428	.427	.176	.178	.182	.188	.172	.178
NA	-	-	.003	-	-	-	-	-	-	-
K	-	-	-	-	-	-	-	-	-	-
SUM	8.020	7.965	8.024	8.020	8.006	8.008	8.018	8.031	8.003	8.008

**** SAMPLE DIRECTORY ****

SAMPLE NO.	DESCRIPTION	SAMPLE NO.	DESCRIPTION
71	JE-14	76	JE-18
72	JE-18	77	JE-19
73	JE-18	78	JE-19
74	JE-18	79	JE-20
75	JE-18	80	JE-20

GARNET

SIO2	38.78	38.87	37.66	37.62	37.91	38.34	36.88	37.16	37.67	37.68
TIO2	.05	.07	.05	-	-	-	-	-	-	-
AL2O3	22.09	21.98	22.26	22.09	22.49	22.33	21.46	21.66	21.85	22.05
CR2O3	-	-	-	.07	-	-	-	-	-	-
FEO	12.83	12.57	27.95	28.38	27.74	27.53	30.58	29.85	29.04	29.94
MNO	15.59	15.51	2.28	2.24	2.25	2.31	3.49	3.25	3.01	3.05
MGO	8.88	8.94	8.38	7.95	8.81	8.38	5.38	6.00	7.06	6.23
CAO	2.14	2.12	1.57	1.65	1.63	1.72	1.60	1.61	1.61	1.63
NA2O	.02	-	-	-	-	-	-	-	-	-
K2O	-	-	-	-	-	-	-	-	-	-
TOTAL	100.38	100.06	100.15	100.00	100.83	100.61	99.39	99.53	100.24	100.58

** ATOMIC PROPORTIONS BASED ON SELECTED NO. OF OXYGENS **

OXYGEN	12	12	12	12	12	12	12	12	12	12
SI	2.980	2.991	2.930	2.939	2.924	2.959	2.951	2.953	2.953	2.955
TI	.003	.004	.003	-	-	-	-	-	-	-
AL	2.001	1.994	2.041	2.034	2.045	2.032	2.024	2.029	2.019	2.038
CR	-	-	-	.004	-	-	-	-	-	-
FE2+	.824	.809	1.819	1.854	1.790	1.777	2.046	1.984	1.904	1.964
MN	1.015	1.011	.150	.148	.147	.151	.237	.219	.200	.203
MG	1.017	1.025	.972	.925	1.013	.964	.642	.711	.825	.728
CA	.176	.175	.131	.138	.135	.142	.137	.137	.135	.137
NA	.003	-	-	-	-	-	-	-	-	-
K	-	-	-	-	-	-	-	-	-	-
SUM	8.019	8.008	8.046	8.042	8.053	8.025	8.037	8.032	8.037	8.025

**** SAMPLE DIRECTORY ****

SAMPLE NO.	DESCRIPTION	SAMPLE NO.	DESCRIPTION
81	JE-20	86	JE-29 RIM
82	JE-20	87	JE-31 CORE
83	JE-29	88	JE-31 RIM
84	JE-29	89	JE-31
85	JE-29 CORE	90	JE-31

GARNET

SIO2	37.78	37.14	37.48	37.54	36.66	37.04	38.46	38.53	38.10	37.28
TIO2	-	-	-	-	-	-	ND	ND	.12	.05
AL2O3	22.13	22.32	22.17	22.20	21.76	21.84	21.92	22.02	21.67	21.62
CR2O3	-	-	-	-	-	-	ND	-	.05	.04
FEO	29.60	30.84	30.54	30.80	30.88	30.60	14.50	14.48	14.43	18.74
MNO	4.34	5.23	5.07	5.34	5.00	5.13	14.15	14.50	15.66	17.50
MGO	6.60	5.31	5.78	5.10	5.21	5.17	8.15	8.19	7.02	3.36
CAO	.70	.71	.61	.59	.62	.67	2.57	2.64	2.86	2.29
NA2O	-	-	-	-	-	-	-	-	-	-
K2O	-	-	-	-	-	-	-	-	-	-
TOTAL	101.15	101.55	101.65	101.57	100.13	100.45	99.80	100.38	99.91	100.88

** ATOMIC PROPORTIONS BASED ON SELECTED NO. OF OXYGENS **

OXYGEN	12	12	12	12	12	12	12	12	12	12
SI	2.950	2.920	2.935	2.947	2.927	2.943	2.982	2.974	2.976	2.965
TI	-	-	-	-	-	-	-	-	.007	.003
AL	2.036	2.068	2.046	2.054	2.048	2.045	2.003	2.004	1.995	2.027
CR	-	-	-	-	-	-	-	-	.003	.003
FE2+	1.933	2.028	2.000	2.022	2.062	2.033	.940	.935	.943	1.247
MN	.287	.348	.336	.355	.338	.345	.929	.948	1.036	1.179
MG	.768	.622	.674	.597	.620	.612	.942	.942	.817	.398
CA	.059	.060	.051	.050	.053	.057	.214	.218	.239	.195
NA	-	-	-	-	-	-	-	-	-	-
K	-	-	-	-	-	-	-	-	-	-
SUM	8.032	8.046	8.042	8.026	8.049	8.035	8.014	8.023	8.017	8.017

**** SAMPLE DIRECTORY ****

SAMPLE NO.	DESCRIPTION	SAMPLE NO.	DESCRIPTION
91	JE-32 CORE	96	JE-32 RIM
92	JE-32 RIM	97	JE-35
93	JE-32 CORE	98	JE-35
94	JE-32 RIM	99	JE-35
95	JE-32 CORE	100	JE-36

GARNET

SIO2	37.55	37.79	37.45	37.50	37.15	37.01	38.05	37.94	37.76	38.04
TIO2	.05	.08	.11	.06	.09	.06	-	-	-	-
AL2O3	20.73	20.87	20.63	21.00	20.55	20.63	21.70	21.61	21.57	21.62
CR2O3	ND	-	ND	ND	ND	.04	-	-	-	-
FEO	18.38	18.01	17.71	18.07	17.79	17.94	15.70	16.57	16.79	16.98
MNO	17.39	17.18	17.42	17.33	17.12	17.06	14.04	11.70	11.70	11.53
MGO	3.19	3.59	3.69	3.74	3.64	3.56	8.56	9.07	9.20	9.22
CAO	2.36	2.31	2.42	2.36	2.31	2.33	1.58	1.86	1.78	1.80
NA2O	-	-	-	-	.02	-	-	-	-	-
K2O	-	-	-	-	-	-	-	-	-	-
TOTAL	99.68	99.83	99.46	100.09	98.70	98.63	99.63	98.75	98.80	99.19

** ATOMIC PROPORTIONS BASED ON SELECTED NO. OF OXYGENS **

OXYGEN	12	12	12	12	12	12	12	12	12	12
SI	3.019	3.022	3.011	2.997	3.010	3.003	2.966	2.969	2.957	2.965
TI	.003	.005	.007	.004	.005	.004	-	-	-	-
AL	1.965	1.967	1.955	1.978	1.963	1.973	1.994	1.993	1.991	1.986
CR	-	-	-	-	-	.003	-	-	-	-
FE2+	1.236	1.205	1.191	1.208	1.206	1.217	1.024	1.084	1.100	1.107
MN	1.184	1.164	1.187	1.173	1.175	1.173	.927	.775	.776	.761
MG	.382	.428	.442	.445	.440	.431	.994	1.058	1.074	1.071
CA	.203	.198	.209	.202	.201	.203	.132	.156	.149	.150
NA	-	-	-	-	.003	-	-	-	-	-
K	-	-	-	-	-	-	-	-	-	-
SUM	7.995	7.989	8.003	8.009	8.004	8.005	8.037	8.035	8.047	8.041

**** SAMPLE DIRECTORY ****

SAMPLE NO.	DESCRIPTION	SAMPLE NO.	DESCRIPTION
101	JE-36	106	JE-36
102	JE-36	107	JE-74
103	JE-36	108	JE-82 CORE
104	JE-36	109	JE-82 RIM
105	JE-36	110	JE-82 CORE

GARNET

SIO2	37.96	37.57	37.81
TIO2	.05	.06	.05
AL2O3	21.58	21.87	22.09
CR2O3	-	-	-
FEO	16.55	18.74	18.00
MNO	11.51	10.03	9.01
MGO	9.19	8.49	9.61
CAO	1.85	2.03	2.16
NA2O	-	-	-
K2O	-	-	-
TOTAL	98.69	98.79	98.73

** ATOMIC PROPORTIONS BASED ON SELECTED NO. OF OXYGENS **

OXYGEN	12	12	12
SI	2.969	2.949	2.945
TI	.003	.004	.003
AL	1.990	2.023	2.028
CR	-	-	-
FE2+	1.083	1.230	1.172
MN	.763	.667	.594
MG	1.071	.993	1.115
CA	.155	.171	.180
NA	-	-	-
K	-	-	-
SUM	8.033	8.036	8.038

**** SAMPLE DIRECTORY ****

SAMPLE NO.	DESCRIPTION	SAMPLE NO.	DESCRIPTION
111	JE-82 RIM		
112	OF-7		
113	OF-7		

TOURMALINE

SIO2	34.55	34.20	35.11	35.19	35.22	35.66	35.14	35.03	34.69	34.35
TIO2	.82	.86	.63	.41	.75	.46	.73	.74	.75	.73
AL2O3	33.35	34.69	34.03	34.20	33.78	33.59	34.34	34.93	35.10	35.11
CR2O3	ND	-	.06	.06	-	.04	.05	.05	ND	-
FE2O3	-	-	-	-	-	-	-	-	-	-
FEO	10.30	9.05	8.25	7.84	10.24	10.02	6.36	5.89	6.28	6.23
MNO	.19	.27	.22	.18	.24	.21	.05	ND	.09	ND
MGO	4.16	4.54	5.44	5.89	4.34	4.67	6.57	6.75	6.42	6.82
CAO	.51	1.04	.80	.79	.49	.51	.72	.79	.50	1.03
NA2O	1.47	1.29	1.77	1.71	1.77	1.67	1.82	1.68	2.03	1.72
K2O	.14	.19	.07	.06	.11	ND	.05	.13	.04	.07
TOTAL	85.51	86.13	86.38	86.33	86.94	86.86	85.83	86.01	85.92	86.08

** ATOMIC PROPORTIONS BASED ON SELECTED NO. OF OXYGENS **

OXYGEN	31	31	31	31	31	31	31	31	31	31
SI	7.318	7.160	7.294	7.294	7.336	7.412	7.268	7.213	7.169	7.095
TI	.131	.135	.098	.064	.117	.072	.114	.115	.117	.113
AL	8.326	8.560	8.333	8.355	8.293	8.229	8.372	8.478	8.549	8.548
CR	-	-	.010	.010	-	.007	.008	.008	-	-
FE3+	-	-	-	-	-	-	-	-	-	-
FE2+	1.825	1.585	1.433	1.359	1.784	1.742	1.100	1.014	1.085	1.076
MN	.034	.048	.039	.032	.042	.037	.009	-	.016	-
MG	1.313	1.416	1.684	1.819	1.347	1.447	2.025	2.071	1.977	2.099
CA	.116	.233	.178	.175	.109	.114	.160	.174	.111	.228
NA	.604	.524	.713	.687	.715	.673	.730	.671	.813	.689
K	.038	.051	.019	.016	.029	-	.013	.034	.011	.018
SUM	19.707	19.712	19.802	19.811	19.773	19.739	19.799	19.782	19.851	19.871

**** SAMPLE DIRECTORY ****

SAMPLE NO.	DESCRIPTION	SAMPLE NO.	DESCRIPTION
1	BH LO-1	6	BH LO-1
2	BH LO-1	7	ABN-7
3	BH LO-1	8	ABN-7
4	BH LO-1 CORE	9	ABN-7 CORE
5	BH LO-1 RIM	10	ABN-7 RIM

TOURMALINE

SIO2	34.69	34.51	34.70	34.45	34.50	34.61	34.74	34.17	34.76	34.35
TIO2	.78	.74	.79	.77	.74	.73	.67	.81	.78	.77
AL2O3	35.05	34.95	34.74	35.12	35.44	35.33	35.17	35.15	35.31	35.15
CR2O3	.06	-	ND	-	ND	-	ND	.06	.04	ND
FE2O3	-	-	-	-	-	-	-	-	-	-
FEO	5.98	6.19	6.01	6.15	5.94	6.33	6.18	6.20	6.03	6.36
MNO	.04	ND	ND	ND	-	-	ND	.05	ND	ND
MGO	6.75	6.79	6.76	6.88	6.73	6.98	6.87	6.85	6.87	6.89
CAO	.97	1.06	.83	1.12	.78	1.20	.80	1.13	.90	1.21
NA2O	1.69	1.72	1.80	1.73	1.77	1.71	1.84	1.69	1.77	1.71
K2O	.10	.09	.12	.10	.06	.07	ND	.07	.10	.07
TOTAL	86.11	86.07	85.80	86.34	85.99	86.96	86.34	86.18	86.59	86.55

** ATOMIC PROPORTIONS BASED ON SELECTED NO. OF OXYGENS **

OXYGEN	31	31	31	31	31	31	31	31	31	31
SI	7.149	7.127	7.177	7.096	7.111	7.083	7.143	7.057	7.126	7.069
TI	.121	.115	.123	.119	.115	.112	.104	.126	.120	.119
AL	8.514	8.508	8.470	8.526	8.610	8.523	8.523	8.556	8.532	8.527
CR	.010	-	-	-	-	-	-	.010	.006	-
FE3+	-	-	-	-	-	-	-	-	-	-
FE2+	1.031	1.069	1.040	1.059	1.024	1.083	1.063	1.071	1.034	1.095
MN	.007	-	-	-	-	-	-	.009	-	-
MG	2.073	2.090	2.084	2.112	2.067	2.129	2.105	2.108	2.099	2.113
CA	.214	.235	.184	.247	.172	.263	.176	.250	.198	.267
NA	.675	.689	.722	.691	.707	.679	.734	.677	.704	.682
K	.026	.024	.032	.026	.016	.018	-	.018	.026	.018
SUM	19.819	19.860	19.839	19.880	19.828	19.891	19.861	19.882	19.850	19.897

**** SAMPLE DIRECTORY ****

SAMPLE NO.	DESCRIPTION	SAMPLE NO.	DESCRIPTION
11	ABN-7 CORE	16	ABN-7 RIM
12	ABN-7 RIM	17	ABN-7 CORE
13	ABN-7 CORE	18	ABN-7 RIM
14	ABN-7 RIM	19	ABN-7 CORE
15	ABN-7	20	ABN-7 RIM

EPIDOTE

SIO2	37.35	37.54	37.30	39.56	36.78	37.22	32.33	37.27	36.17
TIO2	.07	-	-	-	-	-	-	-	-
AL2O3	25.37	24.76	24.51	26.09	22.82	23.85	19.02	24.88	21.79
CR2O3	-	-	-	-	-	-	-	-	-
FE2O3	12.20	12.57	12.97	11.20	11.17	11.14	3.64	10.81	8.06
FEO	-	-	-	-	-	-	-	-	-
MNO	1.39	.62	.31	.76	3.35	2.12	11.18	.93	7.96
MGO	ND	-	-	-	.33	.07	-	.13	.05
CAO	22.29	23.52	23.14	22.20	22.52	22.61	19.56	23.37	21.71
NA2O	-	-	-	-	-	-	-	-	-
K2O	-	-	-	-	-	-	-	-	-
TOTAL	98.69	99.01	98.23	99.81	96.97	97.01	85.73	97.39	95.74

** ATOMIC PROPORTIONS BASED ON SELECTED NO. OF OXYGENS **

OXYGEN	12	12	12	12	12	12	12	12	12
SI	2.827	2.837	2.840	2.925	2.866	2.876	2.921	2.853	2.893
TI	.004	-	-	-	-	-	-	-	-
AL	2.264	2.206	2.199	2.273	2.096	2.172	2.025	2.245	2.054
CR	-	-	-	-	-	-	-	-	-
FE3+	.695	.715	.743	.623	.655	.648	.247	.623	.485
FE2+	-	-	-	-	-	-	-	-	-
MN	.089	.040	.020	.048	.221	.139	.856	.060	.539
MG	-	-	-	-	.038	.008	-	.015	.006
CA	1.808	1.905	1.888	1.759	1.881	1.872	1.893	1.917	1.860
NA	-	-	-	-	-	-	-	-	-
K	-	-	-	-	-	-	-	-	-
SUM	7.689	7.702	7.689	7.627	7.758	7.714	7.943	7.713	7.838

**** SAMPLE DIRECTORY ****

SAMPLE NO.	DESCRIPTION	SAMPLE NO.	DESCRIPTION
1	JE-16	6	JE-7
2	JE-16	7	JE-7
3	JE-16	8	JE-7
4	JE-16	9	JE-7
5	JE-7		

EPIDOTE

SIO2	37.35	37.54	37.30	39.56	36.78	37.22	32.33	37.27	36.17
TIO2	.07	-	-	-	-	-	-	-	-
AL2O3	25.37	24.76	24.51	26.09	22.82	23.85	19.02	24.88	21.79
CR2O3	-	-	-	-	-	-	-	-	-
FE2O3	12.20	12.57	12.97	11.20	11.17	11.14	3.64	10.81	8.06
FEO	-	-	-	-	-	-	-	-	-
MNO	1.39	.62	.31	.76	3.35	2.12	11.18	.93	7.96
MGO	ND	-	-	-	.33	.07	-	.13	.05
CAO	22.29	23.52	23.14	22.20	22.52	22.61	19.56	23.37	21.71
NA2O	-	-	-	-	-	-	-	-	-
K2O	-	-	-	-	-	-	-	-	-
TOTAL	98.69	99.01	98.23	99.81	96.97	97.01	85.73	97.39	95.74

** ATOMIC PROPORTIONS BASED ON SELECTED NO. OF OXYGENS **

OXYGEN	12	12	12	12	12	12	12	12	12
SI	2.827	2.837	2.840	2.925	2.866	2.876	2.921	2.853	2.893
TI	.004	-	-	-	-	-	-	-	-
AL	2.264	2.206	2.199	2.273	2.096	2.172	2.025	2.245	2.054
CR	-	-	-	-	-	-	-	-	-
FE3+	.695	.715	.743	.623	.655	.648	.247	.623	.485
FE2+	-	-	-	-	-	-	-	-	-
MN	.089	.040	.020	.048	.221	.139	.856	.060	.539
MG	-	-	-	-	.038	.008	-	.015	.006
CA	1.808	1.905	1.888	1.759	1.881	1.872	1.893	1.917	1.860
NA	-	-	-	-	-	-	-	-	-
K	-	-	-	-	-	-	-	-	-
SUM	7.689	7.702	7.689	7.627	7.758	7.714	7.943	7.713	7.838

CA .01	CA .01	CA .01	CA .01	CA .01	CA .01	CA .01	CA .01	CA .01
MG 50.00	MG 50.00	MG 50.00	MG 50.00	MG .00	MG .00	MG 50.00	MG .00	MG .00
FE 50.00	FE 50.00	FE 50.00	FE 50.00	FE 99.99	FE 99.99	FE 50.00	FE 99.99	FE 99.99
M: 50.00	M: 50.00	M: 50.00	M: 50.00	M: .00	M: .00	M: 50.00	M: .00	M: .00

**** SAMPLE DIRECTORY ****

SAMPLE NO.	DESCRIPTION	SAMPLE NO.	DESCRIPTION
1	JE-16	6	JE-7
2	JE-16	7	JE-7
3	JE-16	8	JE-7
4	JE-16	9	JE-7
5	JE-7		

AMPHIBOLE

SIO2	53.25	53.35	53.60	53.56	53.29	50.98	45.08	44.02	43.72	42.54
TIO2	-	.26	-	-	-	.04	.14	.11	.18	.29
AL2O3	.12	-	.17	.18	.24	4.14	13.09	13.03	15.42	16.08
CR2O3	ND	-	-	-	-	-	-	ND	-	-
FEO	14.07	13.88	13.35	14.45	14.09	24.41	25.43	25.89	23.80	23.73
MNO	16.04	15.66	16.27	16.04	14.53	.30	.27	.28	.58	.53
MGO	14.06	14.43	14.43	13.90	15.19	18.03	13.84	13.32	13.34	13.33
CAO	.13	.26	.18	.19	.27	.07	.12	.12	.51	.52
NA2O	.06	.14	.08	.12	.13	.26	1.09	.98	1.71	1.74
K2O	-	-	-	-	-	-	-	-	-	ND
TOTAL	97.75	97.98	98.08	98.44	97.74	98.23	99.06	97.77	99.26	98.78

** ATOMIC PROPORTIONS BASED ON SELECTED NO. OF OXYGENS **

OXYGEN	24	24	24	24	24	24	24	24	24	24
SI	8.340	8.321	8.341	8.339	8.297	7.783	6.899	6.856	6.664	6.529
TI	-	.030	-	-	-	.005	.016	.013	.021	.033
AL	.022	-	.031	.033	.044	.745	2.361	2.392	2.770	2.909
CR	-	-	-	-	-	-	-	-	-	-
FE2+	1.843	1.810	1.737	1.882	1.835	3.117	3.255	3.373	3.034	3.046
MN	2.128	2.069	2.145	2.115	1.916	.039	.035	.037	.075	.069
MG	3.282	3.354	3.347	3.225	3.525	4.102	3.157	3.092	3.030	3.049
CA	.022	.043	.030	.032	.045	.011	.020	.020	.083	.086
NA	.018	.042	.024	.036	.039	.077	.323	.296	.505	.518
K	-	-	-	-	-	-	-	-	-	-
SUM	15.657	15.670	15.655	15.662	15.701	15.879	16.066	16.081	16.183	16.243

**** SAMPLE DIRECTORY ****

SAMPLE NO.	DESCRIPTION	SAMPLE NO.	DESCRIPTION
1	BH-3	6	240 AG 56
2	BH-3	7	240 AG 56
3	BH-3	8	240 AG 56
4	BH-3	9	ABN-6
5	BH-3	10	ABN-6

AMPHIBOLE

SIO2	43.39	41.05	41.92	42.39
TIO2	.30	1.64	1.39	.53
AL2O3	15.59	15.91	15.81	19.02
CR2O3	-	-	-	.09
FEO	24.04	9.50	9.59	14.59
MNO	.49	.73	.70	.17
MGO	12.98	14.56	15.03	18.49
CAO	.56	11.22	11.22	.62
NA2O	1.80	2.17	2.15	2.08
K2O	-	.67	.60	ND
ZNO	.09	-	-	-
TOTAL	99.24	97.45	98.41	98.00

** ATOMIC PROPORTIONS BASED ON SELECTED NO. OF OXYGENS **

OXYGEN	24	24	24	24
SI	6.630	6.255	6.312	6.284
TI	.034	.188	.157	.059
AL	2.808	2.857	2.806	3.323
CR	-	-	-	.011
FE2+	3.072	1.211	1.208	1.809
MN	.063	.094	.089	.021
MG	2.956	3.306	3.373	4.085
CA	.092	1.832	1.810	.098
NA	.533	.641	.628	.598
K	-	.130	.115	-
ZN	.010	-	-	-
SUM	16.198	16.514	16.499	16.291

**** SAMPLE DIRECTORY ****

SAMPLE NO.	DESCRIPTION	SAMPLE NO.	DESCRIPTION
11	ABM-16		
12	JE-A		
13	JE-A		
14	JE-G		

PYROXENE

SIO2	46.89	46.16	47.17	52.47	52.81	51.79	50.58	50.20
TIO2	-	-	-	.14	.10	.11	.08	.10
AL2O3	-	-	-	5.87	5.22	5.68	7.53	8.44
CR2O3	-	-	-	-	-	-	-	ND
FEO	8.30	8.75	10.29	15.26	15.07	15.11	17.61	18.08
MNO	43.07	43.23	38.85	1.54	1.69	1.61	.16	.15
MGO	1.19	.46	3.13	26.37	26.86	25.92	25.13	24.61
CAO	.15	.98	.29	.27	.24	.21	.08	.12
NA2O	-	-	.03	-	-	-	-	-
K2O	-	-	-	-	-	-	-	-
TOTAL	99.60	99.58	99.76	101.92	101.99	100.43	101.17	101.73

** ATOMIC PROPORTIONS BASED ON SELECTED NO. OF OXYGENS **

OXYGEN	6	6	6	6	6	6	6	6
SI	2.022	2.007	2.009	1.861	1.871	1.865	1.817	1.798
TI	-	-	-	.004	.003	.003	.002	.003
AL	-	-	-	.245	.218	.241	.319	.356
CR	-	-	-	-	-	-	-	-
FE2+	.299	.318	.367	.453	.447	.455	.529	.541
MN	1.573	1.592	1.402	.046	.051	.049	.005	.005
MG	.076	.030	.199	1.394	1.418	1.391	1.346	1.313
CA	.007	.046	.013	.010	.009	.008	.003	.005
NA	-	-	.002	-	-	-	-	-
K	-	-	-	-	-	-	-	-
SUM	3.978	3.993	3.992	4.013	4.017	4.012	4.021	4.021

**** SAMPLE DIRECTORY ****

SAMPLE NO.	DESCRIPTION	SAMPLE NO.	DESCRIPTION
1	BH-1	6	JE-A
2	BH-1	7	JE-G
3	BH-1	8	JE-G
4	JE-A		
5	JE-A		

OXIDES

SIO2	-	-	-	-	-	-	-	-	-	-
TIO2	.17	.13	.15	.11	.13	.11	.07	ND	ND	.06
AL2O3	.51	.34	.35	.33	.38	.28	.32	.08	.19	.13
CR2O3	-	-	-	-	-	-	-	-	-	ND
FE2O3	71.29	71.42	70.96	70.59	71.44	71.01	71.68	71.97	71.63	71.81
FEO	32.23	32.30	32.11	31.81	32.25	32.03	32.22	30.67	30.51	30.71
MNO	.45	.30	.33	.34	.39	.24	.34	1.78	1.79	1.72
MGO	ND	-	-	ND	-	.04	ND	-	.05	.04
CAO	-	-	-	-	-	-	-	-	-	-
NA2O	-	-	-	-	-	-	-	-	-	-
K2O	-	-	-	-	-	-	-	-	-	-
TOTAL	104.69	104.49	103.90	103.20	104.59	103.71	104.65	104.52	104.20	104.50

** ATOMIC PROPORTIONS BASED ON SELECTED NO. OF OXYGENS **

OXYGEN	4	4	4	4	4	4	4	4	4	4
SI	-	-	-	-	-	-	-	-	-	-
TI	.005	.004	.004	.003	.004	.003	.002	-	-	.002
AL	.022	.015	.015	.014	.016	.012	.014	.003	.008	.006
CR	-	-	-	-	-	-	-	-	-	-
FE3+	1.969	1.978	1.976	1.979	1.976	1.982	1.982	1.995	1.990	1.990
FE2+	.989	.994	.994	.991	.991	.993	.990	.945	.942	.946
MN	.014	.009	.010	.011	.012	.008	.011	.056	.056	.054
MG	-	-	-	-	-	.002	-	-	.003	.002
CA	-	-	-	-	-	-	-	-	-	-
NA	-	-	-	-	-	-	-	-	-	-
K	-	-	-	-	-	-	-	-	-	-
SUM	3.000	3.000	3.000	3.000	3.000	3.000	3.000	3.000	3.000	3.000

**** SAMPLE DIRECTORY ****

SAMPLE NO.	DESCRIPTION	SAMPLE NO.	DESCRIPTION
1	BH WE-2	6	BH WE-1
2	BH WE-2	7	BH WE-1
3	BH WE-2	8	BH-1
4	BH WE-1	9	BH-1
5	BH WE-1	10	BH-1

OXIDES

SIO2	-	-	-	-	-	-	-	-	-	-
TIO2	.21	.25	.13	.16	.15	.14	53.16	53.44	.09	50.93
AL2O3	.20	.83	.42	.34	.49	.23	-	-	-	-
CR2O3	-	-	-	ND	ND	.18	ND	-	.13	.05
FE2O3	69.58	68.58	69.42	69.15	69.64	70.11	-	-	60.31	.75
FEO	29.48	31.38	31.41	31.36	31.61	32.04	44.63	44.75	26.95	44.84
MNO	2.26	.45	.31	.24	.30	-	2.19	2.18	.09	.86
MGO	ND	ND	ND	ND	ND	-	ND	-	.06	.05
CAO	-	-	-	-	-	-	-	-	-	-
NA2O	-	-	-	-	-	-	-	-	-	-
K2O	-	-	-	-	-	-	-	-	-	-
ZNO		-	-	-	-	-	-	-	.24	-
TOTAL	101.75	101.51	101.72	101.31	102.23	102.71	100.02	100.37	87.86	97.47

** ATOMIC PROPORTIONS BASED ON SELECTED NO. OF OXYGENS **

OXYGEN	4	4	4	4	4	4	3	3	4	3
SI	-	-	-	-	-	-	-	-	-	-
TI	.006	.007	.004	.005	.004	.004	1.006	1.008	.003	.992
AL	.009	.037	.019	.015	.022	.010	-	-	-	-
CR	-	-	-	-	-	.005	-	-	.005	.001
FE3+	1.979	1.949	1.974	1.975	1.969	1.977	-	-	1.990	.015
FE2+	.932	.991	.993	.995	.994	1.004	.939	.938	.988	.971
MN	.072	.014	.010	.008	.010	-	.047	.046	.003	.019
MG	-	-	-	-	-	-	-	-	.004	.002
CA	-	-	-	-	-	-	-	-	-	-
NA	-	-	-	-	-	-	-	-	-	-
K	-	-	-	-	-	-	-	-	-	-
ZN	-	-	-	-	-	-	-	-	.008	-
SUM	3.000	3.000	3.000	3.000	3.000	3.000	1.994	1.992	3.000	2.000

**** SAMPLE DIRECTORY ****

SAMPLE NO.	DESCRIPTION	SAMPLE NO.	DESCRIPTION
11	BH-3	16	240 AG 56
12	BHG-302	17	ABN-1
13	BHG-302	18	ABN-1
14	BHG-302	19	ABN-3
15	BHG-302	20	ABN-5

OXIDES

SIO2	-	-	-	-	-	-	-	-	-	-
TIO2	48.59	50.13	48.06	52.69	.05	.06	49.43	51.21	-	.15
AL2O3	-	-	-	-	2.44	4.95	ND	-	-	.45
CR2O3	ND	.07	.10	-	.06	.06	-	.04	.75	ND
FE2O3	4.98	4.16	8.66	.15	56.39	51.57	.79	-	69.71	69.86
FEO	42.02	43.90	42.57	43.59	25.89	26.08	44.33	43.91	31.72	31.73
MNO	.98	.67	.54	2.71	.05	ND	.08	.12	-	ND
MGO	.38	.04	ND	.59	.19	.07	ND	-	-	.16
CAO	-	.03	.04	-	.60	.28	-	-	-	-
NA2O	-	-	-	-	-	-	-	-	-	-
K2O	-	-	-	-	-	-	-	-	-	-
ZNO	-	.44	-	-	.18	.27	-	-	-	-
TOTAL	96.98	99.45	100.00	99.72	85.85	83.36	94.68	95.28	102.18	102.40

** ATOMIC PROPORTIONS BASED ON SELECTED NO. OF OXYGENS **

OXYGEN	3	3	3	3	4	4	3	3	4	4
SI	-	-	-	-	-	-	-	-	-	-
TI	.951	.959	.916	.999	.002	.002	.992	1.014	-	.004
AL	-	-	-	-	.127	.261	-	-	-	.020
CR	-	.001	.002	-	.002	.002	-	.001	.022	-
FE3+	.098	.080	.165	.003	1.868	1.733	.016	-	1.978	1.971
FE2+	.915	.934	.903	.919	.953	.974	.989	.967	1.000	.995
MN	.022	.014	.012	.058	.002	-	.002	.003	-	-
MG	.015	.002	-	.022	.012	.005	-	-	-	.009
CA	-	.001	.001	-	.028	.013	-	-	-	-
NA	-	-	-	-	-	-	-	-	-	-
K	-	-	-	-	-	-	-	-	-	-
ZN	-	.008	-	-	.006	.009	-	-	-	-
SUM	2.000	2.000	2.000	2.000	3.000	3.000	2.000	1.985	3.000	3.000

**** SAMPLE DIRECTORY ****

SAMPLE NO.	DESCRIPTION	SAMPLE NO.	DESCRIPTION
21	ABN-5	26	ABN-16
22	ABN-6	27	JE-19
23	ABN-6	28	JE-19
24	ABN-13	29	JE-29
25	ABN-16	30	JE-A

OXIDES

SIO2	-	-	-	-	-
TIO2	.09	48.92	47.87	11.08	12.63
AL2O3	.35	-	-	.49	.14
CR2O3	.12	.04	ND	.48	.17
FE2O3	69.96	8.78	10.31	46.16	42.96
FEO	31.80	36.25	35.11	38.93	42.06
MNO	.08	6.29	7.64	ND	-
MGO	ND	.72	.11	1.30	.09
CAO	-	.07	-	-	-
NA2O	-	-	-	-	-
K2O	-	-	-	-	-
TOTAL	102.43	101.07	101.07	98.47	98.04

** ATOMIC PROPORTIONS BASED ON SELECTED NO. OF OXYGENS **

OXYGEN	4	3	3	4	4
SI	-	-	-	-	-
TI	.003	.917	.902	.318	.368
AL	.015	-	-	.022	.006
CR	.004	.001	-	.014	.005
FE3+	1.976	.165	.194	1.327	1.252
FE2+	.998	.756	.736	1.244	1.363
MN	.003	.133	.162	-	-
MG	-	.027	.004	.074	.005
CA	-	.002	-	-	-
NA	-	-	-	-	-
K	-	-	-	-	-
SUM	3.000	2.000	2.000	3.000	3.000

**** SAMPLE DIRECTORY ****

SAMPLE NO.	DESCRIPTION	SAMPLE NO.	DESCRIPTION
31	JE-A		
32	JE-A		
33	JE-A		
34	JE-G		
35	JE-G		

GAHNITE

SIO2	-	-	-	-	-	-	-	-	-	-
TIO2	ND	-	-	-	-	-	-	-	-	-
AL2O3	57.00	57.13	57.65	57.01	56.94	56.74	56.60	56.96	56.74	56.92
CR2O3	.12	.10	.09	.12	.09	.09	.06	-	-	-
FEO	12.30	11.90	12.24	12.54	14.29	14.25	11.66	13.35	13.82	14.01
MNO	.23	.19	.16	.22	.43	.44	.36	.44	.44	.43
MGO	1.98	2.04	2.09	2.05	1.60	1.69	1.69	1.71	1.81	1.83
CAO	-	-	-	-	-	-	-	-	-	-
NA2O	-	-	-	-	-	-	-	-	-	-
K2O	-	-	-	-	-	-	-	-	-	-
ZNO	27.64	28.09	28.11	27.61	26.50	26.60	28.72	26.83	26.77	26.75
TOTAL	99.29	99.45	100.34	99.55	99.85	99.81	99.09	99.29	99.58	99.94

** ATOMIC PROPORTIONS BASED ON SELECTED NO. OF OXYGENS **

OXYGEN	4	4	4	4	4	4	4	4	4	4
SI	-	-	-	-	-	-	-	-	-	-
TI	-	-	-	-	-	-	-	-	-	-
AL	1.993	1.994	1.993	1.988	1.985	1.979	1.991	1.993	1.981	1.980
CR	.003	.002	.002	.003	.002	.002	.001	-	-	-
FE3+	.003	.004	.005	.009	.013	.019	.008	.007	.019	.020
FE2+	.302	.291	.296	.301	.340	.333	.283	.325	.323	.326
MN	.006	.005	.004	.006	.011	.011	.009	.011	.011	.011
MG	.088	.090	.091	.090	.071	.075	.075	.076	.080	.080
CA	-	-	-	-	-	-	-	-	-	-
NA	-	-	-	-	-	-	-	-	-	-
K	-	-	-	-	-	-	-	-	-	-
ZN	.605	.614	.609	.603	.579	.581	.633	.588	.586	.583
SUM	3.000	3.000	3.000	3.000	3.000	3.000	3.000	3.000	3.000	3.000

**** SAMPLE DIRECTORY ****

SAMPLE NO.	DESCRIPTION	SAMPLE NO.	DESCRIPTION
1	ABN-12	6	ABN-13
2	ABN-12	7	ABN-13
3	ABN-12	8	ABN-13
4	ABN-12	9	ABN-13
5	ABN-13	10	ABN-13

GAHNITE

SIO2	-	-	-	-	-	-	-	-	-	-
TIO2	-	-	-	-	-	-	-	-	-	-
AL2O3	57.44	56.92	58.98	59.47	59.38	58.95	59.47	59.93	55.93	56.54
CR2O3	-	-	-	.11	.05	-	.05	-	.09	.16
FEO	12.45	10.62	9.73	10.76	10.33	10.19	10.09	10.16	14.76	14.66
MNO	.41	.28	.33	.29	.31	.33	.24	.28	.22	.29
MGO	1.86	1.66	1.66	1.70	1.65	1.68	1.62	1.61	1.24	1.18
CAO	-	-	-	-	-	-	-	-	-	-
NA2O	-	-	-	-	-	-	-	-	-	-
K2O	-	-	-	-	-	-	-	-	-	-
ZNO	28.29	29.22	30.67	29.21	29.39	29.31	29.64	29.80	27.10	27.20
TOTAL	100.45	98.70	101.37	101.54	101.11	100.46	101.11	101.78	99.34	100.03

** ATOMIC PROPORTIONS BASED ON SELECTED NO. OF OXYGENS **

OXYGEN	4	4	4	4	4	4	4	4	4	4
SI	-	-	-	-	-	-	-	-	-	-
TI	-	-	-	-	-	-	-	-	-	-
AL	1.989	2.006	2.018	2.023	2.027	2.026	2.030	2.031	1.970	1.977
CR	-	-	-	.003	.001	-	.001	-	.002	.004
FE3+	.011	-	-	-	-	-	-	-	.028	.019
FE2+	.295	.266	.236	.260	.250	.249	.244	.244	.341	.345
MN	.010	.007	.008	.007	.008	.008	.006	.007	.006	.007
MG	.081	.074	.072	.073	.071	.073	.070	.069	.055	.052
CA	-	-	-	-	-	-	-	-	-	-
NA	-	-	-	-	-	-	-	-	-	-
K	-	-	-	-	-	-	-	-	-	-
ZN	.614	.645	.657	.622	.629	.631	.634	.633	.598	.596
SUM	3.000	2.997	2.991	2.987	2.986	2.987	2.985	2.984	3.000	3.000

**** SAMPLE DIRECTORY ****

SAMPLE NO.	DESCRIPTION	SAMPLE NO.	DESCRIPTION
11	ABN-13	16	ABN-14
12	ABN-14	17	ABN-14
13	ABN-14	18	ABN-14
14	ABN-14	19	ABN-16
15	ABN-14	20	ABN-16

GAHNITE

SIO2	-	-	-	-	-	-	-	-	-	-
TIO2	-	-	-	-	-	-	-	-	-	-
AL2O3	56.26	57.05	56.02	57.28	56.01	56.93	55.57	54.92	56.28	55.31
CR2O3	.08	.07	-	.06	.05	-	-	.07	-	-
FEO	15.10	15.26	15.09	14.81	14.85	14.94	16.45	12.46	13.26	16.45
MNO	.22	.30	.29	.30	.25	.25	.36	.16	.38	.44
MGO	1.53	1.36	1.51	1.49	1.45	1.53	2.50	2.15	1.93	2.08
CAO	-	-	-	-	-	-	-	-	-	-
NA2O	-	-	-	-	-	-	-	-	-	-
K2O	-	-	-	-	-	-	-	-	-	-
ZNO	26.79	26.99	26.63	26.94	26.53	26.82	23.93	28.32	27.60	24.86
TOTAL	99.98	101.03	99.54	100.88	99.14	100.47	98.81	98.08	99.45	99.14

** ATOMIC PROPORTIONS BASED ON SELECTED NO. OF OXYGENS **

OXYGEN	4	4	4	4	4	4	4	4	4	4
SI	-	-	-	-	-	-	-	-	-	-
TI	-	-	-	-	-	-	-	-	-	-
AL	1.965	1.972	1.965	1.980	1.972	1.976	1.946	1.952	1.970	1.941
CR	.002	.002	-	.001	.001	-	-	.002	-	-
FE3+	.033	.026	.035	.019	.027	.024	.054	.046	.030	.059
FE2+	.341	.348	.341	.344	.344	.344	.355	.268	.300	.350
MN	.006	.007	.007	.007	.006	.006	.009	.004	.010	.011
MG	.068	.059	.067	.065	.065	.067	.111	.097	.085	.092
CA	-	-	-	-	-	-	-	-	-	-
NA	-	-	-	-	-	-	-	-	-	-
K	-	-	-	-	-	-	-	-	-	-
ZN	.586	.585	.585	.583	.585	.583	.525	.631	.605	.546
SUM	3.000	3.000	3.000	3.000	3.000	3.000	3.000	3.000	3.000	3.000

**** SAMPLE DIRECTORY ****

SAMPLE NO.	DESCRIPTION	SAMPLE NO.	DESCRIPTION
21	ABN-16	26	ABN-16
22	ABN-16	27	ABN-3
23	ABN-16	28	ABN-3
24	ABN-16	29	ABN-3
25	ABN-16	30	ABN-3

GAHNITE

SIO2	-	-	-	-	-	-	-	-	-	-
TIO2	-	-	-	-	-	-	-	-	-	-
AL2O3	55.13	55.29	56.31	55.99	56.05	55.64	56.64	57.08	56.57	56.07
CR2O3	-	.05	.15	.34	.21	.42	.33	ND	-	.04
FEO	16.95	15.49	9.76	14.87	14.82	13.83	14.10	21.56	23.79	9.37
MNO	.48	.46	.28	.29	.39	.35	.30	.14	.15	.14
MGO	2.36	1.87	.82	1.30	1.28	1.27	1.36	5.76	6.78	1.35
CAO	-	-	-	-	-	-	-	-	-	-
NA2O	-	-	-	-	-	-	-	-	-	-
K2O	-	-	-	-	-	-	-	-	-	-
ZNO	22.70	25.36	32.71	26.77	26.42	27.80	27.78	14.57	11.88	33.11
TOTAL	97.62	98.52	100.03	99.56	99.17	99.31	100.51	99.13	99.17	100.08

** ATOMIC PROPORTIONS BASED ON SELECTED NO. OF OXYGENS **

OXYGEN	4	4	4	4	4	4	4	4	4	4
SI	-	-	-	-	-	-	-	-	-	-
TI	-	-	-	-	-	-	-	-	-	-
AL	1.952	1.954	1.986	1.967	1.975	1.964	1.971	1.926	1.895	1.972
CR	-	.001	.004	.008	.005	.010	.008	-	-	.001
FE3+	.048	.045	.011	.025	.020	.027	.021	.073	.105	.027
FE2+	.378	.343	.234	.346	.350	.320	.327	.443	.460	.207
MN	.012	.012	.007	.007	.010	.009	.008	.003	.004	.004
MG	.106	.084	.037	.058	.057	.057	.060	.246	.287	.060
CA	-	-	-	-	-	-	-	-	-	-
NA	-	-	-	-	-	-	-	-	-	-
K	-	-	-	-	-	-	-	-	-	-
ZN	.504	.561	.723	.589	.583	.615	.606	.308	.249	.730
SUM	3.000	3.000	3.000	3.000	3.000	3.000	3.000	3.000	3.000	3.000

**** SAMPLE DIRECTORY ****

SAMPLE NO.	DESCRIPTION	SAMPLE NO.	DESCRIPTION
31	ABN-3	36	ABN-4
32	ABN-3	37	ABN-4
33	ABN-4	38	ABN-6
34	ABN-4	39	ABN-6
35	ABN-4	40	ABN-8

GAHNITE

SIO2	-	-	-	-	-	-	-	-	-	-
TIO2	-	-	-	-	-	-	-	-	-	-
AL2O3	55.88	56.53	56.37	55.96	56.05	55.79	55.87	55.69	56.38	56.11
CR2O3	.07	.04	-	.11	.07	-	ND	.06	.14	.09
FEO	9.59	9.56	9.00	9.82	9.64	9.79	9.78	9.77	9.97	9.23
MNO	.15	.17	.22	.20	.21	.21	.19	.23	.26	.18
MGO	1.37	1.38	1.36	1.36	1.38	1.36	1.39	1.29	1.35	1.39
CAO	-	-	-	-	-	-	-	-	-	-
NA2O	-	-	-	-	-	-	-	-	-	-
K2O	-	-	-	-	-	-	-	-	-	-
ZNO	32.87	32.86	32.99	33.03	32.69	32.59	32.95	32.82	32.39	32.78
TOTAL	99.93	100.54	99.94	100.48	100.04	99.74	100.21	99.86	100.49	99.78

** ATOMIC PROPORTIONS BASED ON SELECTED NO. OF OXYGENS **

OXYGEN	4	4	4	4	4	4	4	4	4	4
SI	-	-	-	-	-	-	-	-	-	-
TI	-	-	-	-	-	-	-	-	-	-
AL	1.968	1.977	1.982	1.962	1.971	1.968	1.963	1.965	1.973	1.977
CR	.002	.001	-	.003	.002	-	-	.001	.003	.002
FE3+	.030	.022	.018	.035	.027	.032	.036	.034	.024	.021
FE2+	.210	.215	.207	.209	.213	.214	.208	.211	.224	.210
MN	.004	.004	.006	.005	.005	.005	.005	.006	.007	.005
MG	.061	.061	.060	.060	.061	.061	.062	.058	.060	.062
CA	-	-	-	-	-	-	-	-	-	-
NA	-	-	-	-	-	-	-	-	-	-
K	-	-	-	-	-	-	-	-	-	-
ZN	.725	.720	.727	.726	.720	.720	.725	.726	.710	.724
SUM	3.000	3.000	3.000	3.000	3.000	3.000	3.000	3.000	3.000	3.000

**** SAMPLE DIRECTORY ****

SAMPLE NO.	DESCRIPTION	SAMPLE NO.	DESCRIPTION
41	ABN-8	46	ABN-8
42	ABN-8	47	ABN-8
43	ABN-8	48	ABN-8
44	ABN-8	49	ABN-8
45	ABN-8	50	ABN-8

GAHNITE

SIO2	-	-	-	-	-	-	-	-	-	-
TIO2	-	-	-	-	-	-	-	-	-	-
AL2O3	58.38	58.80	59.02	57.76	58.27	57.79	55.66	55.61	56.19	55.72
CR2O3	-	-	-	-	-	-	.37	-	-	-
FEO	13.88	14.32	13.59	13.57	13.95	13.61	13.92	12.66	8.52	9.88
MNO	.29	.31	.32	.32	.37	.28	.41	.39	.32	.32
MGO	3.84	3.95	3.58	3.32	3.41	3.61	2.05	2.19	1.77	1.91
CAO	-	-	-	-	-	-	-	-	-	-
NA2O	-	-	-	-	-	-	-	-	-	-
K2O	-	-	-	-	-	-	-	-	-	-
ZNO	24.69	24.32	25.27	24.65	24.89	24.23	27.42	28.15	33.56	31.50
TOTAL	101.08	101.70	101.78	99.62	100.89	99.52	99.83	99.00	100.36	99.33

** ATOMIC PROPORTIONS BASED ON SELECTED NO. OF OXYGENS **

OXYGEN	4	4	4	4	4	4	4	4	4	4
SI	-	-	-	-	-	-	-	-	-	-
TI	-	-	-	-	-	-	-	-	-	-
AL	1.973	1.973	1.984	1.986	1.979	1.984	1.945	1.956	1.966	1.964
CR	-	-	-	-	-	-	.009	-	-	-
FE3+	.027	.027	.016	.014	.021	.016	.046	.044	.034	.036
FE2+	.306	.314	.308	.317	.315	.315	.299	.272	.178	.211
MN	.007	.007	.008	.008	.009	.007	.010	.010	.008	.008
MG	.164	.168	.152	.144	.146	.157	.091	.097	.078	.085
CA	-	-	-	-	-	-	-	-	-	-
NA	-	-	-	-	-	-	-	-	-	-
K	-	-	-	-	-	-	-	-	-	-
ZN	.523	.511	.532	.531	.530	.521	.600	.620	.736	.696
SUM	3.000	3.000	3.000	3.000	3.000	3.000	3.000	3.000	3.000	3.000

**** SAMPLE DIRECTORY ****

SAMPLE NO.	DESCRIPTION	SAMPLE NO.	DESCRIPTION
51	ABN-9	56	ABN-9
52	ABN-9	57	ABN-10
53	ABN-9	58	ABN-10
54	ABN-9	59	ABN-10
55	ABN-9	60	ABN-10

GAHNITE

SIO2	-	-	-	-	-	-	-	-	-	-
TIO2	-	-	-	-	-	-	-	-	-	-
AL2O3	56.98	56.49	56.54	56.08	56.36	56.82	56.94	56.94	56.85	56.54
CR2O3	-	-	-	-	-	-	-	-	-	-
FEO	13.17	15.23	15.27	15.76	12.61	14.97	15.74	15.57	15.78	15.06
MNO	.28	.27	.23	.26	.22	.31	.29	.28	.24	.27
MGO	1.50	1.57	1.42	1.36	1.41	1.57	1.58	1.64	1.59	1.31
CAO	-	-	-	-	-	-	-	-	-	-
NA2O	-	-	-	-	-	-	-	-	-	-
K2O	-	-	-	-	-	-	-	-	-	-
ZNO	27.59	25.76	26.31	25.65	28.44	25.38	25.31	25.38	25.41	25.57
TOTAL	99.52	99.32	99.77	99.11	99.04	99.05	99.86	99.81	99.87	98.75

** ATOMIC PROPORTIONS BASED ON SELECTED NO. OF OXYGENS **

OXYGEN	4	4	4	4	4	4	4	4	4	4
SI	-	-	-	-	-	-	-	-	-	-
TI	-	-	-	-	-	-	-	-	-	-
AL	1.994	1.979	1.976	1.974	1.988	1.993	1.982	1.983	1.980	1.993
CR	-	-	-	-	-	-	-	-	-	-
FE3+	.006	.021	.024	.026	.012	.007	.018	.017	.020	.007
FE2+	.322	.358	.355	.367	.303	.365	.371	.367	.370	.370
MN	.007	.007	.006	.007	.006	.008	.007	.007	.006	.007
MG	.066	.070	.063	.061	.063	.070	.070	.072	.070	.058
CA	-	-	-	-	-	-	-	-	-	-
NA	-	-	-	-	-	-	-	-	-	-
K	-	-	-	-	-	-	-	-	-	-
ZN	.605	.566	.576	.566	.628	.558	.552	.554	.554	.565
SUM	3.000	3.000	3.000	3.000	3.000	3.000	3.000	3.000	3.000	3.000

**** SAMPLE DIRECTORY ****

SAMPLE NO.	DESCRIPTION	SAMPLE NO.	DESCRIPTION
61	ABN-11	66	ABN-11 CENTRE
62	ABN-11	67	ABN-11 RIM
63	ABN-11	68	ABN-11 CENTRE
64	ABN-11	69	ABN-11 RIM
65	ABN-11	70	ABN-11

GAHNITE

SIO2	-	-	-	-	-	-	-	-	-	-
TIO2	-	-	-	-	-	-	-	-	-	-
AL2O3	56.82	57.53	58.86	58.33	58.23	57.62	58.35	57.89	58.43	58.69
CR2O3	-	-	.07	.07	.15	-	.07	.06	-	-
FEO	15.49	15.99	15.54	15.36	15.52	16.35	15.63	15.73	15.56	15.09
MNO	.30	.14	.13	.20	.14	.14	.15	.14	.16	.17
MGO	1.17	1.84	1.98	2.09	1.98	1.95	2.02	2.01	2.08	2.09
CAO	-	-	-	-	-	-	-	-	-	-
NA2O	-	-	-	-	-	-	-	-	-	-
K2O	-	-	-	-	-	-	-	-	-	-
ZNO	25.83	23.85	24.79	24.34	24.00	24.08	24.42	24.56	24.18	24.73
TOTAL	99.61	99.35	101.37	100.39	100.02	100.14	100.64	100.39	100.41	100.77

** ATOMIC PROPORTIONS BASED ON SELECTED NO. OF OXYGENS **

OXYGEN	4	4	4	4	4	4	4	4	4	4
SI	-	-	-	-	-	-	-	-	-	-
TI	-	-	-	-	-	-	-	-	-	-
AL	1.989	2.001	2.003	2.003	2.005	1.990	2.001	1.993	2.005	2.006
CR	-	-	.002	.002	.003	-	.002	.001	-	-
FE3+	.011	-	-	-	-	.010	-	.005	-	-
FE2+	.374	.395	.375	.374	.379	.390	.380	.379	.379	.366
MN	.008	.003	.003	.005	.003	.003	.004	.003	.004	.004
MG	.052	.081	.085	.091	.086	.085	.088	.088	.090	.090
CA	-	-	-	-	-	-	-	-	-	-
NA	-	-	-	-	-	-	-	-	-	-
K	-	-	-	-	-	-	-	-	-	-
ZN	.567	.520	.529	.524	.518	.521	.525	.530	.520	.530
SUM	3.000	3.000	2.997	2.998	2.996	3.000	2.999	3.000	2.998	2.997

**** SAMPLE DIRECTORY ****

SAMPLE NO.	DESCRIPTION	SAMPLE NO.	DESCRIPTION
71	ABN-11	76	SK-2 CENTRE
72	SK-2 CENTRE	77	SK-2 RIM
73	SK-2 RIM	78	SK-2 CENTRE
74	SK-2	79	SK-2 RIM
75	SK-2	80	SK-2

GAHNITE

SIO2	-	-	-	-	-	-	-	-	-	-
TIO2	-	-	-	-	-	-	-	-	-	-
AL2O3	58.26	58.85	57.86	58.71	58.39	57.89	57.34	57.90	57.71	57.73
CR2O3	.08	.10	-	-	.23	.26	.26	.26	.24	.24
FEO	14.91	15.57	16.74	15.82	24.71	24.84	24.89	24.90	25.50	25.54
MNO	.20	-	.18	-	.36	.31	.40	.28	.37	.32
MGO	2.05	1.97	2.04	2.04	3.64	3.41	3.40	3.56	3.48	3.41
CAO	-	-	-	-	-	-	-	-	-	-
NA2O	-	-	-	-	-	-	-	-	-	-
K2O	-	-	-	-	-	-	-	-	-	-
ZNO	25.03	24.23	23.78	24.02	13.18	13.16	13.15	12.93	13.31	13.21
TOTAL	100.53	100.72	100.60	100.59	100.51	99.87	99.44	99.83	100.61	100.45

** ATOMIC PROPORTIONS BASED ON SELECTED NO. OF OXYGENS **

OXYGEN	4	4	4	4	4	4	4	4	4	4
SI	-	-	-	-	-	-	-	-	-	-
TI	-	-	-	-	-	-	-	-	-	-
AL	2.001	2.010	1.987	2.009	1.964	1.963	1.955	1.962	1.946	1.950
CR	.002	.002	-	-	.005	.006	.006	.006	.005	.005
FE3+	-	-	.013	-	.031	.031	.039	.032	.049	.045
FE2+	.363	.377	.395	.384	.559	.567	.563	.566	.561	.567
MN	.005	-	.004	-	.009	.008	.010	.007	.009	.008
MG	.089	.085	.089	.088	.155	.146	.147	.153	.148	.146
CA	-	-	-	-	-	-	-	-	-	-
NA	-	-	-	-	-	-	-	-	-	-
K	-	-	-	-	-	-	-	-	-	-
ZN	.539	.519	.512	.515	.278	.280	.281	.274	.281	.280
SUM	2.999	2.994	3.000	2.996	3.000	3.000	3.000	3.000	3.000	3.000

**** SAMPLE DIRECTORY ****

SAMPLE NO.	DESCRIPTION	SAMPLE NO.	DESCRIPTION
81	SK-2	86	SK-3
82	SK-2	87	SK-3
83	SK-2 CENTRE	88	SK-3 CENTRE
84	SK-2 RIM	89	SK-3 RIM
85	SK-3	90	SK-3 CENTRE

GAHNITE

SIO2	-	-	-	-	-	-	-	-	-	-
TIO2	-	-	-	-	-	-	-	-	-	-
AL2O3	58.04	57.69	57.61	57.49	57.53	57.84	57.74	57.26	57.26	57.40
CR2O3	.21	.25	.28	.26	.19	.20	.11	.14	.14	.12
FEO	25.04	24.69	24.63	24.71	25.27	25.57	21.39	21.46	21.31	20.95
MNO	.33	.36	.36	.36	.34	.35	.23	.26	.28	.30
MGO	3.37	3.30	3.50	3.62	3.64	3.50	2.78	2.78	2.60	2.89
CAO	-	-	-	-	-	-	-	-	-	-
NA2O	-	-	-	-	-	-	-	-	-	-
K2O	-	-	-	-	-	-	-	-	-	-
ZNO	13.17	14.03	13.33	12.90	13.20	13.28	18.03	17.90	18.28	18.39
TOTAL	100.16	100.32	99.71	99.34	100.17	100.74	100.28	99.80	99.87	100.05

** ATOMIC PROPORTIONS BASED ON SELECTED NO. OF OXYGENS **

OXYGEN	4	4	4	4	4	4	4	4	4	4
SI	-	-	-	-	-	-	-	-	-	-
TI	-	-	-	-	-	-	-	-	-	-
AL	1.963	1.953	1.957	1.957	1.946	1.947	1.969	1.963	1.965	1.963
CR	.005	.006	.006	.006	.004	.005	.003	.003	.003	.003
FE3+	.032	.041	.037	.037	.050	.048	.028	.034	.032	.035
FE2+	.569	.552	.557	.560	.556	.562	.489	.489	.487	.474
MN	.008	.009	.009	.009	.008	.008	.006	.006	.007	.007
MG	.144	.141	.150	.156	.156	.149	.120	.121	.113	.125
CA	-	-	-	-	-	-	-	-	-	-
NA	-	-	-	-	-	-	-	-	-	-
K	-	-	-	-	-	-	-	-	-	-
ZN	.279	.298	.284	.275	.280	.280	.385	.385	.393	.394
SUM	3.000	3.000	3.000	3.000	3.000	3.000	3.000	3.000	3.000	3.000

**** SAMPLE DIRECTORY ****

SAMPLE NO.	DESCRIPTION	SAMPLE NO.	DESCRIPTION
91	SK-3 RIM	96	SK-3
92	SK-3 CENTRE	97	SK-4
93	SK-3 RIM	98	SK-4 CENTRE
94	SK-3 CENTRE	99	SK-4 RIM
95	SK-3 RIM	100	SK-4 CENTRE

GAHNITE

SIO2	-	-	-	-	-	-	-	-	-	-
TIO2	-	-	-	-	-	-	-	-	-	-
AL2O3	57.89	57.70	58.75	57.52	58.18	57.70	56.66	56.30	56.33	55.69
CR2O3	.10	.05	.07	.11	.14	.13	.08	-	-	-
FEO	20.20	21.39	19.42	20.87	20.28	21.40	20.80	15.64	16.32	16.53
MNO	.21	.25	.22	.31	.27	.27	.31	.17	.21	.22
MGO	2.91	2.83	2.91	2.94	2.90	2.80	2.66	1.67	1.79	1.78
CAO	-	-	-	-	-	-	-	-	-	-
NA2O	-	-	-	-	-	-	-	-	-	-
K2O	-	-	-	-	-	-	-	-	-	-
ZNO	18.93	17.90	19.08	18.41	18.59	18.38	18.49	25.70	24.34	24.29
TOTAL	100.24	100.12	100.45	100.16	100.36	100.68	99.00	99.48	98.99	98.51

** ATOMIC PROPORTIONS BASED ON SELECTED NO. OF OXYGENS **

OXYGEN	4	4	4	4	4	4	4	4	4	4
SI	-	-	-	-	-	-	-	-	-	-
TI	-	-	-	-	-	-	-	-	-	-
AL	1.974	1.970	1.995	1.964	1.980	1.962	1.962	1.970	1.975	1.964
CR	.002	.001	.002	.003	.003	.003	.002	-	-	-
FE3+	.024	.029	.004	.034	.017	.035	.036	.030	.025	.036
FE2+	.465	.489	.464	.472	.472	.481	.475	.358	.381	.378
MN	.005	.006	.005	.008	.007	.007	.008	.004	.005	.006
MG	.125	.122	.125	.127	.125	.120	.116	.074	.079	.079
CA	-	-	-	-	-	-	-	-	-	-
NA	-	-	-	-	-	-	-	-	-	-
K	-	-	-	-	-	-	-	-	-	-
ZN	.404	.383	.406	.394	.396	.392	.401	.563	.535	.537
SUM	3.000	3.000	3.000	3.000	3.000	3.000	3.000	3.000	3.000	3.000

**** SAMPLE DIRECTORY ****

SAMPLE NO.	DESCRIPTION	SAMPLE NO.	DESCRIPTION
101	SK-4 RIM	106	SK-4 CENTRE
102	SK-4 CENTRE	107	SK-4 RIM
103	SK-4 RIM	108	SK-10 CENTRE
104	SK-4 CENTRE	109	SK-10 RIM
105	SK-4 RIM	110	SK-10

GAHNITE

SIO2	-	-	-	-	-	-	-	-	-	-
TIO2	-	-	-	-	-	-	-	-	-	-
AL2O3	57.47	56.91	56.34	57.03	56.86	56.72	57.22	57.13	57.08	57.03
CR2O3	.07	.09	.06	.06	.05	.18	.04	.06	.06	.06
FEO	7.79	7.41	6.48	7.04	6.76	7.37	7.38	7.50	7.08	7.36
MNO	.59	.55	.47	.50	.47	.59	.52	.48	.49	.49
MGO	1.29	1.09	1.00	1.19	1.07	1.26	1.26	1.23	1.11	1.11
CAO	-	-	-	-	-	-	-	-	-	-
NA2O	-	-	-	-	-	-	-	-	-	-
K2O	-	-	-	-	-	-	-	-	-	-
ZNO	32.88	33.79	34.03	33.34	33.80	33.32	33.17	33.12	33.76	33.46
TOTAL	100.09	99.84	98.38	99.16	99.01	99.44	99.59	99.52	99.58	99.51

** ATOMIC PROPORTIONS BASED ON SELECTED NO. OF OXYGENS **

OXYGEN	4	4	4	4	4	4	4	4	4	4
SI	-	-	-	-	-	-	-	-	-	-
TI	-	-	-	-	-	-	-	-	-	-
AL	2.008	2.003	2.011	2.012	2.013	2.001	2.010	2.009	2.010	2.009
CR	.002	.002	.001	.001	.001	.004	.001	.001	.001	.001
FE2+	.193	.185	.164	.176	.170	.184	.184	.187	.177	.184
MN	.015	.014	.012	.013	.012	.015	.013	.012	.012	.012
MG	.057	.049	.045	.053	.048	.056	.056	.055	.049	.049
CA	-	-	-	-	-	-	-	-	-	-
NA	-	-	-	-	-	-	-	-	-	-
K	-	-	-	-	-	-	-	-	-	-
ZN	.720	.745	.761	.737	.750	.736	.730	.730	.745	.738
SUM	2.995	2.998	2.994	2.993	2.993	2.997	2.994	2.995	2.994	2.995

**** SAMPLE DIRECTORY ****

SAMPLE NO.	DESCRIPTION	SAMPLE NO.	DESCRIPTION
111	BH-2 CENTRE	116	BH-2
112	BH-2 RIM	117	BH-2
113	BH-2	118	BH-2 CENTRE
114	BH-2	119	BH-2 RIM
115	BH-2	120	BH-2

GAHNITE

SIO2	-	-	-	-	-	-	-	-	-	-
TIO2	-	-	-	-	-	-	-	-	-	-
AL2O3	57.61	56.82	56.84	56.49	56.99	56.89	56.38	56.37	56.89	56.59
CR2O3	ND	-	-	-	-	-	-	-	-	-
FEO	6.10	8.95	9.42	9.80	9.06	9.06	9.29	8.82	9.48	9.15
MNO	.46	.34	.41	.46	.35	.35	.42	.35	.33	.41
MGO	.94	1.10	1.14	.97	1.01	1.15	1.10	1.03	1.12	1.03
CAO	-	-	-	-	-	-	-	-	-	-
NA2O	-	-	-	-	-	-	-	-	-	-
K2O	-	-	-	-	-	-	-	-	-	-
ZNO	34.93	32.81	32.88	31.80	32.82	32.71	31.84	32.85	32.20	32.30
TOTAL	100.07	100.02	100.69	99.52	100.23	100.16	99.03	99.42	100.02	99.48

** ATOMIC PROPORTIONS BASED ON SELECTED NO. OF OXYGENS **

OXYGEN	4	4	4	4	4	4	4	4	4	4
SI	-	-	-	-	-	-	-	-	-	-
TI	-	-	-	-	-	-	-	-	-	-
AL	2.018	1.997	1.986	1.996	1.999	1.996	1.999	1.995	1.997	1.999
CR	-	-	-	-	-	-	-	-	-	-
FE3+	-	.003	.014	.004	-	.004	-	.005	.003	-
FE2+	.152	.220	.220	.241	.225	.221	.233	.217	.234	.229
MN	.012	.009	.010	.012	.009	.009	.011	.009	.008	.010
MG	.042	.049	.050	.043	.045	.051	.049	.046	.050	.046
CA	-	-	-	-	-	-	-	-	-	-
NA	-	-	-	-	-	-	-	-	-	-
K	-	-	-	-	-	-	-	-	-	-
ZN	.767	.722	.720	.704	.721	.719	.707	.728	.708	.715
SUM	2.991	3.000	3.000	3.000	3.000	3.000	3.000	3.000	3.000	3.000

**** SAMPLE DIRECTORY ****

SAMPLE NO.	DESCRIPTION	SAMPLE NO.	DESCRIPTION
121	BH-2	126	BH WE-1
122	BH WE-1	127	BH WE-1
123	BH WE-1	128	BH WE-1
124	BH WE-1	129	BH WE-1
125	BH WE-1	130	BH WE-1

TABLE 1

GAHNITE

SIO2	-	-	-	-	-	-	-	-	-	-
TIO2	-	-	-	-	-	-	-	-	-	-
AL2O3	56.98	56.73	57.54	57.16	56.06	57.04	56.93	57.45	56.75	57.02
CR2O3	-	-	-	-	-	-	-	-	-	-
FEO	10.36	9.09	8.94	10.46	11.96	9.03	8.98	8.90	8.48	8.89
MNO	.53	.60	.67	.63	.88	.46	.47	.50	.41	.54
MGO	1.05	1.11	.98	1.08	1.03	1.00	1.06	1.11	1.00	1.10
CAO	-	-	-	-	-	-	-	-	-	-
NA2O	-	-	-	-	-	-	-	-	-	-
K2O	-	-	-	-	-	-	-	-	-	-
ZNO	31.17	31.71	32.60	31.08	29.35	32.29	32.17	32.20	32.45	32.47
TOTAL	100.09	99.24	100.73	100.41	99.28	99.82	99.61	100.16	99.09	100.02

** ATOMIC PROPORTIONS BASED ON SELECTED NO. OF OXYGENS **

OXYGEN	4	4	4	4	4	4	4	4	4	4
SI	-	-	-	-	-	-	-	-	-	-
TI	-	-	-	-	-	-	-	-	-	-
AL	1.998	2.004	2.005	1.997	1.982	2.005	2.005	2.008	2.008	2.001
CR	-	-	-	-	-	-	-	-	-	-
FE3+	-	-	-	.003	.018	-	-	-	-	-
FE2+	.255	.228	.221	.256	.282	.225	.224	.221	.213	.221
MN	.013	.015	.017	.016	.022	.012	.012	.013	.010	.014
MG	.047	.050	.043	.048	.046	.044	.047	.049	.045	.049
CA	-	-	-	-	-	-	-	-	-	-
NA	-	-	-	-	-	-	-	-	-	-
K	-	-	-	-	-	-	-	-	-	-
ZN	.685	.702	.712	.680	.650	.711	.710	.705	.719	.714
SUM	3.000	2.998	2.998	3.000	3.000	2.997	2.998	2.996	2.996	2.999

**** SAMPLE DIRECTORY ****

SAMPLE NO.	DESCRIPTION	SAMPLE NO.	DESCRIPTION
131	BH WE-2	136	BH WE-2
132	BH WE-2	137	BH WE-2
133	BH WE-2	138	BH WE-2
134	BH WE-2	139	BH WE-2
135	BH WE-2	140	BH WE-2

TABLE 1

GAHNITE

SIO2	-	-	-	-	-	-	-	-	-	-
TIO2	-	-	-	-	-	-	-	-	-	-
AL2O3	56.70	55.99	56.77	56.50	57.23	56.67	56.43	56.47	56.45	55.37
CR2O3	-	-	-	-	-	-	.10	-	-	-
FEO	23.73	28.35	26.84	29.76	26.82	28.78	17.20	18.93	20.30	14.73
MNO	1.63	2.56	2.14	3.04	2.55	2.57	-	-	.09	-
MGO	2.00	1.96	2.05	2.22	2.44	2.10	2.66	2.66	2.70	2.62
CAO	-	-	-	-	-	-	-	-	-	-
NA2O	-	-	-	-	-	-	-	-	-	-
K2O	-	-	-	-	-	-	-	-	-	-
ZNO	15.52	10.28	12.05	8.26	11.30	9.62	23.14	21.94	20.57	26.49
TOTAL	99.58	99.14	99.85	99.78	100.34	99.74	99.53	100.00	100.11	99.21

** ATOMIC PROPORTIONS BASED ON SELECTED NO. OF OXYGENS **

OXYGEN	4	4	4	4	4	4	4	4	4	4
SI	-	-	-	-	-	-	-	-	-	-
TI	-	-	-	-	-	-	-	-	-	-
AL	1.956	1.934	1.947	1.931	1.945	1.940	1.956	1.947	1.942	1.938
CR	-	-	-	-	-	-	.002	-	-	-
FE3+	.044	.066	.053	.069	.055	.060	.042	.053	.058	.062
FE2+	.537	.628	.600	.653	.592	.639	.381	.410	.437	.303
MN	.040	.064	.053	.075	.062	.063	-	-	.002	-
MG	.087	.086	.089	.096	.105	.091	.117	.116	.117	.116
CA	-	-	-	-	-	-	-	-	-	-
NA	-	-	-	-	-	-	-	-	-	-
K	-	-	-	-	-	-	-	-	-	-
ZN	.335	.222	.259	.177	.241	.206	.502	.474	.443	.581
SUM	3.000	3.000	3.000	3.000	3.000	3.000	3.000	3.000	3.000	3.000

**** SAMPLE DIRECTORY ****

SAMPLE NO.	DESCRIPTION	SAMPLE NO.	DESCRIPTION
141	BHG 302	146	BHG 302
142	BHG 302	147	240 AG 56
143	BHG 302	148	240 AG 56
144	BHG 302	149	240 AG 56
145	BHG 302	150	240 AG 56

TABLE 1

GAHNITE

SIO2	-	-	-	-	-	-	-	-	-	-
TIO2	-	-	-	-	-	-	-	-	-	-
AL2O3	55.89	55.63	54.87	57.21	56.79	56.37	55.38	55.33	55.47	54.81
CR2O3	-	.07	-	.06	.05	.11	.04	.04	.04	-
FEO	16.26	16.65	17.88	11.48	11.26	11.55	2.03	2.19	2.21	1.98
MNO	-	.08	-	.42	.37	.43	ND	.05	.04	-
MGO	2.86	2.74	3.03	.55	.57	.59	.08	.08	.10	.07
CAO	-	-	-	-	-	-	-	-	-	-
NA2O	-	-	-	-	-	-	-	-	-	-
K2O	-	-	-	-	-	-	-	-	-	-
ZNO	25.13	24.69	23.24	29.80	30.57	30.05	41.58	41.87	42.03	41.92
TOTAL	100.14	99.86	99.02	99.52	99.61	99.10	99.14	99.56	99.89	98.78

** ATOMIC PROPORTIONS BASED ON SELECTED NO. OF OXYGENS **

OXYGEN	4	4	4	4	4	4	4	4	4	4
SI	-	-	-	-	-	-	-	-	-	-
TI	-	-	-	-	-	-	-	-	-	-
AL	1.932	1.930	1.915	2.013	2.004	2.000	2.001	1.993	1.992	1.991
CR	-	.002	-	.001	.001	.003	.001	.001	.001	-
FE3+	.068	.069	.085	-	-	-	-	.006	.007	.009
FE2+	.331	.341	.358	.287	.282	.291	.052	.050	.049	.043
MN	-	.002	-	.011	.009	.011	-	.001	.001	-
MG	.125	.120	.134	.024	.025	.026	.004	.004	.005	.003
CA	-	-	-	-	-	-	-	-	-	-
NA	-	-	-	-	-	-	-	-	-	-
K	-	-	-	-	-	-	-	-	-	-
ZN	.544	.537	.508	.657	.676	.668	.941	.945	.945	.954
SUM	3.000	3.000	3.000	2.993	2.998	2.999	2.999	3.000	3.000	3.000

**** SAMPLE DIRECTORY ****

SAMPLE NO.	DESCRIPTION	SAMPLE NO.	DESCRIPTION
151	240 AG 56	156	DPB-1
152	240 AG 56	157	JE-2 BLUE
153	240 AG 56	158	JE-2 BLUE
154	DPB-1	159	JE-2 BLUE
155	DPB-1	160	JE 2 BLUE

TABLE 1

GAHNITE

SIO2	-	-	-	-	-	-	-	-	-	-
TIO2	-	-	-	-	-	-	-	-	-	-
AL2O3	55.62	57.81	58.42	58.34	58.72	55.13	54.96	58.21	58.22	55.00
CR2O3	-	.29	.21	.20	.25	-	-	.11	.15	.08
FEO	1.97	6.56	7.48	6.99	7.00	2.24	2.29	8.90	8.29	1.79
MNO	.07	.20	.22	.20	.13	.04	.05	.18	.21	.10
MGO	.09	4.93	4.97	4.97	4.79	.13	.09	5.61	5.67	.06
CAO	-	-	-	-	-	ND	-	-	-	-
NA2O	-	-	-	-	-	-	-	-	-	-
K2O	-	-	-	-	-	-	-	-	-	-
ZNO	42.54	29.28	29.26	29.66	29.68	42.35	42.99	27.61	27.88	45.53
TOTAL	100.29	99.07	100.56	100.36	100.57	99.92	100.38	100.62	100.42	102.56

** ATOMIC PROPORTIONS BASED ON SELECTED NO. OF OXYGENS **

OXYGEN	4	4	4	4	4	4	4	4	4	4
SI	-	-	-	-	-	-	-	-	-	-
TI	-	-	-	-	-	-	-	-	-	-
AL	1.990	1.985	1.977	1.979	1.988	1.981	1.971	1.960	1.963	1.941
CR	-	.007	.005	.005	.006	-	-	.002	.003	.002
FE3+	.010	.009	.018	.017	.006	.019	.029	.038	.034	.045
FE2+	.040	.151	.162	.152	.162	.038	.029	.175	.164	-
MN	.002	.005	.005	.005	.003	.001	.001	.004	.005	.003
MG	.004	.214	.213	.213	.205	.006	.004	.239	.242	.003
CA	-	-	-	-	-	.001	-	-	-	-
NA	-	-	-	-	-	-	-	-	-	-
K	-	-	-	-	-	-	-	-	-	-
ZN	.954	.630	.620	.630	.630	.954	.966	.582	.589	1.007
SUM	3.000	3.000	3.000	3.000	3.000	3.000	3.000	3.000	3.000	3.000

**** SAMPLE DIRECTORY ****

SAMPLE NO.	DESCRIPTION	SAMPLE NO.	DESCRIPTION
161	JE-2 BLUE	166	JE-3 BLUE
162	JE-2 GREEN	167	JE-3 BLUE
163	JE-2 GREEN	168	JE-3 GREEN
164	JE-2 GREEN	169	JE-3 GREEN
165	JE-2 GREEN	170	JE-15 BLUE

TABLE 1

GAHNITE

SIO2	-	-	-	-	-	-	-	-	-	-
TIO2	-	-	-	-	-	-	-	-	-	-
AL2O3	55.34	55.14	54.93	54.19	54.42	55.39	55.54	55.75	56.06	56.26
CR2O3	.06	-	-	.09	.09	-	-	.05	-	.04
FEO	1.91	1.69	1.97	2.14	1.78	1.82	1.83	1.85	1.53	1.40
MNO	.30	.10	-	.16	-	-	.15	-	-	ND
MGO	.06	.08	.06	.22	.13	.07	.06	.07	.06	.11
CAO	-	-	-	-	-	-	-	-	-	-
NA2O	-	-	-	-	-	-	-	-	-	-
K2O	-	-	-	-	-	-	-	-	-	-
ZNO	42.95	43.11	43.67	42.93	43.33	42.42	43.37	42.46	42.08	40.84
TOTAL	100.62	100.12	100.63	99.73	99.75	99.70	100.95	100.18	99.73	98.68

** ATOMIC PROPORTIONS BASED ON SELECTED NO. OF OXYGENS **

OXYGEN	4	4	4	4	4	4	4	4	4	4
SI	-	-	-	-	-	-	-	-	-	-
TI	-	-	-	-	-	-	-	-	-	-
AL	1.978	1.981	1.967	1.957	1.966	1.994	1.979	1.996	2.009	2.024
CR	.001	-	-	.002	.002	-	-	.001	-	.001
FE3+	.021	.019	.033	.041	.032	.006	.021	.003	-	-
FE2+	.028	.024	.017	.014	.013	.040	.025	.044	.039	.036
MN	.008	.003	-	.004	-	-	.004	-	-	-
MG	.003	.004	.003	.010	.006	.003	.003	.003	.003	.005
CA	-	-	-	-	-	-	-	-	-	-
NA	-	-	-	-	-	-	-	-	-	-
K	-	-	-	-	-	-	-	-	-	-
ZN	.962	.970	.980	.971	.981	.957	.968	.952	.945	.921
SUM	3.000	3.000	3.000	3.000	3.000	3.000	3.000	3.000	2.995	2.987

**** SAMPLE DIRECTORY ****

SAMPLE NO.	DESCRIPTION	SAMPLE NO.	DESCRIPTION
171	JE-15 BLUE	176	JE-15 BLUE
172	JE-15 BLUE	177	JE-15 BLUE
173	JE-15 BLUE	178	JE-15 BLUE
174	JE-15 BLUE	179	JE-15 BLUE
175	JE-15 BLUE	180	JE-14 BLUE

TABLE 1

GAHNITE

SIO2	-	-	-	-	-	-	-	-	-	-
TIO2	-	-	-	-	-	-	-	-	-	-
AL2O3	56.68	56.02	55.36	55.63	55.55	55.40	55.15	55.19	58.57	58.59
CR2O3	-	-	ND	-	.07	-	-	-	.05	-
FEO	1.14	1.17	2.81	2.16	2.10	2.26	2.65	2.28	8.66	8.82
MNO	.06	ND	.05	.04	.09	-	-	.04	.48	.42
MGO	.06	.04	.10	.23	.06	.14	.06	.16	6.02	6.01
CAO	-	-	-	-	-	-	-	-	-	-
NA2O	-	-	-	-	-	-	-	-	-	-
K2O	-	-	-	-	-	-	-	-	-	-
ZNO	41.30	41.60	41.51	41.95	42.05	42.08	42.16	42.16	27.00	27.04
TOTAL	99.24	98.86	99.86	100.01	99.92	99.88	100.02	99.83	100.78	100.88

** ATOMIC PROPORTIONS BASED ON SELECTED NO. OF OXYGENS **

OXYGEN	4	4	4	4	4	4	4	4	4	4
SI	-	-	-	-	-	-	-	-	-	-
TI	-	-	-	-	-	-	-	-	-	-
AL	2.027	2.019	1.988	1.992	1.994	1.989	1.981	1.984	1.961	1.960
CR	-	-	-	-	.002	-	-	-	.001	-
FE3+	-	-	.011	.008	.004	.011	.019	.016	.038	.040
FE2+	.029	.030	.060	.047	.049	.047	.048	.042	.167	.169
MN	.002	-	.001	.001	.002	-	-	.001	.012	.010
MG	.003	.002	.005	.010	.003	.006	.003	.007	.255	.254
CA	-	-	-	-	-	-	-	-	-	-
NA	-	-	-	-	-	-	-	-	-	-
K	-	-	-	-	-	-	-	-	-	-
ZN	.926	.939	.934	.941	.946	.947	.949	.950	.566	.567
SUM	2.986	2.991	3.000	3.000	3.000	3.000	3.000	3.000	3.000	3.000

**** SAMPLE DIRECTORY ****

SAMPLE NO.	DESCRIPTION	SAMPLE NO.	DESCRIPTION
181	JE-14 BLUE	186	JE-18 BLUE
182	JE-14 BLUE	187	JE-18 BLUE
183	JE-18 BLUE	188	JE-18 BLUE
184	JE-18 BLUE	189	JE-18 GREEN
185	JE-18 BLUE	190	JE-18 GREEN

TABLE 1

GAHNITE

SIO2	-	-	-	-	-	-	-	-	-	-
TIO2	-	-	-	-	-	-	-	-	-	-
AL2O3	57.70	59.12	59.41	58.60	58.70	58.98	57.79	58.68	58.70	56.20
CR2O3	ND	.10	.06	.13	.05	.10	.09	.08	.06	-
FEO	8.77	8.58	7.20	8.36	7.75	8.69	7.83	7.90	6.99	1.04
MNO	.50	.38	.31	.48	.38	.57	.34	.29	.33	ND
MGO	6.97	7.37	6.92	7.17	7.01	6.97	6.90	6.90	6.86	.14
CAO	-	-	-	-	-	-	-	-	-	-
NA2O	-	-	-	-	-	-	-	-	-	-
K2O	-	-	-	-	-	-	-	-	-	-
ZNO	24.51	24.65	25.08	25.13	25.38	25.51	25.83	26.38	27.00	41.32
TOTAL	98.48	100.20	98.98	99.87	99.27	100.82	98.78	100.23	99.94	98.72

** ATOMIC PROPORTIONS BASED ON SELECTED NO. OF OXYGENS **

OXYGEN	4	4	4	4	4	4	4	4	4	4
SI	-	-	-	-	-	-	-	-	-	-
TI	-	-	-	-	-	-	-	-	-	-
AL	1.957	1.964	1.997	1.958	1.973	1.957	1.958	1.960	1.967	2.023
CR	-	.002	.001	.003	.001	.002	.002	.002	.001	-
FE3+	.043	.034	-	.039	.026	.041	.040	.038	.032	-
FE2+	.168	.168	.170	.159	.159	.164	.148	.149	.135	.027
MN	.012	.009	.007	.012	.009	.014	.008	.007	.008	-
MG	.299	.310	.294	.303	.298	.292	.296	.291	.291	.006
CA	-	-	-	-	-	-	-	-	-	-
NA	-	-	-	-	-	-	-	-	-	-
K	-	-	-	-	-	-	-	-	-	-
ZN	.521	.513	.528	.526	.534	.530	.548	.552	.567	.932
SUM	3.000	3.000	3.000	3.000	3.000	3.000	3.000	3.000	3.000	2.988

**** SAMPLE DIRECTORY ****

SAMPLE NO.	DESCRIPTION	SAMPLE NO.	DESCRIPTION
191	JE-19 GREEN	196	JE-19 GREEN
192	JE-19 GREEN	197	JE-19 GREEN
193	JE-19 GREEN	198	JE-19 GREEN
194	JE-19 GREEN	199	JE-19 GREEN
195	JE-19 GREEN	200	JE-23 BLUE

TABLE 1

GAHNITE

SIO2	-	-	-	-	-	-	-	-	-	-
TIO2	-	-	-	-	-	-	-	-	-	-
AL2O3	56.26	57.05	55.80	60.39	60.67	60.08	60.54	60.83	60.37	60.14
CR2O3	-	-	-	.04	.05	ND	ND	-	-	.04
FEO	1.40	.81	1.61	5.31	5.23	4.96	4.72	4.97	4.84	4.84
MNO	.06	ND	.04	.39	.32	.27	.28	.30	.32	.32
MGO	.25	.11	.06	7.80	7.79	7.89	7.58	7.56	7.62	7.50
CAO	ND	-	-	-	-	-	-	-	-	-
NA2O	-	-	-	-	-	-	-	-	-	-
K2O	-	-	-	-	-	-	-	-	-	-
ZNO	41.65	42.01	42.64	26.23	26.38	26.56	26.57	26.81	26.83	27.00
TOTAL	99.64	100.01	100.15	100.16	100.44	99.79	99.72	100.47	99.98	99.84

** ATOMIC PROPORTIONS BASED ON SELECTED NO. OF OXYGENS **

OXYGEN	4	4	0	4	4	4	4	4	4	4
SI	-	-	-	-	-	-	-	-	-	-
TI	-	-	-	-	-	-	-	-	-	-
AL	2.012	2.026	0.000	1.996	1.999	1.993	2.008	2.005	2.001	1.999
CR	-	-	-	.001	.001	-	-	-	-	.001
FE3+	-	-	-	.003	-	.006	-	-	-	-
FE2+	.036	.020	0.000	.122	.122	.111	.111	.116	.114	.114
MN	.002	-	0.000	.009	.008	.006	.007	.007	.008	.008
MG	.011	.005	0.000	.326	.325	.331	.318	.315	.319	.315
CA	.001	-	-	-	-	-	-	-	-	-
NA	-	-	-	-	-	-	-	-	-	-
K	-	-	-	-	-	-	-	-	-	-
ZN	.933	.935	0.000	.543	.545	.552	.552	.554	.557	.562
SUM	2.994	2.987	0.000	3.000	3.000	3.000	2.996	2.997	2.999	3.000

**** SAMPLE DIRECTORY ****

SAMPLE NO.	DESCRIPTION
201	JE-23 BLUE
202	JE-23 BLUE
203	JE-23 BLUE
204	JE-23 GREEN
205	JE-23 GREEN
206	JE-23 GREEN
207	JE-23 GREEN
208	JE-23 GREEN
209	JE-23 GREEN
210	JE-23 GREEN

TABLE 1

GAHNITE

SIO2	-	-	-	-	-	-	-	-	-	-
TIO2	-	-	-	-	-	-	-	-	-	-
AL2O3	60.52	55.39	54.89	55.26	55.20	54.32	56.07	56.55	56.57	59.72
CR2O3	.04	-	-	.04	.09	-	-	-	-	-
FEO	4.98	1.68	1.84	2.48	2.25	2.02	1.35	1.74	1.77	7.88
MNO	.31	.04	.09	.27	.23	.08	.10	.10	.10	.35
MGO	7.43	.08	.13	.11	.11	.13	.12	.11	.10	6.21
CAO	-	-	-	-	-	ND	.04	-	-	-
NA2O	-	-	-	-	-	-	-	-	-	-
K2O	-	-	-	-	-	-	-	-	-	-
ZNO	27.13	43.31	42.13	42.30	42.36	42.16	42.72	42.95	43.38	26.74
TOTAL	100.41	100.50	99.08	100.46	100.24	98.73	100.40	101.45	101.92	100.90

** ATOMIC PROPORTIONS BASED ON SELECTED NO. OF OXYGENS **

OXYGEN	4	4	4	4	4	4	4	4	4	4
SI	-	-	-	-	-	-	-	-	-	-
TI	-	-	-	-	-	-	-	-	-	-
AL	2.001	1.982	1.988	1.976	1.978	1.977	2.001	1.998	1.992	1.987
CR	.001	-	-	.001	.002	-	-	-	-	-
FE3+	-	.018	.012	.023	.019	.023	-	-	.008	.013
FE2+	.117	.024	.036	.040	.038	.030	.034	.042	.036	.173
MN	.007	.001	.002	.007	.006	.002	.003	.003	.003	.008
MG	.311	.004	.006	.005	.005	.006	.005	.005	.004	.261
CA	-	-	-	-	-	.001	.001	-	-	-
NA	-	-	-	-	-	-	-	-	-	-
K	-	-	-	-	-	-	-	-	-	-
ZN	.562	.971	.956	.948	.951	.962	.955	.951	.957	.557
SUM	2.999	3.000	3.000	3.000	3.000	3.000	3.000	3.000	3.000	3.000

**** SAMPLE DIRECTORY ****

SAMPLE NO.	DESCRIPTION	SAMPLE NO.	DESCRIPTION
211	JE-23 GREEN	216	JE-39 BLUE
212	JE-26 BLUE	217	JE-74 BLUE
213	JE-35 BLUE	218	JE-74 BLUE
214	JE-35 BLUE	219	JE-74 BLUE
215	JE-35 BLUE	220	JE-74 GREEN

TABLE 1

GAHNITE

SIO2	-	-	-	-	-	-	-	-	-	-
TIO2	-	-	-	-	-	-	-	-	-	-
AL2O3	56.03	59.18	53.17	53.29	53.77	59.22	58.16	58.27	58.48	60.61
CR2O3	-	-	-	-	-	-	-	-	-	-
FEO	.60	7.35	3.97	3.54	3.39	7.11	10.79	8.68	10.56	11.29
MNO	-	.35	.10	.09	.12	.27	.58	.38	.50	1.09
MGO	-	5.61	.11	.16	.14	6.00	6.38	4.99	6.21	12.36
CAO	-	-	-	-	-	-	-	-	-	-
NA2O	-	-	-	-	-	-	-	-	-	-
K2O	-	-	-	-	-	-	-	-	-	-
ZNO	41.93	27.89	41.49	40.73	41.16	26.99	23.20	27.25	23.75	14.50
TOTAL	98.56	100.38	98.84	97.81	98.58	99.59	99.11	99.57	99.50	99.85

** ATOMIC PROPORTIONS BASED ON SELECTED NO. OF OXYGENS **

OXYGEN	4	4	4	4	4	4	4	4	4	4
SI	-	-	-	-	-	-	-	-	-	-
TI	-	-	-	-	-	-	-	-	-	-
AL	2.024	1.990	1.941	1.960	1.962	1.997	1.964	1.985	1.970	1.932
CR	-	-	-	-	-	-	-	-	-	-
FE3+	-	.010	.059	.040	.038	.003	.036	.015	.030	.068
FE2+	.015	.165	.044	.052	.050	.167	.223	.194	.222	.187
MN	-	.008	.003	.002	.003	.007	.014	.009	.012	.025
MG	-	.239	.005	.007	.006	.256	.272	.215	.264	.498
CA	-	-	-	-	-	-	-	-	-	-
NA	-	-	-	-	-	-	-	-	-	-
K	-	-	-	-	-	-	-	-	-	-
ZN	.949	.588	.949	.938	.941	.570	.491	.581	.501	.290
SUM	2.988	3.000	3.000	3.000	3.000	3.000	3.000	3.000	3.000	3.000

**** SAMPLE DIRECTORY ****

SAMPLE NO.	DESCRIPTION
221	JE-74 BLUE
222	JE-74 GREEN
223	JE-82 BLUE
224	JE-82 BLUE
225	JE-82 BLUE
226	JE-82 GREEN
227	OF-7 GREEN
228	OF-7 GREEN
229	OF-7 GREEN
230	JE-16

TABLE 1

GAHNITE

SIO2	-	-	-	-	-	-	-	-	-	-
TIO2	-	-	-	-	-	-	-	-	-	-
AL2O3	60.29	54.68	62.77	61.25	61.33	61.22	61.19	61.41	61.06	61.09
CR2O3	-	.67	.15	.05	.07	.07	.11	1.15	.71	1.45
FEO	13.87	27.37	20.25	22.28	21.77	21.91	21.87	20.37	23.54	19.87
MNO	1.35	.39	.75	.90	.88	.80	.82	.07	-	-
MGO	13.13	6.23	15.39	14.36	14.62	14.67	14.54	13.68	13.14	14.55
CAO	-	-	-	-	-	-	-	-	-	-
NA2O	-	-	-	-	-	-	-	-	-	-
K2O	-	-	-	-	-	-	-	-	-	-
ZNO	11.08	8.31	.65	.49	.52	.67	.08	2.34	1.25	2.01
TOTAL	99.72	97.65	99.96	99.33	99.19	99.34	98.61	99.02	99.70	98.97

** ATOMIC PROPORTIONS BASED ON SELECTED NO. OF OXYGENS **

OXYGEN	4	4	4	4	4	4	4	4	4	4
SI	-	-	-	-	-	-	-	-	-	-
TI	-	-	-	-	-	-	-	-	-	-
AL	1.911	1.866	1.929	1.910	1.911	1.906	1.916	1.930	1.915	1.913
CR	-	.015	.003	.001	.001	.001	.002	.024	.015	.030
FE3+	.089	.119	.068	.089	.087	.092	.082	.046	.070	.057
FE2+	.223	.544	.373	.404	.394	.392	.404	.409	.454	.385
MN	.031	.010	.017	.020	.020	.018	.018	.002	-	-
MG	.526	.269	.598	.566	.576	.577	.576	.544	.521	.576
CA	-	-	-	-	-	-	-	-	-	-
NA	-	-	-	-	-	-	-	-	-	-
K	-	-	-	-	-	-	-	-	-	-
ZN	.220	.178	.013	.010	.010	.013	.002	.046	.025	.039
SUM	3.000	3.000	3.000	3.000	3.000	3.000	3.000	3.000	3.000	3.000

**** SAMPLE DIRECTORY ****

SAMPLE NO.	DESCRIPTION	SAMPLE NO.	DESCRIPTION
231	JE-16	236	JE-A
232	JE-29	237	JE-A
233	JE-A	238	JE-G
234	JE-A	239	JE-G
235	JE-A	240	JE-G

TABLE 1

GAHNITE

SIO2	-
TIO2	-
AL2O3	61.27
CR2O3	.42
FEO	22.74
MNO	-
MGO	13.65
CAO	-
NA2O	-
K2O	-
ZNO	1.07
TOTAL	99.15

** ATOMIC PROPORTIONS BASED ON SELECTED NO. OF OXYGENS **

OXYGEN	4
SI	-
TI	-
AL	1.922
CR	.009
FE3+	.069
FE2+	.437
MN	-
MG	.542
CA	-
NA	-
K	-
ZN	.021
SUM	3.000

**** SAMPLE DIRECTORY ****

SAMPLE NO.	DESCRIPTION	SAMPLE NO.	DESCRIPTION
241	JE-6		